Lateral Earth Pressures on Rigid Retaining Walls with Limited Granular Backfills in Clays

by

Mohamed Elchalakani
B.E. (Cairo University, Egypt)

A thesis submitted for the Degree of
Master of Engineering Science

THE UNIVERSITY OF ADELAIDE
Department of Civil and Environmental Engineering
Australia

October 1996

To my wife Noriko

and my parents Farouk and and Karima

Abstract

When retaining walls are constructed in cohesive soils, a zone behind the retaining wall is excavated and backfilled with well-draining granular material to prevent the build up of water and to reduce the lateral pressures acting on the wall.

Use of classical theories to predict the magnitude and distribution of lateral pressures acting on the wall presents a number of issues for which the designer relies on experience and judgement for guidance. Examples of these issues are the choice of appropriate soil parameters to compute the lateral earth pressures, the choice and significance of the extent of the backfilled zone and the effect of the type and stiffness of the retaining wall chosen.

Numerical analyses have been carried out using the finite element method to address the above issues. The investigations have been carried out for a medium wall, with a height of 4.5 m, and for three common types of retaining walls used for residential and highway construction. These walls are cantilever T-wall, cantilever L-wall and gravity wall. The analyses have been carried out for a smooth vertical wall back and a horizontal ground surface.

Also, the focus has been on those walls supporting clay soils and having limited granular backfills of different geometries. Three common geometries of limited granular backfills have been investigated; triangular, rectangular and trapezoidal.

In this thesis, various simplified analytical methods for determining the lateral pressures on rigid retaining walls have been reviewed. The performance of these analytical procedures has been assessed by comparing their predictions with the results of the numerical investigations. Accordingly, the suitability of each analytical method for design has been determined.

The influence of some of the design parameters on the distribution of lateral earth pressures is examined through a parametric study. It is shown that the lateral earth pressures increase as the stiffness of the embankment decreases, but decreases as the stiffness of the foundation subsoil increases.

For small to medium construction, where the overall cost of the project is reasonably low, the costs involved in executing a good soil investigation are relatively high, and a numerical analysis is usually out of the question. Accordingly, the designer has to rely on experience to select suitable design parameters, together with suitable design charts, to estimate the likely behaviour of the retaining wall.

This thesis presents suitable lateral earth pressure distributions for use in design. A rational, step-by-step design process is suggested to improve design of retaining walls. This design process and the design curves, together with the simplified lateral pressure distributions, are applied to a case study of a retaining wall built in the metropolitan area of Adelaide.

Statement of Originality

This work contains no material which has been accepted for the award of any other degree or diploma in any university or other tertiary institution and, to the best of my knowledge and belief, contains no material previously published or written by another person except where due reference has been made in the text.

I give consent to this copy of my thesis, when deposited in the University Library, being available for loan and photocopying.

Signed: Date: 25/10/1996

Acknowledgments

I shall remain indebted to my supervisor Dr. G. W. S. Kaggwa, who gave me the necessary support to complete this research project and to present it appropriately. My thanks and gratitude to Dr. Mark Jaksa for his assistance in obtaining data on the construction of retaining walls and reading the thesis.

Also, I thank Dr. Peter Mitchell of Rust PPK for his useful comments and encouragement. I gratefully thank Dr. A. T. C. Goh for his guidance during the initial stages of the project in obtaining relevant references on interface parameters. I am grateful to James Trezona for the valuable data provided for the case study. I deeply thank the Computing Officer, Dr. Stephen Carr, for his technical assistance with computer problems which arose during the research.

I extend my thanks to Dr. M. C. Griffith, Head of Department of Civil and Environmental Engineering, for his concern for postgraduate students. I appreciate the friendliness and cooperative nature of all the staff members and fellow post graduate students of the department and shall remember with fondness the marvellous time I have shared with them. I wish to thank Barbara Thompson of RFS for reading the thesis, her encouragement and advice.

The financial assistance of the university and facilities, particularly the provision of computing laboratories, is greatly appreciated. I am also grateful to the consulting engineers in Adelaide who provided me with the necessary information on current construction of retaining walls. Most importantly, I express my deep gratitude to my wife, Noriko Seiwa who was extremely patient during this time.

Contents

Abbreviations

The following terms has been used throughout the thesis, and below their full description is given.

ASCE	American Society of Civil Engineers
CP No. 2	Civil Engineers Code of Practice No. 2
CIRIA	Construction Industry Research and Information Association
FE	Finite element
FEM	Finite Element Method
LEMs	Limit Equilibrium Methods
ICSMFE	International Conference on Soil Mechanics and Foundation Engineering
LEPs	Lateral earth pressures
LEPDs	Lateral earth pressure distributions
JSMFD	Journal of Soil Mechanics and Foundation Engineering
Non-homog.	Non-homogeneous backfill
RAVs	Rankine active values
Rect.	Rectangular backfill
SF	Safety factor
SMFE	Soil Mechanics and Foundation Engineering
Trans.	Translation
Trap.	Trapezoidal backfill
TWM	Trial wedge method
Wall yield	Outward lateral movement of the retaining wall

Notation

The following terms refer to the properties presented below.

a/H	backfill size ratio for triangular backfill
B	width of the wall base
b	width between rigid walls
b/H	backfill size ratio for rectangular backfill
c	cohesion of the soil; also horizontal distance quantifies the size of trapezoidal backfill
c_a	interface cohesion
c_u	undrained shear strength of the clay deposit
c/H	backfill size ratio for trapezoidal backfill
E	Young's modulus
E_c	Young's modulus of concrete
E_u	undrained soil modulus
E_cI_c	flexural rigidity of concrete
E_1	Young's modulus of the backfill
E_2	Young's modulus of the embankment
E_3	Young's modulus of the foundation subsoil
G	shear modulus
H	height of the retaining wall
H1	height of the embankment; also height of the stem of the wall
H_c	critical depth
I_c	second moment of area of the concrete cross section of the wall
K	coefficient of lateral earth pressure used in silo equations
K_a	coefficient of active lateral earth pressure
K_{ac}	Coulomb's active lateral earth pressure coefficient
K_{ar}	Rankine active lateral earth pressure coefficient
K_n	normal stiffness
K_0	coefficient of earth pressure at-rest
K_{sb}	interface shear stiffness along the base of the wall
K_{ss}	interface shear stiffness along the back of the wall
K_{st}	tangent stiffness
P	lateral thrust
P_a	Rankine active thrust
p_a	Rankine active lateral earth pressure

p_{hz}	horizontal earth pressure
p_{vz}	vertical earth pressure
p_0	at-rest lateral earth pressure
Y	distance from base of embankment to line of action of lateral thrust
y_i	distance from the base of embankment to the point of application of σ_i
z	depth below ground surface
Δ / H	ratio of wall lateral movement to the height of the wall
Δn	average normal displacement across the element
Δs	average relative shear displacement across the element
[D]	elastic-plastic constitutive matrix
[K]	overall stiffness matrix of the assemblage of elements
{P}	prescribed nodal forces vector
$\{\delta\}$	unknown nodal displacements
α	angle of inclination of the back of the wall to the horizontal; also angle of inclination of excavation surface to the horizontal
β	lateral thrust correction factor
δ	angle of wall friction
δ_s	angle of wall friction within the silo
$\dot{\varepsilon}^p_{ij}$	plastic strain rate
$\dot{\varepsilon}$	rate of strain
η / B	ratio of differential settlement of the wall to its base width
ϕ	angle of shearing resistance
ϕ'	effective angle of shearing resistance
γ	unit weight of soil
λ	limiting value of backfill size ratio; also scalar
ν	Poisson's ratio
ν_2	Poisson's ratio of the embankment
φ	angle between the total reaction acting on rupture plane and the normal; also angle of dilation
ω	angle of inclination of ground surface to the horizontal
ρ	Coulomb's angle of rupture
σ_i	normal horizontal stress
σ'_1	major principle effective normal stress
σ'_3	minor principle effective normal stress
$\dot{\sigma}$	rate of stress
σ_n	normal stress within the element
τ	shear stress within the element

Chapter 1

Introduction

1.1 INTRODUCTION

This research project is aimed at determining the lateral earth pressure distributions behind rigid retaining walls having limited granular backfills and founded on clays. The problem of lateral earth pressure on retaining structures has been the subject of study by many researchers over the last two centuries. This is because the cost of construction is considerably high compared with other structures. Reducing factors of safety and developing a rational design tool were the major aims of these studies, such as Terzaghi (1934). The present research project was first established as an attempt to improve the design of retaining walls and reduce the cost of construction.

Although the impractical assumptions involved in the classical theories of earth pressure of Coulomb (1773) and Rankine (1857), and in spite of the strong arguments accumulated over the last 20 years against these theories, they are still used for design purposes. One of these assumptions is that the backfill should extend a sufficient distance behind the wall to allow for the formation of the inner plane of rupture. However, in design manuals and codes, such as CP No. 2 (1951), it is recommended that when retaining walls are constructed to support clays, a granular zone of at least 18" (457 mm) should be loosely placed between the clay deposit and the retaining wall. This is to prevent the build up of water and to reduce the lateral earth pressures on the

wall. This condition is known in the literature as *the limited backfill condition* (Huntington, 1957). Therefore, using the classical theories to determine the lateral earth pressure distributions for retaining walls with limited backfills involves considerable uncertainties.

Although the limited backfill condition was investigated in a number of studies and simplified analytical methods were established, such as Huntington (1957), Reimbert (1989) and Bang and Tucker (1990), it was not properly addressed. It has been found that these methods are only valid for some particular conditions and a considerable uncertainty is associated with using their solutions. This uncertainty is due to some basic assumptions, namely: zero cohesion along the excavation surface; extreme high stiffness of the natural deposit; using the at-rest coefficient of earth pressures and only treating vertical cuts.

A survey carried out by the author of consulting engineering firms in Adelaide, South Australia, demonstrated that many geotechnical engineers rely on experience and judgement, with little theoretical basis, for the analysis of retaining walls with limited backfills. Although there are some analytical procedures treat the limited backfill condition, the designer still uses the classical theories, as these analytical procedures have not yet been assessed. Also, the results of the survey indicated that there is poor design practice among geotechnical engineers because of low fees associated with retaining wall design, as well as insufficient information on drainage systems. This poor practice not only leads to uneconomical design of stiffer walls but may also result in failure of retaining walls during their service life.

It was with all of these in mind that this research project was initiated to develop a numerical technique to enable the behaviour of retaining walls with limited backfills to be more confidently predicted. Also, the project was established to provide guidance to the consulting engineers in Adelaide and allowing them to deal with limited backfill conditions.

1.2 OBJECTIVES AND SCOPE

The main objective of this project is to determine the lateral earth pressure on rigid retaining walls which are founded on clays and have limited granular backfills. A correction factor for the magnitude of the lateral thrust and its line of action are given for different field conditions. In addition, one important aspect of this project is to

develop simplified lateral earth pressure distributions to assist in routine design. As the results of the survey of consulting engineers indicate poor design practice, a step-by-step design procedure is one of the aims of this project. Another objective is to investigate whether available simplified analytical procedures produce realistic estimates to lateral earth pressure distributions. Therefore, more confidence in these methods would be built up, thus enabling retaining walls to be constructed safely and economically.

This research project involved theoretical computer modelling of rigid retaining walls. The results are compared with a number of field measurements in the literature. Attention is confined to concrete retaining wall problems assuming plane strain conditions and elastic-plastic behaviour of soil.

The numerical investigation of T-walls, presented in the present research, is an extension to the work carried out by Goh (1993). Also, the numerical modelling of gravity walls, presented in this thesis, is based on Clough and Duncan (1971).

The finite element method (FEM) was used to carry out the numerical investigation program as it is able to model more realistically most of the significant variables such as the deformation properties of the soil, construction sequence, wall flexibility, soil-structure interaction, and complex initial conditions.

The finite element program AFENA (Carter and Balaam, 1994), developed at the University of Sydney, was used to carry out the analyses. The numerical studies involve investigation of the behaviour of rigid walls with particular attention being paid to the key factors affecting lateral earth pressures. The focus was on cantilever and gravity walls with smooth vertical rear faces and having different backfill geometries.

The natural clay deposit was categorised into four types: soft; medium; stiff; and very stiff. Undrained conditions were assumed for the clay, and the ground water table was chosen below the foundation level. The clay deposit was modelled as self supporting, ie without allowance for temporary supports during construction.

In order to simulate closely the conditions that exist in the field, finite element models are developed to model, as close as possible, the excavation and construction sequence by using the macro programming option employed in AFENA. The large difference in stiffness between concrete and soil results in relative movements along the interface. This is overcome through employing one dimensional interface elements to simulate the soil-structure interaction and relative movements.

This research project focuses on rigid retaining walls. Flexible walls are beyond the scope of this thesis. Rigid walls are those constructed out of relatively bulky material with large thickness (mass), such as reinforced concrete, masonry and bricks. Flexible walls are used more for temporary construction such as sheet pile walls and are fabricated using metals such as mild steel with much smaller cross sections owing to its large strength and stiffness compared to rigid walls. The major difference between these two types is the behaviour under lateral pressures, which in turn affects the stress-strain field behind the wall. A rigid wall tends to slide along the base and/or to rotate as a rigid body about the toe. On the other hand, flexible walls tend to bend under lateral earth pressures, because of their ductility and flexibility, and most of the movements are lateral deflections under bending action.

Rigid walls with heights more than 4.5 metres or with inclined rear faces (backs) are not included in this study. No tension cracks, or any other discontinuity or softening of the clay deposit due to wetting effects were considered in these analyses. The research focuses on the active pressures behind the wall, as they are a key design factor, while the passive lateral pressures at the front of the wall have been neglected in the problem formulation.

The geometry and size of a limited backfill chiefly relies on the type of drainage system used for a particular site condition. This thesis considers the commonly used backfill geometries. However, different drainage systems including their requirements and applicable field conditions are beyond the scope of this research. Text books such as Huntington (1957) and Bell (1987) can be used for further reading on drainage systems.

1.3 THESIS LAYOUT

This thesis focuses on the evaluation of effects of backfill geometry and size on the distribution of lateral earth pressures behind rigid retaining walls. Also, the key factors which affect the lateral earth pressures in the case of limited backfills are determined through a parametric study. The thesis focuses on walls of moderate heights, 4.5 m high, which are used for residential and highway construction. The main results of this research project are given in Chapters 4 and 5. The cantilever T-wall is the most common type of retaining wall, therefore Chapter 4 is devoted to the analysis of this type of wall. The layout of this thesis is given below.

In Chapter 2 background information on the problem of lateral earth pressures on retaining walls is presented. The developments and major studies of the problem of lateral earth pressures on retaining walls are reviewed in a short historical review. A literature review of the classical theories along with a coverage of the phenomenon and theory of lateral earth pressures are discussed. The factors affecting lateral earth pressures are discussed, focusing on wall and soil movements and the effect of shear stresses. Available simplified analytical procedures for limited backfill conditions are investigated and some of the available solutions are presented at the end of the chapter.

The finite element methodology is described in Chapter 3. Attention is paid to previous finite element studies, and their main assumptions and findings are discussed. The basic formulation of the finite element method relevant to the present problem is briefly presented. The elementary features of the finite element analysis are described with particular attention to constitutive soil models, interface modelling, modelling of construction sequence and time constraints and efficiency. Also, the technique adopted in interpreting the results of the finite element analyses is discussed at the end of the chapter.

Chapter 4 deals with the analysis of cantilever T-walls having limited backfills. The idealised case of unlimited backfill is first examined and the results are compared with other finite element studies in the literature. A parametric study was carried out to identify the critical design parameters. Two different sets of analyses were carried out. The first set involves limited homogeneous backfills with three commonly used backfill geometries which are described in Sections 4.4 to 4.6. The second set covers limited non-homogeneous backfills that are described in Section 4.7. A correction factor for the Rankine active thrust is proposed to allow for variations in backfill geometry and size. The performance of simplified analytical methods is then assessed by comparing their predictions with the results of the numerical investigations.

Chapter 5 deals with the numerical modelling of gravity walls and cantilever L-walls. Also, the unlimited backfill case is again described first followed by the results of a parametric study. Design curves for the variation of the lateral thrust correction factor with backfill geometry, and size and the location of the lateral thrust, are presented. Attention is given to the triangular shaped backfill geometry. However, additional analyses for other geometries are included. Some comparisons between the results of the three types of retaining wall (T-walls, L-walls, and gravity walls) are also discussed.

Chapter 6 describes the application of the results presented in Chapters 4 and 5 for design purposes. The current practice is discussed and the main difficulties are included. Simplified lateral earth pressure distributions, to account for the size and geometry of the backfill, are recommended for routine design. Also, a step-by-step design procedure is presented at the end of the chapter.

Finally, a summary of the main findings of the research undertaken, the conclusions drawn from it and the recommendations for future research, are presented in Chapter 7.

Chapter 2

Analytical Methods Used to Determine Lateral Earth Pressures

2.1 INTRODUCTION

This chapter covers the background of the lateral earth pressure theories including the main concepts of its phenomena and gives a historical overview of the developments since the time of Coulomb (1773). Also, the chapter reviews the classical earth pressure theories. The basic features of each method are covered, including the types of walls that these methods may be applied to. The factors affecting lateral earth pressures (LEPs) are reviewed, focusing on soil-structure interaction effects, in particular, wall stiffness and geometry and associated movements. The available procedures and methods used to predict lateral earth pressures for limited backfill conditions are also investigated.

Although the research is directed at investigating the effects of backfill size and geometry on the LEPs, it was found necessary, not only to review this particular factor, but to cover all key factors which influence the distribution of the LEPs. This results from the fact that the problem is complex and the factors are interrelated. As an example of this complex interaction, changing the size of the backfill affects the mode of deformation of the wall and subsequently varies the LEPs.

2.2 LATERAL EARTH PRESSURE THEORY

In this section, the theory of the lateral earth pressure is presented. First, the main contributions over the last two centuries are briefly reviewed. The complex interaction between the forces acting within the plastic zone (region bounded by the back of the wall and the plane of rupture) is highlighted. The importance of determining the lateral earth pressures, as the key factor in the design of retaining walls, is discussed.

2.2.1 Historical Overview

The analysis of problems in soil mechanics is generally divided into two distinct groups: stability problems and deformation problems. The stability problems deal with the condition of ultimate failure of a mass of soil; for example, problems of earth pressures, bearing capacity, and stability of slopes fall in this category. The most important feature of such problems is the determination of the failure load. Solutions to these problems can often be obtained by satisfying static equilibrium and applying failure criteria, such as the Mohr-Coulomb failure criterion, along the assumed rupture surface, for example, plane, circular or log spiral. These methods are known as the Limit equilibrium Methods (LEMs) in soil mechanics.

The earliest contribution to the evaluation of the active thrust on masonry retaining walls, using the LEMs was made in 1773 by Coulomb. He proposed Coulomb's criterion for soils and also established the concept of limiting equilibrium for a continuum and applied it to determine the lateral thrust of a fill on a retaining wall, employing wall friction in his mathematical formulation. In 1773 he also established a simplified graphical procedure for irregular fills known as the Trial Wedge Method (TWM). Another graphical procedure was introduced later by Culmann in 1866. This method is similar to the TWM, but the only difference being the orientation of the force polygon.

Rankine (1857) investigated the limiting equilibrium of an infinite soil mass and applied, for the first time, his stress-field theory for cohesionless soils for active and passive states. His mathematical formulation confirmed Coulomb's value for the active state. However, the theory of Rankine was restrictive in that the angle of friction on the wall and soil interface was established at failure as being equal to the slope of the ground for a vertical wall.

Nevertheless, Coulomb's and Rankine's contributions are considered as very important developments in the LEMs. In the classical theories of Coulomb and Rankine, the constitutive relation (stress-strain relationship) was neglected, and the theories were developed only for cohesionless soils. Important developments were made during the nineteenth century when the stress circle was introduced and used for clays, the elasticity theory was applied to surcharge loading, and the establishment of the beam on elastic foundation model to account for the flexural rigidity of retaining walls, Chen and Liu (1990).

By the beginning of the 20th century, research trends aimed to develop a simplified theory of limiting equilibrium in order to solve various problems by elementary methods. Kotter (1903) considered the differential equations of equilibrium and the yield condition at each point, forming a set of equations and then transformed them to curvilinear co-ordinates. This also includes developments by Fellenius (1926) who assumed slip surfaces of various simple shapes, such as plane, prismatic and circular-cylindrical. Neither Coulomb's nor Rankine's methods explicitly incorporated cohesion, however in 1915 Bell published his active and passive equations as a solution to this problem, which were directly obtained from Mohr's circle.

Later, Caquot (1934) adopted a completely different approach and derived a system of equations of limiting equilibrium for an ideally granular wedge to solve complicated problems. Sokoloviski (1960) presented a highly mathematical, finite difference solution for the lateral earth pressure problem for cohesive and cohesionless soils.

Parallel developments since 1920, largely due to the influence of Terzaghi (1920), led to a better understanding of the limitations and appropriate applications of the classical earth pressure theories. Due to the variety of types of retaining structures, and his belief that the earth pressure on a retaining structure is an experimental problem, Terzaghi (1934) conducted large scale model tests at the Massachusetts Institute of Technology (MIT). In this significant contribution he confirmed the lateral earth pressure concept, and as well he highlighted the influence of wall movements. Caquot and Kerisel (1948) produced tables for lateral earth pressures based on Boussinesq's non-plane failure method. Hansen (1953) based on Kotter's (1903) equations, developed a new limiting equilibrium method applicable to cohesive and cohesionless soils and a variety of retaining walls with any inclination and roughness, as well as for irregular ground surfaces.

Rosenfarb and Chen (1972) developed a closed form solution for the lateral earth pressures on retaining walls using plasticity theory. Their equations for active and passive coefficients were solved using a computer program with an iteration routine. They considered several failure surfaces, and the combination of a so called *log-sandwich*. More recently, Chen and Liu (1990) established solutions for lateral earth pressure problem, based on an upper bound theorem, in the case of earthquakes. Contributions by Symons and Clayton (1992) used field studies and centrifuge and Pilot-Scale models, with particular attention to diaphragm walls, to examine a number of design factors, such as: wall stiffness; wall and consequent ground movements; compaction and installation effects; and construction sequence.

In most of the afore mentioned studies, the key assumptions of unlimited backfill and enough deformations to reach the active state have been employed. Little or no attention has been paid to drainage requirements, which are specified in current design manuals, where the retaining wall is founded on cohesive soil and the backfill is of finite geometry. However, it is shown in the present study that a limited backfill is often the case for these walls, and wall deformations depend on the size and geometry of the backfill. In Section 2.5 the problem of a limited backfill is discussed and the main analytical methods dealing with this problem are reviewed.

2.2.2 Forces Acting on Retaining Walls

In this section, the problem of lateral earth pressures on retaining walls is explored including all forces contributing to the equilibrium of the wall and soil system. Investigating these forces is essential, as any change in one force will affect the equilibrium condition due to the complex soil-structure interaction.

To study the equilibrium of forces that are imposed on rigid retaining walls, the conventional gravity retaining wall, shown in Figure 2.1, is considered. The bearing force resists the weight of the wall plus the vertical component of the other forces above the foundation level. The total lateral thrust, which develops as the backfill is placed and as any surcharges are placed on the surface of the backfill, acts to push the wall outward, and movements of the supported soil can take place. The total lateral thrust is the integration of the lateral earth pressure distribution along the full height and acts at the centroid of this distribution.

The outward motion of the wall is resisted by sliding (shear) resistance along the base of the wall and the passive resistance of the soil lying above the toe of the wall. The lateral thrust (P) also tends to overturn the wall about the toe. This overturning is resisted by the weight of the wall and the vertical component of the lateral thrust. The wall and the soil above and below the foundation level form an indeterminate system.

The magnitudes of working lateral pressures acting upon the wall are not determined using simple statics, because the behaviour of the wall and the adjoining soil depends, to a large extent, on the associated movements and the interaction along the interfaces. However, the limiting values of the lateral pressures can be determined by using the classical earth pressure theories.

One key factor in retaining wall design is the overall stability which in turn affects the lateral earth pressures. Exceeding the ultimate bearing capacity and/or the ultimate sliding resistance along the base results in large movements. These movements change the equilibrium condition and the geometry of the plastic zone, hence vary the magnitudes of LEPs. The effect of the overall stability on lateral earth pressures is discussed for soft clay soils in Chapters 4 and 5.

2.2.3 Earth Pressure Phenomena

The main aim of this research is to investigate the stress field behind retaining walls. To accomplish this investigation, the basic aspects of the problem should be fully reviewed. Identifying the initial in-situ conditions is of significant importance in this investigation.

(a) Lateral Earth Pressure Concept

Terzaghi (1920) concluded that any development in the determination of lateral earth pressure will be tied to the basic concepts of the theory. There are two main concepts that form the fundamental basis of the lateral earth pressure phenomena. Consider the retaining wall in Figure 2.1. If the wall yields, a slip occurs in the backfill along the inner plane of rupture (am) and a soil wedge moves down. The wedge slides and the slip is considered the only characteristic of failure of the soil mass behind the wall. Hence, wall yield forms the first aspect of the problem.

The second aspect relates to the similarity between lateral earth pressures on retaining walls and the stability of slopes. This can be demonstrated if the wall is entirely

removed, then the slope (that has been supported by the wall) fails, since the angle of the slope is larger than the angle of repose of the backfill. Also, the surface of the front part of the backfill forms an even talus of specific angle. Generally, this angle will be equal to the angle of repose of this soil. In fact, if a retaining wall is constructed inclined to coincide with the surface of the talus, then the lateral thrust acting on this inclined wall will be zero.

The first aspect of wall yield is examined in Section 2.4.2, while the second aspect is discussed through the numerical investigations in Chapters 4 and 5.

(b) In Situ Lateral Earth Pressures

The lateral earth pressures in a soil mass are greatly affected by any lateral deformations that the mass may have experienced before. Such pressures are divided into three classes: earth pressure at-rest, or natural earth pressures; active earth pressures; and passive pressures. The lateral earth pressures in a natural deposit that has remained undisturbed are referred to as *natural earth pressures* or earth pressures at-rest. Also, lateral pressures in deposits formed artificially by some construction operation and in which no lateral deformation has occurred subsequent to deposition are called earth pressures at-rest. The magnitude of these pressures depends upon the manner in which the soil was deposited as well as the physical properties of the soil. Minimum lateral pressures will exist in a loosely dumped fill, whereas the pressures may be relatively high in deposits that have been artificially compacted. The effect of compaction is discussed in Sections 2.4 and 3.3.

Furthermore, earth pressures at-rest may exist in deposits retained laterally by structures that do not yield appreciably under the action of earth pressures, (Huntington, 1957). Examples of such structures are basement walls of buildings supported laterally by rigid floor construction, the vertical legs of rigid frame bridges, some types of bridge abutments, and retaining walls founded on soft rocks. It is not possible to compute magnitudes of natural earth pressures or earth pressures at-rest, but such values can only be determined experimentally. However, Jaky (1948) established a simplified formula for the coefficient of earth pressure at-rest, K_0:

$$K_0 = 1 - \sin\phi \qquad (2.1)$$

where
ϕ = friction angle of the soil

Active earth pressures exist in a soil deposit that has been extended laterally, such as a backfill of a retaining wall that has tilted or moved horizontally. In this case, two inner and outer planes of rupture are mobilised, and both inclined to the horizontal at angles equal to the Coulomb angle of rupture; $\rho = \pm(45 + \phi/2)$. Figure 2.1 shows the inner and outer planes of rupture (defined as am and am') and their relative orientations.

2.3 CLASSICAL EARTH PRESSURE THEORIES

In this current research, the classical earth pressure theories considered are those of Coulomb and Rankine including the Trial Wedge Method (TWM). They are briefly discussed in the current section focussing on their main assumptions. The applicability of the TWM for the limited backfill condition is examined.

2.3.1 Coulomb's Theory

The main assumptions in this theory are that the soil extends a sufficient distance behind the wall and the soil possesses constant properties, (Huntington, 1957). Therefore, this theory can not be used for a limited backfill condition as there are two material zones with different properties.

In this theory, the static equilibrium of the plastic zone is considered in order to determine the lateral thrust of perfect sand against a retaining wall. Coulomb's conditions for the active state of stress assume that a retaining wall yields sufficiently to develop this state of stress. They differ from Rankine's conditions by assuming that the soil slides along the back of the wall, and the obliquity of the resultant pressure on the back of the wall has a value of δ. Therefore, Coulomb's conditions prevail when the active wedge is bounded on one side by the back of the wall and on the other side by the plane of rupture. Coulomb's conditions yield the resultant pressure against the back of a retaining wall directly, whereas Rankine's conditions apply to the resultant pressure against a vertical plane through the heel of the wall.

To derive Coulomb's formula for active earth pressure against the back of a retaining wall, consider the equilibrium of the forces acting throughout the plastic zone behind the wall, shown in Figure 2.1, and differentiating the equation of equilibrium with respect to the angle of obliquity of the inner plane of rupture (ρ). Accordingly, the well-known Coulomb's formula is given as follows:

$$P_a = \frac{1}{2}\gamma H^2 K_{ac} \tag{2.2}$$

where

P_a = total active thrust on a vertical wall

K_{ac} = Coulomb's active lateral pressure coefficient, which is given by:

$$K_{ac} = \frac{\sin^2(\alpha+\phi)}{\sin^2\alpha.\sin(\alpha-\delta)\left[1+\sqrt{\frac{\sin(\phi+\delta).\sin(\phi-\omega)}{\sin(\alpha-\delta).\sin(\alpha+\omega)}}\right]^2} \tag{2.3}$$

where

α = angle of inclination of the back of the wall to the horizontal

δ = angle of wall friction

ω = angle of inclination of the ground surface to the horizontal

It should be realised that there is a theoretical error associated with this method. This error is caused by the assumption that the inner surface of rupture is planar, while, in fact, it is slightly curved (Terzaghi and Peck, 1967). For Coulomb's formula to apply, the first and either the second or third of the following conditions must apply: (1) the back of the wall must be planar, or nearly planar, such that an equivalent planar surface may be substituted for the real surface, for computational purposes; (2) the wall does not interfere with the formation of the outer plane of rupture but sliding occurs along the back of the wall; (3) the wall interferes with the formation of the outer plane of rupture, so sliding occurs along the back of the wall, and an outer plane of rupture does not develop.

2.3.2 Rankine's Theory

The key assumption of a sufficient distance of the backfill behind the wall was employed by Rankine. The method does not allow for variation of the backfill geometry or size. Therefore, this method is inappropriate for the determination of the LEPs in the case of limited backfills.

In this method, the plastic equilibrium of soil elements in the plastic zone is considered to determine active and passive pressures of sand against retaining walls. Rankine's active state of stress exists if the followings two conditions are satisfied: (1) the wall does not interfere with the outer plane of rupture; and (2) the soil in the active wedge

between the outer plane of rupture and the back of the wall does not slide on the back of the wall but moves with the wall. The coefficient of Rankine active earth pressure (K_{ar}) can be determined from assuming the soil elements have reached the active state and according to plastic equilibrium:

$$K_{ar} = \cos\omega \frac{\cos\omega - \sqrt{\cos^2\omega - \cos^2\phi}}{\cos\omega + \sqrt{\cos^2\omega - \cos^2\phi}} \qquad (2.4)$$

where all the variables are as in Eq. 2.3.

The lateral thrust acting upon the wall will be determined using Eq. 2.2, where K_{ac} is to be replaced by K_{ar}. Note that the Rankine active thrust is always parallel to the ground surface, unlike Coulomb's active thrust. In comparison, the value of Coulomb's coefficient of active earth pressures that is given in Eq. 2.3 is less than Rankine's coefficient that is given by Eq. 2.4. Bell (1915) extended Rankine's theory to include cohesive soils in the case of a plane ground surface. This formulation for active state is given by:

$$\sigma_3 = \gamma z K_a - 2c\sqrt{K_a} \qquad (2.5)$$

where

σ_3 = lateral pressure on back of the wall

γ = unit weight of soil

z = depth below ground surface

c = cohesion

K_a = coefficient of active lateral earth pressure

Note that K_a could be either K_{ar} or K_{ac}, as recommended by Bell. The conditions that have been described for the application of the two theories may be summarised as follows:

(1) if the back of the wall is a planar surface or a surface, which can be assumed to be plane without introducing significant errors, either method can be applied depending upon which of the following conditions prevail: (a) if the outer plane of rupture can not form, Coulomb's conditions prevail; or (b) if the outer plane of rupture can form, Coulomb's conditions prevail if the obliquity of the earth pressure on the plane is equal to or greater than δ, while, Rankine's conditions prevail if the obliquity is equal to or less than δ;

(2) if the back of the wall can not be assumed to be a planar surface, Coulomb's conditions can not prevail but Rankine's conditions prevail if the outer plane of rupture can form without being obstructed by the wall.

In general, solid gravity walls with the usual proportions satisfy Coulomb's conditions. Cantilever and counterforted walls do not satisfy the assumptions of either theory but walls with the usual proportions (the proportion of heel to height) can be assumed to satisfy Rankine's conditions without introducing significant error in the computed pressures against the wall. Additionally, Coulomb's conditions prevail in the case of comparatively flexible walls (such as sheet pile walls), where the mobilised movements allow for the development of the shear stresses along the back of the wall. Moreover, both Coulomb's and Rankine's theories were developed for cohesionless soils and plane ground surface conditions. In the case of cohesive soils with irregular ground surface the only method that can be applied is the Trial Wedge Method (TWM).

2.3.3 Trial Wedge Method

This method is a simple graphical procedure to determine the active and passive earth pressures on retaining walls that can be obtained using Rankine's or Coulomb's formulas (Huntington, 1957). The only limitation with this method is that the inner surface of rupture must be a planar or close to a planar. The TWM can be applied successfully to cohesive soils, cohesionless soils and for gravity and cantilever walls with plane or irregular rear faces. Also, the method can be used if the backfill carries line loads or distributed loads. However, the method has a number of disadvantages including: the distribution of lateral earth pressures can not be determined accurately by this method; the method has the same theoretical error as Coulomb's theory; and the method does not allow for point loads.

The procedure of this method is given in most text books, such as Bowles (1988), but herein its applicability for limited backfill condition is discussed. For unlimited backfills, the plane of rupture is determined in the TWM based on the fact that the maximum shearing resistance is mobilised along this plane. The angle of friction along the trial plane is assumed equal to the angle of shearing resistance, ϕ, of the backfill. This assumption is valid only for the actual plane of rupture. The shearing resistance along any trial plane reduces the lateral force on the wall, as shown in the force polygon in Figure 2.1(b). Thus, the shearing resistance along all the trial planes, except the actual one, is larger than it should be. For this reason, the maximum value of the lateral force is chosen. Accordingly, the TWM can not be used in the case of a

limited backfill, since there are two different material zones, and two different values of ϕ. If the TWM is applied, two rupture planes are determined and each one corresponds to the plane with maximum lateral pressure through a zone, and there is uncertainty in selecting the actual plane of rupture between these planes.

2.4 DESIGN PARAMETERS

In general, the lateral earth pressures on a retaining structure are caused by the instability in the backfill material governed by the mobilised shearing stresses in the plastic zone and soil-structure interaction. The effect of soil-structure interaction is investigated in Sections 2.4.2 to 2.4.4 and the influence of shearing stresses is discussed in Section 2.4.5. Other factors affecting the lateral earth pressure are reviewed in the following subsection.

2.4.1 Factors Affecting Lateral Earth Pressure

A number of factors affecting the mobilisation of lateral earth pressures are highlighted, because lack of understanding of their effects may result in erroneous estimation of the lateral earth pressures. These factors are: (a) subsoil conditions; (b) compaction effects; (c) construction sequence; (d) backfill soil properties and wall friction; (e) soil-tension effects; (f) seepage and pore water pressures.

(a) Subsoil Conditions

The New Zealand Ministry of Works and Development Report (1973) includes the effects of wall type and foundation conditions, and recommends design values for lateral earth pressure coefficients, where higher values are recommended for relatively rigid walls on firm soils or rocks. This is because the lateral yield of the wall is likely to be small for a stiffer soil which results in lateral earth pressure close to at-rest conditions.

The subsoil deformation parameters affect the mode of deflection of the wall and, consequently, the lateral earth pressures. The effect of constructing rigid T-walls on soft soils is discussed in Bowles (1988), where there is likely inward wall tilting rather than outside movement due to placement of a heavy backfill. In this particular case there is uncertainty in earth pressures calculations, since the Rankine active wedge will not form. Therefore, he suggested using at-rest lateral pressures in addition to a

uniform surcharge at the ground surface of 15-30 kPa to determine the lateral thrust at the back of the wall.

(b) Compaction Effects

Despite progress made in understanding the phenomenon of compaction-induced pressures, it remains true that compaction induces soil stresses which are not amenable to accurate and reliable analysis with existing theories and procedures (Duncan and Seed, 1986).

Based on the available data provided in field measurements for compaction induced pressures, such as Coyle et al. (1974) and Davis and Stephens (1956), it can be concluded that:

- The compaction of soil represents a process of load application and removal which can result in significant increases in residual lateral earth pressures. The compaction process changes the properties of the backfill soil and may increase the lateral pressures, particularly for rigid unyielding walls;

- The depth which compaction increases the LEPs varies from 2 to 3 m for small hand-operated rollers to 10 to 15 m for very heavy compaction equipments.

- The compaction of soil against a deflected wall: (i) can significantly increase structural deflections of the type reported by Terzaghi (1934); (ii) increases near surface residual stresses to greater than at-rest values; (iii) decreases LEPs at depth due to the increase of structural deflections. The mode of structural deflections affect these later changes in stress distribution;

- Terzaghi (1934), in his large retaining wall tests, noted that compaction significantly affected lateral earth pressures and resulted in considerable deflections. He concluded that, prior to any displacement of the wall, the coefficient of lateral earth pressure at the back of the wall was $K_0 = 0.7$ for compacted dense sand, and $K_0 = 0.4$ for loose sand;

- The compaction of soil against a non-deflected wall generally increases the LEPs along the full height to greater than the at-rest values. This was explained more recently by the analytical model developed by Seed and Duncan (1986).

(c) Construction Sequence

Conventional design methods take no account of effects of construction sequence on lateral pressures as well as lateral performance of retaining walls, because these classical methods assume that the wall appears 'magically' in place without any apparent construction disturbance of the natural soils. The interaction between a structure and the adjacent soil will be affected by the construction sequence, and by the displacements that occur during construction of the structure and placement of the backfill.

Construction sequence has two physical forms: (1) in the case of backfilled walls, the number of lifts placed together represents the sequence; (2) in the case of sunken walls (such as deep excavations), the schedule that is followed in installing the struts represents the sequence. Tschebotarioff (1951) reported a redistribution of lateral pressures during excavation for strutted sheet piling, and this was caused by increasing movements at the top. He also reported that earth pressures developed in the case of braced excavations chiefly depend upon the method of installation of the struts. The effects of construction sequence are larger in the case of sunken walls, where the movements are higher. The use of numerical methods in the analysis of rigid retaining walls allows the determination of the effects of construction sequence on the lateral pressures. These effects are discussed in Section 3.4.3, as one aspect of the finite element methodology.

(d) Backfill Soil Properties and Wall Friction

The effects of the backfill soil strength parameters on the LEPs are considered in the classical theories. However, the effect of the deformation parameters is not considered in these theories. These theories study the equilibrium at limiting state, where the strength parameters determine the ultimate shearing resistance required to achieve equilibrium. The deformation parameters are of negligible importance at this limiting state, since it is assumed that large movements have already occurred along the rupture plane. However, as it will be discussed in Section 2.5, the limited backfill condition is a common situation where the active state may not develop, and the deformations of the natural clay deposit control the equilibrium of the plastic zone.

The effects of lower estimation of soil parameters on the developed shear stresses, and consequently on safety factors employed in design were discussed by Huntington (1957). He indicated that low shearing strength results in high lateral pressures and

vice versa. The relation between method of analysis and level of accuracy of soil parameters is discussed in a few contributions, such as Clayton (1993).

Wall friction considerably reduces the magnitude of the active thrust and its horizontal component, as reported by Lambe and Whitman (1969). They found that this reduction is of the order of 7% in the case of gravity walls. Also, the effect of wall friction on the shape of the plastic zone behind retaining walls is discussed by Terzaghi and Peck (1967). Coulomb (1773) included wall friction in his analysis but the results were not accurate due to the assumption of a planar rupture surface. On the other hand, in Rankine's theory (1857) wall friction was implicitly neglected, and this leads to an over-estimation of K_a. Bowles (1988) recommended typical design values for angle of wall friction.

(e) Soil-Tension Effects

When a cohesive soil is used as a backfill, the total lateral force at the back of the wall can be obtained by the integration of Eq. 2.5 along the full depth:

$$P_a = \int_0^H (\gamma z K_a - 2c\sqrt{K_a})\, dz \qquad (2.6)$$

The critical depth, H_c, to which a vertical excavation or embankment in cohesive soils may stand, without support, can be determined by equating Eq. 2.6 to zero and employing a safety factor, SF, hence:

$$H_c = \frac{4c}{SF.\gamma\sqrt{K_a}} \qquad (2.7)$$

In the present research, this formulation of the critical depth is used to determine the safety factor associated with each embankment type in subsequent finite element analyses.

(f) Seepage and Pore Water Pressures

The presence of water behind a retaining wall has marked effects on the forces applied to the wall. Many recorded retaining wall failures may be attributed to the action of water. The design water pressure should be based on the worst expected ground

water conditions. The Hong Kong Geotechnical Engineering Office (1993) reported many factors that influence the water flow pattern and hence the water pressures that act behind retaining walls. These factors are: the nature of the ground (permeability); the ground water conditions; the topography; the land use and the natural drainage of the site; and the layout of the drainage system.

For large retaining walls, the pore pressures under seepage conditions, which are likely to be less than the hydrostatic ones, should be determined by the flow net procedure as in Huntington (1957). In CIRIA (1984), for thin flexible walls, a simplified mathematical procedure was derived for pore pressures under seepage conditions, rather than using a flow-net. When all or a portion of the backfill material is saturated with water, the presence of water will significantly increase the magnitude of the lateral thrust against the wall (Lambe and Whitman, 1969). This, also, will decrease the resistance to sliding along the wall base, and reduce the effective stress throughout the plastic zone due to softening effects. Therefore, it is very important to provide adequate drainage behind a retaining wall and/or to take water pressure into account. For residential retaining walls with adequate drainage provisions, zero water pressures may be assumed for design (Bowles, 1988).

2.4.2 Backfill Soil Movements

Results of a survey of Consulting Engineers in Adelaide conducted by the author indicate that the classical earth pressure theories are used in design regardless of recent developments. However, the arguments accumulated for more than two centuries against their validity are so powerful that many studies have been carried out to develop accurate solutions (Terzaghi, 1920).

In the classical theories, sand is assumed to behave as a rigid-plastic material governed by the Mohr-Coulomb failure criterion, and the structure itself is assumed to be perfectly rigid. Additionally, both methods neglect the plastic deformations of the sand during the development of the lateral pressures. Moreover, they consider only the extreme case, where sliding occurs and minimum active pressures are mobilised.

Away from this extreme condition the theories provide no information about the stresses or deformations. When Coulomb first established his theory, it was assumed that the active wedge would slide as a solid material without any consideration of the soil as a granular material. This demonstrates that, the major error was first introduced by Coulomb, who ignored that sand consists of individual grains, and who

dealt with the sand as if it was a homogeneous material with certain mechanical properties. Coulomb's idea was proved very useful as a working hypothesis for the solution of one special problem (earth pressure on masonry walls), but it was an obstacle for further research to solve other problems (Huntington, 1957).

The way out for the researchers was to start again from the elementary fact that sand consists of individual grains (Terzaghi, 1920). Developments using laboratory or field models, such as Terzaghi (1934), or using numerical modelling, such as Clough and Duncan (1971), were able to account for backfill soil deformation parameters and associated movements.

2.4.3 Wall Stiffness and Geometry

Although the determination of wall stiffness effects on the LEPs has been investigated for flexible walls, few investigations have been carried out for rigid walls (CIRIA, 1984). The effect of wall stiffness and geometry is presented here, because it interacts with the effect of backfill size and geometry on the LEPs which forms the main focus of this research.

(a) Wall Stiffness

The deflections that a flexible wall can accommodate without overstress (failure) are much larger than those for a relatively rigid wall. The flexible wall causes a greater degree of redistribution of pressures behind the wall than the rigid wall, as shown in Figure 2.2. This redistribution of pressures behind the wall reduces the bending moments in the wall, and this enables the support of very deep cuts with relatively slender walls. This also means that, the more flexible the wall is, the lower the lateral pressure developed, the lower the bending moment developed, and the more economic the design is.

However, many geotechnical engineering designs purposely choose relatively stiff wall sections to resist the applied loads. These stiffer walls will likely result in large lateral pressures, as shown in Figure 2.2. These high lateral pressures are unlikely to be taken into account in the final design. Accordingly, when backfilling is completed the wall will most probably crack. Only design methods for flexible sheet pile walls allow for moment reduction, while no such reductions have been established for rigid walls (CIRIA, 1984). Therefore, a suitable method of analysis is required that accounts for the stress-strain behaviour of the soil in the vicinity of rigid retaining walls.

In addition, a number of field measurements, and full-scale modelling, have been carried out to investigate the influence of wall stiffness, and consequent movements, on the stress field behind the wall. In full scale field measurements that were carried out by Tschebotarioff (1951) on a 24.08 m high, rigid, reinforced concrete retaining wall, the average coefficient of earth pressure was K=0.42. This value was found to be very close to the calculated at-rest value of $K_0 = 0.4$. Also, full-scale field measurements were reported by Symons and Wilson (1972) on a reinforced concrete rigid retaining wall, with restrained side ends. In this case, the yield (outward movement) of the wall was insufficient to mobilise active earth pressures. Additionally, settlement of buildings located above the plastic zone behind retaining walls is critical and depends chiefly on wall yielding (CIRIA , 1984).

It will be shown in Chapter 3 that the FEM considers the effect of wall stiffness in modelling retaining walls. The effect of wall stiffness on the lateral earth pressures is examined in Chapters 4 and 5, where it is shown that greater lateral pressures are associated with stiffer walls.

(b) Wall Geometry

Wall geometry affects the formation of the inner plane of rupture and subsequently affects the distribution of the LEPs (Terzaghi and Peck, 1967). In general, it is a common practice to apply the classical theories for a gravity wall with a vertical back. This is because the wall allows the formation of the inner plane of rupture. Coulomb's theory will be the most appropriate method for these walls. For cantilever T-walls with base projection into the soil, the inner plane of rupture does not form and the LEPs at the back of the wall are unknown. However, by assuming that the vertical plane through the heel is a principal plane, Rankine's theory can be adopted to predict the limit active pressures at the virtual back of the wall (Huntington, 1957).

Lambe and Whitman (1969) concluded that gravity walls are designed for active earth pressures, since a small rotation around the toe is often sufficient to drop the pressures to the Rankine active values. For T-walls, placement of the backfill over the base significantly affects the behaviour of the wall. The large backfill weight acting on the base limits any rotation about the toe, and bending rotation is the only rotation that causes active conditions. The bending rotations (deflection) required to achieve active conditions are often large and may cause cracking of the wall. Therefore, cantilever T-walls are often designed for at-rest lateral pressures. In Chapters 4 and 5 different

types of retaining walls are examined to investigate the effect of wall geometry on the LEPs.

2.4.4 Wall Movements

There are a number of factors that control lateral wall movements. One of these factors is wall stiffness, as discussed earlier. High stiffness of the foundation subsoil greatly reduces wall rotation and translation which may increase the lateral earth pressures. The effect of stiffness of the foundation soil will be examined in Chapters 4 and 5. Wall movements are of two opposite directions, outward and inward, as shown in Figure 2.3. Outward yielding (extension) causes an active state of stress, while inward yielding results in a passive state in the backfill soil adjacent to the wall.

The simple linear assumption about active pressures is an over-simplification of very complex variations. In the 20th century, the varieties of retaining structures and the substantial difference in stiffness have led engineers to study whether active pressures are strain dependent. These studies have been based on different methodologies, such as, theoretical analyses, laboratory and field tests, or numerical investigations. In the following, a number of these contributions are discussed.

(a) Laboratory and Field Testing

The influence of wall movements on earth pressure was studied by Terzaghi (1934) in his large retaining wall model tests, using sand as a backfill. He concluded that a slight outward displacement of the wall of the order of 0.001H (where H is the wall height) was sufficient to reduce the lateral pressures to their active values. Tschebotarioff (1951), based on laboratory shear tests, reported that an outward movement close to 0.05H would be needed to fully mobilise the shearing resistance of clay, and to reduce lateral pressures to their active values. Also, after many extensive unloading triaxial tests on sand and undrained tests for clay, he concluded that strains less than 0.005H for sand and 0.04H for clay were sufficient to develop the active state.

Many different investigations, using laboratory and field tests on model retaining walls or controlled field experiments, have measured the movements required to reduce earth pressures to the active values. Table 2.1 summarises the results of some of these studies. These data will be compared against the results of the FEM in Chapters 4 and 5. Also, these data illustrate some significant points regarding active earth pressures:

- The movement (Δ / H) required to reach the minimum active pressure condition is about the same for rotation and translation, provided Δ is the movement of the wall at the top.

- Two definitions of the active conditions have been used. The first corresponds to the resultant active earth pressure force reaching its minimum value. The second corresponds to development of a triangular pressure distribution. In many experiments the first condition is achieved while the earth pressure has a nonlinear variation, with the resultant at an elevation higher than 0.33H. Continuing movement results in a triangular distribution of pressures and the resultant at 0.33H.

- The larger the wall, the greater the value of (Δ / H) required to reduce the active earth pressure resultant to its minimum value. This finding is consistent with the fact that the stiffness of sand does not increase in direct proportion to confining pressure, and therefore does not increase in proportion to wall height. For large walls the movements required to reach the active condition is of the order of $\Delta / H = 0.004$.

- The magnitude of the lateral extension of the soil required to develop the active state of stress depends upon the type of soil, the manner in which it is deposited, and the pattern of deformation. It is larger for soft clays and loose sands than for stiff clays and dense sands.

(b) Analytical Models

The Harr (1977) model appears to be the only analytical model that accounts for the effect of rigid wall movements on the LEPs. The model considers the various modes of rotation about the top and bottom, and translation of rigid retaining walls with unlimited backfills. This method uses the same concepts of the classical earth pressure theories. The main assumption involved in this model is that the angle φ (between the total reaction acting on the rupture plane and the normal) varies linearly with depth. This variation depends on the mode of displacement of the wall, that is, at full active state $\varphi = +\phi$ and at full passive state $\varphi = -\phi$, while for the case of zero rotation $\varphi = 0$.

Five cases were examined, as shown in Figure 2.3, where the distribution of φ with the depth, z, is given: (a) active state with rotation about the top; (b) passive state with

rotation about the bottom; (c) passive state with rotation about the top; (d) active state with rotation about the bottom; and (e) active and passive states with rotation about the mid point. The lateral thrust, P, and the lateral pressure, p, at a depth z are given by :

$$P = \frac{\gamma}{2\cos\delta}\left[\frac{z}{(1/\cos\varphi)+(\tan^2\varphi+\tan\varphi\tan\delta)^{0.5}}\right]^2 \qquad (2.8)$$

$$p = \frac{dP}{dz} = \frac{z\gamma\cos\varphi}{(1+m\sin\varphi)^2\cos\delta}\left[\cos\varphi - \frac{z\left(\sin\varphi+\frac{1+m^2}{2m}\right)}{(1+m\sin\varphi)}\left(\frac{d\varphi}{dz}\right)\right] \qquad (2.9)$$

where

m	=	$[1+\tan\delta/\tan\varphi]^{1/2}$
δ	=	angle of wall friction
φ	=	angle between total reaction acting on the rupture plane and the normal
z	=	depth below ground surface

This model has the advantage of allowing for the effect of wall movements on the lateral pressures. To use this model to calculate the lateral pressure distribution the mode of wall movement has to be assumed, considering the wall geometry and loading conditions. In addition, in Figure 2.3 (e), for rotation about the mid point, the lower rotation was assumed sufficient to achieve the active state, and the upper rotation was sufficient to produce the passive state. However, the passive state requires a rotation much larger than that for the active state. The movements at the upper and lower points are necessarily equal when the rotation of a rigid wall is about the mid point. Hence, the linear assumption of the variation of the angle φ with depth is not justified in this particular case. The results of this model are compared with those of the FEM in Chapter 4 in the case of a T-wall rotated about its bottom point.

2.4.5 Shearing Stresses

According to typical stress-strain curves for soils that are shown in Figure 2.4, it is clear that the shearing stresses do not increase linearly with movement, and also the shearing strength will not be mobilised unless a minimum movement occurs. In situ, a wall starts to move and plastic movements occur along the shear planes in the plastic

zone behind the wall, while the shearing stresses increase due to these movements until they reach the ultimate shearing resistance. At this stage, lateral earth pressures decrease to their minimum active values, and the Mohr's circle of stress touches the failure envelope. This means that the active state and maximum shearing resistance are almost simultaneously reached, and this should be borne to mind when studying the stress-strain field behind retaining walls.

Wall movements affect shearing stresses, and these, in turn, affect the lateral pressures. To determine these effects, the equilibrium of the forces acting throughout the plastic zone and the force polygon in Figure 2.1 are considered. When the wall starts to yield the mobilised shearing stresses increase due to slip along the plane of rupture. Based on equilibrium, any increase in the total shearing resistance, *S*, leads to a reduction in the lateral thrust, P, acting on the wall. Hence, at the early stage prior to yielding the lateral thrust acting is, $P_0 = 0.5K_0\gamma H^2$. When the wall starts to move and the movement is sufficient to mobilise full shearing resistance the total lateral pressure reduces until it reaches the minimum active value, $P_a = 0.5K_a\gamma H^2$.

Another way to recognise the effect of shearing stresses on the lateral pressures and also to show the relation between shearing stresses, lateral stresses and vertical stresses, is to consider full-scale measurements on a silo reported by Tschebotarioff (1951). The measured vertical stresses transmitted to the bottom of the silo were not geostatic ones, but were lower due to the shear stresses along the sides of the silo. These shearing stresses depend on the corresponding horizontal normal stresses, which, in turn, are a function of the vertical pressures. Hence, the change in lateral pressures is due to variations in vertical pressures and not due to changes in the coefficient of lateral earth pressure, K. This silo-analogy, between the vertical pressures, the developed shear stresses and the lateral pressures, is important when analysing the equilibrium of forces in the plastic zone, particularly, in the case of limited backfills.

2.5 EFFECT OF EXTENT OF THE BACKFILL

Commonly used classical earth pressure theories assume unlimited backfill conditions. This is to allow for the formation of the inner plane of rupture that forms the principal boundary of the active wedge. The equilibrium of the forces acting throughout this wedge determine the lateral thrust on the wall. However, site and cost considerations often lead to cases where a limited backfill zone is used. A limited backfill often

results from excavation of the natural clay deposit and backfilling with well draining soil to prevent the development of any hydrostatic pressure behind the wall as required by most retaining wall design manuals, such as CP No. 2 (1951). This free draining soil is a component of a drainage system often used in the construction of retaining walls. Figure 2.5 shows the construction of a retaining with a limited granular backfill, which was designed and constructed in Adelaide, South Australia.

A typical drainage system for a retaining wall is often made up of four elements. The first element is adequate surface drainage to dispose of surface water. The second element is a relatively impervious layer of soil on the top of the backfill to reduce the amount of water which may permeate into the backfill. The third element consists of a freely draining backfill, or pockets, channels or blankets of highly permeable material to collect any water which may seep into the backfill. The final element includes the conveying units, such as weep holes through the wall which collect water from the collecting drains. Huntington (1957) reported some field situations and a number of drainage systems which may be suitable for such cases.

In the case of limited backfill, there is a variation of soil properties which causes an uncertainty in the determination of the LEPs. To explain this uncertainty, the following example may be considered.

Worked Example [1]

Calculate the total lateral force on a 3 m high reinforced concrete cantilever T-wall. The wall has a limited sand backfill and supports a natural clay deposit, with the following properties:

Sand: $\gamma = 16\ kN/m^3$, $\phi_1 = 30^0$, $c_1 = 0$
Clay: $\gamma = 15\ kN/m^3$, $\phi_2 = 0^0$, $c_2 = 20\ kPa$

Solution:

For this type of wall Rankine's conditions prevail as discussed before, hence

(a) Using sand parameters:

For $\phi_1 = 30^0$, $K_a = 0.333$ (Bowles, 1988)

$P_1 = 0.5\gamma K_a H^2$

$P_1 = \underline{\underline{24\ kN/m}}$

(b) Using clay parameters:

For $\phi_2 = 0^0$, $K_a = 1.0$

the lateral pressures at ground surface, $e_0 = \gamma h_0 K_a - 2c\sqrt{K_a} = -40$ kPa

the lateral pressures at the bottom, $e_1 = \gamma H K_a - 2c\sqrt{K_a} = 5.0$ kPa

by integration along the full height, the lateral thrust becomes,

$P_2 = \underline{0.83 \text{ kN/m}}$

Accordingly, the limitation in the backfill causes $\pm 96.5\%$ difference in the magnitude of the lateral thrust. In practice, engineering judgement is used to select the lateral thrust used in the design. Most probably, the largest value will be selected regardless of the large difference between the two values. However, a review of the literature shows that there are a few procedures that treat the case of limited backfill. These procedures are covered in the following subsections.

2.5.1 Huntington's Method

Huntington (1957) studied the effects of: (i) the inclination of the excavation surface; and (ii) the natural deposit and backfill material type, on the LEPs and the formation of the plastic zone. The results of his investigations showed that:

1. In natural cohesionless deposits, which result from excavation and backfilling with the same material compacted to the same density, the same shearing resistance is obtained. This case should be treated as an unlimited backfill, where the classical earth pressure theories can be applied.

2. In the case of c-ϕ soils, where cohesion is lost after excavation and backfilling, but ϕ remains unchanged, the soil will behave as a frictional material along the excavation surface. This assumption leads to the interface shearing resistance always being less than that of the natural deposit, due to loss of cohesion. In this case, two conditions were examined for different steepness of the excavation surface:

   - For gentle cohesive cuts, where the inclination of the excavation surface, α, is less than the inclination of the Coulomb's angle of rupture, $\rho = 45 + \phi/2$, as shown in Figure 2.6 (a). The classical earth pressure theories are valid as the inner plane of rupture can form.

- In steep cohesive cuts, where the inclination of the excavation surface, α, is greater than the Coulomb's angle of rupture, $\rho = 45 + \phi/2$, ie, the rupture surface is located beyond the excavation surface, as shown in Figure 2.6(b). Since the shearing resistance along the excavation surface is less than that along the presumed rupture surface through the natural deposit, sliding will occur along the face of excavation, as the wall moves under the action of the lateral pressures.

  Thus, the excavation surface may be considered as the true rupture surface. By constructing the force polygon for the forces R (total reaction), W (weight of the active wedge) and P (lateral thrust), this latter force can be determined. Huntington also found that the lateral pressures in this case are not linear, but smaller in magnitude than those determined using the classical theories. This reduction can be related to the fact that the earth pressures result from the component of the weight of the active zone, which is relatively small in this case.

The foregoing procedure, that proposed by Huntington, may be criticised on the grounds that: (i) rapid excavation and backfilling has not been considered, where some cohesion remains; and (ii) in the first and the second cases, he neglected the possibility of reduction in friction angle, due to soil disturbance. Accordingly, it would be difficult to determine the true plane of rupture for steep cuts.

2.5.2 New Zealand Ministry of Works Procedure

The New Zealand Ministry of Works and Development Report (1973) concluded that, where an excavation is made to accommodate the wall, the natural deposit usually has a different strength from that of the backfill. When calculating the inclination of the inner plane of rupture to the horizontal, two positions can be determined: the first is based on the backfill parameters; and the second is based on the natural deposit parameters. Three cases were reported as follows:

- if both positions fall within the backfill zone, the critical failure plane is the first one, and if both fall beyond the excavation surface, the critical failure plane is the second one.

- when the critical failure planes occur in both materials, the one giving the maximum pressures should be used. In this case two ruptures will occur, one due to instability in the backfill and the other due to rupture of the natural deposit.

- where the first failure plane, calculated using the backfill parameters, falls beyond the failure plane due to the natural deposit, sliding will occur along the excavation surface, which, in turn, is considered the true plane of rupture.

This procedure was developed without clear theoretical basis. This procedure failed to address the following: (a) the type of soil is not considered; (b) in the third case, the shearing strength along the excavation surface has not been compared with that for the rupture plane located in the natural deposit in order to decide which plane the sliding would occur along; (c) when both rupture planes are located beyond the excavation surface, the procedure provides no solution.

2.5.3 Bell and Reimbert Methods

Using a completely different approach, Reimbert (1989) studied the case of a limited backfill, with a retaining wall built in front of a heavily compacted backfill with a steep slope. In this case the backfill has a special equilibrium state, which can be modelled as a backing material contained between two adjacent walls. An analogy exists between this case and lateral pressures on the side walls of a slender vertical silo.

Also, Bell (1987) suggested using this silo analogy to calculate lateral earth pressures in the case of a limited backfill. If the area behind the wall is very narrow as shown in Figure 2.7, the classical wedge can not develop and consequently there is a reduction of the lateral earth pressures when compared with the active value. This case is best analysed using the modified equations of lateral pressures acting on a silo with vertical walls. These modified silo equations used in this case are given by:

$$p_{vz} = \frac{\gamma b}{2 \tan \delta_s K}\left(1 - e^{-\frac{2zK \tan \delta_s}{b}}\right) \tag{2.10}$$

$$p_{hz} = K p_{vz} = \frac{\gamma b}{2 \tan \delta_s}\left(1 - e^{-\frac{2zK \tan \delta_s}{b}}\right) \tag{2.11}$$

where

p_{vz} = vertical pressure

p_{hz} = horizontal pressure

z	=	depth below ground surface
b	=	backfill width
K	=	coefficient of earth pressure (recommended at-rest values)
δ_s	=	angle of wall friction within the silo

This method is valid only for vertical cuts and does not allow for variation in the angle of inclination of the excavation surface. Also, shearing stresses along both side walls in the silo formulation are essentially equal, which is not the case for a limited backfill. This leads to a significant error in the magnitude of the lateral pressures determined using Eq. 2.12. However, this silo analogy may be suitable for the analysis of retaining walls founded on rocks, because field conditions might be closely approximated by the silo analogy.

2.5.4 Bang and Tucker Analysis

Bang and Tucker (1990) introduced an analytical model based on a limiting equilibrium principle to estimate the developed active lateral thrust exerted by a combination of an interposed cohesionless soil wedge and a natural deposit. The geometry of the backfill soil wedge was defined by horizontal extents at the top (a) and bottom of the retaining wall (b), as shown in Figure 2.8. The rupture surface was assumed to be composed of two planes inclined to the horizontal at angles α_1 and α_2. The orientation of the excavation surface was represented by its angle (n) to the vertical. The total lateral thrust (P) can be determined from the static equilibrium of elements 1 and 2 as follows:

$$P = F_5 \cos n - F_6 \sin n + F_2 \sin \alpha_1 - F_1 \cos \alpha_1 \qquad (2.12)$$

All symbols are defined in Figure 2.8.

To determine the potential failure surface, ie the angles α_1 and α_2, that produces the maximum thrust on the retaining structure, P_{max}, an iterative method is used. It was assumed in the case of $a > b$ that the angle α_2 has a maximum value of 90-n. This means that, the excavation surface is considered as a failure plane for soils that possess comparatively high values of friction angle.

Solutions for maximum thrust have been developed for soil strength parameters that are typically used in practice. These solutions are presented for the normalised lateral thrust versus b/H and for different a/H values. For cohesive natural deposits, it was

found that the lateral thrust decreases as the backfill size increases. As the cohesion of the natural deposit increases, there exists a certain interposed backfill wedge geometry which produces a minimum value of the active thrust. Zero cohesion along the excavation surface was also assumed in this procedure as in the Huntington (1957) method.

Bang and Tucker analyses assume that the lateral thrust is due to instability in the backfill and the natural deposit. This means that, there are two different failure wedges. The first wedge forms in the granular backfill and is bounded by the Coulomb classical plane of rupture that is inclined to the horizontal at an angle $\alpha_1 = 45 + \phi_1 / 2$. The second wedge is due to the failure of the embankment soil that is bounded by the failure plane inclined at an angle $\alpha_2 = 45 + \phi_2 / 2$. Note that they only treat the case when $\phi_1 > \phi_2$ and hence increasing the backfill size will intuitively decrease the lateral thrust.

Stefanoff and Venkov (1972) used a similar analytical procedure for a vertical cut where the angle of friction of the backfill is greater than that of the natural deposit. They concluded that the lateral thrust decreases as the size of the backfill zone increases.

2.5.5 Bowles's Method

For retaining walls founded on cohesive soils and having limited granular backfills, Bowles (1988) concluded that the inner plane of rupture does not form and the backfill soil does not reach the active state. Therefore, the Rankine or Coulomb coefficients for lateral earth pressures can not be used and there is uncertainty in the lateral earth pressure calculations. It was recommended for design purposes to use the at-rest coefficient for lateral pressures (K_0), instead of the active value, as well as a surface surcharge of 15-30 kPa. However, in this procedure it is unclear: (i) which soil parameters K_0 will be determined from, ie the granular backfill or the natural deposit; or (ii) on what basis these recommendations were developed.

2.5.6 Teng's Method

One quick method treating the limited backfill condition, which relied upon engineering judgement without any clear theoretical justification, is that proposed by Teng (1962). In this method, if the sand blanket extends a distance $\leq 0.1H$ in a horizontal direction behind the wall, then the lateral thrust is only due to the natural

deposit, and if it extends more than 0.9H then the lateral thrust is entirely due to the granular backfill. For intermediate values, linear interpolation is recommended.

2.6 SUMMARY

The classical earth pressure theories are not suitable for determining the LEPs for retaining walls with limited backfills as they assume unlimited backfill conditions. There are other limitations of these theories, such as neglecting soil-structure interaction, construction sequence and in situ initial conditions. Accordingly, numerical methods, such as the FEM should be used to investigate the limited backfill condition as these can readily take into account these factors.

Two different approaches treating the limited backfill condition have been reviewed. The results of Bang and Tucker (1990) and Stefanoff and Venkov (1972) demonstrate that the lateral thrust decreases as the cohesionless backfill zone increases. They assume that the lateral thrust is due to the instability in both materials, ie the granular backfill soil and the natural clay deposit. However, these methods assume that the strength of the backfill soil is larger than that of the natural clay deposit. Accordingly, an increase in the size of the granular backfill results in a reduction in the lateral thrust as the relative strength of the active wedge increases. On the other hand, the results of Huntington (1957) and Bell (1987) demonstrate that the lateral thrust increases as the size of the backfill increases. They consider the lateral thrust to be only due to the instability in the granular backfill zone, assuming a stable natural deposit. These two approaches are investigated using the finite element method in Chapters 4 and 5.

Table 2.1 Movements required to achieve active earth pressure conditions

Investigator	**Wall height (m)**	**Backfill soil type**	**Mode of Movement**	**Δ / H to reach active pressure**
Broms and Ingelson (1971)	2.743	sand	rotate	0.0003
Broms and Ingelson (1972)	8.656	sandy gravel	rotate	0.0009 - 0.0024
Carder et al. (1977)	2.017	sand	translate	0.002
Matsumoto et al. (1978)	10	silty clay	rotate	0.006 - 0.008
Matsumoto et al. (1978)	10	silty sand	rotate	0.003-0.005
Sherif et al.(1984)	1.219	sand (compact.)	rotate	0.0005
Sherif et al.(1984)	1.219	sand (No compact.)	rotate	0.0005
Terzaghi (1934)	1.494	sand	rotate	0.0011
Terzaghi (1934)	1.494	sand (No compact.)	translate	0.0011
Terzaghi (1925-1940)	1.494	sand	rotate	0.002
Terzaghi (1925-1940)	1.494	sand	rotate	0.005 to develop triangular pressure distribution.
Terzaghi (1925-1940)	1.494	sand	translate	0.001
Terzaghi (1925-1940)	1.494	sand	translate	0.005 to develop triangular pressure distribution.

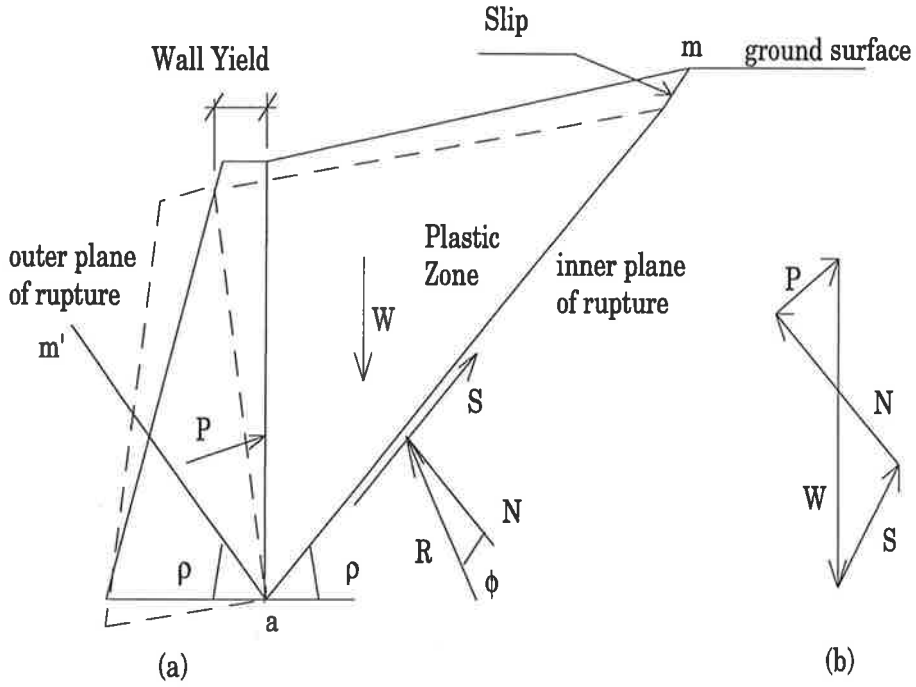

Figure 2.1 Forces act on retaining walls: (a) forces act throughout the plastic zone; and (b) force polygon.

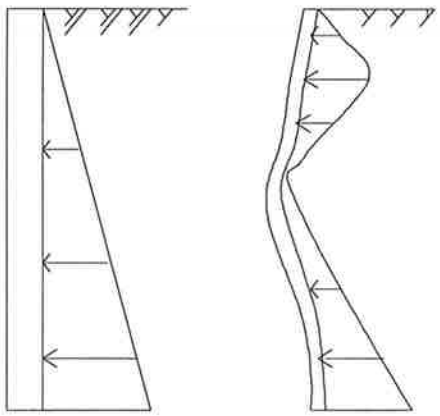

Rigid wall Flexible wall

Figure 2.2 Influence of wall flexibility on lateral earth pressure distribution *(CIRIA, 1984).*

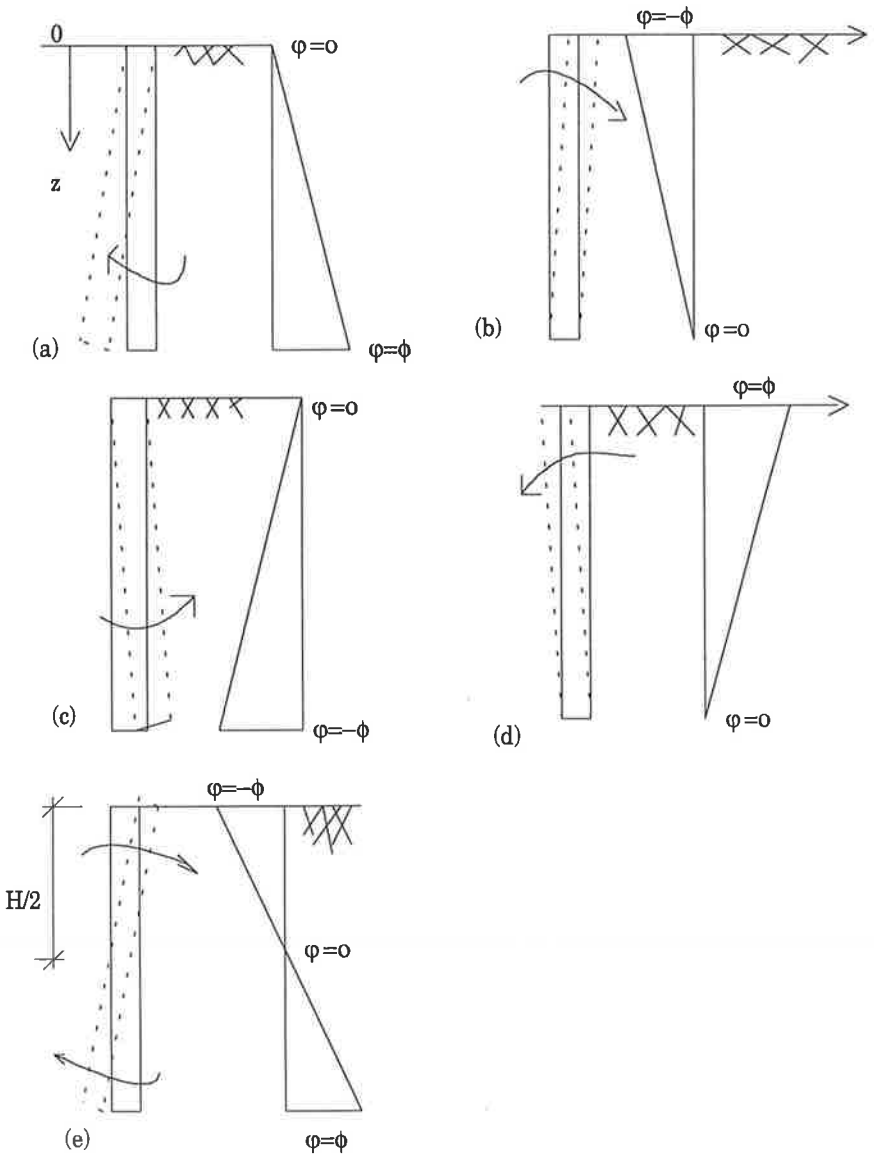

Figure 2.3 Lateral movements of rigid retaining walls and distribution of the parameter φ along the depth, z: (a) active state with rotation about the top; (b) passive state with rotation about the bottom; (c) passive state with rotation about the top; (d) active state with rotation about the bottom; and (e) active and passive states with rotation about the mid point (*Harr, 1977*).

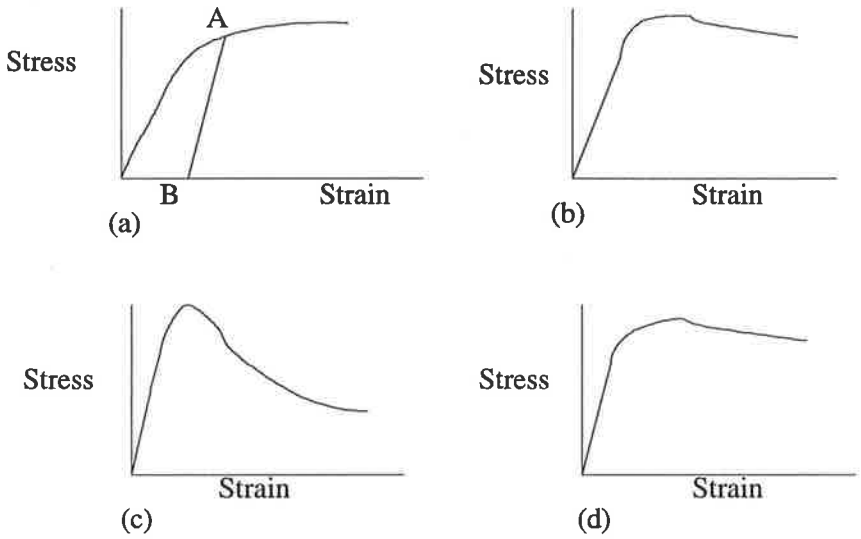

Figure 2.4 Typical stress-strain behaviour of soils: (a) remoulded clay or loose sand; (b) undisturbed insensitive clay or dense sand; (c) sensitive clay; and (d) undrained insensitive clay *(Chen, 1975)*.

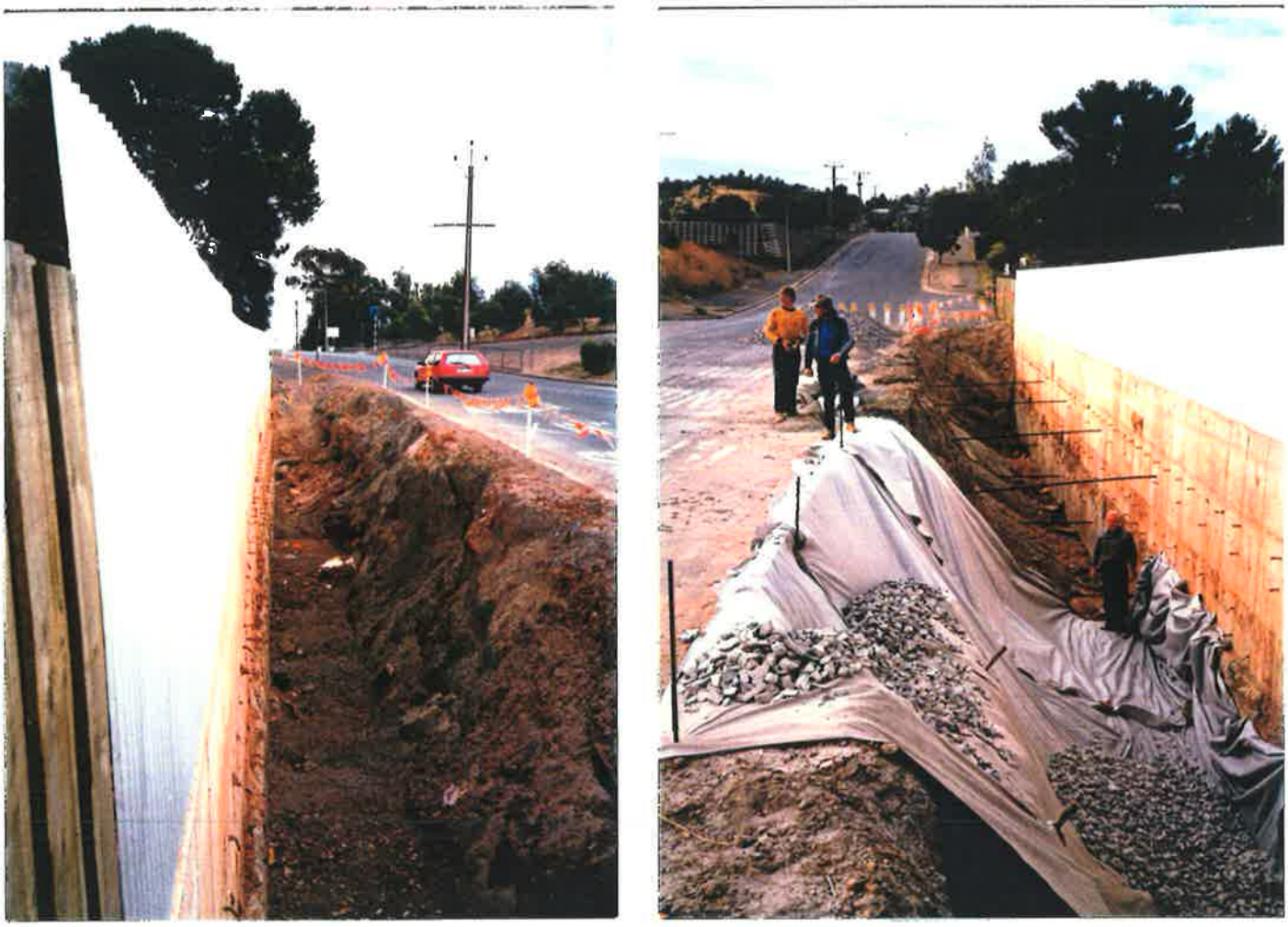

(a) before placement of the backfill

(b) during placement of the backfill

Figure 2.5 Typical construction process of a retaining wall having a limited granular backfill due to provision of a drainage system (*courtesy of M. B. Jaksa*)

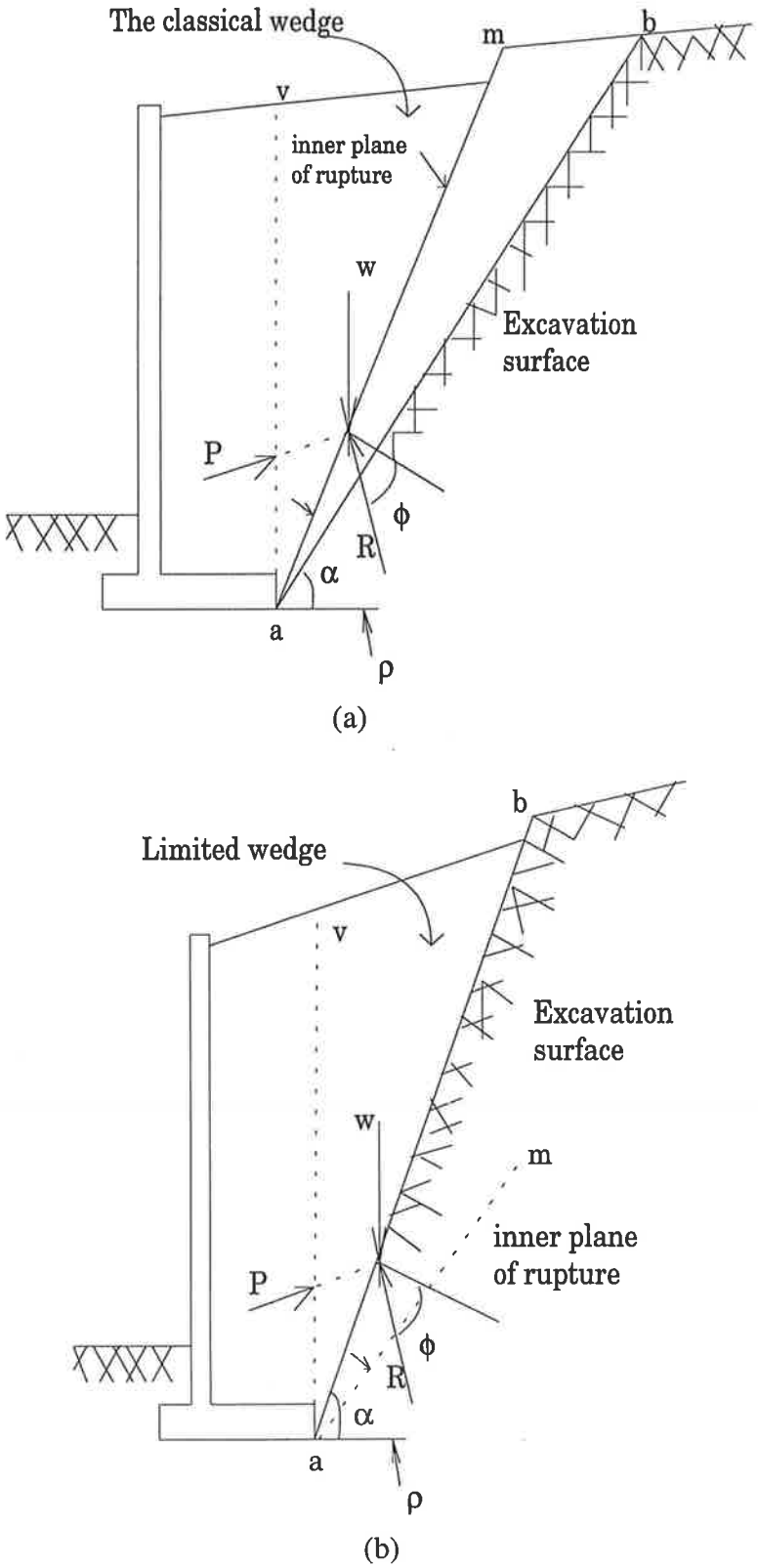

Figure 2.6 Lateral thrust due to limited backfills; (a) gentle cuts; and (b) steep cuts (*Huntington, 1957*).

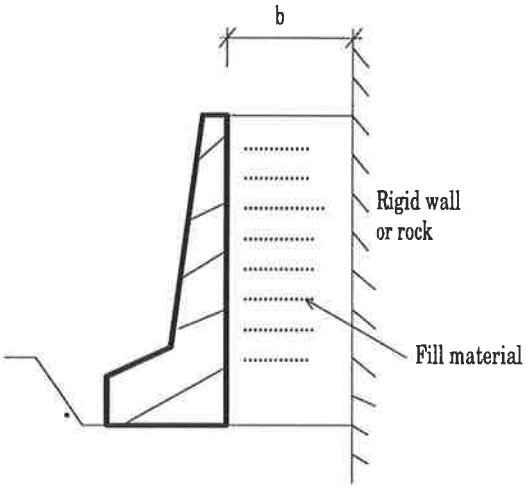

Figure 2.7 Rigid retaining wall with a narrow backfill zone *(Bell, 1987)*

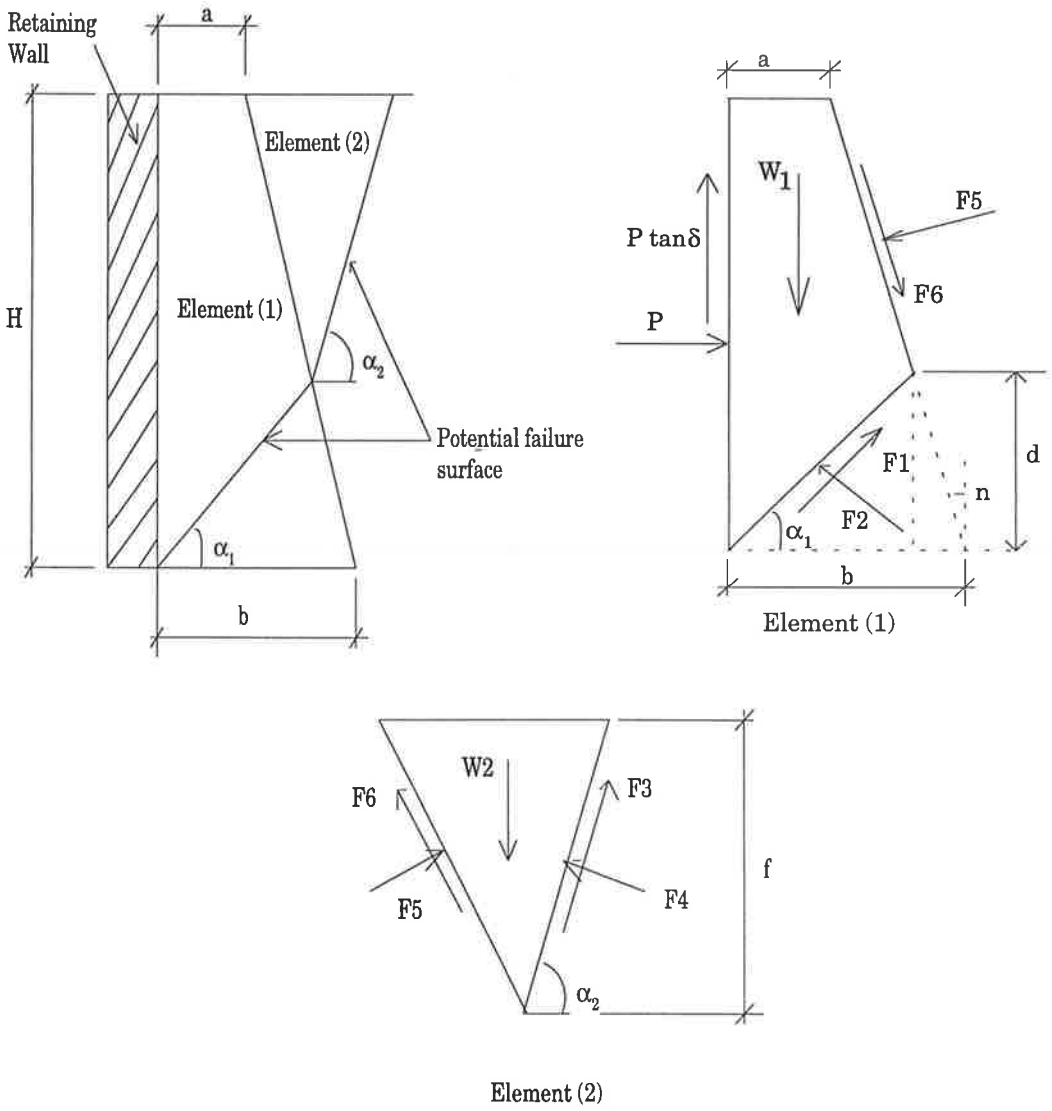

Figure 2.8 Schematic diagram of an interposed backfill wedge system and the free body diagrams *(Bang and Tucker 1990).*

Chapter 3

Finite Element Methodology

3.1 INTRODUCTION

It was observed in Chapter 2 that the classical earth pressure theories fail to determine the lateral pressures in the case of retaining walls having limited backfills, and it was concluded that the best way to determine these pressures is by using numerical modelling. In this chapter, the technique of the finite element method (FEM) is reviewed, focusing on its application to rigid retaining walls since the late 1960s. The basic features of the finite element analysis of rigid retaining walls are covered including: the common constitutive models of soil behaviour; soil-wall interface modelling; construction sequence; and efficiency.

The numerical investigation program is also described, including wall geometries and soil parameters used in the analyses. The finite element program AFENA, used to carry out the analysis, is also briefly described. A full description of the interpretation of the finite element results is also given.

3.2 OVERVIEW OF FINITE ELEMENT METHOD

This part of the work is concerned with the application of the finite element method to the static analysis of stresses and movements in geotechnical engineering problems, especially the lateral pressures on rigid retaining walls. The theory of the finite element method is not covered, nor the details of theoretical or computer aspects of the method, as it is well described elsewhere in the literature. Instead, a description of the potential uses of the method, and a review of different procedures used in the literature, are presented.

Although the FEM was applied to problems in aerospace and structural engineering from the early 1950s, this was not followed up in the field of geomechanics extensively until the late 1960s. This is due to the fact that soils and rocks, unlike other materials, are more complex in their behaviour because they are non-homogeneous, anisotropic, and exhibit non-linear behaviour. Apart from these problems, the extent of the boundary to be considered for numerical modelling posed a real problem. Modelling the interface between the soil and the structure represents a critical problem which controls the accuracy achieved in the numerical analysis. Another problem facing researchers was the modelling of a continuum.

The finite element method was introduced to the geotechnical engineering profession in the late 1960s when Clough and Woodward (1967) demonstrated its usefulness for the analysis of stresses and movements in earth dams. The most significant aspect of these applications was the use of non-linear stress-strain characteristics in their analyses. Geotechnical engineers had long been aware of the limited usefulness of the linear-elastic analyses of soil and rock masses, and it was immediately apparent that the ability to analyse non-linear behaviour gave the FEM great potential for use in geotechnical engineering problems. The method has many great capabilities as well. These include the fact that it can be used for problems involving non-homogeneous materials, complex boundary conditions, sequential loading, and so on. In short, the method can be used to overcome most of the difficulties which had made analysis of realistic conditions previously impossible.

In the late 1960s the FEM was applied to many problems in geotechnical engineering. The method was employed for: the analysis of stresses and deformations in slopes and embankments (Clough and Woodward, 1967); the calculation of movements around excavations (Duncan and Dunlop, 1968; Chang and Duncan, 1970); the analysis of stresses and settlements due to footing loads (Girijavallabhan and Reese, 1968); and the

analysis of earth pressures and wall movements. The main studies concerned with this latter application are presented in the next section.

The fundamental concepts of the FEM are already well established and are adequately covered in texts such as Rockey et al. (1983) and Zienkiewicz and Taylor (1989). Basically, the FEM, as applied to a continuum, may be divided into two basic steps: (1) discretization of the continuum into an assemblage of a finite number of elements connected at their nodes, with the accuracy of the solution relying upon their number; (2) stress-strain analysis of the element assemblage. This latter step essentially involves satisfying the compatibility between displacements and strains, material behaviour, and the equilibrium of this assembly, which involves partial differential equations. This requires replacement of these partial differential equations by matrix equations which take the form of linear algebraic equations suitable for computer programming, as follows:

$$[K] \,.\, \{\delta\} = \{P\} \tag{3.1}$$

The vector $\{\delta\}$ contains the unknown nodal displacements. The square matrix [K] is the overall stiffness matrix of the assemblage of elements relating $\{\delta\}$ to the prescribed nodal forces vector $\{P\}$.

3.3 DEVELOPMENTS OF RETAINING WALL ANALYSIS

The subject of rigid retaining walls is covered in almost every elementary text book and manual on geotechnical engineering. It is always assumed that the behaviour of these walls is simple and can be taken for granted. However, there are important soil-structure interaction effects on rigid walls and a more complete understanding of these effects provide an improved basis for design. The finite element method has provided new insights into the behaviour of these walls and a better understanding of the complex soil-structure interactions. Over the past 30 years the FEM has been used successfully by researchers to investigate the problem of lateral earth pressures on retaining walls. In the following paragraphs, the major finite element studies are described and a summary of some of these studies is given in Table 3.1.

Girijavallabhan and Reese (1968) appear to be the first investigators to establish a realistic relationship between a passive rotation of the wall and the lateral thrust for loose and dense granular backfills. A perfectly smooth wall was assumed. Their predicted values were based on the non-linear stress-strain relationships derived from conventional triaxial

tests. The secant modulus at the specific stress was evaluated based on octahedral shear stress and octahedral shear strain. Poisson's ratio was assumed constant in the analysis. There was remarkable agreement between the predicted and observed experimental values of the lateral thrust as shown Figure 3.1.

Morgenstern and Eisenstein (1970) used a linear-elastic soil model combined with a smooth wall-soil interface to demonstrate the effects of foundation conditions on retaining wall behaviour by varying the depth of the foundation layer from zero to a thickness equal to the height of the wall, and assuming the base of the foundation to be either perfectly rough or smooth. The first set of tests was carried out for a rigid unmoving wall and excavation of the soil in front of the wall. This resulted in an increase in the earth pressure near the bottom and a decrease near the top. In the second set of tests, the wall was translated into and away from the backfill by an amount equal to 0.25% of the wall height. They concluded that the base boundary conditions have a significant effect on the horizontal earth pressures, with the earth pressure distribution becoming non-linear for a rough base. This is possibly the result of the influence of restraining conditions at the base on the behaviour of the wall and its subsequent movements. This study also demonstrated the importance of the initial stress state.

Simpson and Wroth (1972) used the elastic-plastic model to analyse a rigid retaining wall rotating about the top or the base into the soil. A perfectly rough wall was assumed. A subdivision of the finite element mesh was made in the plastic regions. A comparison was made between the predicted values and the experimental data of James and Bransby (1970). It was found that the finite element results tended to exceed the experimental values due to the stress concentration near the base of the wall and the assumption of a perfectly rough wall. However, the computed and measured shear strains were similar. A more satisfactory prediction of the lateral thrust was obtained for the wall rotating about the bottom edge.

In all the previous studies the wall-soil interface was modelled as either perfectly rough (zero relative slip) or perfectly smooth (zero shear). Clough and Duncan (1971) were the first to employ the Goodman et al. (1968) one dimensional interface element to model more realistically the relative movement at the soil-wall interface. Interface tests were carried out on soil-concrete specimens using standard direct shear apparatus and the experimental behaviour was modelled by a non-linear hyperbolic stress dependent relationship similar to that developed by Duncan and Chang (1970) for soils. Clough and Duncan carried out two sets of analyses using the Duncan and Chang formulation to model a medium dense granular backfill.

The first series of analyses were for a rigid 3 m high wall on an incompressible rigid foundation. The wall was displaced incrementally forward and away from the backfill until the passive or active pressures were reached. Figure 3.2 shows that the maximum displacement to wall height ratio required to achieve the active state is 0.23% and 1.95% to achieve the passive state. In the second series, the construction sequence procedure was modelled as illustrated in Figure 3.3. Beginning from at-rest conditions in the granular foundation, the wall and soil placement were simulated in incremental steps, as in a realistic field situation. The finite element results showed that the horizontal earth pressure distribution at the back of the wall was approximately triangular with some concentration of pressure near the base. The earth pressure acting at the back of the wall was greater than the active pressure but lower than the at-rest pressure. It was found that the magnitude of the total force on the wall was in good agreement with the value determined from the classical theories when the passive force was neglected. Figure 3.4 shows the inward tilt of the rigid retaining wall due to placement of the heavy backfill.

Kulhawy (1974) performed a preliminary design of a massive 31.8 m high gravity wall and showed the importance of taking the wall movements into account particularly for high gravity walls. Using the incremental construction sequence procedure, the finite element analysis indicated that the earth pressures on the back of the wall were just slightly reduced from the at-rest condition, as the wall movements were insufficient to develop the full active state. Comparisons with the classical theories showed that these methods overestimated the safety factors.

The construction sequence was examined by Christiano and Chuntranuluck (1974). The wall was idealised by beam elements that were stiff relative to the backfill. A dry granular backfill was represented by a non-linear shear modulus which was related to the octahedral normal stress and the octahedral shear stress. The wall-soil interface was smooth and the soil-base interface was rough. The wall was rotated about the base. The behaviour of the wall using 10 increments was compared with that of the backfill soil placed in a single construction stage. They found significant differences in the horizontal and vertical stresses in the region close to the wall but these differences were negligible elsewhere. The lateral movements were approximately 40% greater and the lateral thrust was 4% larger in the case of incremental backfilling than those of a single construction stage.

A review of some of the limitations of the hyperbolic stress-strain model was presented by Ozawa and Duncan (1976). They compared the predicted results using the hyperbolic elastic soil model and an elastic-plastic dilatant model. There was significant difference in the predicted values. They pointed out that the hyperbolic model gave reasonable results in

the earlier stages of the wall movement but led to unsatisfactory predictions near failure. An attempt to improve the model was made by the use of a combination of the hyperbolic model and a plastic region which manifested dilation.

The potential usefulness of various soil constitutive models for application to finite element retaining wall analysis was comprehensively studied by Wong (1978). Experimental studies were carried out for a model wall (passive rotation about the toe) and comparisons made with the finite element results. Three different constitutive models were used: (i) a non-linear hyperbolic model; (ii) a Mohr-Coulomb simple plastic model; (iii) a stress dilatancy model. The numerical results of these three models agreed reasonably well with the measured experimental results. As these models were incapable of simulating strain-softening behaviour, the finite element (FE) analyses tended to overestimate the stiffness of the soil in the failure regions and underestimated the stiffness in the remaining regions, leading to approximately correct results. Wong found that the Mohr-coulomb model is suitable for modelling where large portions of the soil mass are in failure.

To better model the soil behaviour during failure and post yield conditions, Richards (1980), developed a joint element based on a non-linear hyperbolic soil model. This joint element was automatically incorporated in the finite element mesh to replace the element that has reached peak strength, and it was oriented in the direction of the failure plane. This model has been used to back-analyse post-yield behaviour in the triaxial test and direct shear tests. This model is useful in modelling retaining walls founded on soft clays where large plastic zones are likely to develop.

Goh (1984) determined the effect of compaction of a cohesionless backfill in the case of rigid retaining walls using the finite element method. He used two different methods to model the effect of compaction: (1) he assigned a large value to K_o to represent a high density of the backfill due to the compaction process, and assumed the compaction equipment was at a sufficient distance away from the wall; (2) he used a large value of K_o and additional horizontal forces at the corresponding nodes. He concluded that the first method is more realistic and suitable to represent field situations. Figure 3.5 shows that the lateral pressures are close to the at-rest values when using the first method, which is represented by Case CS28.

Seed and Duncan (1986) investigated the compaction induced stresses on a rigid undeflecting retaining wall with a granular backfill using the incremental finite element methodology. Compaction loading was modelled as a transient, moving load of finite

lateral extent, which passes one or more times over some specified portion of the backfill surface at each stage of the incremental backfilling. The finite element results were compared with physical model measurements. There was good agreement between the calculated lateral pressures and the measured values. They concluded that, the inclusion of the compaction induced stresses nearly doubled the lateral thrust and tripled the overturning moment about the base.

Recent finite element investigations by Duncan et al. (1990) is of importance as it gives new insights into the soil-structure interaction of the Fifteen Miles Gravity Wall. The wall is a 46 m high massive gravity retaining wall having granular backfill and founded on rock. They reported that current design manuals require that gravity walls built on rock foundations should be designed for at-rest conditions. They assessed the wall based on these recommendations and the wall was found unstable, in spite of the fact that the wall has performed well over the past 60 years. The results of their finite element analyses illustrated that, the wall rotated about the bottom and that the lateral pressures were less than the at-rest values. Also, the results indicated that, for this massive wall, a large downward shear force develops at the heel which significantly improves the stability. This shear force is neglected by the current design methods, as they assume zero relative movements due to the large stiffness of the wall. However, the FE results demonstrated that a large relative movement developed along the interface due to settlement of the backfill.

Goh (1993) studied the behaviour of a cantilever (T-shape) retaining wall by using a linear elastic-perfect plastic soil model, an he assumed a smooth back of the wall and a rough base. The significance of this study is that design distributions of the LEPs were developed based on extensive investigations of the key design factors. In these distributions, the lateral earth pressures exceed the Rankine active values and they were close to the at-rest values, particularly in the lower half. This was attributed to the restraint at the bottom of the wall.

Based on the investigations presented in the current section, it can be concluded that, the FEM has been successfully used over the last 30 years to investigate the behaviour of retaining walls. However, none of these numerical investigations has adequately studied the significance of a limited backfill. In the current research detailed investigations are carried out to examine the effect of backfill geometry and size on the lateral earth pressures. In the remaining part of this chapter the procedure used in the current investigation is described, while the results of these investigations are given in Chapters 4 and 5.

3.4 BASIC FEATURES OF FINITE ELEMENT ANALYSIS

3.4.1 Constitutive Models of Soil Behaviour

Although a large number of constitutive equations for soil have been established, it has been essential to use numerical methods for implementation of these models. The stress-strain constitutive equations which have been proposed over the last 4 decades or so for granular and clay soils, such as Schofield and Wroth (1968), have the merit that they adequately represent the main features of the observed behaviour of soil. But their complexity is such that exact analytical solutions are unlikely to be derived. Numerical solutions, such as the finite element method, have become possible with the increased availability of powerful digital computers. The FEM develops an approximate solution to the mathematical formulation of soil behaviour.

In the studies that have been described in the preceding section the soil behaviour was modelled by using one of the following: (1) linear-elastic model, such as Morgenstern and Eisenstein (1970); (2) non-linear (hyperbolic) elastic model, such as Clough and Duncan (1971); (3) linear elastic-perfect plastic model, such as Goh (1993); and (4) Cam-clay model, or elastic-plastic strain hardening model, such as Simpson and Wroth (1972).

One of these four models should be used to perform the FE analyses in the current research. Valliappan (1978) reported that the linear-elastic model is unsuitable for modelling the non-linear behaviour of soil, particularly the plastic response in the active zone behind retaining walls. Limited studies by Wong (1978) have shown that the hyperbolic model is unsuitable for modelling systems undergoing continuous failure, as the stresses tend to fluctuate above and below the failure surface causing elements to behave erratically.

Cam-clay, or the elastic-plastic strain hardening model, is a very comprehensive model that is used where soil parameters can be accurately determined from a detailed soil investigation. However, these parameters are not readily available. Accordingly, the linear elastic-perfect plastic model, with associated flow rule condition, was adopted in the current research, as it better represents the soil behaviour close to failure which occurs in the vicinity of a retaining wall due to placement of the backfill. This model is a simplified formulation that accounts for volume change and plastic deformations. Although the associated flow rule was used in the current research, it is accepted that the volume change will be slightly over predicted, as reported by Chen (1975).

Linear Elastic-Perfect Plastic Soil Model

In this model, typical non-linear stress-strain curves, that are shown in Figure 2.4, can be approximated to some degree by a linear elastic-perfect plastic model. The complete description of this model entails appropriate elastic constants, yield function, and flow rule. There exists a number of failure criteria that reflect the fundamental feature of soil behaviour, that is soil failure. The Coulomb criterion is the best known of these criteria.

Drucker et al. (1952) discussed an extension of the well-known *Von Mises failure criterion* that is recommended for the FEM due to its simplicity. Consequently, Drucker (1953) presented the so called *extended Tresca yield condition.* However, for plane stress and/or plane strain conditions, both the extended Tresca and the extended Von Mises yield the same result as the Coulomb failure criterion. For example, for two dimensional, plane-strain problems, the Coulomb failure criterion can be written as:

$$f = \sigma'_1(1-\sin\phi') - \sigma'_3(1+\sin\phi') - 2c\cos\phi' = 0 \qquad (3.2)$$

where

f	=	yield function
σ'_1	=	major principle effective normal stress
σ'_3	=	minor principle effective normal stress
c	=	cohesion
ϕ'	=	effective angle of shearing resistance

In the elastic analysis, the elastic strains depend upon the stress increments, while the plastic strains depend on the magnitude of stresses. When analysing the plastic state, it is necessary to consider the rate of strain not the total strain. The concept of flow rule is to relate the strain rate to the stress state at yield (Chen, 1975).

In other words, the definition of the flow rule is that the plastic strain rate is related to the effective stress state at yield, and the strain tensor at yield is normal to the yield surface. The mathematical formulation of the flow rule is represented by the following equation:

$$\dot{\varepsilon}^{p}_{ij} = \lambda \frac{\partial f}{\partial \sigma_{ij}} \qquad (3.3)$$

where

f	=	yield function
λ	=	scalar

$\dot{\varepsilon}^{p}_{ij}$ = plastic strain rate

σ_{ij} = stress level

There are a number of definitions encountered with respect to the flow rule concept or normality principle. For example, the associated flow rule material expresses the condition that the material deforms with the angle of dilation, φ, equal to the angle of shearing resistance, ϕ, whereas if $\varphi \neq \phi$ the material is said to obey a non-associated flow rule. The plastic behaviour of soils could be modelled by either an associated flow rule or a non-associated flow rule.

Limited finite element investigations carried out on retaining walls by Potts and Burland (1983) indicated no significant difference between associated flow rule material and non-associated flow rule material. Also, Goh (1984) concluded that there was a 10% the difference in magnitude of the lateral thrust between associated and non-associated flow conditions. Preliminary analyses, which were carried out as part of this research, showed minimal difference between both conditions. Therefore, the associated flow rule was assumed in all the analyses conducted in this project.

The plastic behaviour is a load path dependent, therefore, this requires a step-by-step calculation. This incremental procedure involves the calculation of the rate of strain, $\dot{\varepsilon}$, and the rate of stress, $\dot{\sigma}$, as well as the elastic-plastic constitutive matrix, [D]. The relation between these variables can be expressed in matrix form as:

$$\{\dot{\sigma}\} = [D]\{\dot{\varepsilon}\} \tag{3.4}$$

The mathematical formulation of the constitutive matrix is given in several finite element programming text books, such as Hinton and Owen (1977) and Smith (1982). Once this matrix has been determined the principle of virtual work is applied to the assembly of elements and the overall stiffness matrix is determined. The nodal displacement and nodal forces are then computed by solving the developed linear algebraic equations similar to Eq. 3.1.

3.4.2 Interface Modelling

The use of FEM for analysing soil-structure interaction problems was limited to some extent, until difficulties in representing the interface between the structure and the soil were overcome. Most analyses undertaken before the development of interface joint

elements were performed using one of two limiting assumptions concerning the characteristics of soil-structure interface: (1) the interface was assumed to be perfectly rough with no possibility for relative movements between the structure and the soil; or (2) the interface was assumed to be perfectly smooth with no shear stress transfer between the structure and the soil.

Furthermore, in geomechanics, it is often necessary to model the continuum that may include shear failure planes, where a slip would occur. For this purpose, several types of joint elements have been developed that can represent the interface behaviour, such as Goodman et al. (1968). A joint element with four relative displacements was developed, and the adjacent elements were allowed to penetrate into each other.

In the present research, a six-noded, zero-thickness, one dimensional interface joint element based on Goodman et al. (1968) was used to model the soil-structure interface along the base and the back of the retaining wall. In evaluating the stiffness of this element it was assumed that both normal and shear displacements vary linearly along the length of the element, which is compatible with the external boundary displacements of the two dimensional elements of the soil and wall. The linear equations expressing this element are:

$$\sigma_n = K_n \Delta n \tag{3.5}$$

$$\tau = K_{st} \Delta s \tag{3.6}$$

where

σ_n	=	normal stress within the element
k_n	=	normal stiffness
Δn	=	average normal displacement across the element
τ	=	shear stress within the element
K_{st}	=	tangent stiffness for a particular increment
Δs	=	average relative shear displacement across the element

Zero-thickness interface elements have been successfully used over the last 30 years in finite element analysis to model soil-structure interaction. Recently, Kaliakin and Li (1995) have argued that zero-thickness interface elements suffer from: (1) stress oscillations attributed to inappropriate quadrature schemes; (2) lack of accuracy due to excessively large normal stiffness parameters; (3) inaccurate interface stress predictions due to insufficient mesh fineness. In spite of this argument against the use of zero-thickness interface element, it has been adopted in this work with due care. The finite

element program AFENA (Carter and Balaam, 1994) automatically incorporates the zero-thickness elements along the selected interface surface, and this was found to be much more efficient than manually inserting non- zero-thickness elements.

Extensive modified simple shear tests by Goh (1984) of soil-structure interaction behaviour showed that the sand-wall interface behaviour was a tri-linear response, but the clay-wall interface is a hyperbolic response. However, the interface laboratory shear tests on granular soils by Acar et al. (1982), indicated that the sand-wall interface had a hyperbolic response. This hyperbolic response was employed in a number of finite element analyses of retaining walls, eg. Clough and Duncan (1971).

In the current research, a compatible linear elastic-perfect plastic interface model with the other soil and wall model has been adopted to model the interface behaviour along the back and base of the wall.

3.4.3 Modelling of Construction Sequence

Conventional design methods assume that the construction of the wall and placement of the backfill is a single stage process with gravity applied to the whole system at the end of construction. Clough and Woodward (1967) showed that neglecting incremental stage construction in an embankment led to significant differences from the observed vertical displacements. Goh (1984) reported that there were large differences in the results between the "gravity turn-on" procedure and multi-layered (stage-by-stage) analysis.

The stage-by-stage placement of the wall and backfill, developed by Clough (1969), is the most commonly used method for modelling the construction sequence. In this model, as each new layer of backfill is placed, it is assumed to behave as a dense liquid, and the interface elements between the newly placed backfill and the wall are assumed to be frictionless. The main advantage of modelling the construction sequence by the stage-by-stage construction procedure is that it accurately represents the mode of displacement at each stage of construction.

In any analysis, the actual construction sequence should be followed as closely as possible in order to achieve accurate results. This is often impractical from computer storage and solution time considerations, particularly where large earthworks are involved, since this would require many layers of backfill. About 10 layers have typically been used in the analysis of major dams, eg. Clough and Woodward (1967), and retaining walls, eg. Goh (1993).

In the present research, the stage-by-stage placement of the wall and backfill was modelled using the technique developed by Clough (1969). It should be noted that, the backfill was loosely placed as no compaction is allowed in the drainage zone as required by retaining walls design codes, such as CP No. 2 (1951). This is to facilitate the drainage of the water which penetrates and accumulated behind the wall. However, it is accepted that compaction of regions beyond the drainage zone will improve the strength characteristics of the backfill.

The cohesionless backfill was assumed to be loosely placed, and the backfilling and casting of the wall were simultaneously carried out in 10 lifts. The newly placed elements were assigned the following properties: (i) K_o conditions for lateral pressures; (ii) their strains were set to zero; (iii) same strength and stiffness as existing layers; (iv) initial vertical stresses were set equal to the overburden pressures at the centroid of the layer. In addition, an interface element was placed between the newly backfilled layer and the new concrete portion. Note that if the consolidation settlements had been considered in the analysis this would more accurately represent the in situ displacements and hence the stresses. Due to time constraint, the consolidation of the foundation subsoil was not considered, and gravity was directly switched on for the newly placed layer of backfill.

Figure 3.6 shows the construction sequence of a T-wall with a non-homogeneous backfill. It can be seen that, the wall rotated about the toe due to construction of the backfill, and the movements increased as a new layer was added.

As part of the current research a preliminary set of analyses was performed to examine two different construction sequences. In the first one, the wall was assumed in place with no effect on the soil. The stresses were then set to the at-rest values, followed by the placement of the backfill. In the second method, simultaneous construction was allowed, in which both the wall and the backfill were incrementally constructed. The results showed that there were considerable differences, but less than 1 mm, in lateral deflections of the wall. Also, there were small differences (less than 2%) in the lateral thrust acting at the back of the wall.

Figure 3.7 shows one of the analyses of a cantilever T-wall with a limited backfill performed using the first method, where the wall deflections appear to be similar to a cantilever beam fixed at the base level with its maximum deformations at the top. This is because, as a new backfill layer was placed, the wall deflected as a rigid body. In the second method, the deflections were different, with the maximum deflection close to a distance of H/3 from the ground surface. This results from a subsequent construction

segment of the wall is jointed to a deflected portion of the wall from preceding construction. The second method of simultaneous construction, however, has been used in this research as it is more realistic and accounts for the effects of the weight of the wall. Typical deflections of the wall associated with different backfill geometries are presented in Chapters 4 and 5.

3.4.4 Isoparametric Elements

Extensive investigations by Goh (1984) indicated that, for gravity walls, four-noded isoparametric elements, with 2×2 integration points, were sufficient to model the wall and the soil system. Also, he concluded that, for cantilever walls, 8-noded isoparametric elements were employed, as these were found to be more effective in modelling the bending effects of the wall stem. Other elements were used, such as the triangular elements by Christiano and Chuntranuluck (1974). However, the quadrilateral elements are geometrically suitable in the case of excavating and backfilling horizontal soil layers. In the present research, 8-noded isoparametric quadrilateral elements with 3×3 integration points were used for modelling rigid retaining walls.

Two techniques can be used to model the concrete section of cantilever T-walls, these being: (1) one dimensional flexible beam elements which approximate the flexural effects of cantilever walls; and (2) using two dimensional plane strain elements with adjacent interface elements. In this research, the second technique was used to better model the boundary conditions and to account for vertical and horizontal wall movements.

3.4.5 Time Limitations and Efficiency

Time, or computational effort, is an important factor which needs consideration in any finite element analysis. Increasing the number of elements, nodes, and the number of lifts gives greater accuracy, but also increases the computational time and hence the cost. Therefore, in any analysis, there needs to be a balance between accuracy and computational time. This balance was the governing factor in the selection of various mesh sizes, number of nodes and elements, and the number of backfilling lifts.

The effect of the number of construction lifts and the number of gravity application increments on the lateral pressures were examined during the preliminary stage. Three cases were considered for constructing the wall and backfilling: (1) using 5 lifts; (2) using 10 lifts; and (3) using 10 lifts and 5 increments for switching on the gravity. It was found that, using 10 lifts requires a reasonable computational time and leads to satisfactory

results. The validation of the results is discussed in Chapters 4 and 5, where the results of unlimited backfill analyses are compared with those of recent FE studies, as well as against the classical theories.

The central processing unit of the server, HYDRA, of the Department of Civil and Environmental Engineering at the University of Adelaide, was used to carry out the numerical investigations. A typical run using a 486 IBM PC terminal, with 8 MB extended memory, requires 120 to 150 minutes depending on the network load.

3.5 DESCRIPTION OF PROGRAM OF NUMERICAL INVESTIGATIONS

The main aim of these numerical investigations is to demonstrate the significance of backfill size and geometry in the analysis of retaining walls. The previous work by Goh (1993) and Clough and Duncan (1971) represents the basis of the present investigation.

3.5.1 Wall Type and Backfill Geometry

(a) Type of retaining wall

The response of three types of rigid retaining walls was investigated to determine the effect of a limited backfill on the distribution of the LEPs. These three types represent the most common geometries encountered in residential and highway construction. These types are the cantilever T-wall, the cantilever L-wall (with its base projected in the front of the wall) and the gravity wall with constant width and vertical back. Figure 3.8 shows the geometries of the three walls, and Table 3.2 gives the adopted dimensions of these walls.

Cantilever T-walls are the most common type used in practice, because the concrete base provides a significant stability against sliding in addition to its good performance on soft clays. Accordingly, cantilever T-walls form the major component of the present research.

In the geotechnical design of T-walls, the lateral earth pressures acting along the virtual back of the wall are used in the calculations of safety factors against sliding and overturning. In the structural design of cantilever T-walls, the lateral earth pressures along the back of the wall are used as the working pressures. The classical earth pressure theories do not provide any information about these pressures, which are usually estimated by multiplying the limiting active pressures at the wall heel by a load factor. In this

research, both the lateral pressures acting along the back of the wall and at the virtual back of the wall are investigated.

(b) Wall Dimensions

The task of selecting wall dimensions for the present research involves some difficulties. Measurements of earth pressures on rigid retaining walls in service have been reported in many field studies, such as Rehnman and Broms (1972) and Broms and Ingelson (1972). These studies observed that the measured earth pressures were higher than the active values. Also, the numerical investigations by Goh (1993) drew the same conclusions. This is to be expected because the margins of safety used against sliding and overturning are such that the wall is not allowed to move far enough to develop active earth pressures. In the present research, the wall dimensions have been selected to ensure sufficient movements and to provide appropriate stability, particularly for walls founded on soft clay.

(c) Backfill Geometry

The backfill geometry and size is chiefly determined from the required drainage system. Huntington (1957) gave a wide range of drainage systems showing their requirements and applicable field situations where each system may be used. Three different homogeneous backfill geometries were investigated in this present research: triangular, rectangular and trapezoidal, as they form the possible geometry of any drainage system. Also, the case of non-homogeneous backfill is examined. Figure 3.8 shows the selected retaining walls and backfill geometries. The triangular and rectangular shapes are found when the required drainage zone is narrow and/or the granular material is not readily available.

On the other hand, when there is no limitation on the width of excavation nor availability of backfill material, the trapezoidal backfill is used, where a relatively wide excavation is made to allow for construction of the base of the wall. Also, when there is no limitation on the width of excavation, but the backfill material is not readily available a non-homogeneous backfill may be used. A non-homogeneous backfill identifies the case where a simultaneous construction is carried out using both the granular material and a part of the excavated clay as a backfill.

Bowles (1988) reported that there are situations associated with the construction of T-walls, where the zone of the granular backfill used for drainage is very narrow, as shown in Figure 3.9 (a). This situation may be found in a naturally stratified deposit. On the other hand, this condition may arise when the backfill soil is not readily available and/or

there is a limitation on the width of excavation behind the wall. It is accepted that this situation is rare, as it requires very stiff deposit, but preliminary analyses showed that it represents an upper bound for the lateral pressures, hence it was examined.

This latter situation is idealised in the present analyses by a homogeneous triangular or rectangular backfill. The construction of such walls may be carried out in two steps as follows (i) excavating a narrow zone along the stem height, then widening the width of excavation close to the base of the wall to allow its casting; and (ii) constructing a granular blanket between the clay deposit and the back of the wall. This possible construction method is shown in Figure 3.9 (b).

The size of a triangular backfill is determined by the normalised distance, a/H, as shown in Figure 3.8 (a). For the three wall types, the variable, a, represents the horizontal distance from the back of the wall to the point where the excavation surface cuts the ground surface, and H represents the wall height. It was discussed in Chapter 2 that Huntington (1957) concluded that the backfill size has no effect on the lateral thrust when $a/H > \cot\rho$, where ρ is the Coulomb's angle of rupture. However, preliminary investigations carried out by the author indicated that there were significant variations in the lateral earth pressures even when $a/H > \cot\rho$. Therefore, the backfill size ratio (a/H) was investigated for a relatively wide range, a/H=0.2 to 2.0.

The case of a rectangular backfill was only investigated for T-walls. The excavation surface was assumed vertical and the backfill size was determined by the ratio (b/H) which was varied between 0.06 and 0.53, with increments b/H=0.07. These small increments were considered essential in the case of a rectangular backfill, as large variations in the lateral thrust were obtained for a small change in the ratio (b/H).

The size of a trapezoidal backfill was represented by the normalised distance (c/H). For T-walls, the distance, c, was measured from the vertical section through the heel to the point where the excavation surface cuts the ground surface. While, for L-walls and gravity walls, the distance, c, was measured from the back of the wall to the point where the excavation surface cuts the ground surface. The value of c/H was varied between 0.2 to 2.0. This case is more common, however, it is not as critical as the triangular backfill.

(d) Embankment Height

The cohesive natural deposit is made of the embankment soil above the wall base level and the subsoil beneath the foundation level. The embankment was modelled as a self supporting with an adequate safety factor. The maximum height of the self supported embankment, used in this research, was H1= 4.1 m, and Eq. 2.7 was used to determine the associated safety factor against collapse. Table 3.3 gives these safety factors (SF) for each clay type, which demonstrates that, prior to any placement of the granular backfill, the soft clay embankment has at least a safety factor of 1.5 against collapse. Note that the soil in the front of the wall, with height h_1, was neglected in the analyses.

3.5.2 Model Parameters

Duncan et al. (1990) reported a survey of railroad engineers to gather information about retaining walls and abutments that had performed in an unsatisfactory manner. The results of this survey showed that all of the walls that showed progressive movements were backfilled with clay or were founded on clay. They also recommended that more attention should be paid to the evaluation of foundation conditions beneath walls which are founded on clay subsoils. Also, a survey carried out by the author indicated that there is uncertainty in lateral earth pressure computations associated with retaining walls founded on clayey soils. Therefore, this research project focuses on those walls founded on clayey deposits.

There are numerous practical problems in which the soil within the backfill behind a retaining wall is stressed quickly compared to the consolidation time of the soil. These occur particularly when the backfill is constructed on clays. Lambe and Whitman (1969) concluded that, for such problems, it is appropriate to use undrained strength analyses to determine the lateral thrust acting upon the back of retaining walls. In the present research, the backfill was assumed to be constructed quickly and the consolidation of the natural clay deposit was neglected. On the other hand, it is accepted that the consolidation will influence the behaviour of the backfill in the long term. The clay deposit was assumed to be saturated, although the ground water table was assumed to be at a distance greater than H below the foundation level. This condition is common in Adelaide, where soil suction is very high.

Since rapid construction was assumed, total stress ($\phi = 0$) analyses were used for modelling the construction on clays. Also, for simplicity, the stiffness and strength parameters of the soil were assumed constant with depth, even though in many situations the strength and stiffness do vary with depth. In the following, the basis for the choice of these parameters is described.

(a) Shear Strength Parameters

The key factor of any finite element analysis is the choice of model parameters, since the applicability of the results relies upon how well these properties represent the field conditions. The angle of shearing resistance of the granular backfill was assigned a value of 30^0. Four categories of clay were adopted, these being, soft, medium, stiff and very stiff (hard) clays. The undrained shear strength of the clay deposit, c_u, was assigned values of 25 kPa, 60 kPa, 100 kPa, and 150 kPa, for soft , medium, stiff and very stiff clays, respectively. The wall was modelled to behave linearly elastic by assigning relatively high values for strength parameters compared with the stresses within the elements. A summary of these parameters is given in Table 3.3.

In modelling the natural clay deposit, tension cracks were neglected and any other discontinuities likely to occur in situ. In other words, the clay was modelled as a homogeneous mass with constant soil properties.

(b) Stiffness Parameters

Although the use of the shear modulus, G, and the bulk modulus, K, offers the advantage of improved representation of the bulk compressibility especially after failure, the Young's modulus, E, and the Poisson ratio, ν, were used in this work to represent soil behaviour due to the availability of reasonable correlations for these parameters.

(i) Young's Modulus

Estimation of a single value for Young's modulus to represent the stress-strain behaviour of clayey soils within a certain range of strain level is extremely difficult. Islam (1994), after extensive undrained triaxial tests on remoulded Keswick Clay, developed useful relationships where the value of (E_u / c_u) was found between 160-300 for different overconsoildation ratios between 1 to 13. Bowles (1988) suggested using values of the normalised Young's modulus (E_u / c_u) between 200-500 for finite element analyses.

Figure 3.10 shows the variation of secant modulus normalised with respect to the undrained shear strength (E_u / c_u) with increasing shear strain, developed by Simpson et al. (1979) from back analyses of field measurements and laboratory testing using FE linear-elastic model for London Clay. Preliminary finite element analyses by the author showed large differences in strain level between the chosen four clay types. Therefore, a single value of E_u / c_u, based on Simpson et al. (1979) was used for each type of clay according to the average mobilised shear strains within the elements. Table 3.3 gives the adopted values of E_u / c_u for the four clay types.

(ii) Poisson's Ratio

A number of studies have been conducted to determine appropriate values of Poisson's ratio for use in finite element analyses. For analysis of undrained conditions in saturated clays, the value of $\nu \approx 0.5$ is consistent with the numerical stability of computer solutions (Desai, 1972). Bowles (1988) recommended using ν between 0.4 to 0.5 for undrained analysis and saturated clays. In this research, values of ν of 0.49, 0.47, 0.45 and 0.40 for soft, medium, stiff, and very stiff clays, respectively, were adopted. Desai (1972) reported that, for drained conditions, or undrained conditions in partially saturated soils, the value of ν can be determined from the relationship:

$$\nu = \frac{K_0}{1 + K_0} \tag{3.7}$$

where K_0 is the coefficient of earth pressure at-rest.

In the present research, the above relationship was used only to determine the value of ν for the granular backfill, which is given in Table 3.3.

(c) Coefficient of Earth Pressure at-rest

The initial stresses in the ground are required to define the initial conditions for any incremental analysis. In this work, the ground surface was modelled as a horizontal surface, and the soil-wall interface as vertical, hence, the at-rest condition should prevail. The vertical initial stress within an element was taken as the geostatic stress at the centroid of this element. The horizontal initial stress was taken as K_0 times the overburden pressure. The value of K_0 is frequently estimated using empirical relationships, such as Bishop (1958) for granular soils and Booker and Ireland (1965) for clays. Also, Jha (1994) presented a summary for some of these empirical correlations that have been used

in geotechnical design to estimate the value of K_0. In this research, the value of K_0 was determined based on the Jaky (1948) formulation which was presented in Eq. 2.1.

(d) Interface Parameters

A smooth-wall condition was used to carry out the analyses, as it represents the critical case where the lateral earth pressures are large. In order to model a smooth concrete surface the interface elements adjacent to the back of the wall were assigned a relatively small shear stiffness of $K_s = 0.001$MPa/m, and $\delta/\phi = 0.76$. The interface elements adjacent to the base were assigned relatively high values, $K_s = 490$ MPa/m and $c_a / c = 0.95$. A high arbitrary value was assigned to the interface normal stiffness (K_n) to prevent overlap of adjacent two dimensional solid elements. Table 3.4 shows the interface parameters used in this research, which are similar to those used by Clough and Duncan (1971).

The developed shear stresses were relatively small compared to the horizontal stresses because of the low value of the interface shear stiffness that was selected to represent a smooth interface. Therefore, only the horizontal pressures were considered as the lateral earth pressures throughout the analyses.

3.5.3 Finite Element Mesh

Although the model chosen might not be applicable to every retaining wall, the model dimensions have been chosen in such a way that they are representative of many situations likely to be encountered in the field. Boundary conditions have a significant effect in finite element analyses. In the study conducted by Morgenstern and Eisenstein (1970), they found that the boundary condition has a significant effect on the horizontal earth pressures. Therefore, roller constraints have been assumed at horizontal distances of 8H behind the wall, 2H in front of the wall, and 2H beneath the wall; where H is the height of the wall.

Four different finite element meshes were used to carry out the analyses. Figure 3.11 shows the FE mesh used to analyse cantilever T-walls with limited triangular backfills. This mesh consists of 466 8-noded isoparametric elements having 9 integration points with 1438 nodes. Figure 3.12 illustrates the FE mesh used for the analysis of T-walls with trapezoidal and rectangular backfills. This mesh consists of 587 8-noded isoparametric elements with 1814 nodes, with almost half of the elements concentrated in the zones of high stress gradients at the back of the wall and beneath the base of the wall. Figure 3.13 shows the FE mesh used for the analysis of gravity walls with 485 8-noded isoparametric

elements and having 1461 nodes. Figure 3.14 shows the FE mesh used for the analysis of L-walls consisting of 467 8-noded isoparametric elements with 1448 nodes. The soil in the front of the wall that provides passive resistance was neglected in the analyses.

3.5.4 Computer Program

The finite element program AFENA (Algorithm for Finite Element Numerical Analyses) has been used to carry out the investigations. Over the past 15 years AFENA has been used successfully in Australia as a research tool. AFENA was first developed by Carter and Balaam in 1979 at the University of Sydney, based on Fortran 77. The program is made up of three parts: (i) the main module, AFENA, that does the arithmetical computations; (ii) the program GENTOP, which is an automatic 2-D mesh generator; (iii) FELPA, the graphic post-processor. Using macro-programming makes AFENA a versatile algorithm program capable of solving a variety of problems in geotechnical engineering. In the present research, a 2-D plane strain finite element model has been analysed using the latest version AFENA v4.6. AFENA is described in detail by Carter and Balaam (1994).

AFENA is an MS-DOS Extended Memory Program (EMP) that utilises a large memory space while running in DOS Shell. It was found that, a model of about 500 8-noded elements as shown in Figure 3.12, requires at least 8 MB RAM, with 7 MB available memory. The solution time was found to be very sensitive to the available memory, particularly for out-of-core solutions. In these solutions, AFENA requires a comparatively large disk space as the number of elements increases. AFENA was found suitable for modelling a variety of construction sequences including excavation, backfilling and gravity turning-on.

3.6 INTERPRETATION OF THE FINITE ELEMENT RESULTS

The key results to be determined from the numerical investigation are the magnitudes of the lateral earth pressures and the location of the lateral thrust. Accordingly, a detailed study of the stress-strain output of AFENA, to determine the distribution of the lateral earth pressures, has been carried out.

3.6.1 Lateral Earth Pressures

The backfill height was divided into 10 equal layers, each of height h_i. The horizontal normal stress (σ_i), from the AFENA output, at the centroid of the element, was considered to represent the lateral earth pressure at the corresponding height. In the incremental analysis, the lateral pressures were determined from the accumulated horizontal stresses of the backfill elements adjacent to the back of the wall. While, at the virtual back of the T-wall, the elements behind the section through the heel were used. The developed shear stresses were comparatively small, and have therefore been neglected in the computation of the lateral earth pressures.

Although AFENA gives solutions at 3 Gauss points along the side of the element adjacent to the wall, only one value was used to represent the average lateral earth pressure of an element. The developed average lateral earth pressure at a depth z from the ground surface was determined at the Gauss point located at the mid-height of the element. This value was compared with the magnitude of the classical Rankine active pressure, p_a, and with the at-rest lateral earth pressure, p_0, according to:

$$p_a = \gamma z K_{ar} \tag{3.8}$$

$$p_0 = \gamma z K_0 \tag{3.9}$$

where K_{ar} and K_0 are the Rankine and at-rest coefficients of earth pressures, respectively. Although both the L-wall and the gravity wall satisfy Coulomb conditions, Rankine values were used to compare the results with those from the finite element analyses. This is because the three types of retaining walls were modelled using smooth back of the wall, and also for comparison reasons.

3.6.2 Lateral Thrust

The lateral thrust is the summation of the lateral pressure distribution along the back of the wall. In the finite element analyses, the lateral thrust was determined as the summation of the average horizontal stresses of the chosen 10 backfill layers (σ_i) as follows:

$$P = \sum_{i=1}^{10} \sigma_i h_i \tag{3.10}$$

The lateral thrust was compared with the Rankine active thrust (P_a) as given in Eq. 2.2. For the granular backfill properties given in Table 3.3, the Rankine lateral thrust, due to a height H1=4.1 m, is 44.2 kN/m and acts at the classical height (H1/3) from the base of the embankment. In the following chapters, the lateral thrust was determined and normalised with respect to P_a, and its location was determined and normalised with respect to H1.

3.6.3 Location of the Lateral Thrust

In this research, the line of action of the lateral thrust is measured from the base (toe) of the embankment. This was found to be appropriate, as the lateral earth pressures developed only along the embankment height (H1). The location of the lateral thrust (due to 10 backfill layers) was determined from the backfill elements adjacent to the wall as follows:

$$Y = \frac{\sum_{i=1}^{10} \sigma_i h_i y_i}{\sum_{i=1}^{10} \sigma_i h_i} \qquad (3.11)$$

where

Y	=	distance from the base of the embankment to line of action of lateral thrust
σ_i	=	normal horizontal stress
y_i	=	distance from the base of the embankment to the point of application of σ_i
n	=	number of layers
h_i	=	thickness of layer

3.7 SUMMARY

In this chapter, some of the previous finite element studies for retaining walls have been reviewed, focussing on their major assumptions, procedures and conclusions. The procedures used in a number of these studies were the basis for the present research. In addition, this chapter has described the finite element methodology that was used to carry out the numerical investigation. A linear elastic-plastic model and soil-structure interface model, together with incremental construction sequence have been described. The three types of retaining walls that are dealt with have been presented and the different geometries of the backfill have also been described. Furthermore, the basis on which model parameters were selected and the interpretation of the results of the FE analyses have also been presented. The results of these finite element analyses are presented in Chapters 4 and 5.

Table 3.1 Summary of previous finite element analyses of retaining walls

Investigator	Soil Description	Soil Constitutive Low	Boundaries	Element Type	Type of Wall Movement
Girijavallabhan & Reese (1968)	dense and loose granular	non-linear elastic	smooth wall	quadrilateral	passive translation
Morgenstern & Eisenstein (1970)		linear elastic	smooth wall smooth base	triangle	active and passive trans.
Simpson & Wroth (1972)	dense granular	elastic-plastic	rough wall	triangle	passive translation
Clough & Duncan (1971)	medium dense granular	non-linear hyperbolic	interface elements	triangle	active rotation
Kulhway (1974)	stiff and soft clay	non-linear hyperbolic	interface elements	quadrilateral	incremental construction
Christiano & Chuntranuluck (1974)	loose & dense granular	non-linear hyperbolic	smooth wall rough base interfaces	triangle soil & stiff beam wall element	incremental construction
Wong (1978)	granular	4 different soil models	interface elements	isoparametric quadrilateral	active and passive trans.
Goh (1984)	granular and clay	elastic plastic	interface elements	isoparametric quadrilateral	active and passive trans.
Goh (1993)	granular	elastic plastic	interface elements	isoparametric quadrilateral	active translation

Table 3.2 Dimensions of walls used in analyses

Property	Symbol	T-wall	L-wall	Gravity wall
Wall-base width (m)	B	3.4	4.0	1.6
Wall-toe width (m)	t	0.4		
Wall-stem thickness (m)	s	0.4	0.4	
Wall-heel thickness (m)	h	0.4	0.4	
Wall height (m)	H	4.5	4.5	4.5
Wall stem height (m)	H1	4.1	4.1	

Table 3.3 Parameters of soil and concrete used in the analyses

Material	SF	c_u (kPa)	ϕ (deg.)	γ (kN/m^3)	K_0	E_u (MPa)	ν_u	E_u / c_u
Soft clay	1.5	25	0	16	1.0	2	0.49	80
Medium clay	3.4	60	0	17	1.0	10	0.47	165
Stiff clay	5.4	100	0	18	1.0	25	0.45	250
Very stiff clay	7.3	150	0	20	1.0	50	0.40	330
Granular backfill		0	30	16	0.50	40	0.35	
Concrete		1.E+9	40	22	0.2	25, 000	0.20	

Table 3.4 Interface parameters adopted in the analyses

Interface Properties	K_s (MPa/m)	K_n (MPa/m)	c_a (kPa)	δ (deg.)
Wall-granular soil interface	0.001	1×10^9	0	22.8
Base-soft clay interface	490	1×10^9	23.75	0
Base-medium clay interface	490	1×10^9	57	0
Base-stiff clay interface	490	1×10^9	95	0
Base-very stiff clay interface	490	1×10^9	142.5	0

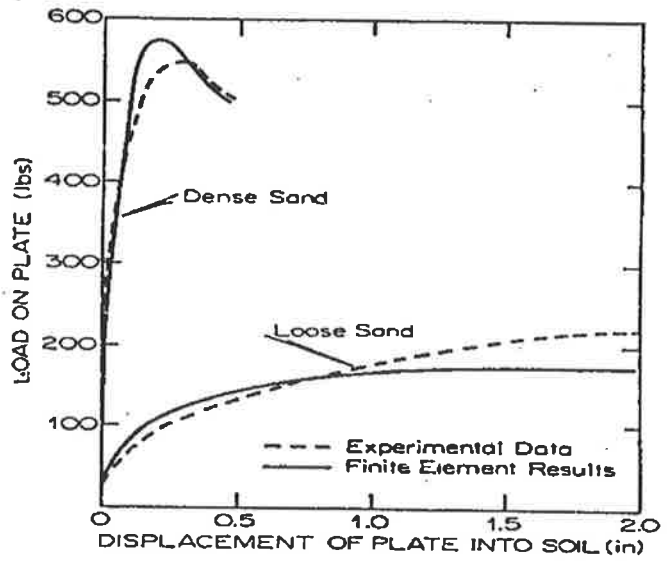

Figure 3.1 **Passive earth pressure tests (*Girijavallabhan and Reese, 1968*).**

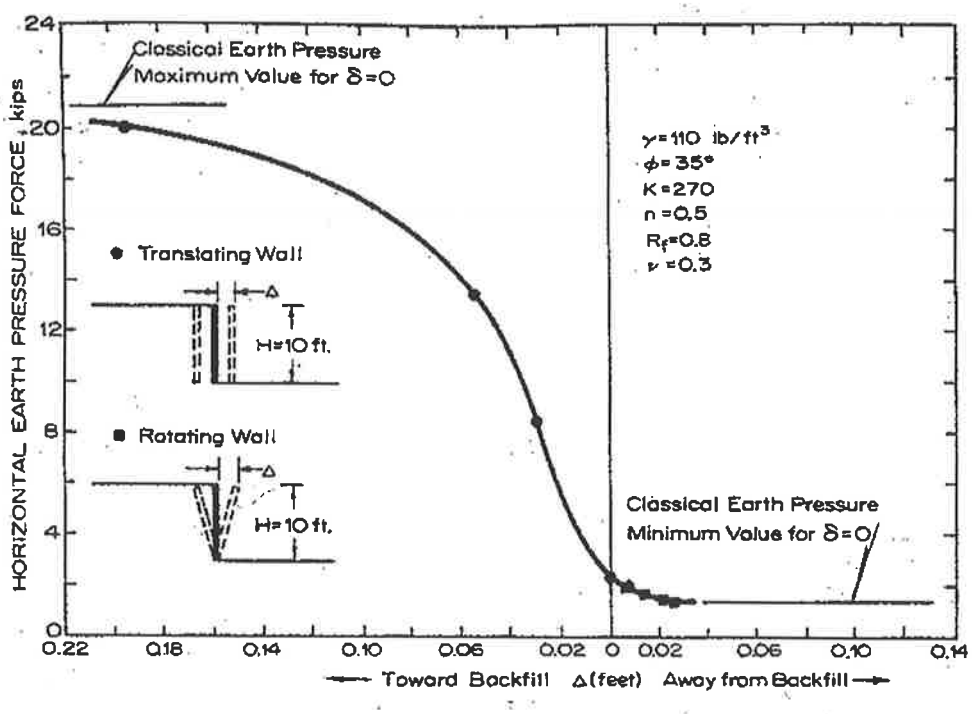

Figure 3.2 **Variation of horizontal earth pressure with wall movement from finite element analyses (*Clough and Duncan, 1971*).**

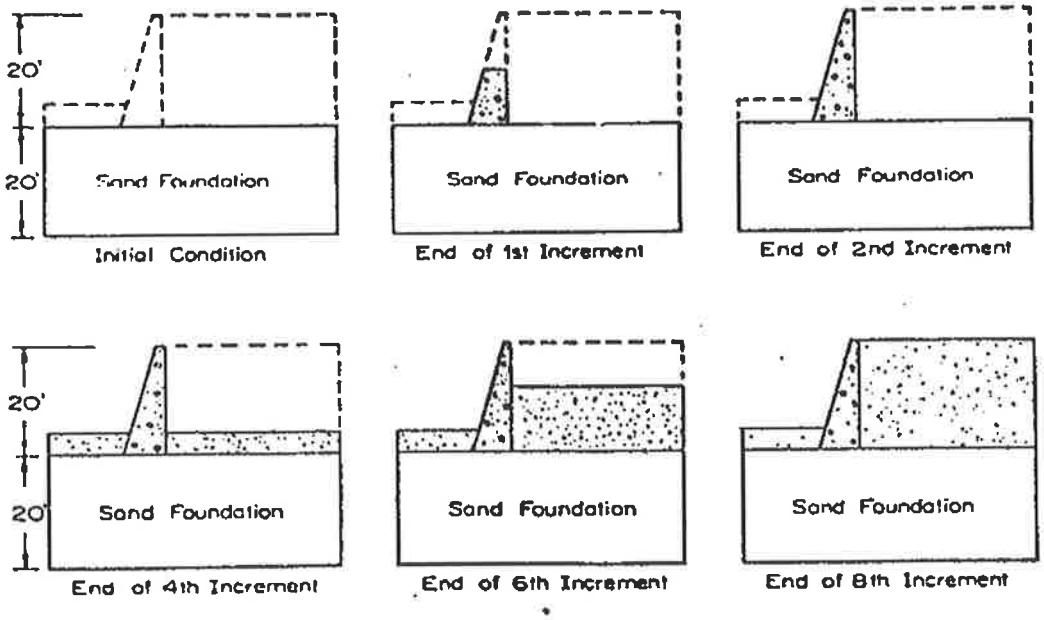

Figure 3.3 Construction simulation of gravity walls (*Clough and Duncan, 1971*).

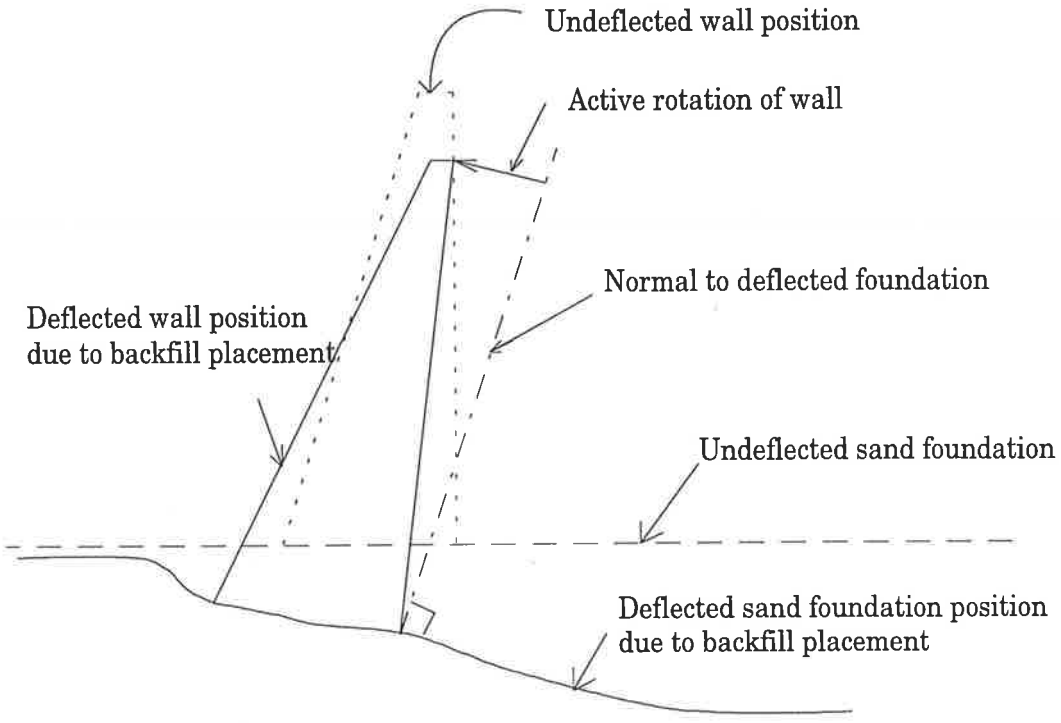

Figure 3.4 Wall tilt determined from finite element analyses (*Clough and Duncan, 1971*).

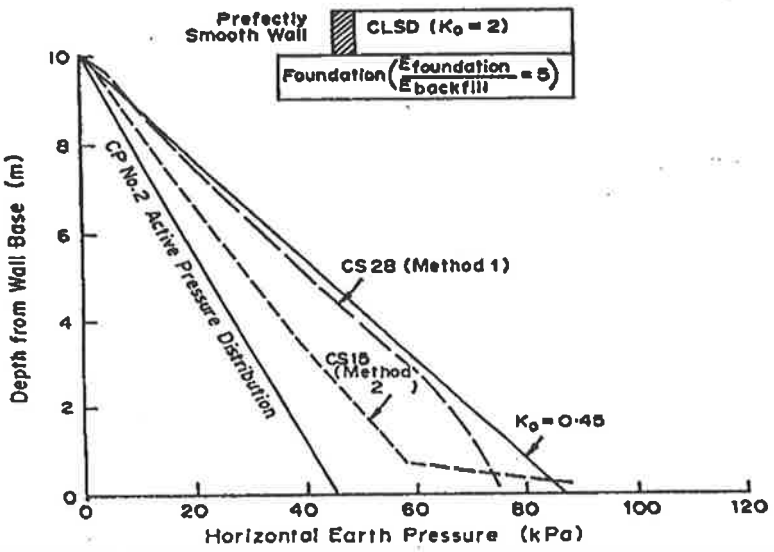

Figure 3.5 Effect of compaction on the lateral earth pressure distribution from finite element analyses (*Goh, 1984*).

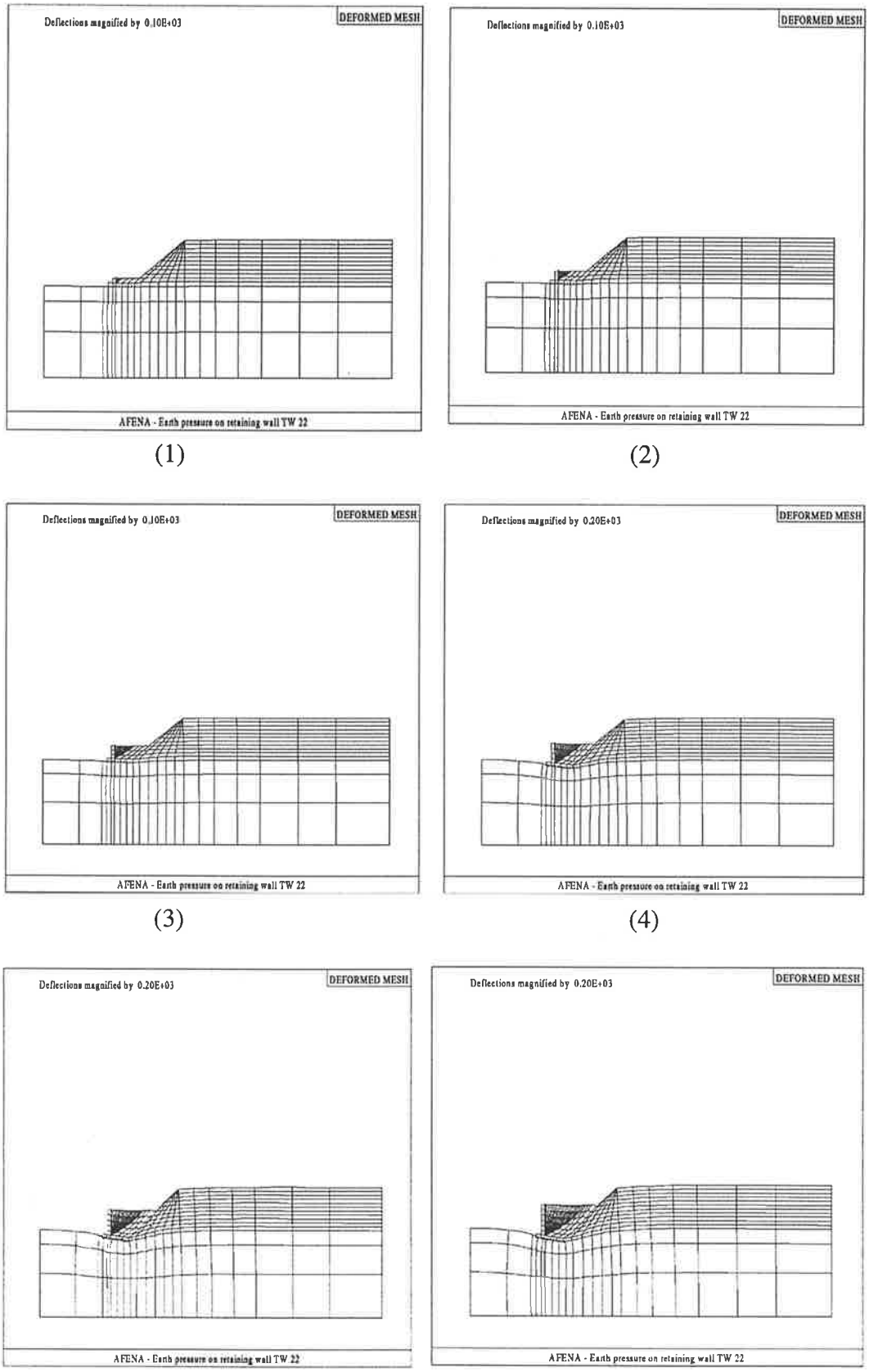

Figure 3.6 Construction of the wall and the non-homogeneous backfill on 10 lifts.

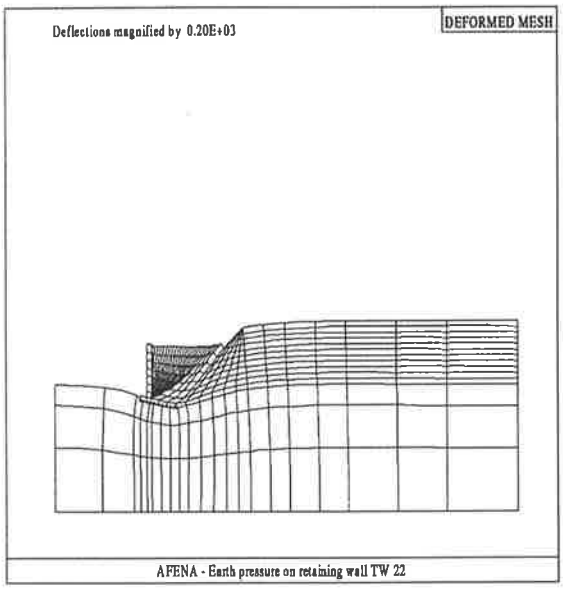

(7)

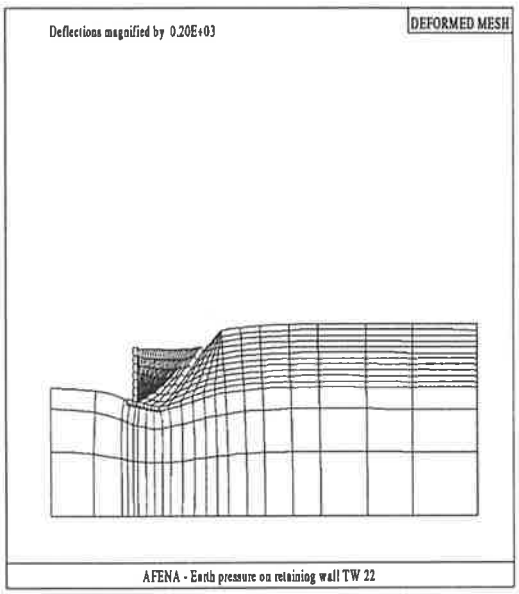

(8)

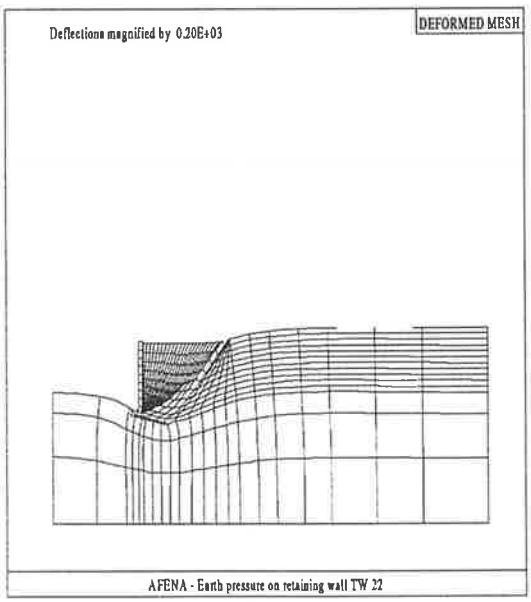

(9)

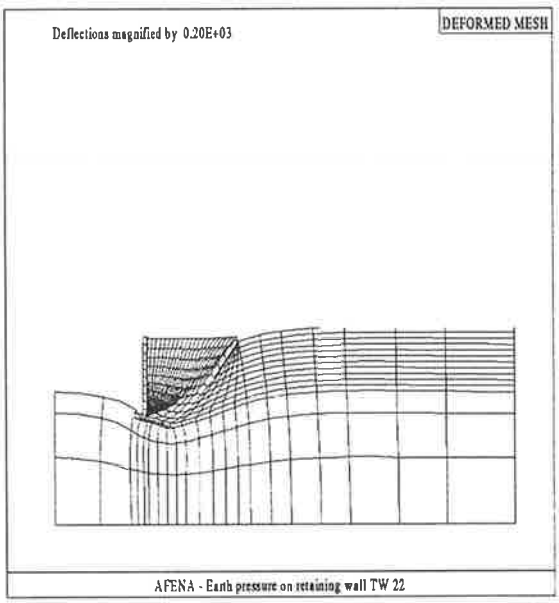

(10)

Figure 3.6 Construction of the wall and the non-homogeneous backfill on 10 lifts (cont.).

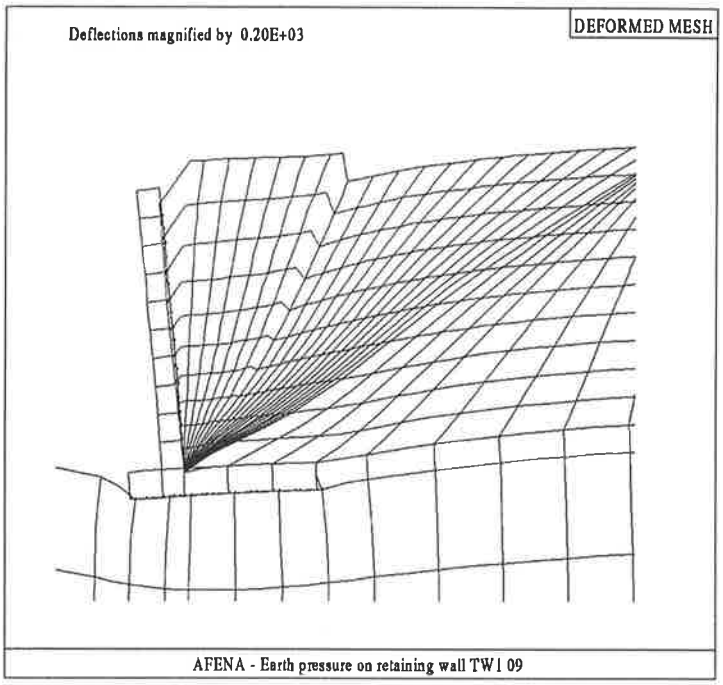

(a)

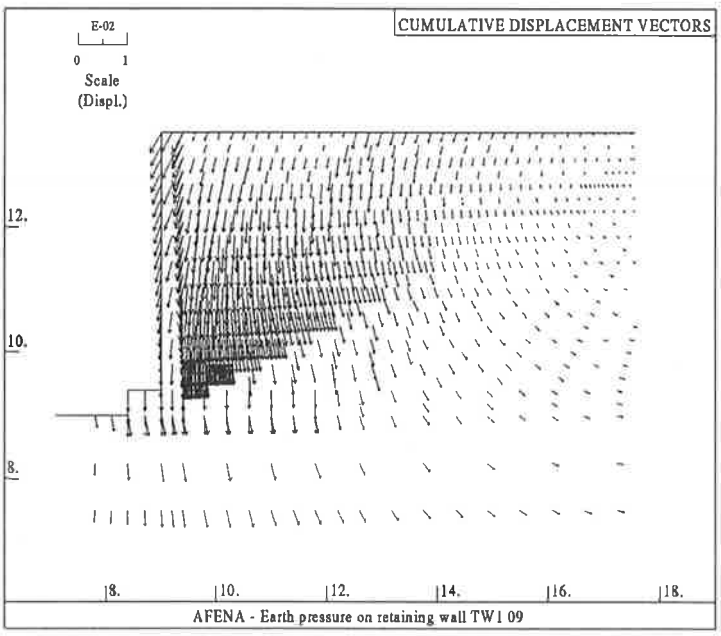

(b)

Figure 3.7 Wall movements when the wall was assumed in place before placement of the backfill: (a) wall and soil movements; and (b) accumulated displacement vectors.

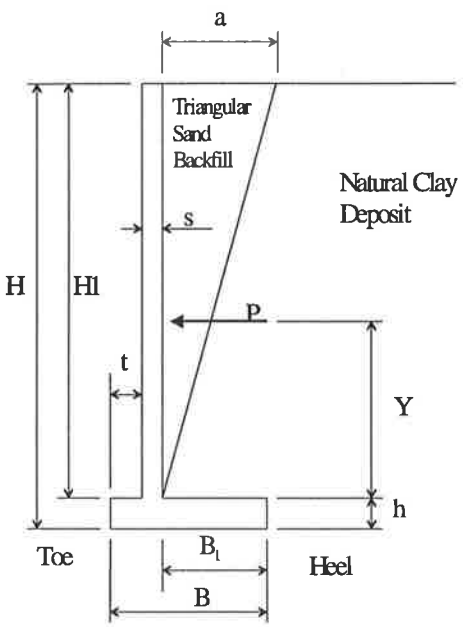

(a) T-walls with triangular backfills

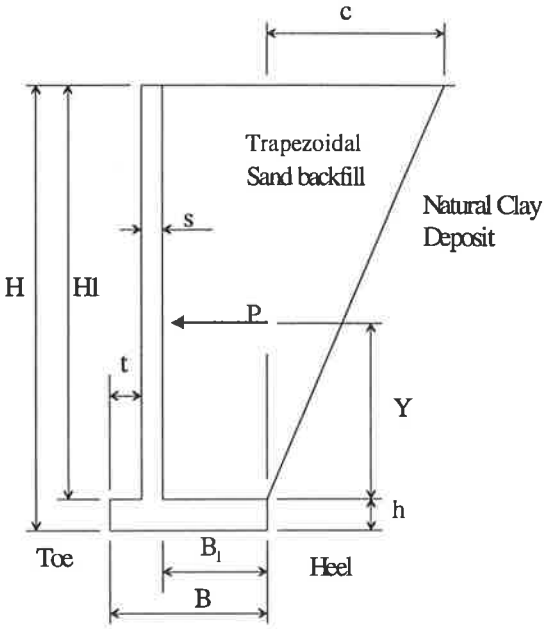

(b) T-walls with trapezoidal backfills

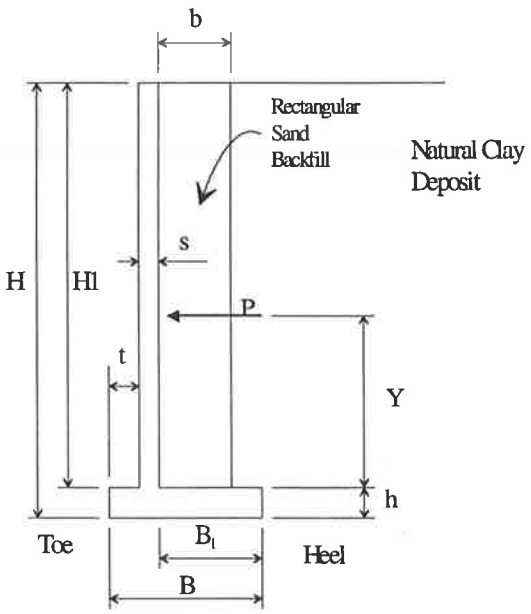

(c) T-walls with rectangular backfills

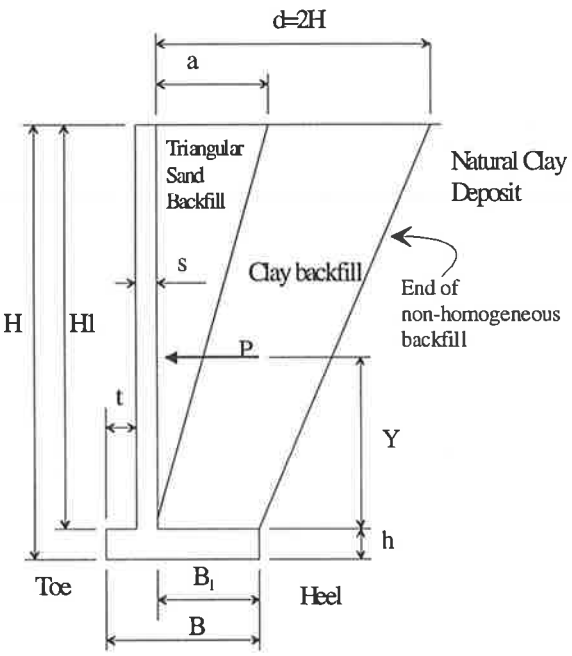

(d) T-walls with non-homogeneous backfills

Figure 3.8 The selected retaining walls and backfill geometries.

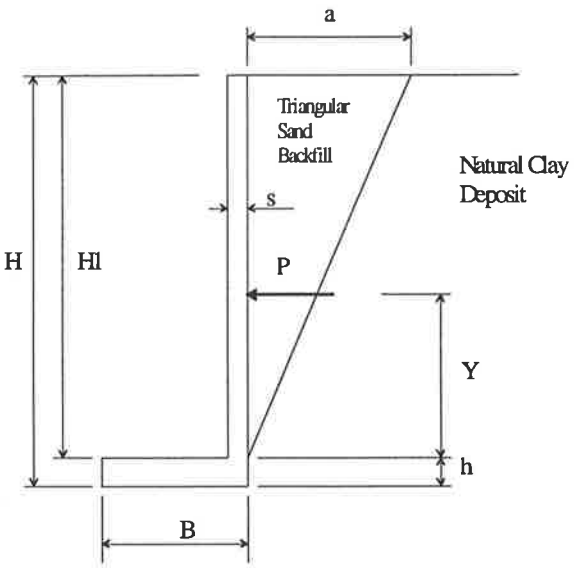

(e) L-walls with triangular backfills

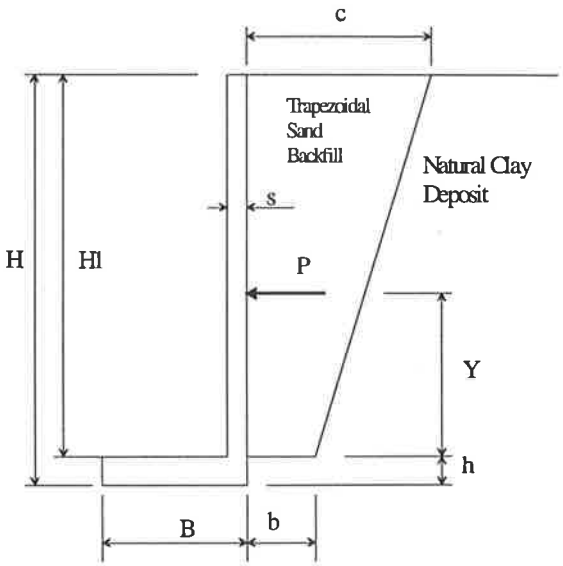

(f) L-walls with trapezoidal backfills

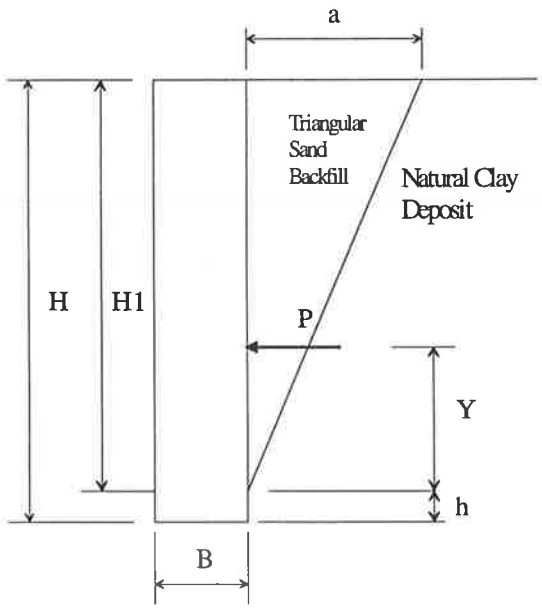

(g) Gravity walls with triangular backfills

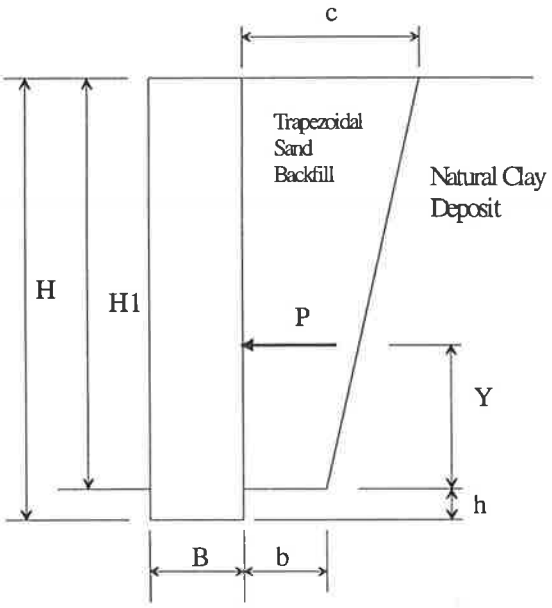

(h) Gravity walls with trapezoidal backfills

Figure 3.8 The selected retaining walls and backfill geometries (cont.).

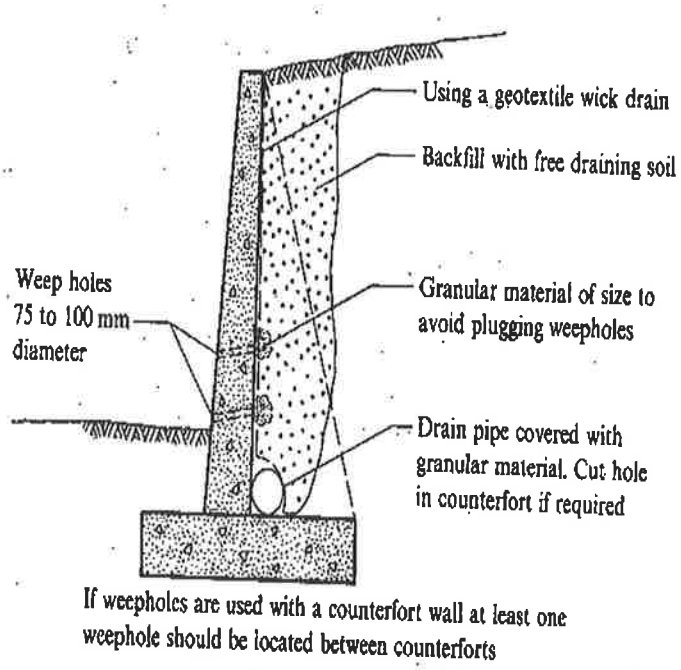

(a)

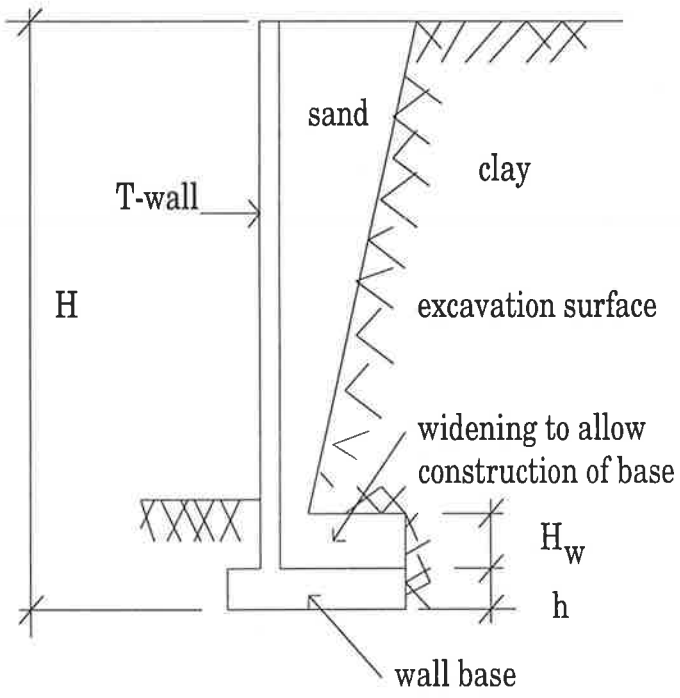

(b)

Figure 3.9 Narrow backfills: (a) cantilever T-walls with narrow granular backfills (*Bowles, 1988*); and (b) possible construction of the wall.

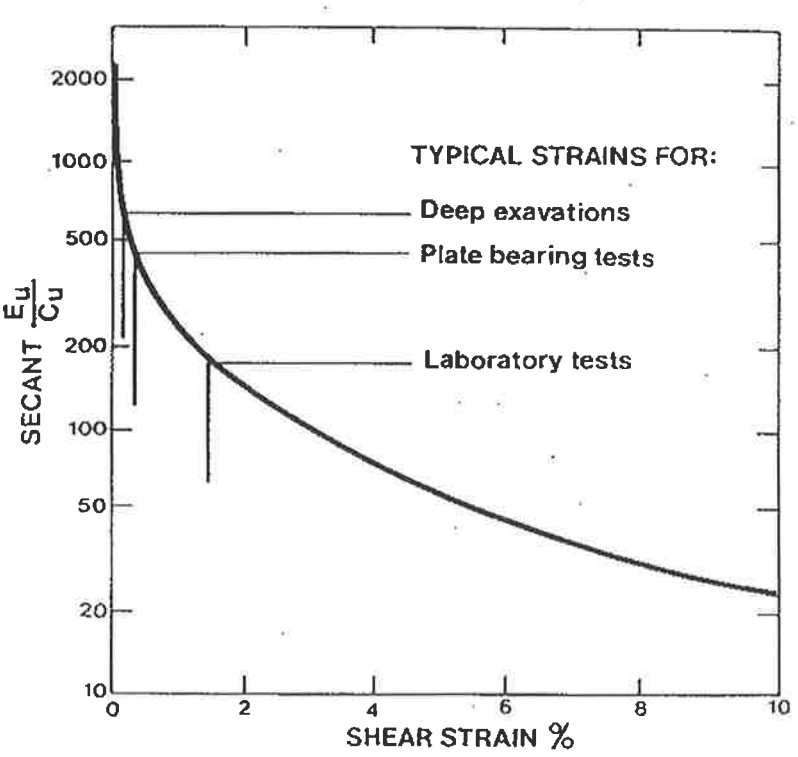

Figure 3.10 Variation of secant Young's modulus with shear strain, derived from the mathematical model of the London Clay (*Simpson et al., 1979*).

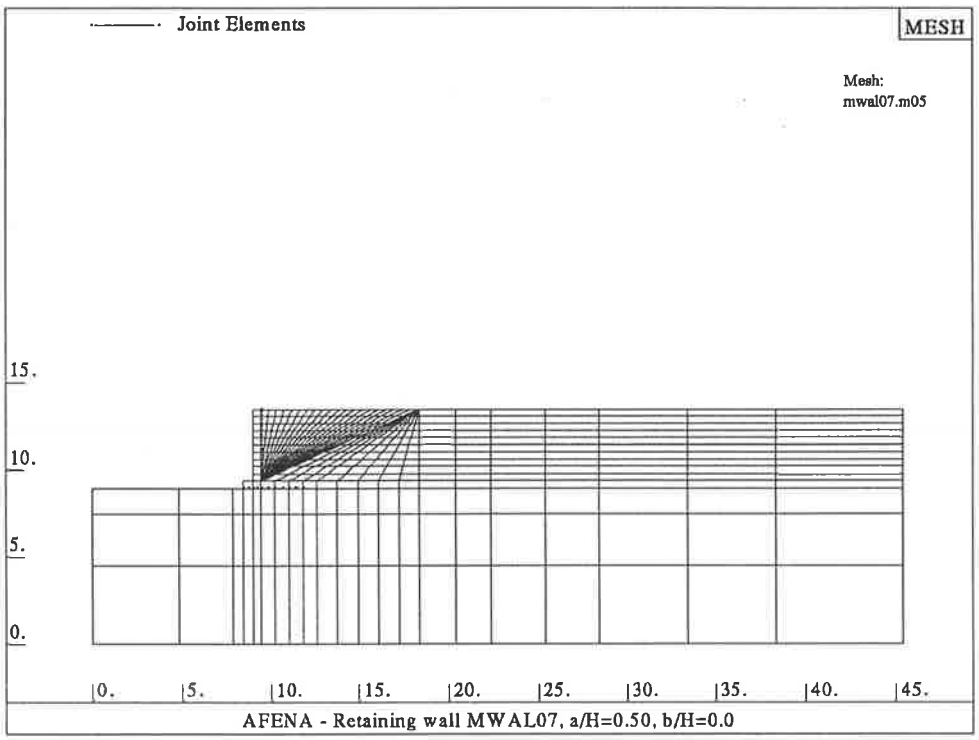

Figure 3.11 The finite element mesh used for cantilever T-walls with triangular backfills.

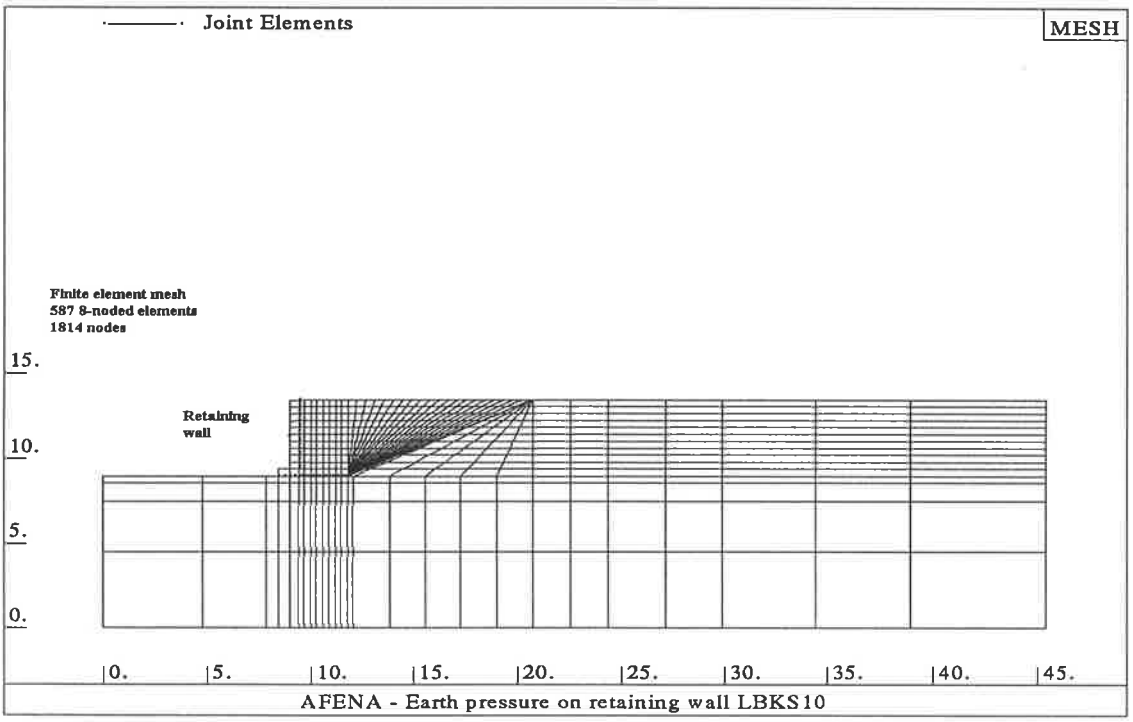

Figure 3.12 The finite element mesh used for cantilever T-walls with rectangular and trapezoidal backfills.

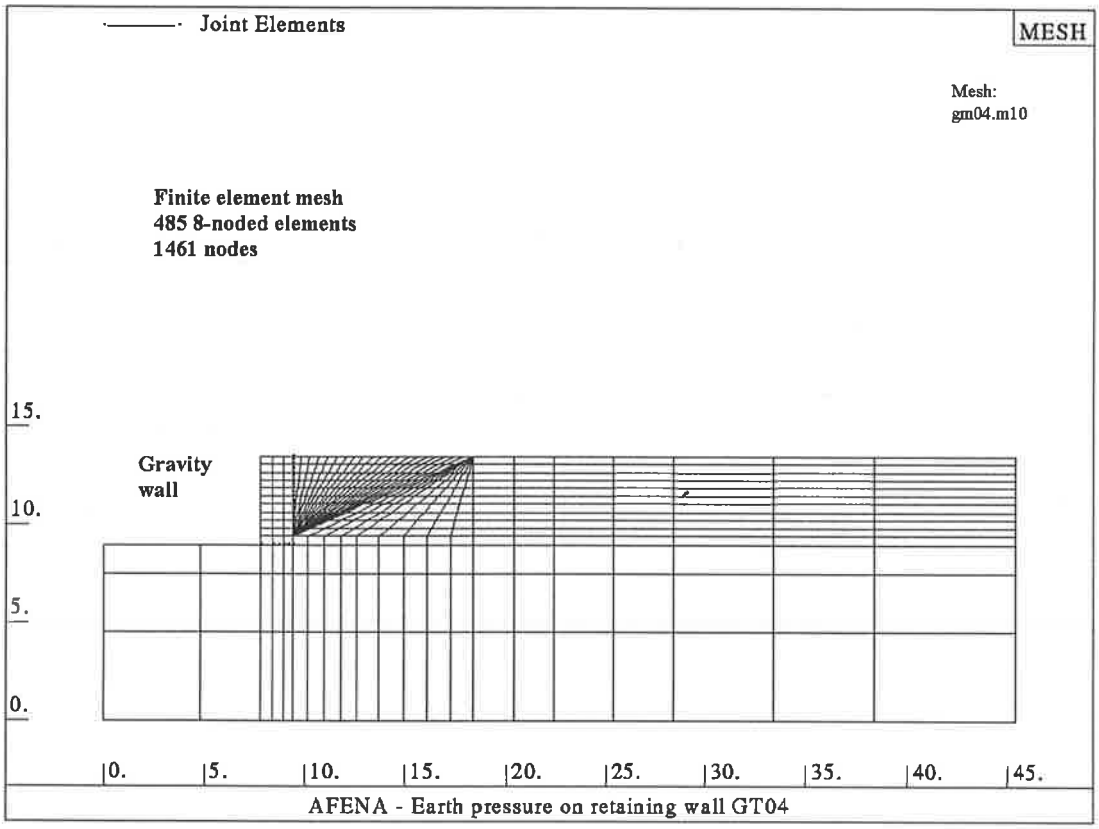

Figure 3.13 The finite element mesh used for gravity walls with triangular backfills.

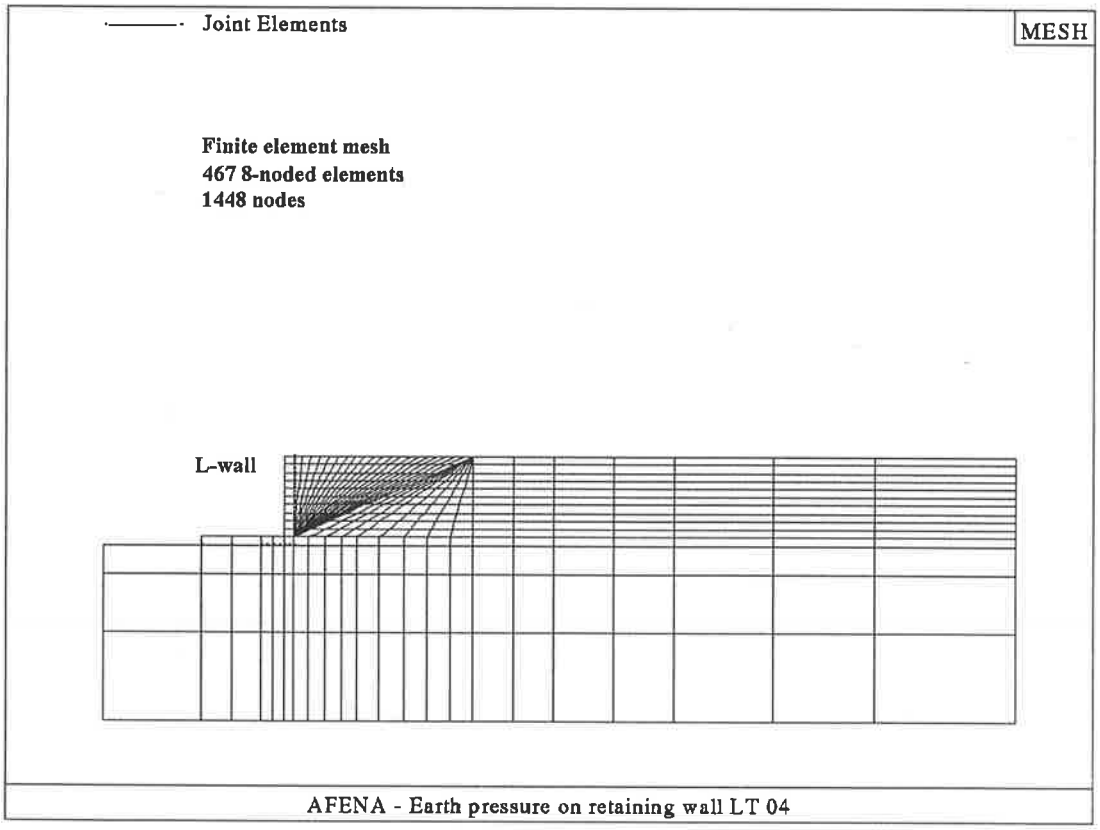

Figure 3.14 The finite element mesh used for cantilever L-walls with triangular backfills.

Chapter 4

Analysis of Cantilever T-Walls

4.1 INTRODUCTION

This chapter deals with the finite element (FE) analysis of cantilever T-walls supporting cohesive soils and having limited granular backfills. First, the unlimited backfill case is examined and the results are compared with another finite element study that was reviewed in Chapter 3. Also, a parametric study was performed to determine the key factors affecting the LEPs and to quantify their effects. Two different sets of analyses were carried out: limited homogeneous backfills, which are described in Sections 4.4 to 4.6; and limited non-homogeneous backfills that are described in Section 4.7.

In the first set, limited homogeneous backfill analyses have been carried out for three commonly used limited backfill geometries, namely: a triangular zone through the bottom of the stem; a rectangular zone; and a trapezoidal zone through the heel point. For each backfill geometry, lateral earth pressure distributions (LEPDs) and the maximum horizontal wall movements are given, together with the magnitude and location of the lateral thrust. Design curves are then given based on the FE results, which quantify the correction factor to be applied to Rankine active lateral thrust values.

In the second set, the case of a non-homogeneous limited backfill was examined where both materials, the granular backfill and the clay soil produced from excavation, are used in backfilling. The results of non-homogenous limited backfill analyses were compared with those of one analytical model in the literature.

The performance of simplified analytical methods that were reviewed in Chapter 2 is assessed to determine their suitability for design by comparing their predictions with those of the present numerical investigations.

4.2 UNLIMITED BACKFILL

(a) Unlimited Granular Backfill

First, the idealised case of a T-wall founded on granular soil with unlimited granular backfill was investigated. This was to validate the methodology described in Chapter 3 and to compare the results with those given by previous FE analyses of rigid walls with unlimited backfills. The unlimited backfill was modelled by backfilling the entire granular soil layers located between the back of the wall and the right boundary of the FE mesh.

The results indicated that the wall rotated about the toe with full outward movements. The settlement of the base of the wall was greater at the heel of the wall than at the toe, due to the larger settlement of the foundation subsoil in the vicinity of the heel compared with the toe. The maximum outward lateral movement of the wall due to rotation and sliding was $\Delta / H = 0.068\%$. This value is comparatively small and only 68% of that recommended by Terzaghi (1934) to develop the active state. However, the results are consistent with those of Goh (1993) and in good agreement with the findings of Broms and Ingelson (1972) that were presented in Table 2.1 of this thesis.

Figure 4.1 shows the distributions of the horizontal (lateral) earth pressures at two vertical planes; immediately adjacent to the back of the wall, and on a vertical plane passing through the heel. The lateral movements of the wall resulted in a reduction of the horizontal earth pressures on the back of the wall from the at-rest condition to the Rankine active values (RAVs) in the upper two-thirds of the wall height. In the lower third of the wall, the lateral pressures are significantly greater than the active pressures, and are close to the at-rest values. This is due to: (i) the effect of the large shear

stresses developed along the wall-base interface; and (ii) insufficient outward yielding of the wall within the lower third due to wall rigidity.

The lateral thrust at the heel of the wall was approximately 7% greater than that at the back of the wall. This may be attributed to the diminished influence of the lateral wall movement with increasing distance from the back of the wall. Also, the lateral thrust, with respect to the Rankine active thrust, was 1.285 times at the back of the wall, and 1.434 times at the heel of the wall.

These results are in good agreement with the results of the FE analyses of cantilever walls by Goh (1993). The lateral pressures developed at the back of the wall and heel of the wall were slightly larger than those predicted by Goh. This may be attributed to the difference in the construction sequence used in this research and that used by Goh (1993). He assumed that the wall had been already constructed before commencing the backfilling. This would result in a variation of the magnitude of wall movements as described in Section 3.4.3. In the present research, the wall has been constructed using simultaneous incremental construction of the wall and backfilling, as described in Section 3.4.3.

(b) Unlimited Clay Backfill

The case of unlimited clay backfill was examined, where the entire zone behind the wall was backfilled using a clay backfill. The maximum outward lateral movement of the wall due to rotation and sliding was $\Delta / H = 0.24\%$, for the stiff clay. This value is comparatively small when compared with the 5% that recommended by Tschebotarioff (1951) to develop the active state. Figure 4.2 shows the distributions of LEPs developed along the back of the wall and the virtual back, for the four clay types. Note that K_0 values in the latter figure are based on the soft clay parameters.

In general, the lateral earth pressures were less than the at-rest values, but significantly larger than the RAVs. The lateral thrust acting at the back of the wall was approximately 10% smaller than that developed at the heel of the wall. This is attributed to the effect of tension cracks developed at the back of the wall. The depth of tension cracks was approximately 0.1H for the soft clay and 0.23H for the very stiff clay. These values are significantly small when compared with those determined from Eq. 2.6.

4.3 PARAMETRIC STUDY

A set of analyses to measure the sensitivity of the results to the model parameters has been carried out, using models and parameters described in Chapter 3. It was found that, the key factors affecting the lateral pressures are: backfill size and geometry; wall stiffness and roughness; properties of the natural clay deposit; and the method of construction.

Shear stresses were very small because a smooth wall interface was assumed. Therefore, they have been neglected and the horizontal normal stresses have been taken as the lateral pressures acting on the wall. The lateral earth pressure distributions have been determined and compared with the linear at-rest and Rankine distributions. Note that the distributions of LEPs are plotted only along the height of the embankment, H1.

4.3.1 Effect of Wall Stiffness

(a) Wall Stiffness

The stiffness of the wall is represented by the flexural rigidity (E_cI_c), where E_c is the Young's modulus of concrete, and I_c is the second moment of area of the cross section of the wall. In practice, using a stiffer wall requires increasing the thickness of the stem of the wall, or using a higher grade concrete with a higher E_c. In this work, to model a stiffer wall, the thickness of the wall was kept unchanged, but the Young's modulus was increased.

The stiffness of the wall was examined for both trapezoidal and triangular backfill geometries. There was a minimal effect of the stiffness of the wall for a trapezoidal backfill as the large weight of the backfill limits the effect of wall deformations on the LEPs. However, for the triangular backfill there were significant effects. Figure 4.3 shows the LEPs distributions for: (i) $E_c = 25\times10^6$ kPa, which represents the typical design value of a reinforced concrete section; (ii) $E_c = 25\times10^9$ kPa, that corresponds to a very rigid wall. It can be seen that, the very rigid wall resulted in significantly higher lateral pressures on the back of the wall, compared to the first case, in the upper two-thirds of the wall.

This may be attributed to a decrease in the outward lateral deflection at the top of the wall in the second case, which was only 29% of the typical wall. The lateral pressures on the stiffer wall were close to the at-rest values over the full height of the wall. The lateral thrust was 13% higher than the corresponding value for the typical wall. The location of the lateral thrust has negligibly changed, therefore, the bending moments of the stiffer wall were approximately 13% larger than the corresponding values for the typical wall.

Based on these findings, it can be concluded that, the Adelaide Local Government Council's requirements of using a stiffer wall is unsuitable as it leads to higher lateral pressures and the possible cracking of the wall during its service life.

(b) Wall Movements

Figure 4.4 (a) shows the deflected shape of a T-wall, founded on the very stiff clay and having relatively wide rectangular backfill, after completion of backfilling. It can be seen that, the wall deflected laterally with a pure rotation about the base. There was approximately zero translation due to the large stiffness of the foundation subsoil and the large stiffness and strength parameters assigned to the base interface elements. The results of Harr (1977), for the case of outward rotation about the base, which is shown in Figure 2.3(d), will be compared with those of the FEM, for the wall shown in Figure 4.4 (a). Harr recommended the use of a simplified form, for Eq. 2.9, for a specific range of the angle of wall friction, $\phi/2 \leq \delta \leq 2\phi/3$. The angle of wall friction employed in the FE model was $\delta = 2\phi/3$. This simplified form of Eq. 2.9 is:

$$p = \frac{z\gamma\cos\varphi}{(1+1.2\sin\varphi)^2\cos\delta}\left[\cos\varphi - z\left(\frac{d\varphi}{dz}\right)\right] \qquad (4.1)$$

where

φ = $\varphi = \phi - \frac{\phi z}{H}$

m = $[1+\tan\delta/\tan\varphi]^{1/2}$

δ = angle of wall friction

φ = angle between the normal to the plane of rupture and the total reaction acting upon it

Figure 4.4 (b) shows the lateral pressure distributions determined from Eq. 4.1 (using $\delta = 22.8^0$) and that developed from the FE analysis. It can be seen that the lateral pressures predicted using Eq. 4.1 are significantly larger than those of the finite

element method. The lateral thrust using Eq. 4.1 is approximately twice that of the FEM. Based on these findings, it can be concluded that Harr (1977) model significantly overestimates the lateral pressure distribution in the case of outward rotation about the base.

4.3.2 Effect of Interface Roughness

In the FE analyses, the interface along the back of the wall was assumed smooth with the interface shear stiffness, $K_{ss} = 0.001$ MPa / m. The case of a rough back of the wall, with the interface shear stiffness, $K_{ss} = 490$ MPa / m, was examined. The lateral pressure distributions for the smooth and rough walls are shown in Figure 4.5.

The rough back of the wall resulted in slightly lower lateral pressures in comparison to the perfectly smooth wall. The magnitude of the horizontal component of the lateral thrust of the rough wall was lower than that of the smooth wall by approximately 10%, which compares well with the 7% reduction reported by Lambe and Whitman (1969).

The wall base roughness was also examined for the case of a comparatively smooth interface, with the interface shear stiffness along the base, $K_{sb} = 49 \times 10^3$ MPa / m. The smooth base resulted in a reduction of 2% in the lateral thrust with larger relative horizontal movements along the base of the wall in comparison to the rough base.

4.3.3 Effect of Stiffness of the Clay Deposit

The results showed that the stiffness parameters that affect the lateral pressure distribution at the back of the wall are: (i) Poisson's ratio of the embankment; (ii) Young's modulus of the embankment; and (iii) Young's modulus of the foundation subsoil. In the following, the effect of these variables are examined.

Two values were examined to determine the effect of the Poisson's ratio of the embankment: (i) $\nu_2 = 0.25$; and (ii) $\nu_2 = 0.49$. Figure 4.6 shows the lateral earth pressure distributions for these cases, where the lateral pressures in the second case are larger than those for the first case, particularly at the lower third of the wall. The magnitude of the lateral thrust in the second case was found to be 8% larger than that of the first case.

Young's modulus of the embankment was examined for three values: (i) E_2=20 MPa; (ii) E_2=70 MPa; and (iii) E_2=7 GPa. Figure 4.7 shows the lateral pressure distributions for these cases. It can be seen that the lateral pressures decrease as E_2 increases, particularly at the lower half of the wall. It was found that the magnitude of the lateral thrust of the second case is smaller than that of the first case by about 13%. Also, the lateral thrust of the third case was found 7% smaller than that of the second case.

The effect of the Young's modulus of the foundation subsoil, E_3, on the lateral pressure distribution was examined for two values: (i) E_3=70 MPa; (ii) E_3=7 GPa. Figure 4.8 shows the lateral pressure distributions for these cases, where larger lateral pressures at the lower half of the wall are associated with the stiffer subsoil. It was found that, for the second case of a stiffer subsoil, the lateral thrust increased by 5% and the settlements decreased to only 2%, in comparison to the first case.

The results show that there is minimal effect of the undrained shear strength of the embankment, c_u, on the lateral pressure distribution and the magnitude and location of the lateral thrust. When c_u was reduced by a factor of 4 the lateral thrust increased by only 0.3%. This may be attributed to the fact that a great part of the load was transmitted vertically to the subsoil.

The results showed that, large movements of the embankment soil, in the case of soft clay, cause comparatively large LEPs. On the contrary, lowers LEPs are associated with large deformations in the foundation subsoil (settlements). For T-walls, the stiffness of the embankment has the prime effect on the LEPs over the stiffness of the foundation subsoil, as the projected base of the wall limits the effect of settlements.

4.3.4 Method of Construction

Two methods of construction have been examined for T-walls with limited triangular backfills: (i) backfilling behind the wall; and (ii) excavating in the front of the wall. Figure 4.9 (a) shows the variation of the normalised lateral thrust, with respect to the Rankine active thrust, for different backfill size ratio (a/H). In the case of excavation, most of the movements were due to swelling, while for the case of backfilling they were mostly due to settlement. Typical wall movements, due to swelling, for the case of excavation in front of the wall are shown in Figure 4.9 (b). The normalised lateral thrust for the case of excavation was approximately 100% higher than the corresponding value for the case of backfilling.

On the basis of these sensitivity analyses it can be concluded that:

- the behaviour of the wall is complex and involves rotation and translation of the stem of the wall and the base of the wall. These movements appear to be influenced primarily by the stiffness of the stem of the wall, the wall-base interface, the stiffness of embankment soil, and the stiffness of foundation subsoil. These movements, in turn, affect the lateral soil pressures in the backfill; and

- the theoretical active pressures at the lower half of the wall are unlikely to develop, due to the employed safety factors against sliding and overturning that lead to relatively small wall movements and consequently large lateral pressures.

4.4 INFLUENCE OF TRIANGULAR BACKFILL ZONE

The methodology of the incremental finite element modelling used to simulate retaining walls having limited backfills was described in Chapter 3, and in the following only the results are presented. The results of limited homogenous granular backfills are presented and will be discussed in terms of: (i) the distribution of the LEPs and the associated wall movements; and (ii) the magnitude and location of the lateral thrust.

4.4.1 Distribution of Lateral Earth Pressures

The results of the triangular backfill indicate that the wall has typically rotated about the heel point, as shown in Figure 4.10. The magnitudes of outward wall movements increase as a/H increases and the stiffness of the embankment decreases, while they decrease as the stiffness of the subsoil increases. The maximum outward movements for the stiff clay was $\Delta / H = 0.02\%$ for a/H=2.0. The magnitudes of wall movements for the soft clays are larger by 10 to 15 times. Also, the results demonstrate that most of the wall movements are due to the horizontal deflection of the stem rather than sliding or rotation of the wall. For the case of an unlimited backfill, the wall rotated about the heel point due to the heavy backfill that extends a distance of 8H placed over the base. However, in the case of a limited triangular backfill, the rotation of the wall is typically about the toe, which is as expected due to the fact that the centre of gravity of the triangular backfill is closer to the toe than that of the unlimited backfill.

The lateral earth pressure distributions at the back of the wall for a/H values between 0.1-1.0 are shown in Figure 4.11. It can be seen that the lateral pressures increase as the backfill size ratio (a/H) increases. In general, there is a critical limiting value of the backfill size ratio (λ) at which the lateral thrust is equal to the Rankine active thrust. This value can be used to distinguish between two categories of backfills; narrow and wide backfills. This limiting value (λ) was 0.5, 0.6 and 0.7 for medium, stiff and very stiff clay, respectively. The value of λ was found to have a relatively small value of 0.1 for soft clay.

Huntington (1957) used the terms: *"steep slopes"* to identify narrow backfills; and *"gentle slopes"* to identify wide backfills. He suggested the value of λ to be the Coulomb classical value of $\cot\rho$ for all types of embankment soil, regardless of the type of natural deposit. Only the predicted value of λ for medium and stiff clay agree with this classical value. In the following, factors affecting the results for narrow and wide backfills are discussed.

(a) Narrow Backfills

In the case of narrow backfills, the plane of rupture can not form within the backfill zone and the classical theories are invalid. The wall movements at the upper part were much larger than those within the lower part. Figure 4.11 (a) shows the distribution of lateral earth pressures where they are uniform and significantly less than the Rankine active values for small a/H values. This uniform distribution was found due to: (i) the developed shear force along the excavation surface; and (ii) the stress redistribution within the backfill soil and the natural deposit. Below, this latter factor is explained to some depth.

The backfill soil in narrow backfills behaves in a confined manner. This confinement affects the behaviour of the granular backfill soil and the natural clay deposit. A considerable part of the load resulting from backfilling was absorbed and turned laterally to the embankment rather than taken by the vertical stresses within the backfill. Accordingly, the vertical pressures within the natural deposit and close to the excavation surface exceeded the geostatic pressures, while the vertical pressures decreased within the backfill zone and were less than the geostatic ones (γh).

Another factor relates to the plastic behaviour that contributes to the reduction of the horizontal stresses, is the dilation effect. Since an associated flow rule was adopted with $\varphi = \phi$, this considerably reduces the horizontal pressures at failure.

The confined behaviour and stress redistribution effects were reported in a number of field measurements on retaining walls having limited backfills. Kany (1972) reported that the stress redistribution was responsible for the lateral pressures decreasing during placement of the backfill behind a buried concrete pump storage plant. This pump house had a cylindrical shape and the backfill was trapezoidal. Measurements on a 2 m high model retaining wall with a limited trapezoidal granular backfill, conducted by Rehnman and Broms (1972), also demonstrated that the stress redistribution was responsible for the low vertical pressures within the natural deposit, particularly at the bottom of the excavation surface.

(b) Wide Backfills

Figure 4.11 (b) shows typical lateral earth pressure distributions for wide backfills. The effects of stress redistribution and lateral confinement diminished with increasing size of the backfill. Two zones in the distribution of the LEPs can be observed:

- in the upper half of the wall, the overburden pressures within the backfill zone decrease due to the combined effect of the wall yield and the shear stresses developed along the excavation surface. As a result, the lateral pressures are close to the Rankine active values; and

- in the lower half, the vertical stresses within the backfill zone are close to, but less than, the geostatic ones, but the horizontal pressures are very large and exceed the at-rest values. The increase of the LEPs within the lower half of the wall most probably results from the confinement at the apex of the triangular shaped backfill.

4.4.2 Magnitude and Location of Lateral Thrust

(a) Magnitude of Lateral Thrust

It was pointed out in Section 4.4.1 that the magnitude of the lateral earth pressure significantly increases with the backfill size ratio (a/H). Since the lateral thrust being the integral of horizontal pressures, the lateral thrust increases with the ratio (a/H). For example, in the case of stiff clay, the lateral thrust increases from a small value of $0.25P_a$, for a/H=0.1, to $2.3P_a$, for a/H=2.0, where P_a is the Rankine active thrust for an unlimited granular backfill. To account for the variation of the lateral thrust with the

backfill size ratio (a/H), a correction factor β is used to relate the predicted lateral thrust to the classical Rankine active thrust:

$$P = \beta . P_a \qquad (4.2)$$

where

P = lateral thrust obtained from the FEM

P_a = Rankine active thrust for unlimited granular backfill.

Figure 4.12 shows the variation of the lateral thrust correction factor, β, for the four clay types, for a/H values between 0.1-2.0. It can be seen that, the general trend for the four clay types is that β increases with a/H in a non linear form. However, for the soft clay there is a large scatter in the results due to large movements associated with the soft clay, which lead to apparent numerical instability in the solution.

The lateral thrust correction factor determined using Huntington's (1957) analysis is also shown in Figure 4.12. It can be seen that, Huntington's values are larger for narrow backfills in comparison to those of the FEM except for the soft clay. The trend of the numerical results agrees well with Huntington's trend only for narrow backfills. Huntington assumed that the sliding surface in narrow backfills is the excavation surface which agrees well with the extension of the plastic zone developed from the numerical analyses. However, Huntington's assumption, that the type of the embankment soil does not affect the results, is not shown by the FEM results.

Further, as suggested by Huntington, the assumption of zero cohesion along the excavation surface was used to determine β in Figure 4.12. This explains, to some extent, why the FE values are less than those of Huntington for narrow backfills. He also concluded that, for wide backfills, the classical theories are valid, and $\beta=1.0$, regardless of the backfill size. However, the numerical results demonstrate that the lateral thrust continues to increase with a/H, even beyond the limiting value λ, due to the backfill-embankment interaction.

Figure 4.13 shows suggested design curves for the correction factor β based on the curves of best fit to β versus a/H which were determined by least squares regression. Hyperbolic models were found to give the best correlations.

(b) Location of Lateral Thrust

The distance of the line of action of the lateral thrust, measured from the base of the embankment, Y, was determined and normalised with respect to the height of the stem, H1. Figure 4.14 shows the variation of Y/H1 for a/H values between 0.1-2.0. It can be seen that, the trend for the four clay types is Y/H1 decreases as a/H increases. It was explained in Section 4.4.1 that the lateral pressure distributions for narrow backfills are uniform, and this explains why the lateral thrust is located close to the mid height of the stem. On the other hand, the lateral pressure distributions for wide backfills increase linearly with depth, and this explains why Y/H1 is close to the classical value of 1/3 for the range of a/H between 0.5-1.0.

Figure 4.15 shows the proposed design curves for Y/H1, which are the curves of the best fit for the data shown in Figure 4.14. The design curves for magnitude and location of the lateral thrust can be of benefit for design purposes. For example, for the stiff clay, the lateral thrust predicted using the design curves in Figure 4.13 and Figure 4.15 yields that (i) for a/H=0.1; $P=0.25P_a$ and Y/H1=0.42; and (ii) for a/H=2.0; $P=1.80P_a$ and Y/H1=0.24. This would result in a reduction of 68% and an increase of 30%, respectively, in the corresponding maximum bending moment based on Rankine's method.

4.5 INFLUENCE OF RECTANGULAR BACKFILL ZONE

The rectangular geometry results from a relatively steep cut which might be founded within a comparatively stiff clay deposit. The analyses have been carried out for the four clay types, and for b/H values between 1/15-8/15, where the ratio 8/15 is the value of B_1 / H in Figure 3.8 (c). The analyses have been carried out for these fine increments as large variations in the lateral pressures were obtained from a small increase of b/H. Only the lateral pressure distributions at the back of the wall are investigated. The results of the modified silo equations developed by Bell (1987) are examined.

4.5.1 Distribution of Lateral Earth Pressures

The results demonstrated that, for narrow backfills with b/H less than λ, the wall rotated about the heel with a maximum active movement being $\Delta / H = 0.01\%$, for the stiff clay, as the centroid of the backfill was close to the toe. On the other hand, for wide backfills with comparatively large weight, the wall rotated about the toe with a maximum active movement of $\Delta / H = 0.023\%$. These values are small when compared with those of 0.1%, reported in the literature in Chapter 2, which are required to reach the active state. These trends of wall movements were typical for stiffer clays, but for medium and soft clays, there was more tendency for rotation about the heel, as there were large settlements at the toe due to the low stiffness of the subsoil.

Although the mode of rotation of the wall varies with the backfill size, the magnitudes of wall movements were sufficient for the backfill soil to reach the plastic state. The results showed that, the extension of the plastic zone behind the wall depends on the backfill size, and AFENA showed that the inner plane of rupture did not completely form, as assumed in the classical theories. Figure 4.16 shows the plastic zones formed behind a T-wall founded on a stiff clay with b/H=8/15, where the plane of rupture cuts the wall within its lower third.

The lateral earth pressure distributions at the back of the wall for a/H values between 1/15 and 8/15 are shown in Figure 4.17. The LEPs significantly increase as the size of backfill increases, as is the case for triangular backfills. The limiting value, λ, was also used to distinguish between narrow and wide backfills. It was found that λ was equal to 0.18, 0.28, 0.33 and 0.4 for soft, medium, stiff and very stiff clays respectively. In these distributions two types of backfill can be distinguished; narrow and wide backfills.

(a) Narrow Backfills

In this case, b/H is less than λ and the LEPs are less than the Rankine active values, particularly within the lower half of the wall, as shown in Figure 4.17 (a). A small increase in b/H from 1/15 to 2/15, produces a large increase in the LEPs, particularly within the upper part of the wall. The lateral pressures increase very rapidly with b/H and reach the Rankine active condition at small values of b/H compared to triangular backfills. As it was explained in Section 4.4.1, stress redistribution due to confinement of the backfill soil and shear stresses along the excavation surface are responsible for the lateral pressures being less than the RAVs.

(b) Wide Backfills

In this case, b/H is larger than λ and the lateral pressures are approximately linear and close to the RAVs along the full height of the wall, as shown in Figure 4.17 (b). The analyses demonstrate that the plane of rupture has partially formed but intersects with the wall at a point within the lower third. Accordingly, the lateral thrust is very close to the Rankine active thrust. The backfill-embankment interaction has a slight effect when compared with the triangular zone. This is as expected since the excavation surface is vertical and there is less lateral effect of placement of backfill on the embankment soil, unlike triangular backfills.

The modified silo equations developed by Bell (1987), are examined for the case of T-walls founded on stiff clay and having relatively wide rectangular backfill, with b/H=8/15. Figure 4.18 (a) shows the vertical pressure distribution predicted using the FEM and those given by Eq. 2.10. Figure 4.18 (b) shows the lateral pressure distributions predicted using Eq. 2.11 and those resulted from the FEM. It can be seen that, the lateral pressures predicted using Eq. 2.11 are larger, particularly at the upper two thirds of the wall. Accordingly, the lateral thrust of Eq. 2.11 is 10.4% larger than that of the FEM.

4.5.2 Magnitude and Location of Lateral Thrust

(a) Magnitude of Lateral Thrust

Figure 4.19 (a) shows the variation of the lateral thrust correction factor, β, with b/H, where β increases with the size of backfill, b/H, for the four clay types. The values of β determined from Eq. 2.11 are also shown. The properties of the granular backfill which were used in Eq. 2.11, are $\phi = 30^0$, $\delta_s = 2\phi/3$ and K=0.5. It can be seen that, the values of β of the medium clay obtained from the FEM are well represented by Eq. 2.11.

Figure 4.19 (b) shows the design curves for the correction factor, β. It can be seen that the values of β for rectangular backfills are larger than the corresponding values for triangular backfills, ie for a/H=b/H. For example: (i) for a triangular zone in a stiff clay with a/H=0.4, β=0.75 from Figure 4.14; (ii) for a rectangular zone in a stiff clay with b/H=0.4, β=1.25 from Figure 4.19 (b). In the case of rectangular backfill the weight of the backfill zone is twice that of the triangular backfill, and this accounts for the lateral thrust being 1.7 times larger.

(b) Location of Lateral Thrust

Figure 4.20 (a) shows the magnitude of the normalised distance of the lateral thrust, Y/H1, measured from the base of the embankment. It can be seen that Y/H1 slightly decreases with increasing b/H, with a maximum value of 0.42 and a minimum value of 0.32. The suggested design curves for Y/H1 are shown in Figure 4.20 (b). It can be seen that the classical value of 1/3 is only valid for the very stiff clay between b/H= 0.4-0.6. For the other cases Y/H1 was slightly larger than the classical value.

4.6 INFLUENCE OF TRAPEZOIDAL BACKFILL ZONE

The trapezoidal backfill is a commonly used form of construction for cantilever T-walls. Both the stresses acting on the back of the wall and at the virtual back of the wall (vertical section through the heel) are investigated. These locations are of interest to present a detailed summary of the behaviour of the soil throughout the limited trapezoidal backfill zone. The distributions of the LEPs at both the back of the wall and the virtual back were presented only along the embankment height (H1). The analyses have been carried out for values of c/H between 0.1-2.0, where the distance, c, is shown in Figure 3.8 (b).

4.6.1 Distribution of Lateral Earth Pressures

The results demonstrated that for the four clay types, the wall rotated about the toe, with full active movements, as shown in Figure 4.21. The maximum active movement at the bottom of the wall was $\Delta / H = 0.022\%$, for the case of stiff clay. The backfill weight was relatively large and its center of gravity was located closer to the heel. Accordingly, the wall rotated about the toe, unlike triangular backfills. The results demonstrated that the lateral wall movements, in the case of soft clay, were of the order of 10 to 15 times larger than those for the stiff clay. The average settlements under the base of the wall, in the case of soft clay, were of the order of 10 times larger than those of the stiff clay.

The shear force developed along the excavation surface is a direct function of the relative movements along this surface which, in turn, depends on the settlements of the backfill relative to the embankment. Since the settlements, in the case of soft clay, are larger, the magnitude of the lateral force acting on the virtual back (based on

equilibrium) is comparatively less than a stiffer clay. Therefore, it is expected that the correction factor, β, possesses small values for soft clay, compared with the medium, stiff and very stiff clay at the virtual back of the wall.

(a) Wall Back

Typical lateral earth pressure distributions are shown in Figure 4.22 (a) and (b). The results show that there are minimal variations in the distribution of the lateral earth pressure for c/H larger than 1.0. It can be seen that, when c/H increases, there are negligible changes in the magnitudes of the LEPs within the upper two thirds of the wall. However, there is a significant increase in the LEPs within the lower third of the wall. This increase is responsible for the increasing nature of the lateral thrust acting on the back of the wall as c/H increases.

The results reveal that, for a relatively narrow backfill having a small value of c/H, the LEPs slightly exceed the RAVs along the full height, except for the lower region where values of the LEPs are between the RAVs and the at-rest values. Accordingly, the lateral thrust is slightly more than the Rankine active thrust, and the magnitude of the correction factor, β, exceeds 1.0 for all values of c/H.

For wide backfills, the nature of the distribution of the LEPs was similar to narrow backfills, but the magnitudes of the LEPs exceed the at-rest values in the lower third of the wall, as shown in Figure 4.22 (b). It is of importance to realise that the distribution of the LEPs at the back of the wall, for a wide trapezoidal backfill, is close to that of an unlimited granular backfill shown in Figure 4.1.

(b) Virtual Wall Back

Typical lateral earth pressure distributions along the virtual back of the wall are shown in Figure 4.23 (a) and (b). It can be seen that, the distributions at the virtual back are significantly different in nature than those at the virtual back of the wall. This is because the confinement effects are larger, whereas base effects are smaller, at the virtual back. There are minimal variations in the distributions of lateral earth pressures for c/H larger than 1.0, therefore typical distributions of lateral earth pressure are given for c/H between 0.1-1.0. For a relatively narrow backfill zone (c/H=0.1) the LEPs are close to the RAVs, and the correction factor (β) is less than, but close to, 1.0. Also, Figure 4.23 shows that as c/H increases, the LEPs increase along the full height of the wall. For soft and medium clays, the LEPs are significantly less than the RAVs.

4.6.2 Magnitude and Location of Lateral Thrust

(a) Magnitude of Lateral Thrust

Figure 4.24 shows the variation of the lateral thrust correction factor, β, at the back of the wall for backfill size ratios (c/H) between 0.1-2.0. It can be seen that, for the four clay types, β increases as c/H increases. Also, the values of β for stiff and very stiff clays are essentially identical.

It can be seen that, the lateral thrust correction factor, β, is larger for medium clay than for stiff and very stiff clays for narrow backfills, whereas it is smaller for wide backfills. This is likely to be due to increasing settlements as c/H increases. The settlements produce large shear forces along the excavation surface which, in turn, cause lower LEPs. Figure 4.25 shows the proposed design curves, where only a single design curve is given for both stiff and very stiff clays.

Figure 4.26 shows the variation of β with c/H values between 0.1-2.0 obtained at the virtual back of the wall. It can be seen that the value of β for soft clay is smaller than the corresponding value for the very stiff clay. The scatter in the results most probably results from the complex interaction between the embankment movements, wall movements and settlements of the backfill and the subsoil. This interaction is discussed in some depth in Section 4.8. In comparison, the values of β at the back of the wall are more consistent because the base of the wall limits the relative movements. Figure 4.27 shows the design curves for β at the virtual back of the wall.

It can be seen that, at the virtual back of the wall, the value of β is less than 1.0 for narrow backfills, indicating confined behaviour of the backfill soil located between the excavation surface and the vertical section through the heel. However, β values shown in Figure 4.27 are comparatively large compared to those of narrow triangular backfills shown in Figure 4.13. This likely results from different boundary conditions which affect the stress redistribution between the backfill soil, embankment soil and the retaining wall.

(b) Location of Lateral Thrust

At the back of the wall, the distance measured from the base of the embankment to the line of action of the lateral thrust (Y/H1) is shown in Figure 4.28. It can be seen that, for the four clay types, Y/H1 decreases as c/H increases. The design curves for Y/H1

applicable at the back of the wall are shown in Figure 4.29. Only a single curve is given for the stiff and very stiff clays owing to the very close values of Y/H1 obtained from the analyses.

For the virtual back of the wall, the normalised distance (Y/H1) is given in Figure 4.30. It can be seen that, there is a scatter in the results with small variations between maximum and minimum values of Y/H1=0.411 and Y/H1=0.33, respectively. As discussed, complex interaction of backfill settlements, embankment and wall movements causes considerable scatter in the results. In comparison, most of the values of Y/H1 for the back of the wall are less than the classical value of 1/3 while, for the virtual back, most of the values are greater than 1/3. The design curves for Y/H1 at the virtual back are shown in Figure 4.31.

4.7 INFLUENCE OF NON-HOMOGENEOUS LIMITED BACKFILL

The limited homogeneous backfills with three different geometries have been investigated in the previous three sections where the backfill was made entirely of a granular material. In the current section only the case of a trapezoidal non-homogeneous backfill is examined.

Cost factors lead to situations where it is not possible to backfill the entire excavated zone using a granular material. One of these situations results when a large excavation is made to allow for the construction of the base of the T-wall. This field situation is shown in Figure 3.8 (d), where the backfill zone is made partially of a granular triangular zone and the remaining part of the trapezoidal backfill contains a part of the excavated cohesive deposit. This case is termed here as the non-homogeneous backfill.

In this set of analyses the backfill size remains unchanged throughout the analyses, and the only variation was the *"relative size"* of the triangular, granular zone to the clay zone (a/H). This set of analyses is different from the other backfill geometries presented in the previous sections. The main difference is that the backfill size in the other geometries is made entirely of a granular soil, but here the total size that is actually constructed is constant and the relative size is varied. The analyses have been carried out for values of the relative size (a/H) between 0.2-2.0.

4.7.1 Distribution of Lateral Earth Pressures

Figure 4.32 (a) shows one example for a T-wall having a non-homogeneous backfill with a/H=2.0 and founded in the stiff clay deposit. It can be seen that the plastic zone extends in both the granular and the clay backfills. The right boundary for the plastic zone is the excavation surface, ie the boundary at a distance from the back of the wall, d=2H. The stage-by stage construction of this wall was shown in Figure 3.6. It can be seen that the embankment and the subsoil remain in the elastic stage.

The results showed that wall typically rotated about the toe, as was the case for trapezoidal backfills, with a maximum movement of $\Delta / H = 0.01$ for the stiff clay. There was a little variation in the magnitudes of wall movements as a/H increases. This results from the fact that the overall size of the backfill was kept unchanged.

Typical lateral earth pressure distributions at the back of the wall, for different a/H values, are shown in Figure 4.32 (b). It can be seen that, the lateral earth pressures are linear and close to the RAVs in the upper two thirds of the wall and exceed the at-rest values in the lower third. It can also be seen that the magnitudes of the lateral pressures significantly decrease as a/H increases, particularly within the lower half of the wall. Due to large initial lateral pressures from the clay backfill (K_0=1.0) and since there was minimal changes in the wall movements, the LEPs decreased as a/H increased. Although the wall rotated about the toe, the nature of the distribution of the LEPs is close to that of wide triangular backfills presented in Section 4.4.1.

4.7.2 Magnitude and Location of Lateral Thrust

(a) Magnitude of Lateral thrust

Figure 4.33 shows the variation of the lateral thrust correction factor, β, with the relative size, a/H, where β decreases as a/H increases for all clay types. It can be seen that the magnitude of β is considerably large, and reaches a value of 2.35 for soft clay at a/H=1.0. The term *"narrow backfills"* is invalid in this case as the magnitudes of β, for all a/H values, are larger than 1.0. Figure 4.34 shows the design curves for the lateral thrust correction factor.

Figure 4.35 shows some of the results of Bang and Tucker (1990) where the lateral thrust is normalised with respect to $\gamma_2 H^2$ (γ_2 is the embankment unit weight). It can be seen that, the lateral thrust decreases as the backfill size increases, which agrees

with the design curves shown in Figure 4.34. This primarily results from their assumption that failure is due to instability in both materials (the backfill and the natural deposit). Accordingly, the failure zone is composed of two zones: (i) the zone in the backfill with a large strength and hence a lower lateral thrust; and (ii) the other zone in the embankment with low a strength and hence a large lateral thrust. Increasing the backfill size leads to the case of the active wedge possesses a relatively large strength and consequently the lateral thrust decreases.

Also, similar results were obtained by limit equilibrium analysis of limited rectangular backfill by Stefanoff and Venkov (1972), where the lateral thrust decreases as the backfill size increases.

(b) Location of Lateral Thrust

Figure 4.36 shows the magnitude of the normalised distance (Y/H1) measured from the base of the embankment. It can be seen that all the values of Y/H1 are less than the classical value of 1/3 with a maximum value of 0.282. This resulted from the concentration of stresses at the lower third of the wall. Figure 4.37 shows the design curves for the location of the lateral thrust.

4.8 DISCUSSION OF RESULTS

A summary of the results of the FE analyses presented in this chapter is given in Table 4.1. The magnitudes of maximum and minimum values of β and Y/H1 are given, together with their maximum variation. The magnitude of the maximum wall movement with its mode of rotation are also given.

The results demonstrated that there was a confined behaviour within the backfill zone in the limited homogeneous narrow backfills. This confined behaviour is different from the confined behaviour in the oedemeter where the soil is fully laterally restrained. In comparison, in the limited backfill condition, the soil can deform laterally but limited by the stiffness of the embankment and the retaining wall. The confined behaviour depends on the state of stress along the boundary of the plastic zone, and the geometry of that boundary. The geometry of the boundary includes the geometry of the wall, the excavation surface and the ground surface. A very slight change in the state or the geometry of the boundary, changes the equilibrium of the forces acting within that

boundary which, in turn, produces a significant variation in the lateral pressures on the retaining wall.

In general, when the size of the backfill zone is increased, there are three different factors that control the lateral pressures:

- with respect to slope stability, the additional backfill weight shifts the centroid away from the retaining wall, thereby increasing the rotational movements which, in turn, decreases the lateral pressures;

- the lateral component of the additional backfill weight directly increases the lateral pressures; and

- the settlements beneath the base increase as the loading increases by the additional backfill weight, thereby reducing the lateral pressures.

The interaction between the latter factors is responsible for the lateral thrust to continue varying with the size of the backfill, even for stiff and very stiff clays. However, Huntington (1957) expected that, for stiff natural deposits, the lateral thrust will reach a maximum active value when $a / H = \cot \rho$.

The effect of the base of the wall on the distribution of the lateral earth pressures on T-walls having limited backfills is of considerable importance. The reinforced concrete base of the retaining wall can be viewed from two different respects:

- the base leads to a concentration of the LEPs, as a strut in a braced excavation. This analogy helps in answering the question of why the LEPs are very large at the lower part of the wall; and

- the base acts as an equivalent soil stratum with a stiffness greater than 60 times the average stiffness of soil used in the analyses, that greatly reduces the settlement effect.

As a result, large local lateral earth pressures at the critical section, where the stem meets the base, will be associated with wide homogeneous and non-homogeneous backfills. It is therefore, providing haunches at this critical section will be suitable to account for these large local pressures.

Although sufficient base width of the wall was selected, the results demonstrated that the distributions of lateral earth pressure for retaining walls founded on soft clays were erratic. This primarily resulted from the large difference in stiffness between the granular backfill and the soft clay deposit. Decreasing the stiffness of the clay leads to a case where the stability of the embankment controls the stress redistribution behind the wall and, consequently, the lateral behaviour of the wall. This represents a difficulty in obtaining confident results for soft clays.

In addition, the results of the homogeneous backfills indicated that, for a particular backfill size, the associated plastic zone extended only in the granular backfill between the back of the wall and the excavation surface, while the embankment soil remained in the elastic range. However, for the case of soft clay, an additional small zone under the heel went plastic.

4.9 SUMMARY

The finite element results, of a cantilever T-wall supporting cohesive clay deposits and having limited backfills, were presented. Two sets of analyses were investigated: the homogeneous granular backfills with three different geometries; and the non-homogeneous backfill. The nature of variation of the lateral thrust with the size of granular backfill zone for homogeneous backfills was significantly different from the non-homogeneous backfills. The limited homogeneous triangular backfill zone represents a severe case and significantly high lateral pressures are associated with this case, particularly near the bottom of the stem of the wall.

In homogeneous limited backfills, the embankment movements control the distribution of the LEPs for triangular backfills, while the settlements of the foundation subsoil primarily influence this distribution for trapezoidal shaped backfills.

Huntington (1957) procedure can be used only for narrow triangular backfills and trapezoidal backfills, but only at the heel of the wall for the latter. The modified silo equations developed by Bell (1987) can be used for homogeneous rectangular backfills founded on cohesive deposits except for soft clays. Bang and Tucker (1990) design curves are valid only for limited non-homogeneous backfills.

Table 4.1 Summary of the FE results of a cantilever T-wall with limited backfills

	unlimited granular backfill	Triang. zone	Rect. zone	Trap. zone		Non-homog.	Notes
				back	heel		
β_{max}	1.434	2.28	1.35	1.32	1.27	2.35	
β_{min}	1.285	0.24	0.25	1.07	0.44	1.32	
Maximum variation %	-	> 100	> 100	24	> 100	78	for the soft clay.
Max difference %			70	22	100	68	between soft and very stiff clays.
$(Y / H1)_{max}$	0.3	0.47	0.4	0.35	0.45	0.282	
$(Y / H1)_{min}$	0.3	0.25	0.32	0.29	0.32	0.241	
Maximum variation %	-	96	20	20	35	17	
Active mov. (Δ / H%)	0.068	0.02	0.01	0.02	-	0.01	these values are for stiff clay, but for soft clay wall movements are of the order of 10-15 times these values.
Wall rotation	toe	heel	toe / heel	toe		toe	
Lateral Earth pressures	linear						
- backfill size ratio		a/H	b/H	c/H	c/H		
- narrow backfills		uniform	uniform	linear	linear		
- wide backfills	-	linear	linear	linear	linear		
- limiting value (λ)		0.5-0.7	0.28-0.4	-	0.5-0.7		excluding the soft clay.

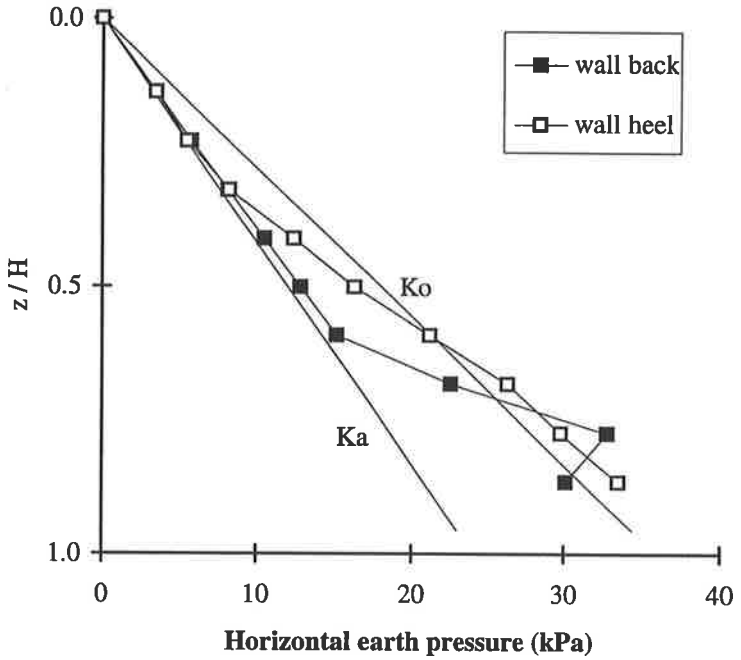

Figure 4.1 Lateral earth pressure distributions for T-walls with unlimited granular backfills.

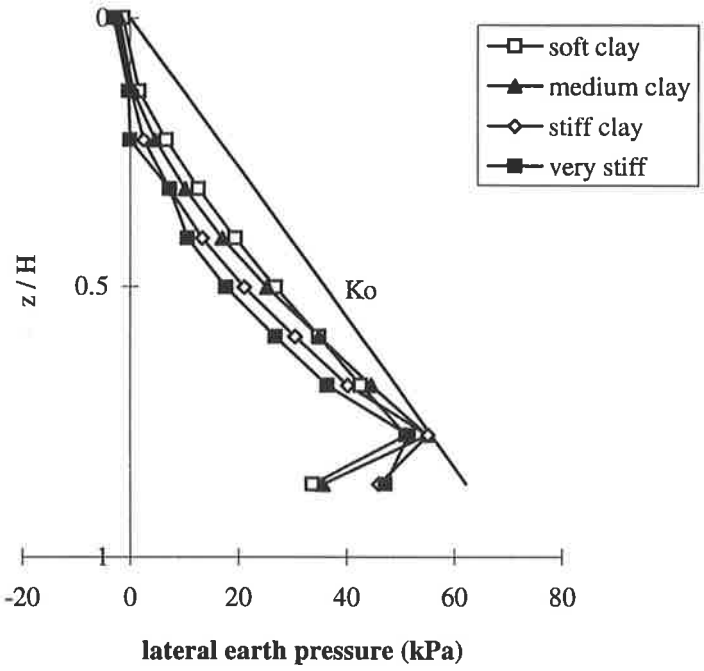

(a)

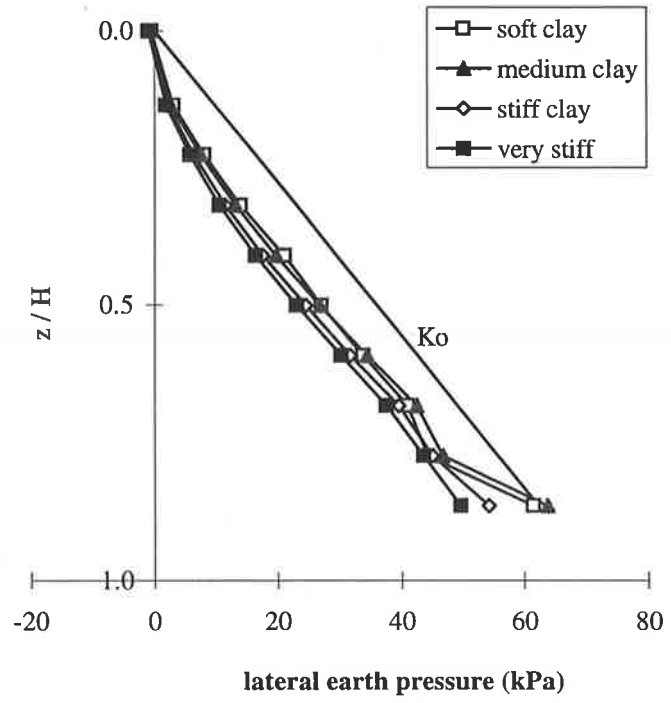

(b)

Figure 4.2 Lateral earth pressure distributions for T-walls with unlimited clay backfills: (a) along the back of the wall; and (b) along the virtual back of the wall.

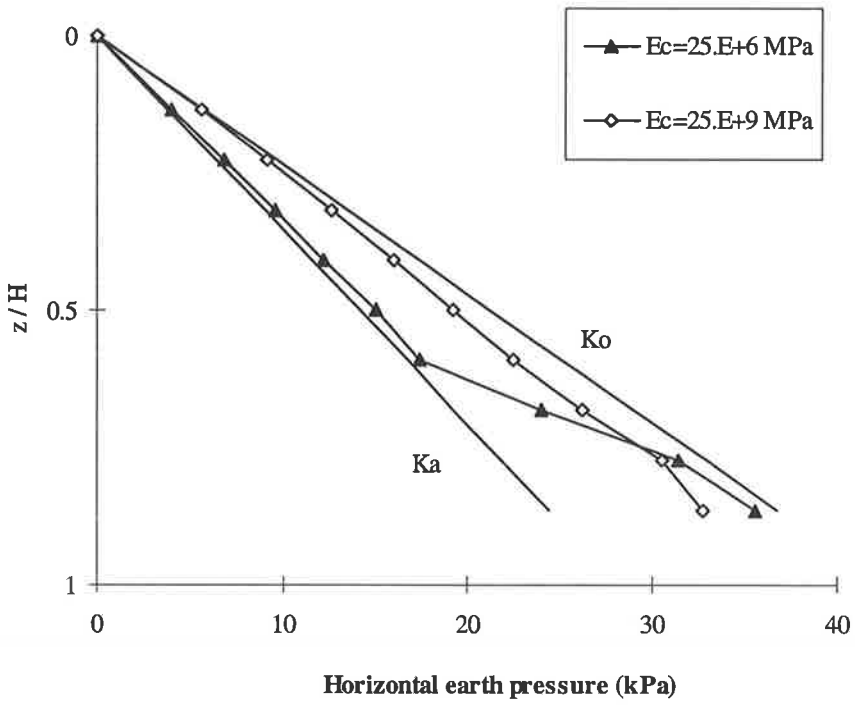

Figure 4.3 Effect of wall stiffness on the lateral pressures at the back of the wall.

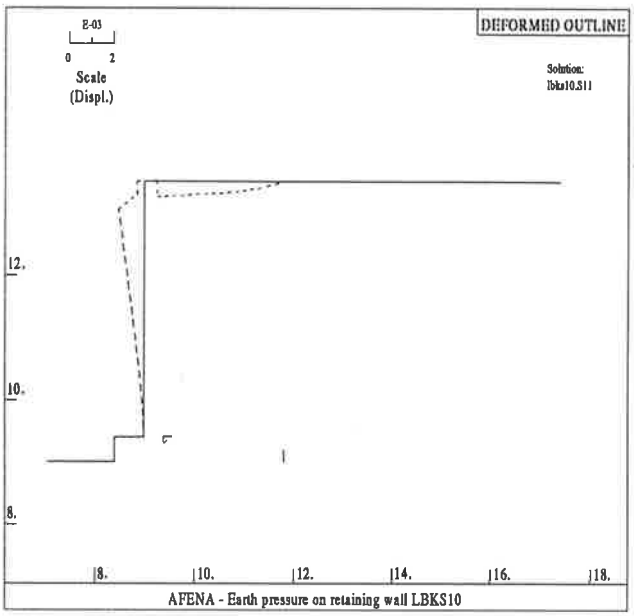

(a)

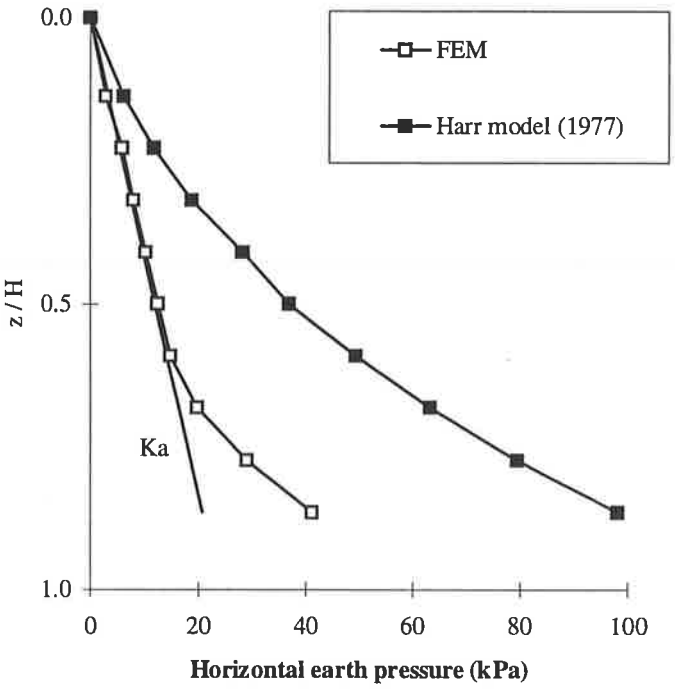

(b)

Figure 4.4 Comparison between the FEM and the results of the Harr (1977) model for T-walls founded on very stiff clays with unlimited backfills:(a) lateral wall movements from AFENA; and (b) lateral earth pressure distributions.

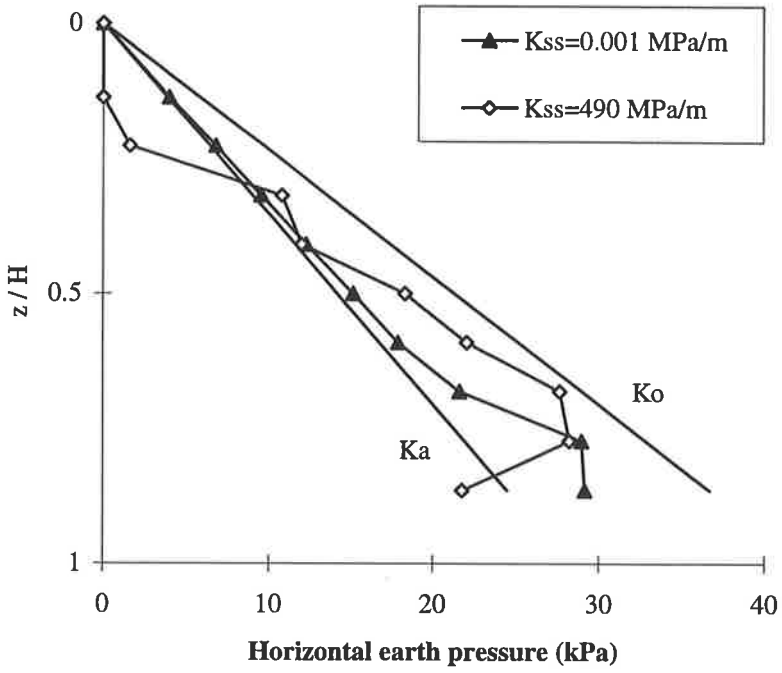

Figure 4.5 Effect of wall stem roughness on the lateral earth pressure distribution.

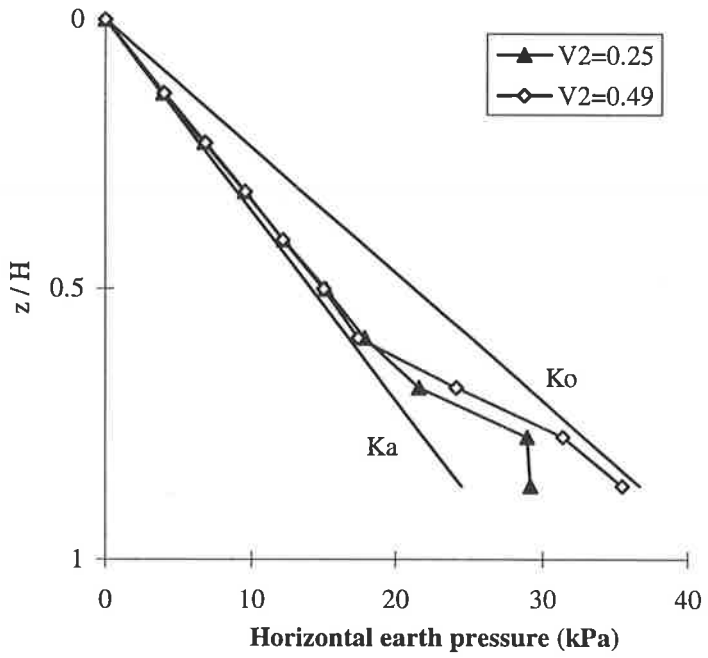

Figure 4.6 Effect of Poisson's ratio of the embankment on the lateral earth pressure distribution.

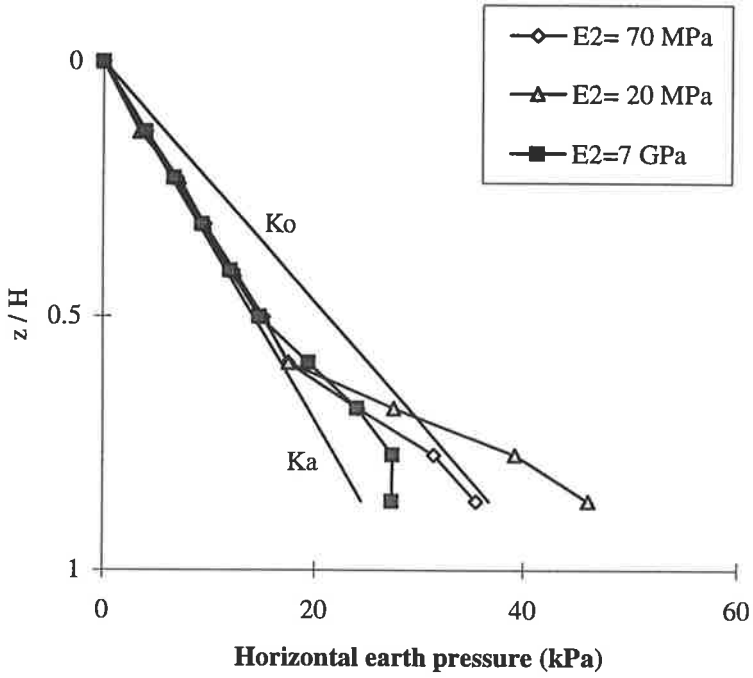

Figure 4.7 **Effect of Young's modulus of the embankment on the lateral earth pressure distribution.**

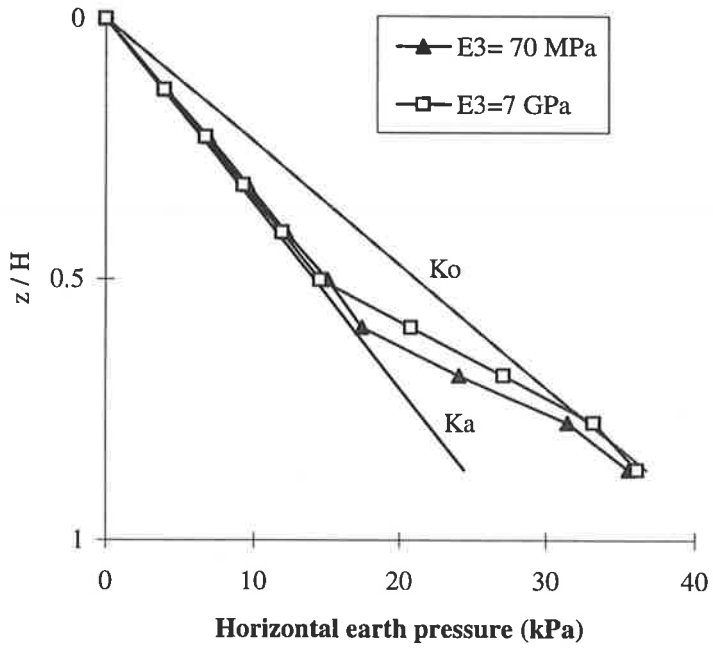

Figure 4.8 **Effect of Young's modulus of the foundation subsoil on the lateral earth pressure distribution.**

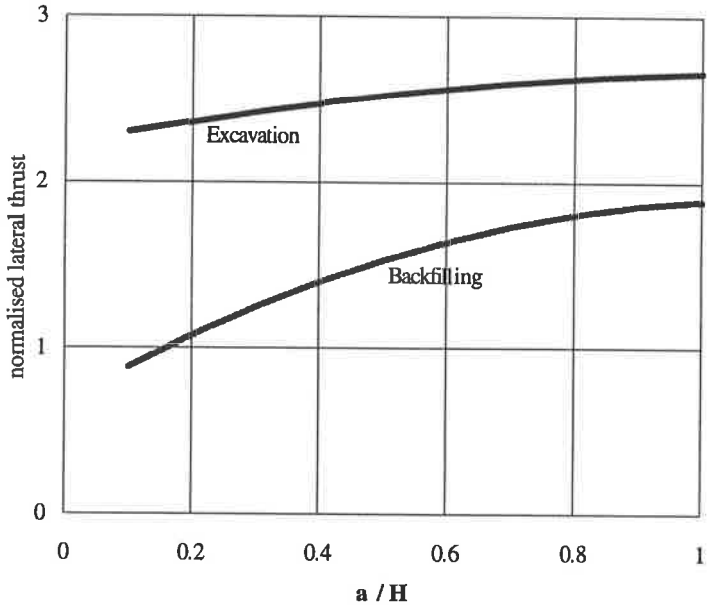

(a)

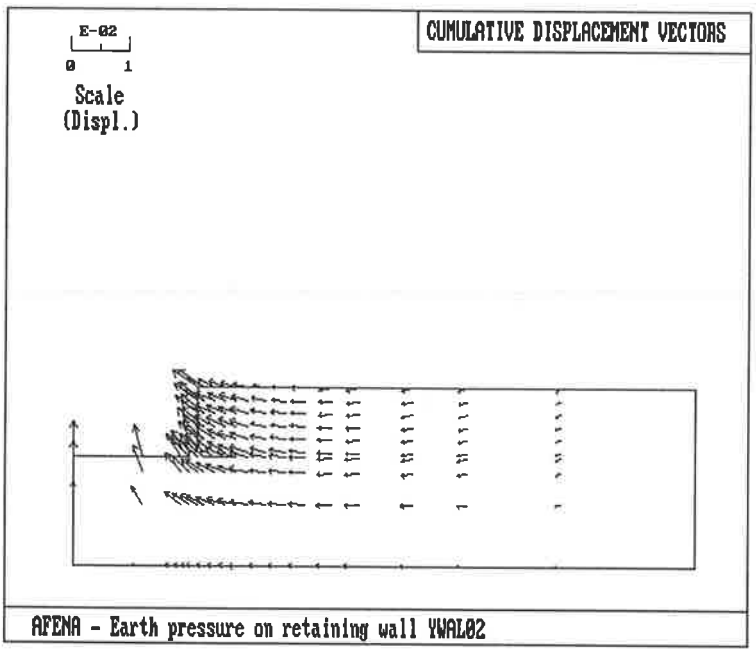

(b)

Figure 4.9 (a) Effect of the method of construction on the normalised lateral thrust; and (b) typical wall and soil movements for the case of excavation in the front of the wall.

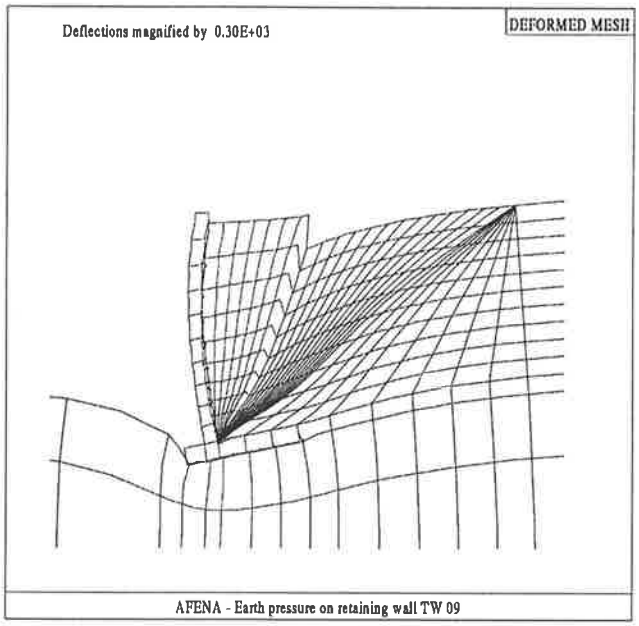

(a)

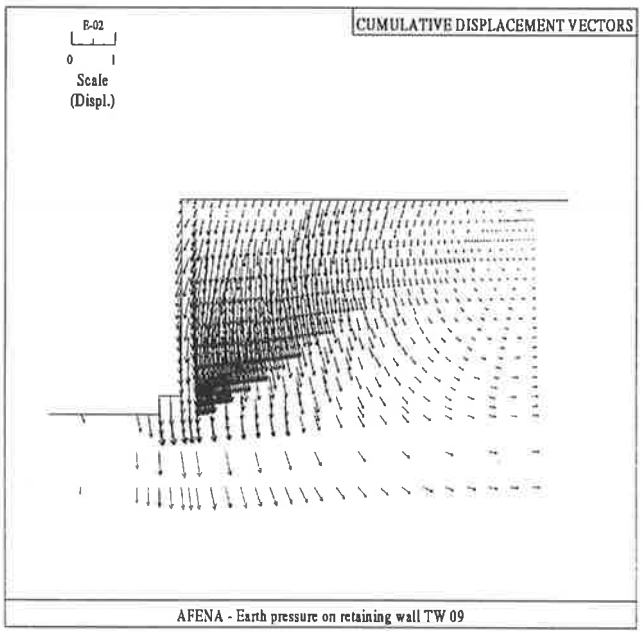

(b)

Figure 4.10 Typical wall and soil movements for T-walls having triangular backfills: (a) wall and soil movements; (b) accumulated displacement vectors.

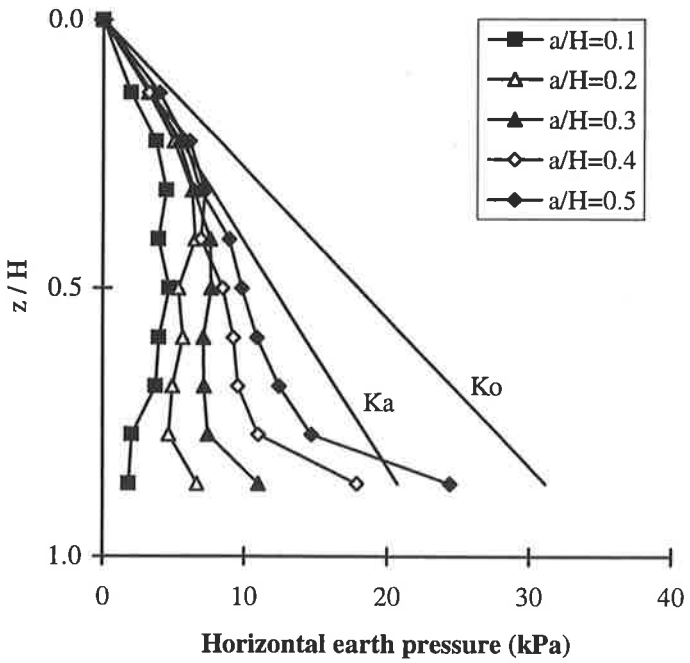

(a)

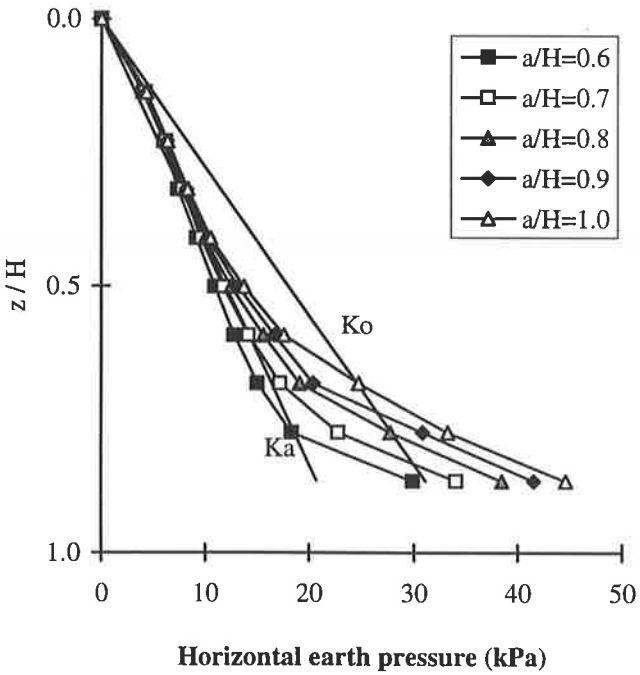

(b)

Figure 4.11 Typical lateral earth pressure distributions for T-walls with triangular backfills and founded on stiff clays: (a) a/H between 0.1-0.5; and (b) a/H between 0.6-1.0.

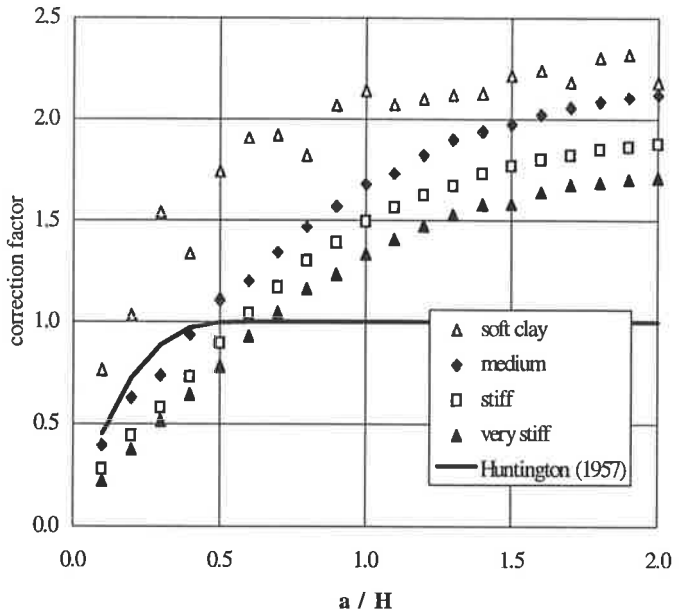

Figure 4.12 Variation of the lateral thrust correction factor with a/H for T-walls having triangular backfills and founded on cohesive soils.

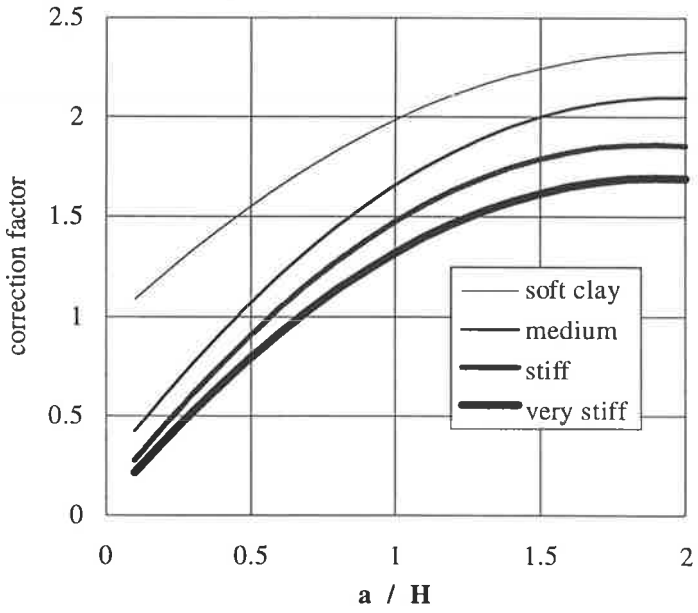

Figure 4.13 Design curves for the lateral thrust correction factor versus a/H for T-walls with triangular backfills founded on cohesive soils.

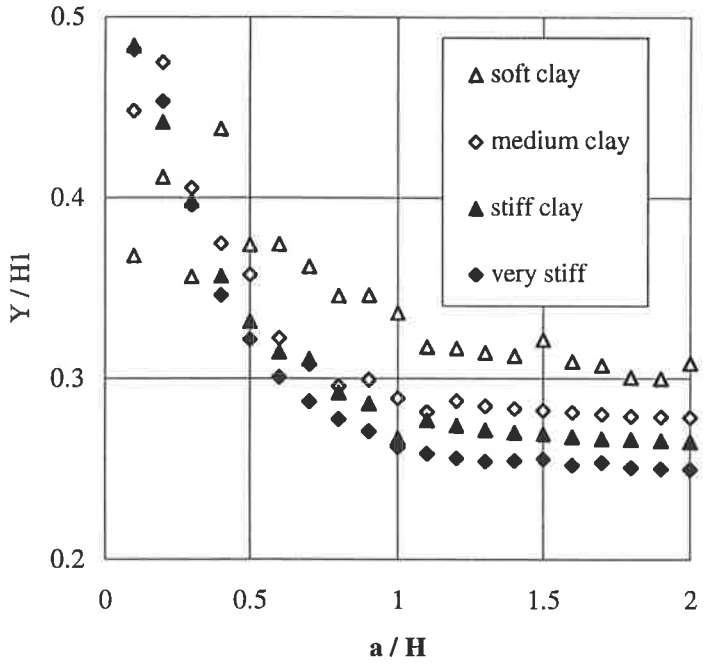

Figure 4.14 Normalised distance of the lateral thrust, Y/H1, versus the backfill size ratio, a/H, for T-walls with triangular backfills.

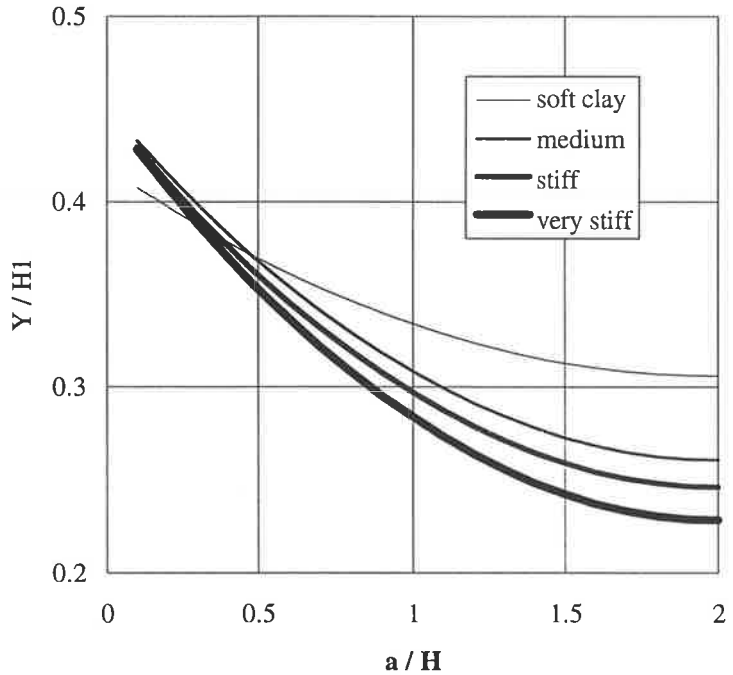

Figure 4.15 Design curves for the normalised distance of the lateral thrust, Y/H1, for T-walls with triangular backfills.

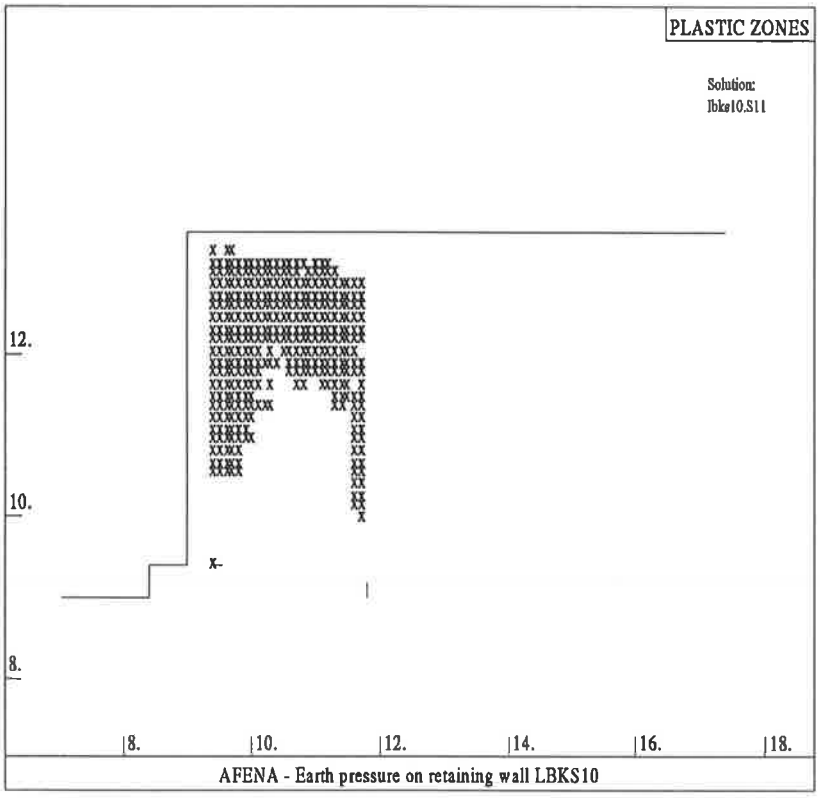

Figure 4.16 The plastic zone of a T-wall with rectangular backfill having b/H = 8/15, where the "X"s indicate soil in the plastic zone.

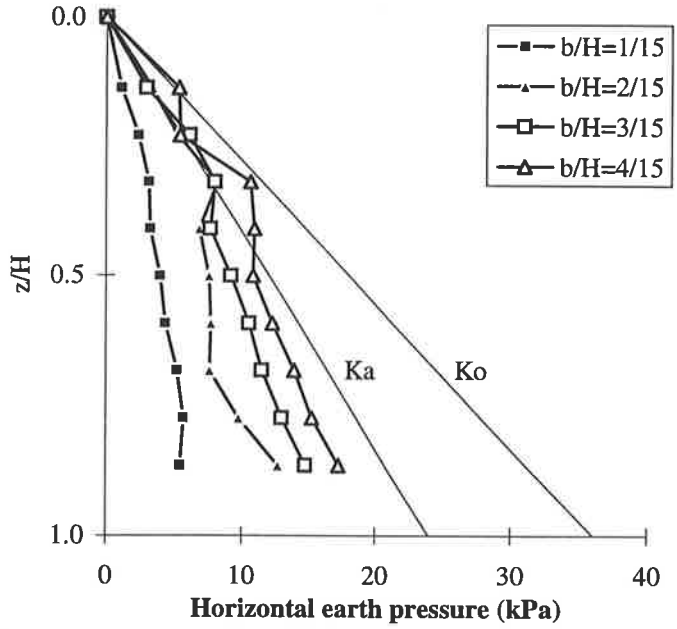

(a)

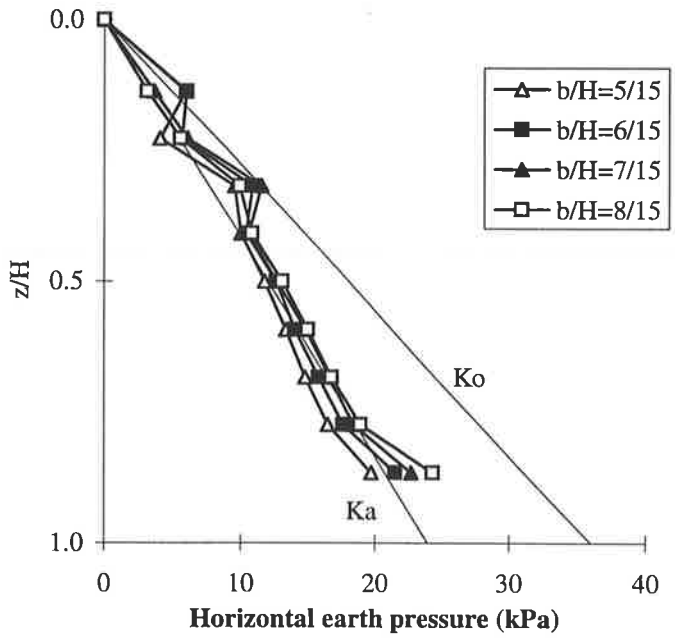

(b)

Figure 4.17 Typical lateral earth pressure distributions for T-walls with limited rectangular backfills and founded on stiff clay deposits: (a) b/H between 1/15-4/15; and (b) b/H between 5/15-8/15.

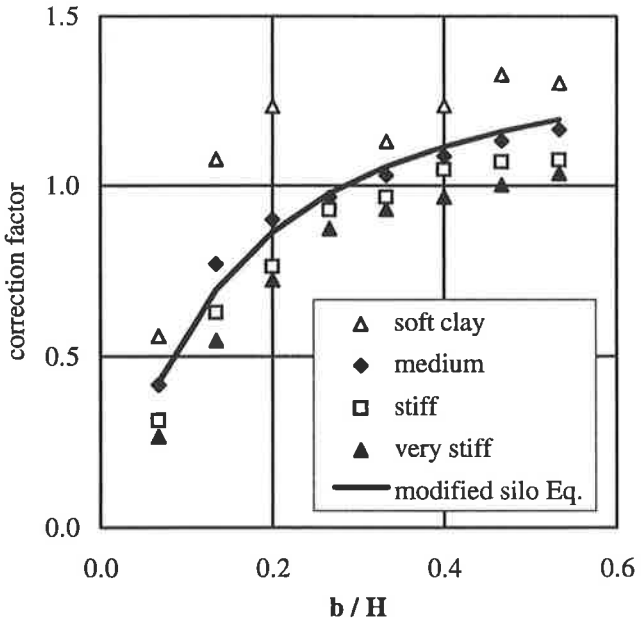

(a)

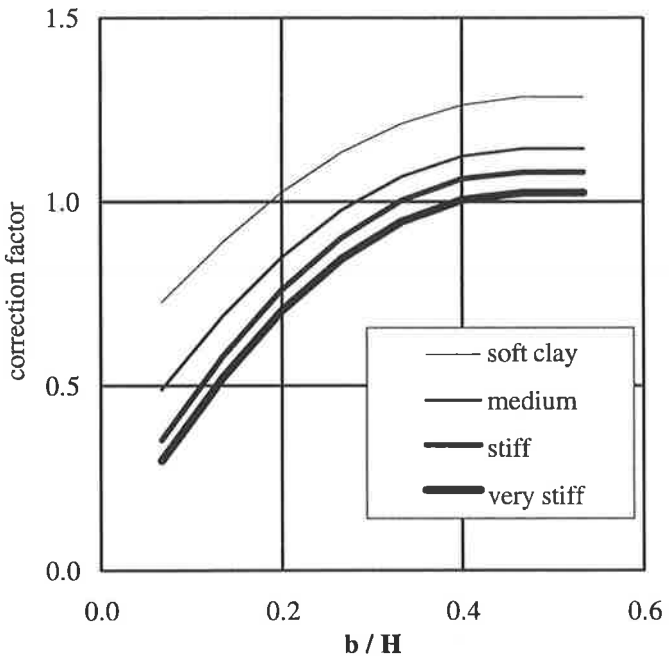

(b)

Figure 4.19 (a) Variation of the lateral thrust correction factor with b/H for T-walls with rectangular backfills; and (b) design curves for the lateral thrust correction factor.

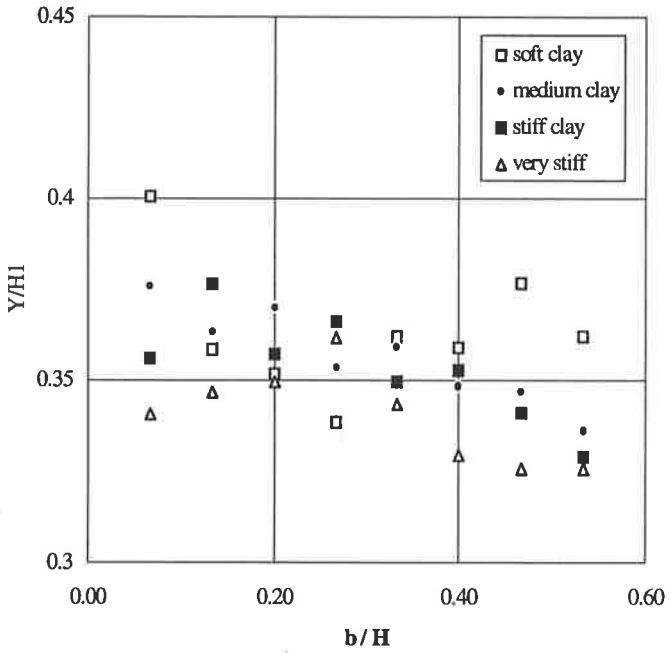

(a)

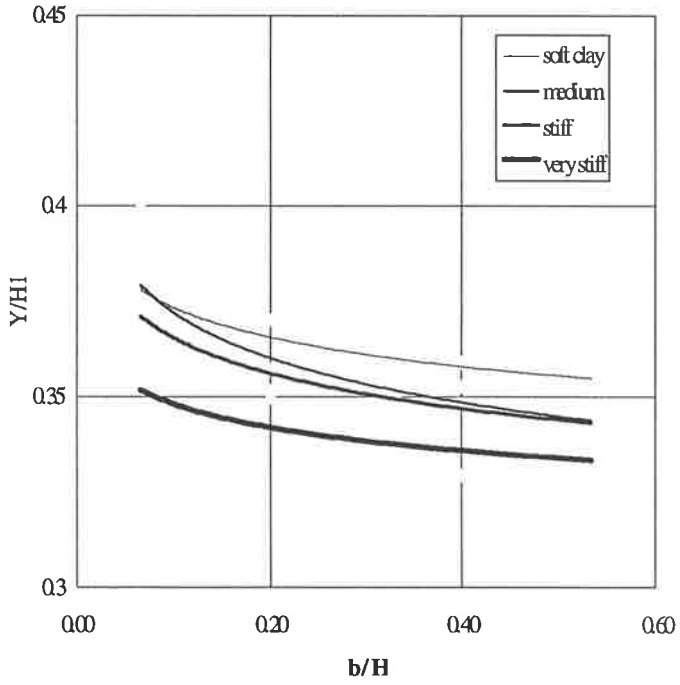

(b)

Figure 4.20 T-walls with rectangular backfills: (a) variation of the normalised distance of the lateral thrust, Y/H1, with b/H; and (b) design curves for Y/H1.

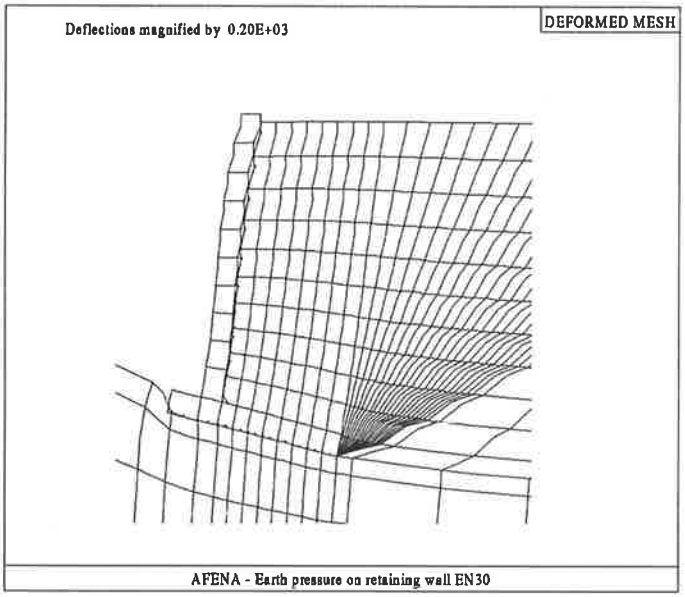

(a)

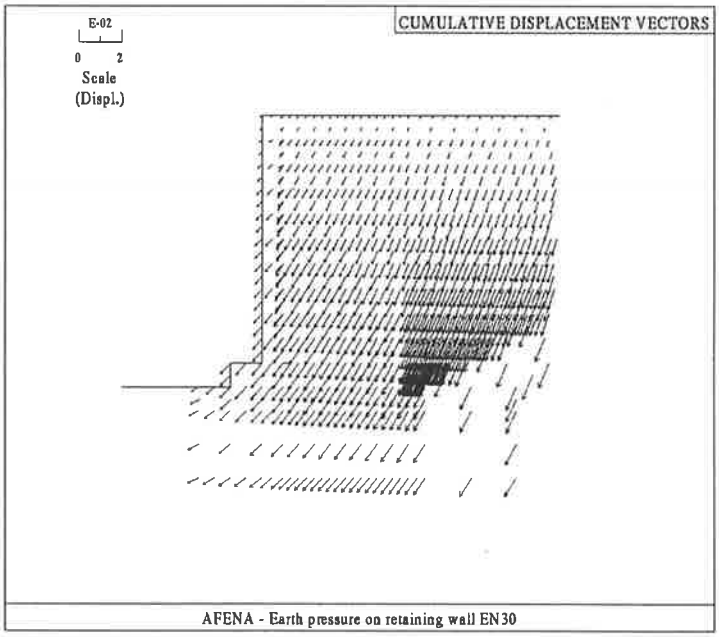

(b)

Figure 4.21 Typical wall and soil movements for T-walls having trapezoidal backfills: (a) wall and soil movements; (b) accumulated displacement vectors.

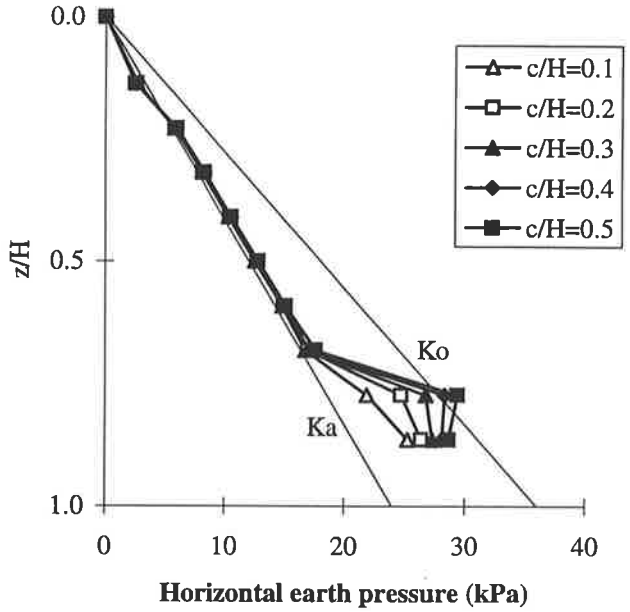

(a) c/H=0.1-0.5

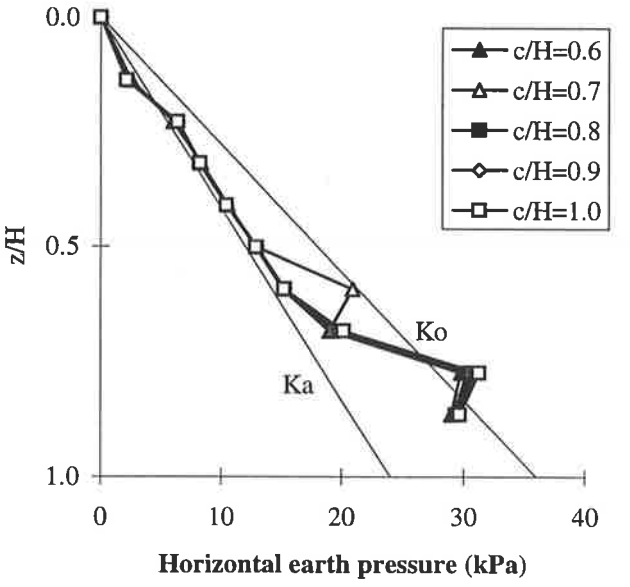

(b) c/H=0.6-1.0

Figure 4.22 Typical lateral earth pressure distributions at the back of the wall for T-walls having trapezoidal backfills and founded on stiff clays: (a) c/H between 0.1-0.5; and (b) c/H between 0.6-1.0.

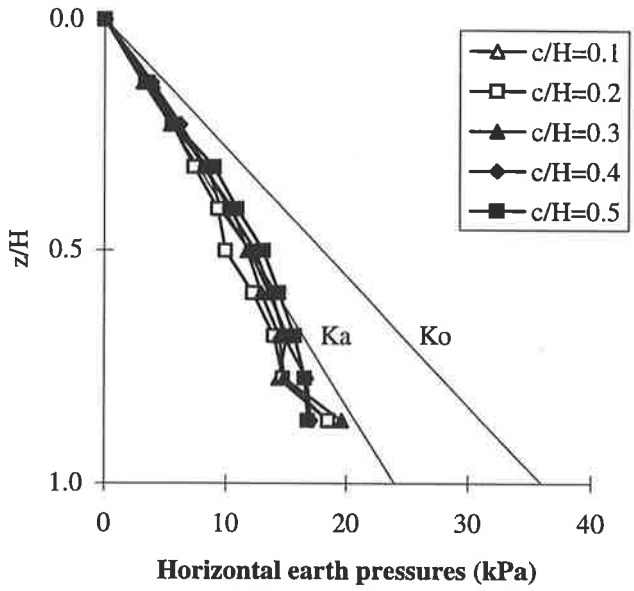

(a)

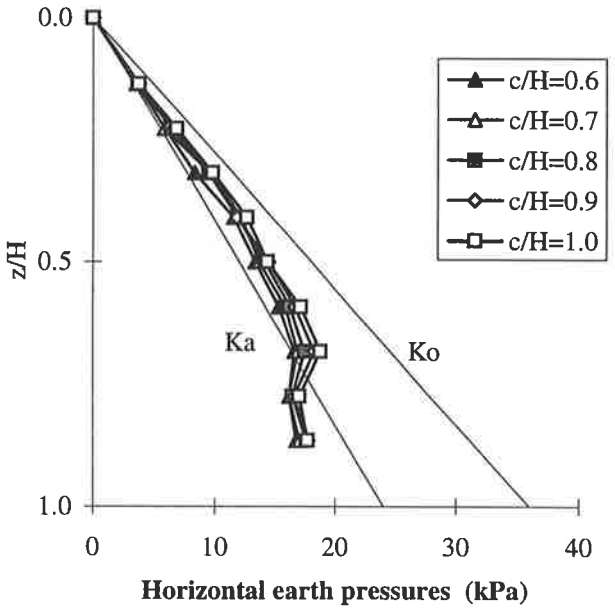

(b)

Figure 4.23 Typical lateral earth pressure distributions at the virtual back of the wall for T-walls with trapezoidal backfills and founded on stiff clays: (a) c/H between 0.1-0.5; and (b) c/H between 0.6-1.0.

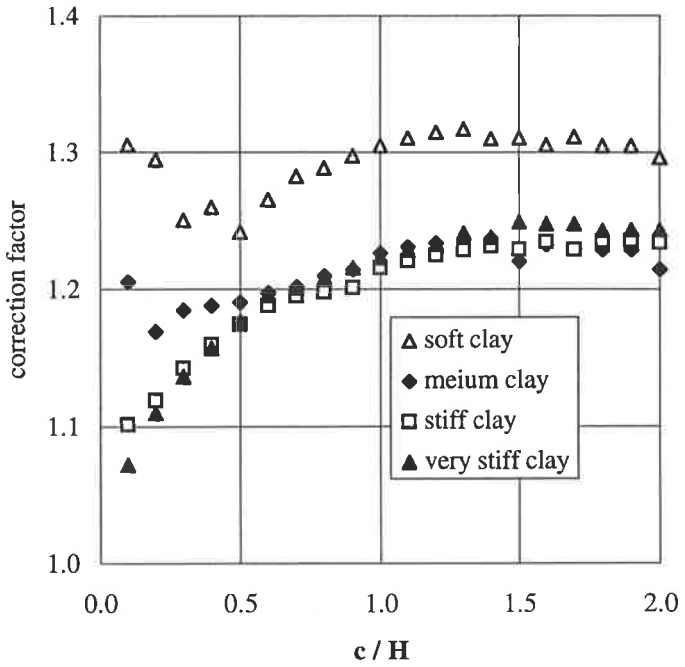

Figure 4.24 Variation of the lateral thrust correction factor at the back of the wall for T-walls with trapezoidal backfills.

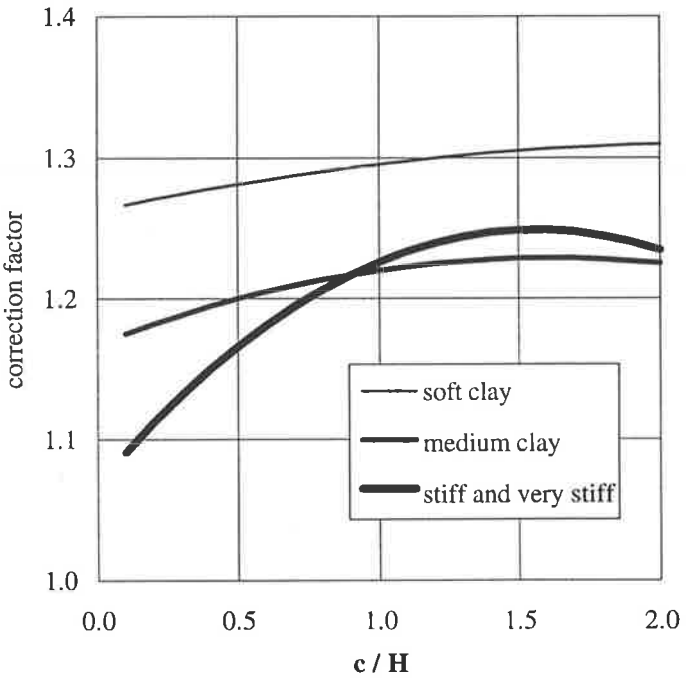

Figure 4.25 Design curves for the lateral thrust correction factor at the back of the wall for trapezoidal backfills.

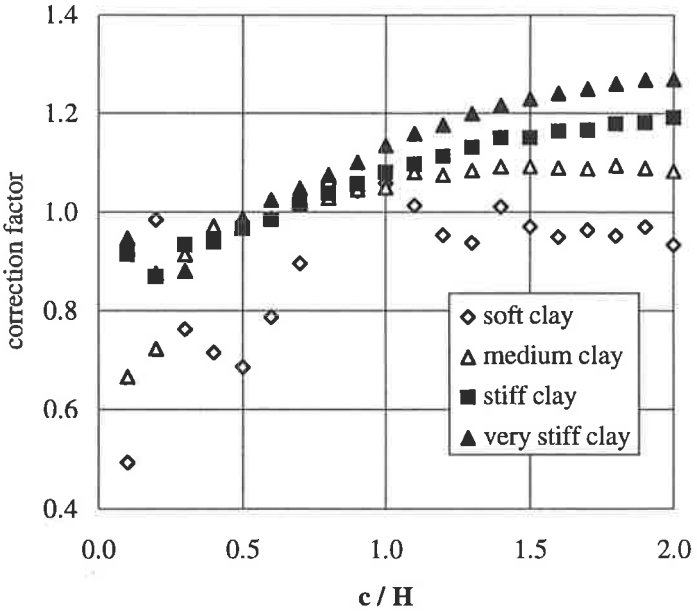

Figure 4.26 Variation of the lateral thrust correction factor at the virtual back of the wall for T-walls with trapezoidal backfills.

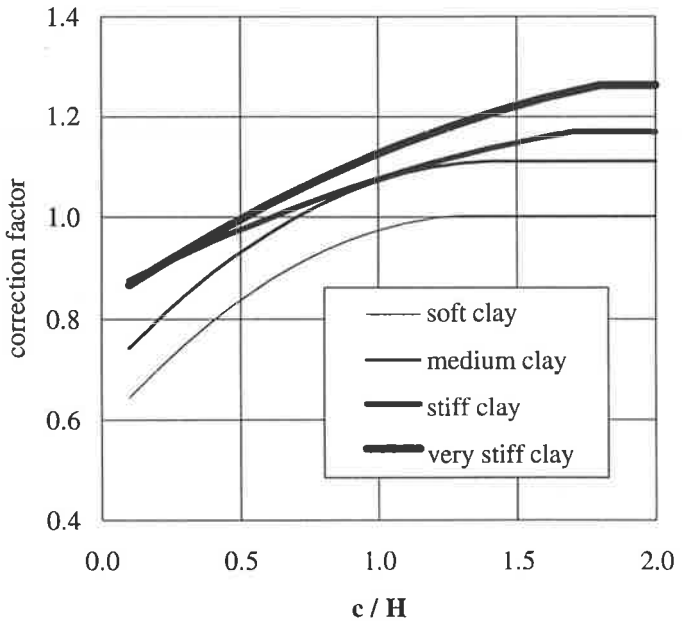

Figure 4.27 Design curves for the lateral thrust correction factor at the virtual back of the wall for trapezoidal backfills.

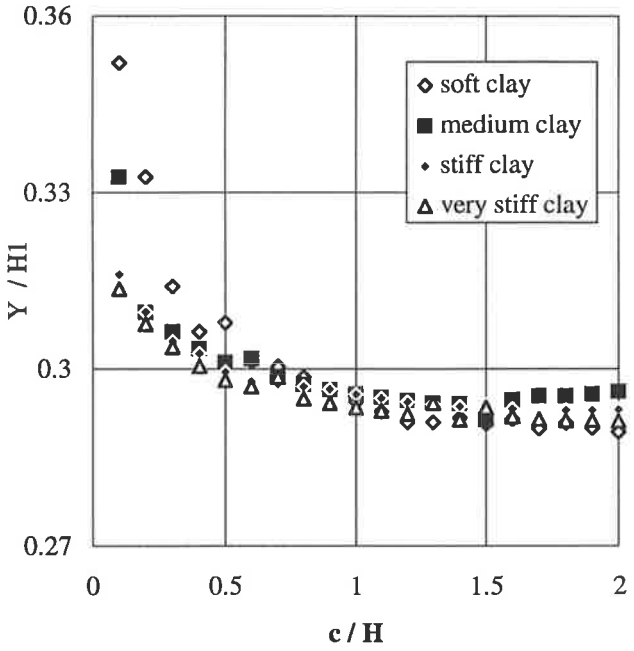

Figure 4.28 Variation of Y/H1 with c/H at the back of the wall for T-walls with trapezoidal backfills.

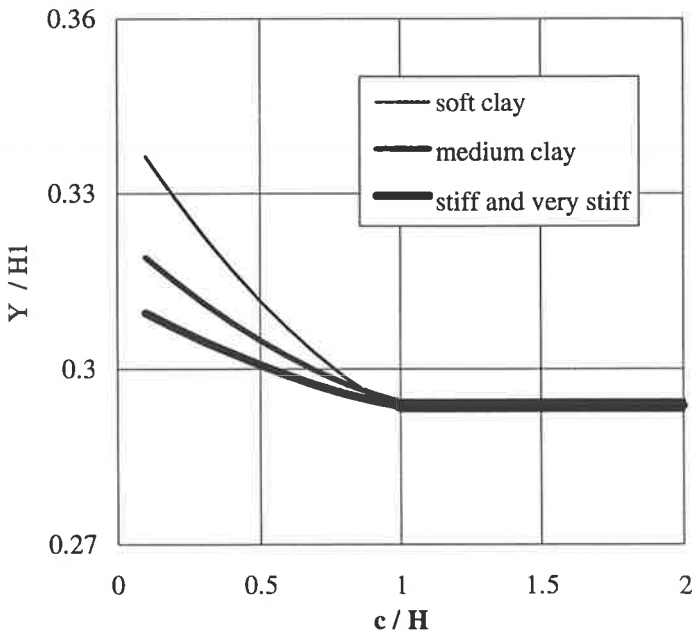

Figure 4.29 Design curves for Y/H1 at the back of the wall for T-walls having trapezoidal backfills.

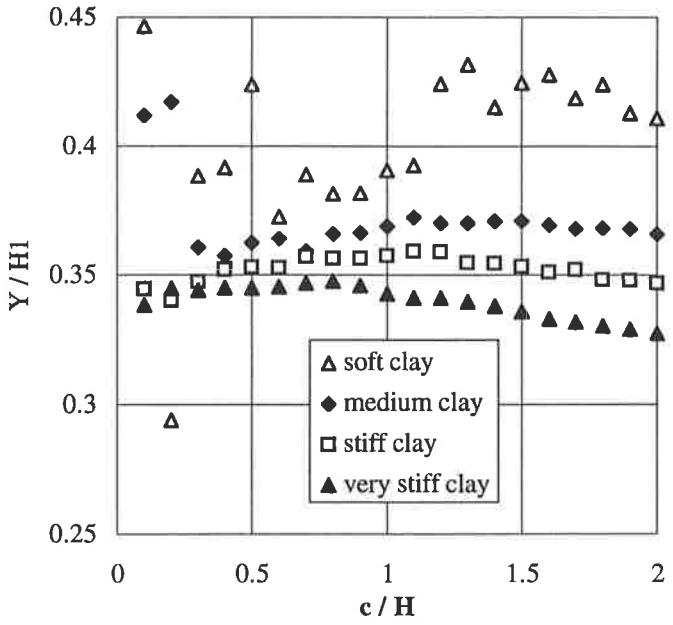

Figure 4.30 Variation of Y/H1 at the virtual back of the wall with c/H for T-walls with trapezoidal backfills.

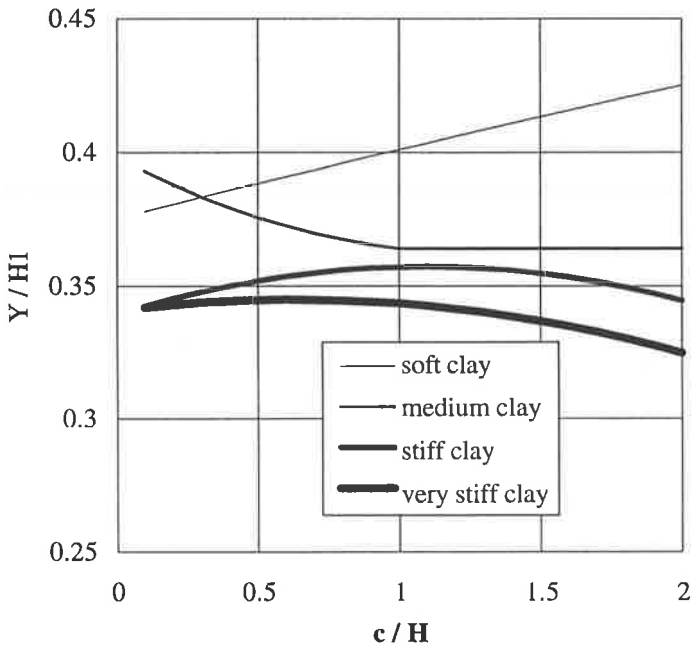

Figure 4.31 Design curves for Y/H1 at the virtual back of the wall for T-walls having trapezoidal backfills.

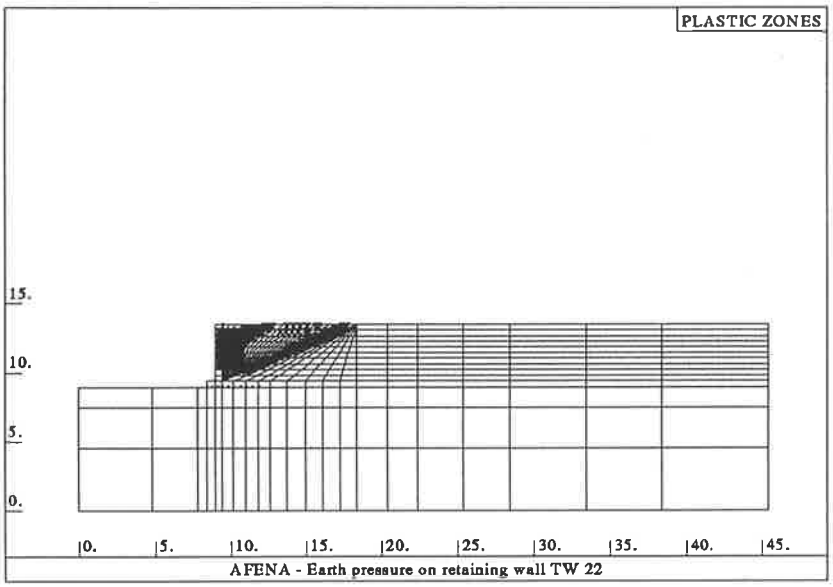

(a)

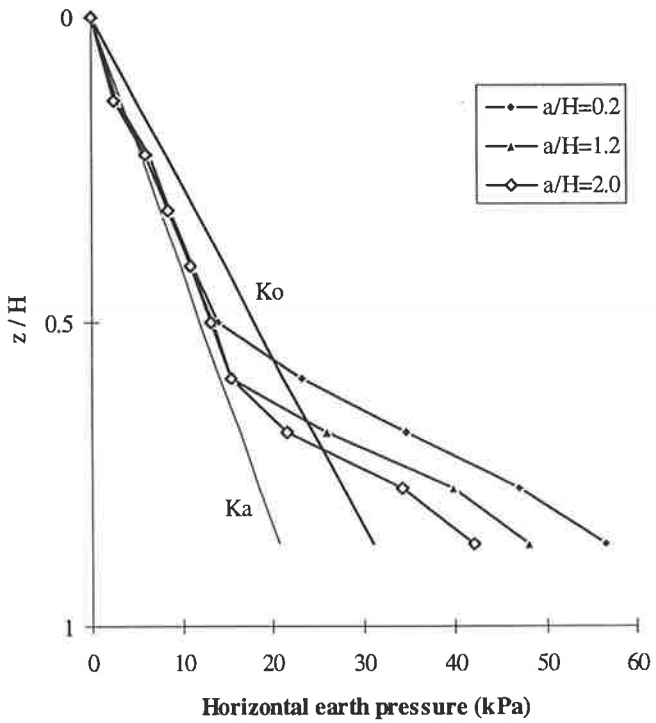

(b)

Figure 4.32 T-walls with non-homogeneous backfills: (a) formation of plastic zones for a/H=2.0; and (b) typical lateral pressure distributions for T-walls founded on stiff clays.

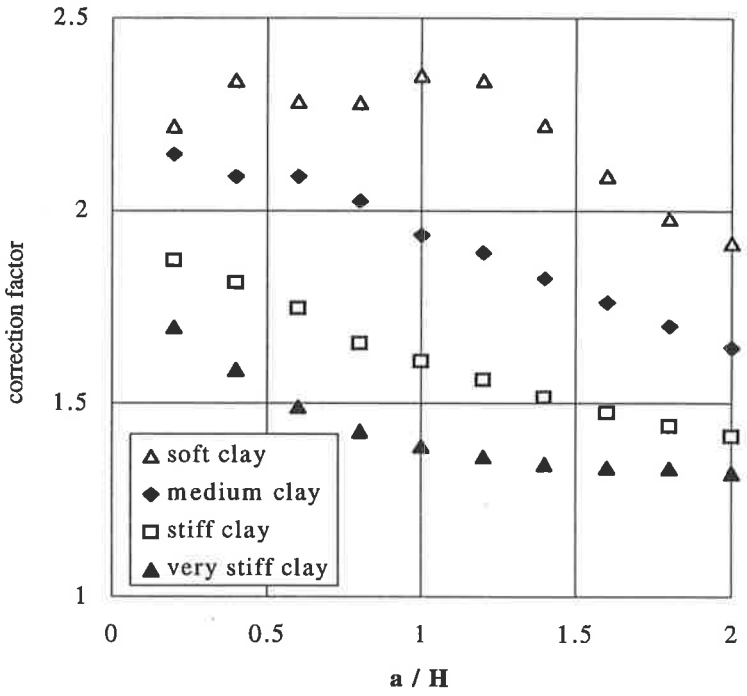

Figure 4.33 Variation of the lateral thrust correction factor with a/H for T-walls with non-homogeneous backfills.

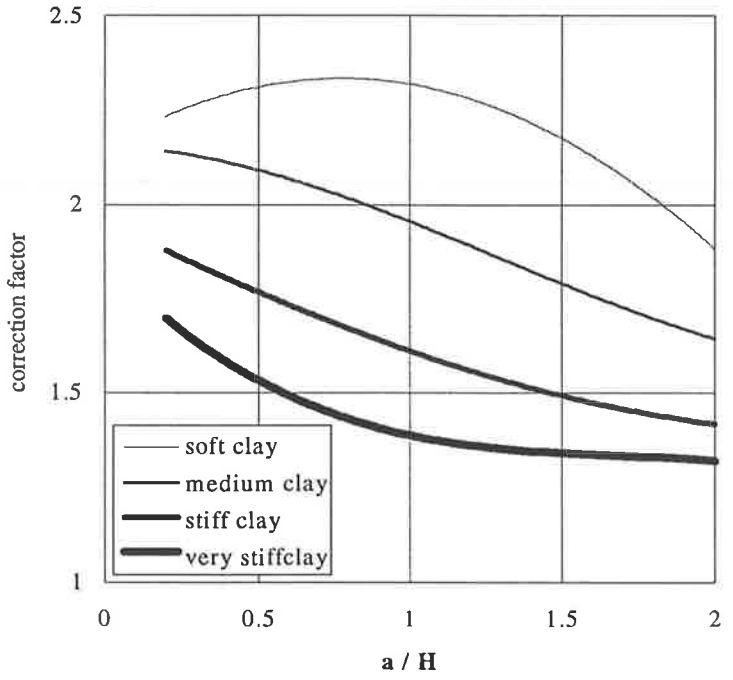

Figure 4.34 Design curves for the lateral thrust correction factor for T-walls with non-homogeneous backfills.

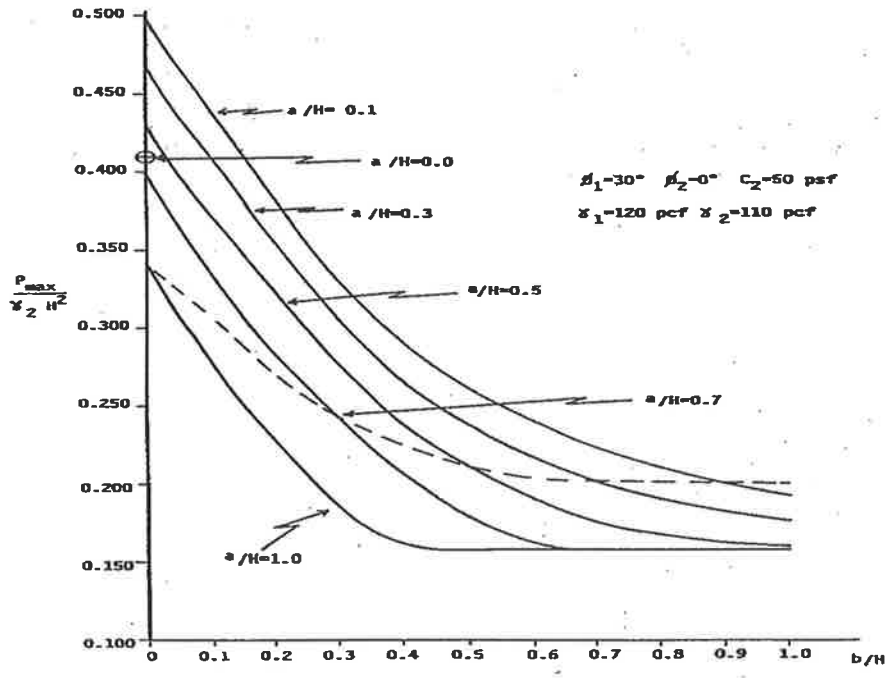

(a)

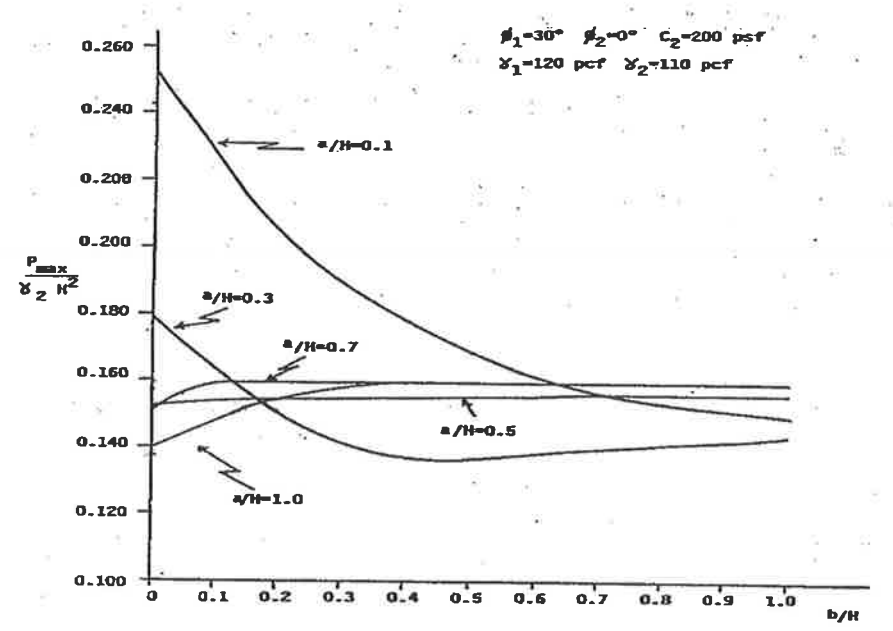

(b)

Figure 4.35 Variation of the normalised lateral thrust with backfill size ratios, a/H and b/H, for rigid walls with granular backfills and founded on cohesive soils: (a) c_2 = 50 psf, c_2 = 2.4 kPa; and (b) c_2 = 200 psf, c_2 = 8.8 kPa (*Bang and Tucker, 1990*).

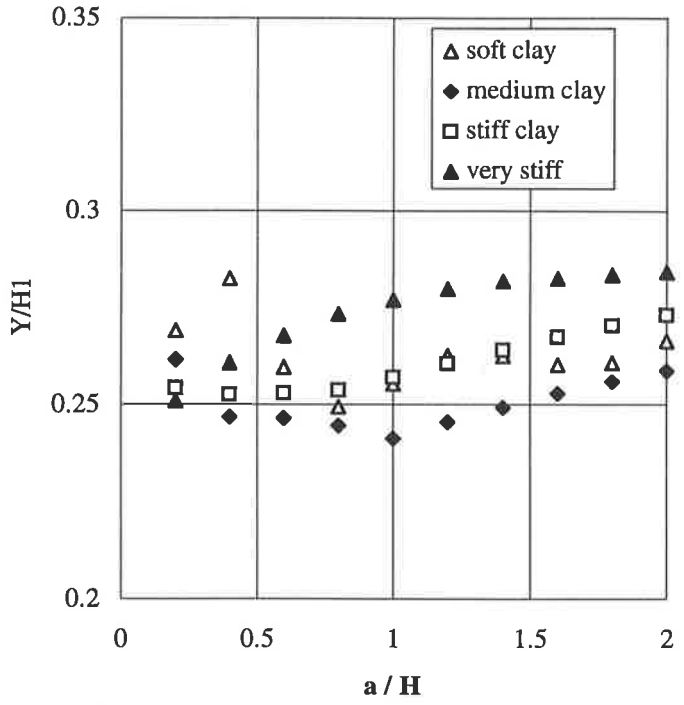

Figure 4.36 Variation of Y/H1 at the back of the wall with a/H for T-walls with non- homogeneous backfills.

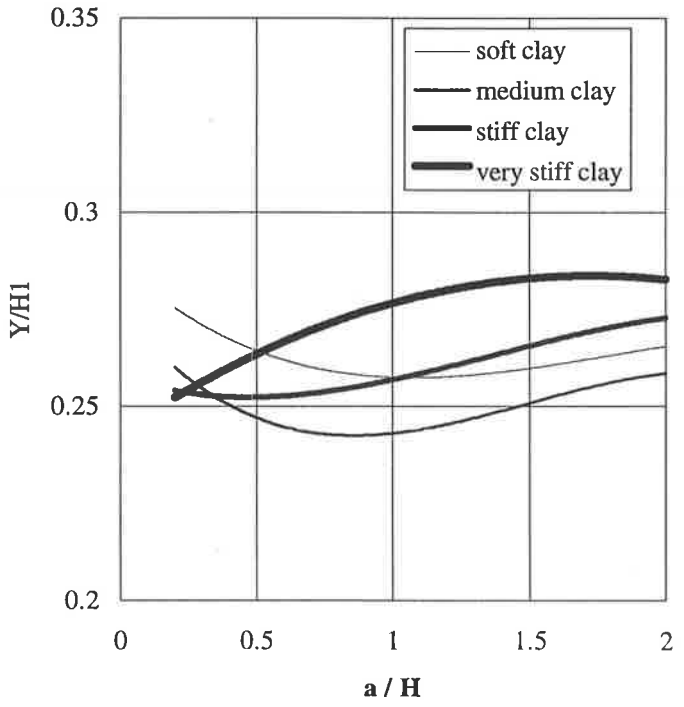

Figure 4.37 Design curves for Y/H1 at the back of the wall for T-walls with non-homogeneous backfills.

Chapter 5

Analysis of Gravity Walls and Cantilever L-Walls

5.1 INTRODUCTION

This chapter deals with the investigation of the lateral earth pressure distributions behind gravity walls and cantilever L-walls having granular backfills and founded on clays. The case of unlimited backfill is first examined and the results are compared with those of FE studies reviewed in Chapter 3. The parameters that affect the lateral earth pressure distribution are determined through a parametric study. Only the case of limited homogeneous triangular backfill is covered fully. Additional analyses have been carried out to investigate the significance of trapezoidal and non- homogeneous backfills.

Proposed design curves for the magnitude and location of the lateral thrust are presented. The lateral thrust correction factor and the normalised location of the lateral thrust are also developed. Typical lateral earth pressure distributions, at the back of the wall, are given. In these distributions, the lateral (horizontal) earth pressure is plotted on the horizontal axis, against the normalised depth z/H, on the vertical axis, where z is the depth from the ground surface behind the wall.

5.2 ANALYSIS OF GRAVITY WALLS

The unlimited and limited backfills are examined in this section. The geometry of the gravity wall and different backfills are shown in Figure 3.8. The case of limited homogeneous triangular backfill is presented below, whereas the trapezoidal and non-homogeneous backfills are investigated in Section 5.4.

5.2.1 Unlimited Backfill

(a) Unlimited Granular Backfill

The same procedure for the unlimited granular backfill, discussed in Section 4.2, was used for gravity walls. The results indicated that the wall rotated slightly (as a rigid body) about the toe due to placement of the backfill and construction of the wall itself, with a maximum lateral outward (active) movement of the wall $\Delta / H = 0.024\%$. This value of Δ / H is close to $\Delta / H = 0.03\%$ which was reported by Broms and Ingelson (1971) for a 3.3 m high retaining wall with an unlimited granular backfill. On the other hand, this value is comparatively small when compared with $\Delta / H = 0.23\%$ reported by Clough and Duncan (1971) for a 3.3 m high gravity wall with an unlimited sand backfill.

Figure 5.1 (a) shows the distributions of lateral earth pressure developed for a gravity wall having an unlimited backfill. It can be seen that the movements of the wall resulted in a reduction of the horizontal earth pressures acting on the wall from the at-rest condition to the Rankine active condition in the upper half of the wall. In the lower half of the wall, the horizontal pressures are in excess of the active pressures and they are less than the at-rest values. This is because of the insufficient active movements at the bottom as a result of the rough base.

For a rotation about the toe, it would be expected that the wall rotated into the granular backfill and developed a passive state of stresses, however the mechanism was somewhat more complex. The foundation and the wall tilted *"backward"* rather than forward, as would be expected from the classical theories. This backward tilt is due to placement of the backfill and the consequent uneven foundation settlement of $\eta / B = 0.044\%$, which is greater beneath the heel of the wall than the toe.

Thus, even though the wall tilted backward, it moved and tilted forward, in a relative sense to the backfill. This backward movement, reported by Clough and Duncan (1971), for a gravity wall with a sand backfill, as shown in Figure 3.4. The results agree with those of Clough and Duncan, and their results of lateral earth pressure distributions for various amounts of rotation of the wall are shown in Figure 5.1 (b).

The lateral thrust acting on the wall was 5.6% larger than the Rankine active thrust. This value is small compared with the corresponding increase of 28.5% for T-walls. Thus, the active conditions assumed in the classical theories better predict the behaviour of gravity walls than cantilever T-walls, because the base of a T-wall limits soil and wall movements.

(b) Unlimited Clay Backfill

The case of unlimited clay backfill was examined, where the entire zone behind the wall was backfilled using a clay backfill. Figure 5.2 shows the distributions of LEPs developed along the back of the wall, for the four clay types. Note that K_0 values in the latter figure are based on the soft clay parameters. The magnitudes of the lateral thrust for gravity walls are 70%, 37%, 30% and 27% lower than the corresponding ones for T-walls, for soft, medium, stiff, and very stiff clay, respectively. These reductions in the lateral thrust are also attributed to the effect of the base of T-walls.

The depth of tension cracks was approximately 0.08H, 0.1H and 0.2H for medium, stiff and very stiff clays, respectively. These values are also significantly small when compared with those determined from Eq. 2.6. The analyses did not show any tension cracks in the soft clay.

5.2.2 Parametric Study

A parametric study was carried out to determine the sensitivity of the model to a number of parameters, and to determine the critical factors affecting the distribution of lateral earth pressure. Preliminary analyses showed that the interface roughness and the stiffness of the clay deposit were the key factors.

5.2.2.1 Effect of Wall Stiffness

It was found that a large change in Young's modulus of the wall resulted in negligible changes in both wall movements and the associated distribution of lateral earth

pressures. This may result from the comparatively large width which gives the gravity wall high lateral stiffness. In comparison, the stiffness of the cantilever T-wall has a significant effect on the distribution of lateral earth pressure, as it was demonstrated in Section 4.3.1, because it is relatively slender and most of the deformations result from the bending action of the stem. However, in the case of a gravity wall the lateral movements are due mostly to the rotation of the wall as a rigid body. This rotation of the gravity wall is due to the uneven foundation settlement underneath the wall which results from the construction of the wall and placement of the backfill.

5.2.2.2 Effect of Interface Roughness

The results demonstrated that there was a large variation in the distribution of lateral earth pressures when the wall back shear stiffness, K_{ss}, was increased as shown in Figure 5.3. Two values were examined: $K_{ss} = 490$ MPa to represent a rough wall back; and $K_{ss} = 0.001$ MPa to represent a smooth wall back. It can be seen that, the rough wall produces a relatively large scatter in the results, while the smooth wall produces a more favourable linear distribution.

The results of the FE analyses were found to be sensitive to the value of the interface base shear stiffness (K_{sb}), as shown in Figure 5.4. It can be seen that, the rough base resulted in a linear distribution, but the relatively smooth base resulted in a large scatter. It is therefore, the rough wall base and smooth wall back conditions were adopted in modelling gravity walls.

5.2.2.3 Effect of Stiffness of the Clay Deposit

The Young's modulus of the embankment (E_2) was found to have a significant effect on the distribution of lateral earth pressures, while Poisson's ratio had a negligible effect. Figure 5.5 shows that the magnitudes of the LEPs are comparatively low, particularly in the lower third of the wall, when E_2=2.5 GPa compared to the case of E_2=25 MPa. This reduction in the lateral pressures can be attributed to a reduction in soil movement and, hence stress redistribution within the soil as the stiffness of the embankment increases. It was also found that the lateral thrust in the case of E_2=2.5 GPa is 80% of the lateral thrust for E_2=25 MPa.

The effect of Young's modulus of the foundation subsoil (E_3) was also examined. Figure 5.6 shows the distributions of lateral earth pressure for two cases: E_3=2.5 GPa; and E_3=25 MPa. It can be seen that, the lateral earth pressures for E_3=2.5 GPa are

significantly larger than those for E_3=25 MPa. Hence, the lateral thrust increased by 22%. This is attributed to the smaller settlements of the foundation subsoil as the stiffness of the subsoil increases, which reduces the rotation of the wall. In comparison, for T-walls, when E_3 was increased by the same factor, the lateral thrust increased by only 5.3%. This difference is possibly due to the effect of the base of the wall as it limits the effect of settlements beneath the T-wall and within the backfill.

5.2.3 Influence of Triangular Backfill Zone

The size of the triangular backfill was represented by the ratio a/H, where a and H are shown in Figure 3.8. In the following, the results of an investigation into the significance of limited homogeneous triangular backfills are presented. Note that the term homogeneous represents a single granular material used as a backfill. The triangular backfill is the focus of the investigation, while other geometries, including non-homogeneous backfills, are examined in Section 5.4. The results are discussed in terms of the distribution of the LEPs and magnitude and location of the lateral thrust.

5.2.3.1 Distribution of Lateral Earth Pressures

The results demonstrated that the gravity wall rotated backward slightly about the toe, as for the case of unlimited backfills. For a gravity wall founded on stiff clay, with a/H=2.0, the maximum deflection measured at the top of the wall was Δ / H=0.01 and the differential settlement under the wall was η / B=0.02. Figure 5.7 shows wall and soil movements for a gravity wall founded on stiff clay and having limited granular backfill with a/H=1.0. It can be seen that, the wall rotated slightly about the toe and most of the wall movements are due to the settlement underneath the wall, whereas the lateral movements are relatively small. This is primarily due to the large lateral stiffness of the gravity wall and its comparatively large weight.

The limiting value λ has been chosen to distinguish between narrow and wide backfills, and has been found to be 0.9, 0.6, 0.55 and 0.75 for soft, medium, stiff and very stiff clays, respectively. Figure 5.8 (a) shows typical lateral earth pressure distributions for a gravity wall founded on a stiff clay and having narrow limited homogeneous triangular backfills with $a / H < \lambda$. The lateral earth pressure distributions are curved and less than the active values in the lower half of the wall. This results from a stress redistribution within the soil. Figure 5.8 (b) shows the lateral earth pressure distributions for wide backfills with $a / H > \lambda$. It can be seen that, the distributions are essentially linear and close to the active values over the full height.

Figure 5.8 shows that the lateral earth pressures increase rapidly for narrow backfills but marginally for wide backfills as a/H increases. The effect of the size of the backfill on the lateral earth pressure distributions is similar to T-walls with triangular backfills, except that the magnitudes of the lateral pressures for wide backfills are larger for T-walls due to base effects.

5.2.3.2 Magnitude and Location of Lateral Thrust

(a) Magnitude of Lateral Thrust

Figure 5.9 shows the variation of the lateral thrust correction factor (β), for the four clay types, for a/H between 0.2-2.0. Also, the values of β, determined using the Huntington (1957) procedure, are also shown. It can be seen that, the general trend for the four clays is that β increases with a/H in a non linear form. It can also be seen that the values of β for stiff and very stiff clays are closer to the Huntington (1957) value of 1.0 for wide backfills than those for medium and soft clays. In addition, Huntington's values are larger than those of the FEM for narrow backfills, whereas they are smaller for wide backfills. The assumption of zero cohesion along the excavation surface was used to determine Huntington's values for the lateral thrust correction factor. This explains why Huntington's values for narrow backfills are larger than those of the FEM. There is obvious scatter for medium and soft clays due to instability and interaction between movements in the embankment and settlements of the foundation subsoil. Table 5.1 gives maximum and minimum values of β developed from the FE analyses.

The values of β for wide backfills are closer to the classical solution of $\beta=1.0$ than those of a T-wall with a triangular backfill presented in Section 4.4.2. This may be attributed to: (i) cantilever T-wall base effects which lead to concentration of stresses and limited settlements; and (ii) the assumptions of the classical theories are best approximated by the geometry of a gravity wall. Figure 5.10 shows the design curves for a gravity wall with limited granular backfills and founded on clays, which are based on curves of best fit for β versus a/H. A logarithmic model was found to give the best correlations.

(b) Location of Lateral Thrust

The distance of the line of action of the lateral thrust (Y) acting at the vertical back of the wall measured from the base of the embankment was determined and normalised

with respect to the height of the embankment (H1). Figure 5.11 shows the variation of Y/H1 with increasing a/H values from 0.2 to 2.0. It can be seen that, for the four clay types, Y/H1 decreases as a/H increases. Figure 5.12 shows the proposed design curves for Y/H1 which are the curves of best fit for the data shown in Figure 5.11. Based on these design curves, it can be concluded that using the classical value of 1/3 will overestimate the value of Y/H1 for wide backfills, but underestimate it for narrow backfills.

5.3 ANALYSIS OF CANTILEVER L-WALLS

The geometry of the L-wall and the chosen backfill geometries are shown in Figure 3.8. The case of unlimited backfill is first examined and the results of L-walls with homogeneous triangular backfills are then presented. The trapezoidal and non-homogeneous backfills are examined in Section 5.4.

5.3.1 Unlimited Backfill

(b) Unlimited Granular Backfill

Examination of the results of L-walls with unlimited granular backfills indicated slight wall rotation about the toe with outward lateral movements along the full height of the wall. The maximum outward movement $\Delta / H = 0.02\%$ is slightly less than that of gravity walls. This outward tilt is caused by a non-uniform foundation settlement resulting in a tilt of $\eta / B = 0.018\%$, greater beneath the heel than the toe. The outward movements resulted in horizontal earth pressures close to the active values in the upper two thirds of the wall, while in the lower third, the horizontal pressures exceeded the active values but were less than the at-rest values.

Figure 5.13 (a) shows the lateral earth pressure distributions for T-walls, gravity walls and L-walls with unlimited granular backfills. It can be seen that, most of the variations in the lateral earth pressure distributions are near the bottom of the wall. This may be attributed to the effect of the base for both L-walls and T-walls, where the base acts as a stiff structural member which limits both the lateral movements and causes a concentration of lateral pressures.

(b) Unlimited Clay Backfill

The case of unlimited clay backfill was also examined for the four clay types. Figure 5.13 (b) shows the distributions of LEPs developed along the back of the wall, for the four clay types. Note that K_0 values in the latter figure are based on the soft clay parameters. The magnitudes of the lateral thrust for L-walls are 10%, 36%, 2% and 7% lower than the corresponding ones for T-walls, for soft, medium, stiff, and very stiff clays, respectively. These reductions in the lateral thrust are also attributed to the effect of the base of T-walls. The depths of tension cracks were the same for gravity walls.

5.3.2 Parametric Study

Wall stiffness, interface roughness and stiffness of clay deposit were found to be the key factors affecting the lateral earth pressures behind cantilever L-walls. These factors are examined below, and the results are compared with those of cantilever T-walls.

5.3.2.1 Effect of Wall Stiffness

Two values of Young's modulus of the wall (E_c) were examined: $E_c = 25\times10^6$ kN/m^2; and a relatively stiffer wall with $E_c = 25\times10^9$ kN/m^2. There was a slight increase in the lateral pressures for the stiffer wall, and the lateral thrust was 8% larger than that of the wall with lower stiffness. In comparison, for a T-wall, when the Young's modulus of the wall was increased by the same factor, the lateral thrust increased by 13%.

5.3.2.2 Effect of Interface Roughness

Similar investigations as those presented in Section 4.3.2 for T-walls have been carried out to examine the effect of interface parameters on the distribution of LEPs at the back of L-walls. The results show that the lateral earth pressure distribution at the back of L-walls is very sensitive to the strength and stiffness parameters of the soil-wall interface.

Figure 5.14 shows the lateral earth pressure distributions for three values of the angle of wall friction along the wall base interface (δ). It can be seen that the there are only slight variations in the lateral earth pressures. Figure 5.15 shows the variation of the

lateral earth pressure distribution for different values of the wall base interface shear stiffness, K_{sb}. It can be seen that the rough wall base, with $K_{sb} = 490$ MPa, resulted in relatively large LEPs in the lower third of the wall, whereas the smooth wall base, with $K_{sb} = 0.001$ MPa, resulted in significantly smaller lateral earth pressures along the full height. The value of $K_{sb} = 4.9$ MPa resulted in an active state along the full height of the wall.

Figure 5.16 shows the lateral earth pressure distributions for a smooth wall back with $K_{ss} = 0.001$ MPa and a rough wall back with $K_{ss} = 490$ MPa. It can be seen that the lateral pressure distribution is comparatively linear for a smooth wall back, while a large scatter is associated with the rough wall. The rough wall base and smooth wall back conditions have been used to model L-walls with limited backfills.

5.3.2.3 Effect of Stiffness of the Clay Deposit

The numerical study demonstrated that variation of the Young's modulus of the embankment (E_2) resulted in large effects compared to those observed for gravity walls. Figure 5.17 shows that, when E_2 was increased from 25 MPa to 2.5 GPa, the lateral earth pressures decrease, particularly in the lower third of the wall. Accordingly, the lateral thrust decreased by 16%. In comparison, for T-walls, when E_2 was increased by the same factor, the lateral thrust decreased only by 7%.

The Young's modulus of the foundation subsoil (E_3) was also examined. Figure 5.18 shows the lateral earth pressure distributions for two cases: $E_3 = 25$ MPa; and $E_3 = 2.5$ GPa. It can be seen that, the lateral earth pressures are significantly larger for the latter case, particularly in the lower third of the wall. As a result, the lateral thrust increased by 27%. This increase is due to the reduction of settlements and rotation of the wall with increasing stiffness of the foundation subsoil.

5.3.3 Influence of Triangular Backfill Zone

The methodology of the FE modelling used to simulate the construction of L-walls with limited homogenous triangular backfills was described in Chapter 3. The size of the triangular backfill was represented by the ratio a/H, where a and H are shown in Figure 3.8 (e). Note that the base of the embankment is located at a distance, h, from the base of the wall.

5.3.3.1 Distribution of Lateral Earth Pressures

The results showed that the wall typically rotated about the toe with full active (outward) horizontal movements. The maximum wall movement was $\Delta / H = 0.02\%$ and the associated differential settlement under the wall was $\eta / B = 0.02\%$, for L-walls founded on stiff clays with a/H=2.0. Figure 5.19 shows one example of the deformations of the wall and the soil in the vicinity of an L-wall with a triangular backfill, having a/H=0.8, and founded on a stiff clay. It can be seen that, there is a slight backward rotation about the toe and the relative displacements, along both the excavation surface and the back of the wall, are evident.

The lateral earth pressure distributions are shown in Figure 5.20. It can be seen that, the distributions are curved for narrow backfills, while they are essentially linear for wide backfills. These pressure distributions are close in magnitude to those of gravity walls with limited triangular backfills. It should be realised that the gravity wall has a shorter base width which causes lower shear along the base. On the other hand, the L-wall has a significant lateral stiffness and, accordingly, undergoes larger lateral bending deflections. These two factors, of base width and lateral stiffness, are of opposite effects and control the lateral pressure distribution.

5.3.3.2 Magnitude and Location of Lateral Thrust

(a) Magnitude of Lateral Thrust

Figure 5.21 shows the variation of the lateral thrust correction factor (β), with a/H values between 0.2 and 2.0. Also, it shows the corresponding magnitudes of β based on Huntington (1957). It can be readily seen that large scatter exists the results of the soft clay which is caused by the opposite effects of the embankment movements and the settlements in the subsoil. The maximum variation of β between wide and narrow backfills is for the soft clay and is larger than 100%. In general, for narrow backfills, β is typically small for the very stiff clay and large for the soft clay.

The values of β for wide backfills are slightly lower than the corresponding values for gravity walls with limited triangular backfills. Figure 5.22 shows the design curves for determining the lateral thrust correction factor, β, for L-walls with limited triangular backfills.

(b) Location of Lateral Thrust

Figure 5.23 shows the variation of Y/H1 with a/H values between 0.2 and 2.0. It can be seen that, Y/H1 decreases as a/H increases, except for the soft clay where there is a large scatter. Also, it can be seen that the values of Y/H1 are concentrated close to the classical value of 1/3. Figure 5.24 shows the design curves for Y/H1 for the four clay types.

5.4 ADDITIONAL NUMERICAL ANALYSES

Additional analyses were carried out to investigate different field conditions encountered with cantilever L-walls and gravity walls. Although detailed analyses were not carried out, as for the triangular backfill, the aim was to obtain possible variations in the lateral thrust due to large changes in the size or the geometry of the backfill.

(a) Trapezoidal Backfill

The case of a trapezoidal backfill has been investigated for L-walls and gravity walls. Only a single case of trapezoidal backfill, with a/H=2.0 and b/H=0.5, founded in a stiff clay was examined. Figure 5.25 shows the lateral pressure distributions for both walls. It can be seen that, there is only a slight variation in these distributions (less than 1%), which are close to those of wide triangular backfills. Thus, it can be concluded that the lateral pressure distributions for wide triangular backfills are valid for trapezoidal backfills with $b / H \geq 0.5$.

(b) Non-Homogeneous Backfill

As discussed in Section 4.7, a non-homogeneous backfill defines a backfill composed of two different soils: a granular backfill used for drainage; and a part of the excavated cohesive deposit. Figure 5.26 shows the lateral pressure distributions for a gravity wall having non-homogeneous backfills and founded on stiff clays. It was found that, $\beta = 1.14$ for a/H=0.2 and $\beta = 1.08$ for a/H=2.0. Therefore, as the granular zone is enlarged the lateral force on the wall decreases. This variation of β with a/H is similar to that for T-walls with non-homogeneous backfills.

Figure 5.27 shows the lateral pressure distributions for L-walls founded on stiff clays and having non-homogeneous backfills. It can be seen that, the backfill, with a comparatively large granular zone, produces lower LEPs. It was found that, $\beta = 1.18$ for a/H=0.2 and $\beta = 1.02$ for a/H=2.0. However, the corresponding values for T-walls with non-homogeneous backfills are $\beta = 1.87$ for a/H=0.2, and $\beta = 1.42$ for a/H=2.0. The magnitudes of β for T-walls with non-homogeneous backfills are comparatively large due to effects of the base of the T-wall.

(c) Effect of Young's Modulus of the Embankment

Additional analyses have been carried out to examine the relative effects of Young's modulus of the embankment soil (E_2) for gravity walls with limited homogenous triangular backfills. The case of $E_2 / E_3 = E_2 / E_1$ for different practical values was examined and the corresponding β-a/H curves were developed. Figure 5.28 shows the variation of the lateral thrust correction factor (β) for a/H values between 0.2-1.0 and for different values of E_2 / E_1. It can be seen that β increases as the ratio E_2 / E_1 decreases, ie, the lateral thrust of an embankment with a low stiffness is larger than that having a larger stiffness. Similar analyses have been carried out for L-walls and about 5% difference in the corresponding values of β were observed.

5.5 SUMMARY

The results of numerical analyses of gravity walls and cantilever L-walls with limited, granular, triangular backfills have been presented. Design curves for determining correction factors for the magnitude of the lateral thrust and its location have been presented. The embankment-subsoil interaction and base interface parameters are more critical for L-walls and gravity walls than T-walls.

The variation of β with the size of the granular backfill for homogeneous and non-homogeneous backfills is essentially the same for L-walls and gravity walls. In general, there are some differences in the corresponding lateral pressure distributions between the two types of retaining walls, due to the difference in geometry. However, from a design standpoint these differences are slight and in most cases can be neglected.

Table 5.1 Summary of the FE results of gravity wall and L-wall

	Gravity Walls		L-walls		Notes
	unlimited	Triangular	Unlimited	Triangular	
β_{max}	1.056	1.284	1.303	1.55	
β_{min}	-	0.41	-	0.53	
max variation %		> 100		>100	
$(Y/H1)_{max}$	0.3	0.51	0.3	0.442	
$(Y/H1)_{min}$	-	0.29		0.252	
maximum variation %	-	76	-	0.75	
active movement, (Δ / H) %*	0.024	0.01	0.019	0.02	for stiff clay
differential settlement	0.044	0.02	0.018	0.017	for stiff clay
wall rotation about	toe	toe	toe	toe	
Lateral Earth pressures	linear		linear		
- backfill size ratio		a/H		a/H	
- narrow backfills		curved		curved	
- wide backfills	-	linear		linear	
- limiting value (λ)		0.55-0.9		0.40-1.15	

* for the soft clay, wall movements are of the order of 10-15 times these values

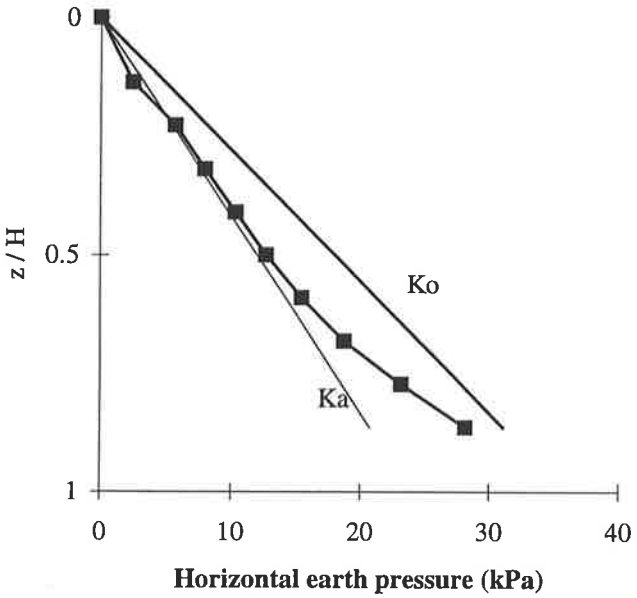

(a)

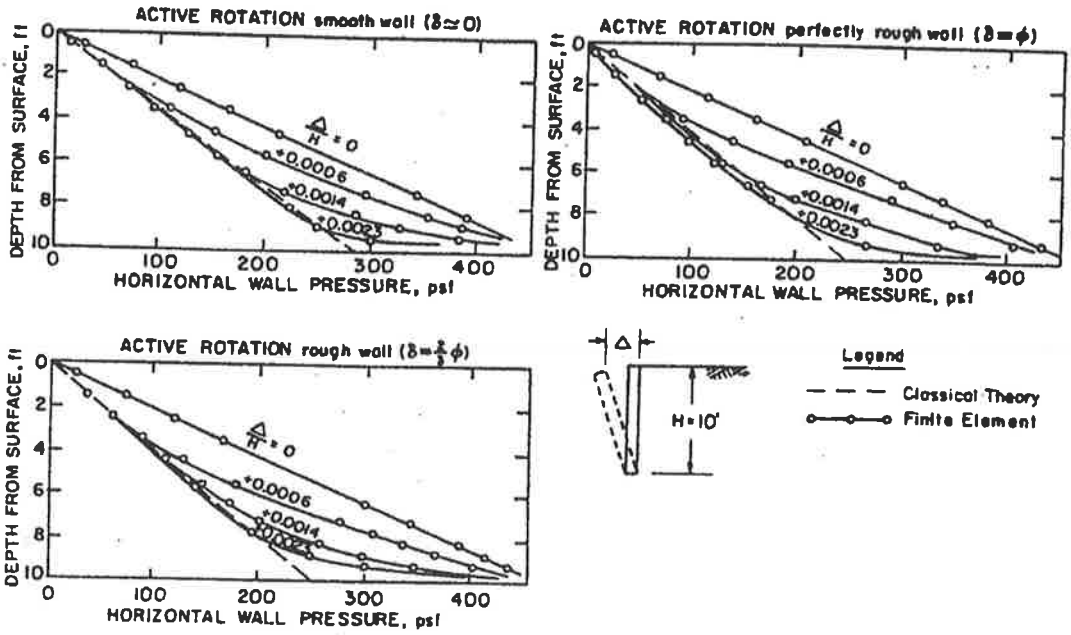

(b)

Figure 5.1 (a) lateral earth pressure distributions for gravity walls with unlimited granular backfills; (b) lateral earth pressure distributions for different deflection ratios for gravity walls with unlimited granular backfills (*Clough and Duncan, 1971*).

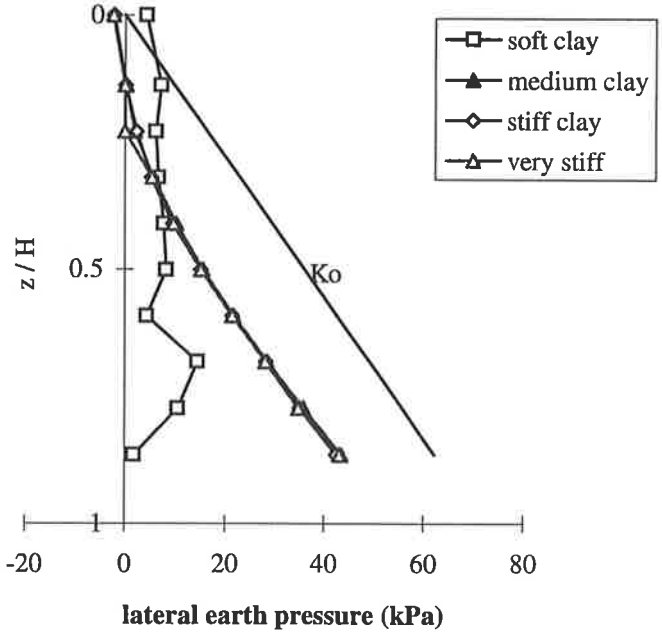

Figure 5.2 Lateral earth pressure distributions for gravity walls with unlimited clay backfills.

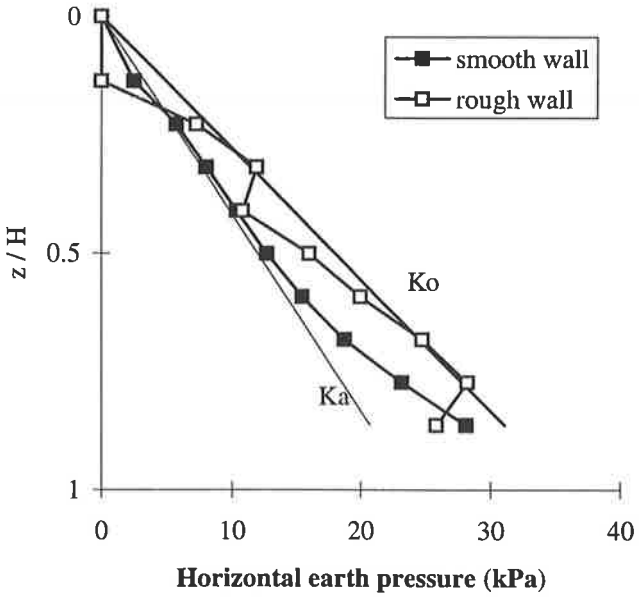

Figure 5.3 Effect of wall back shear stiffness, K_{ss}, on the lateral earth pressure distribution behind gravity walls.

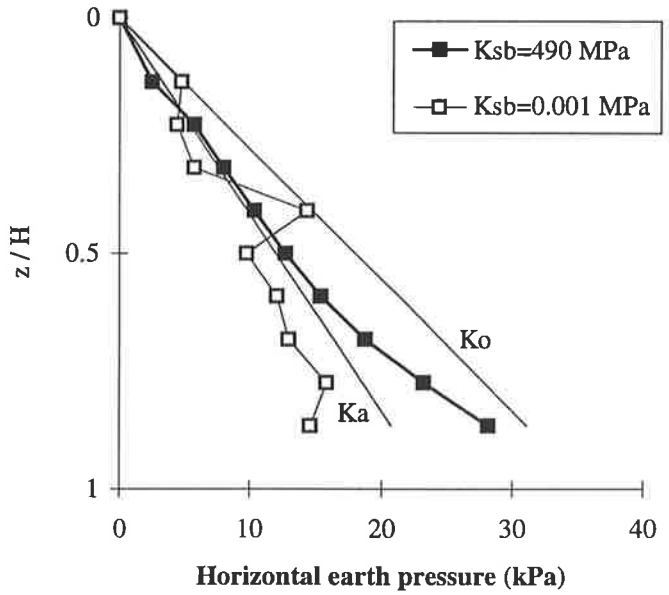

Figure 5.4 Effect of wall base shear stiffness, K_{sb}, on the lateral earth pressure distribution behind gravity walls.

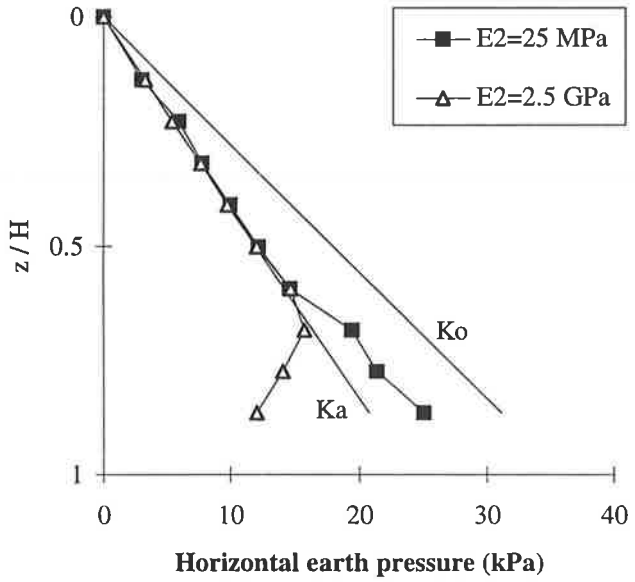

Figure 5.5 Effect of Young's modulus, E_2, of the embankment on the lateral earth pressure distribution behind gravity walls.

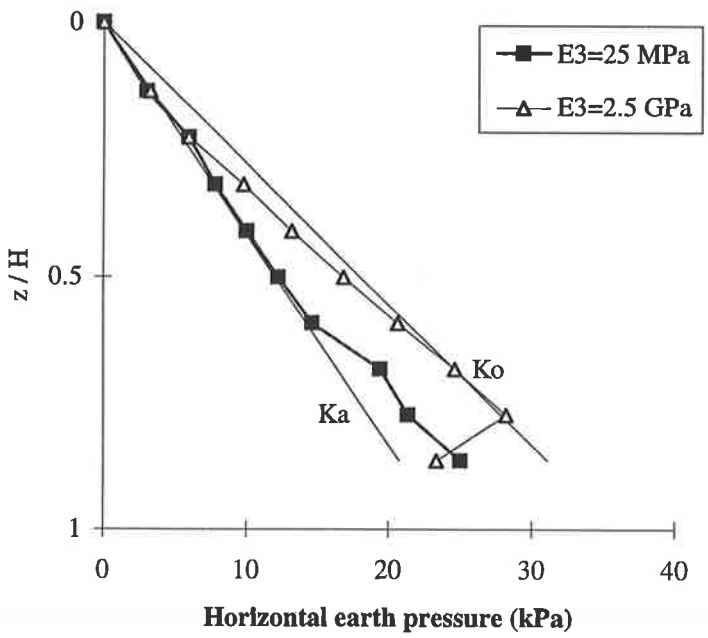

Figure 5.6 Effect of Young's modulus, E_3, of the foundation subsoil on the lateral earth pressure distribution behind gravity walls.

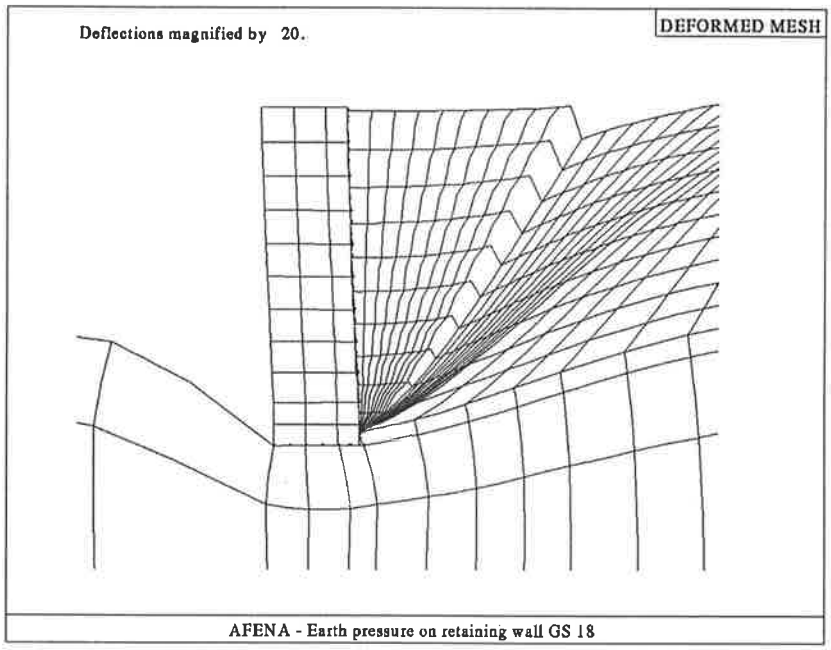

(a)

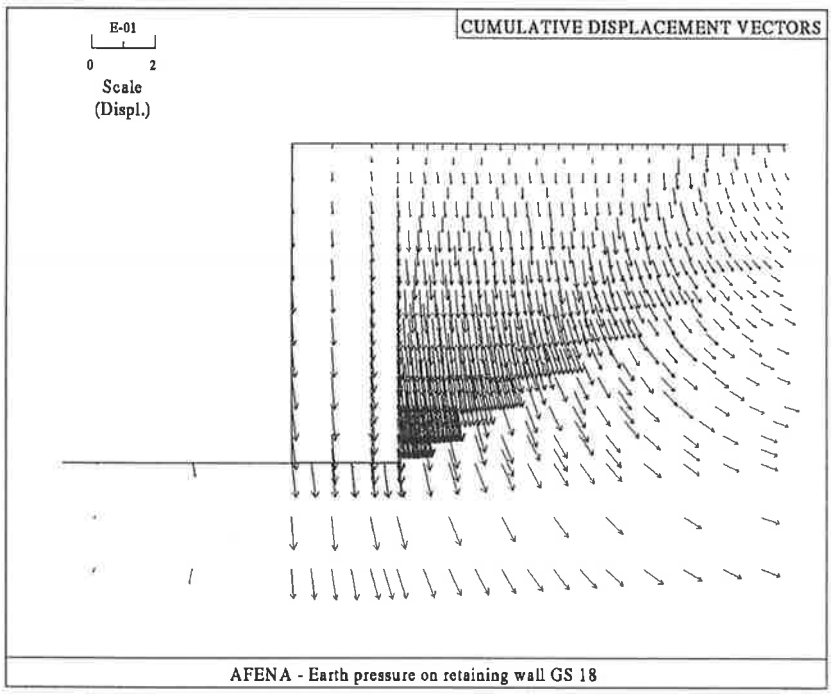

(b)

Figure 5.7 Gravity wall with a triangular backfill and having a/H=1.0: (a) wall and soil movements; and (b) accumulative displacement vectors.

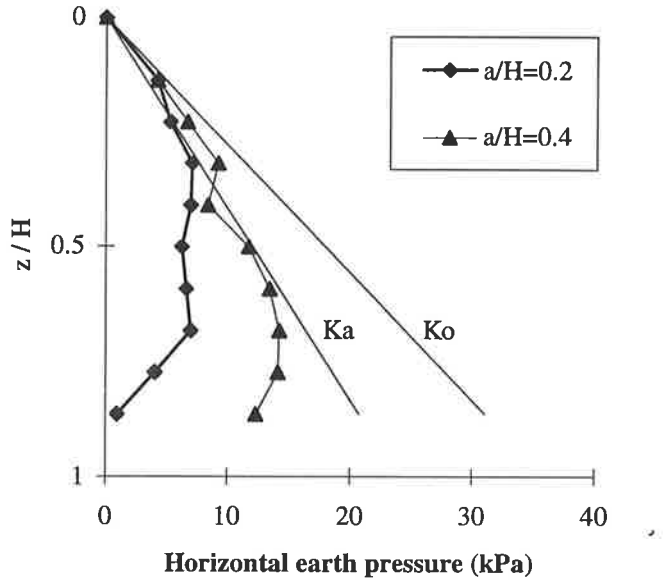

(a)

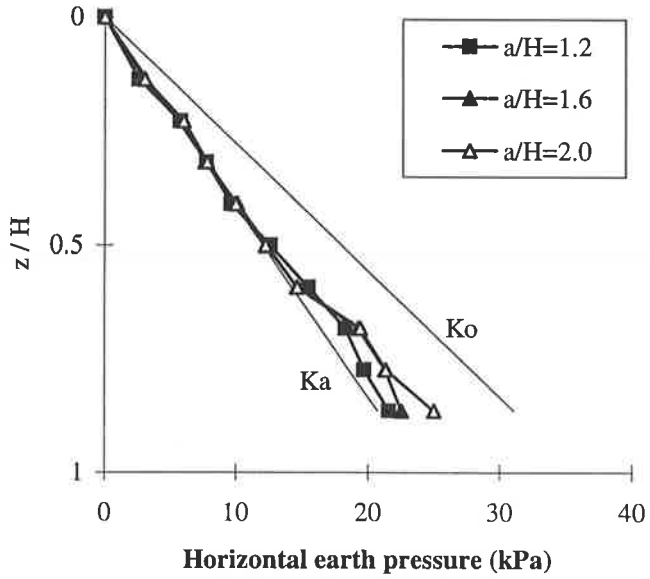

(b)

Figure 5.8 Typical lateral earth pressure distributions for gravity walls founded on stiff clays with triangular backfills: (a) narrow backfills; and (b) wide backfills.

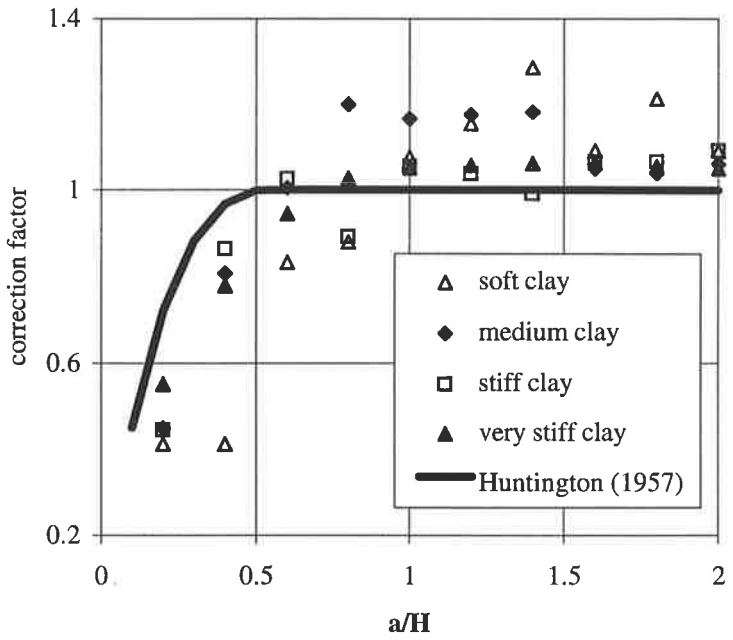

Figure 5.9 Variation of lateral thrust correction factor, β, with backfill size ratio (a/H) for gravity walls having triangular backfills and founded in clays.

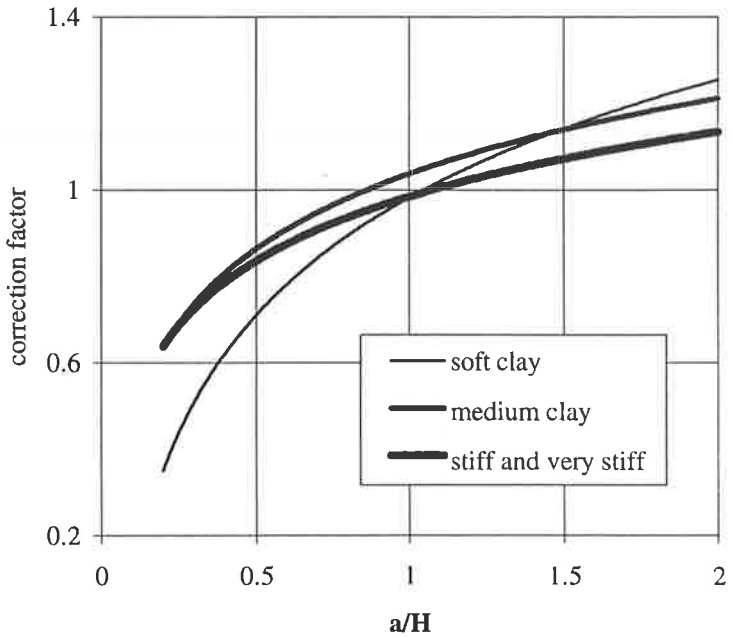

Figure 5.10 Design curves for lateral thrust correction factor, β, for gravity walls having triangular backfills and founded in clays.

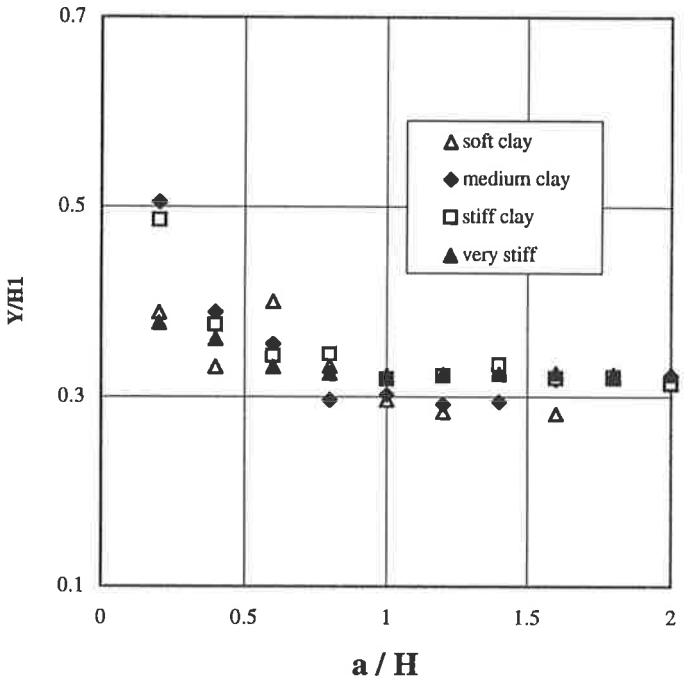

Figure 5.11 Variation of Y/H1 with a/H for gravity walls with triangular backfills and founded in clays.

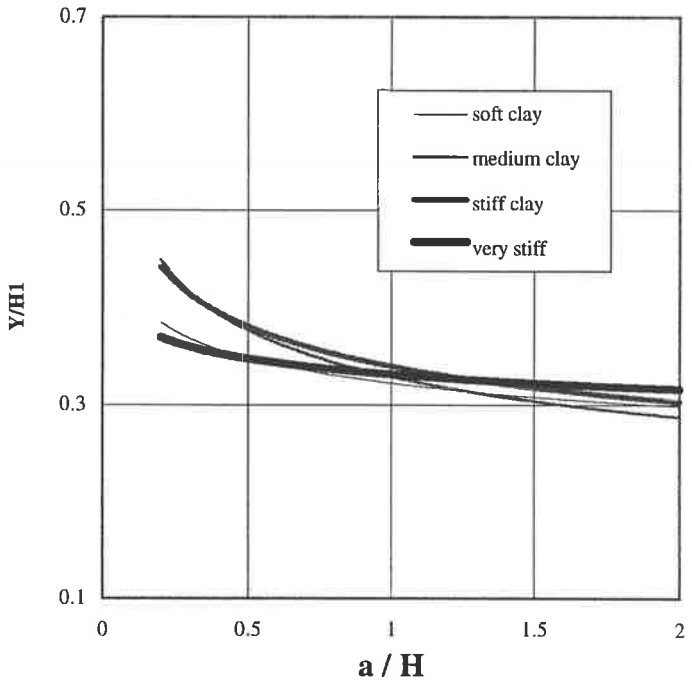

Figure 5.12 Design curves for Y/H1 for gravity walls with triangular backfills and founded in clays.

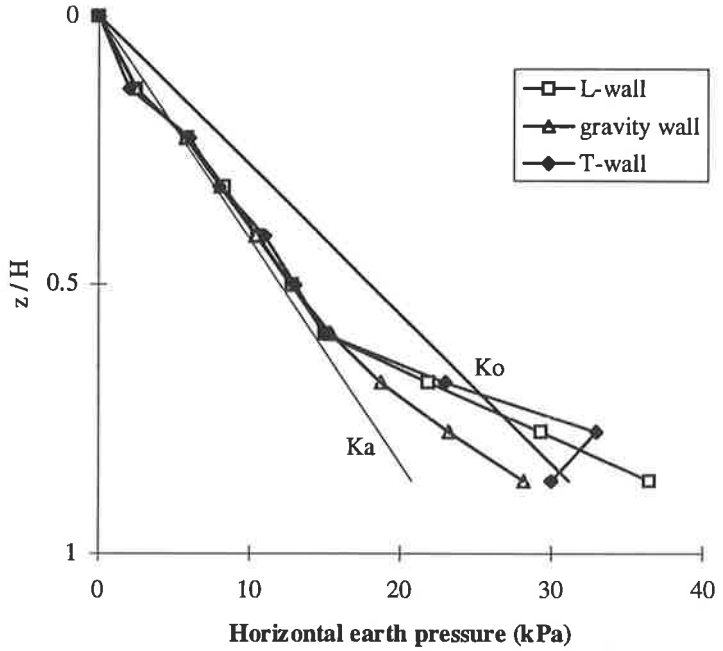

(a)

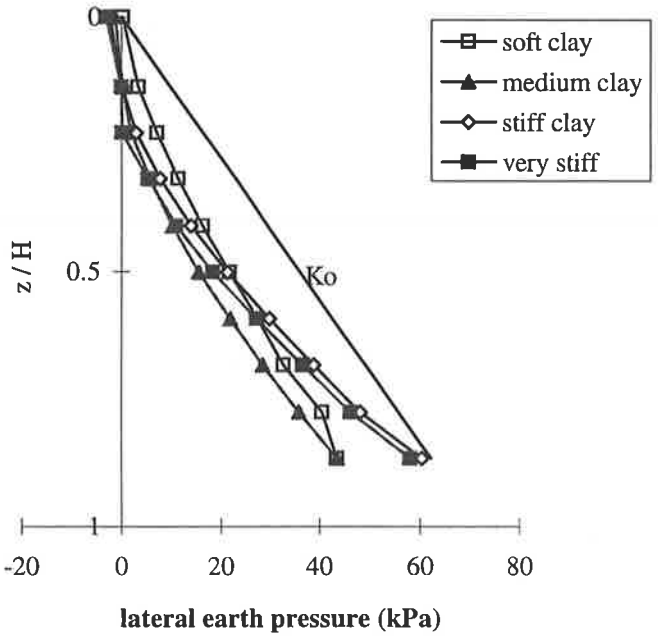

(b)

Figure 5.13 Lateral earth pressure distributions for L-walls with: (i) unlimited granular backfills; and (b) unlimited clay backfills.

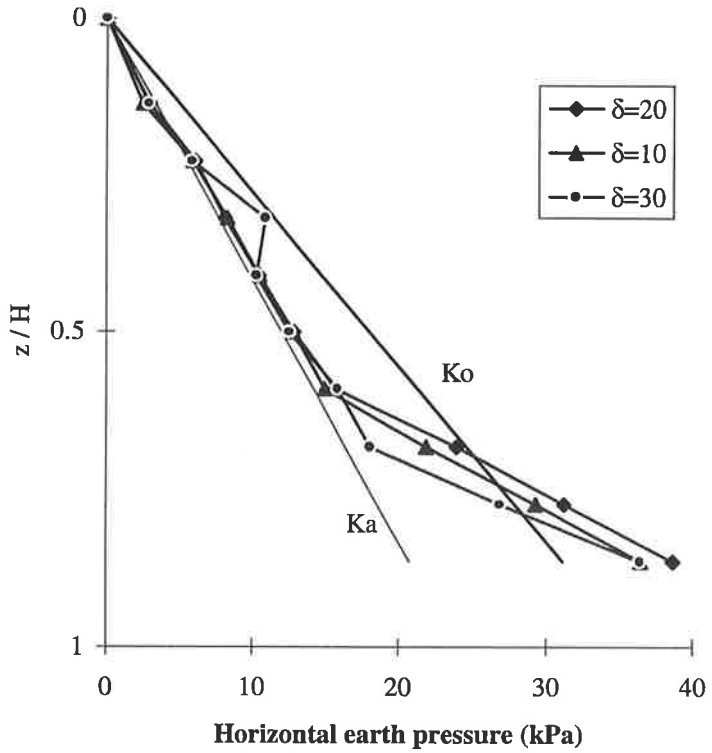

Figure 5.14 Effect of angle of wall base friction, δ, on the lateral earth pressure distribution behind cantilever L-walls.

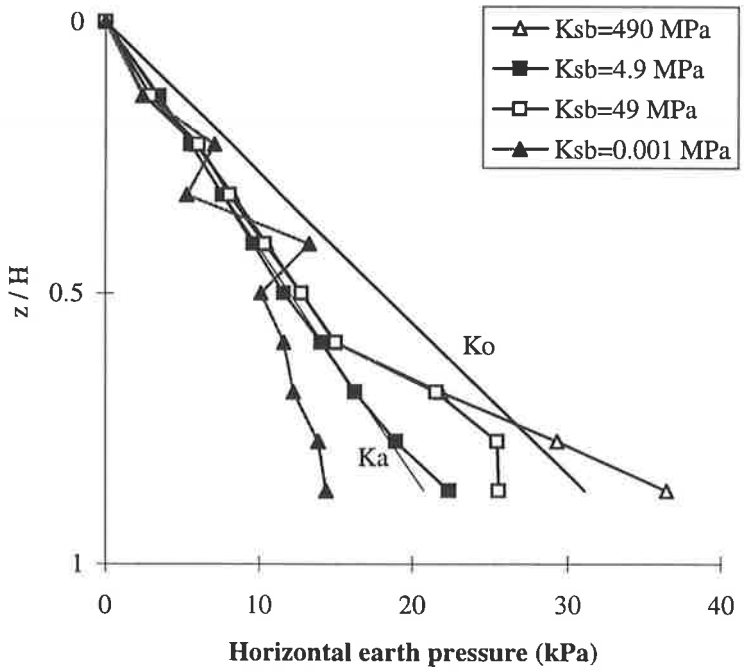

Figure 5.15 Effect of wall base shear stiffness, K_{sb}, on the lateral earth pressure distribution behind cantilever L-walls.

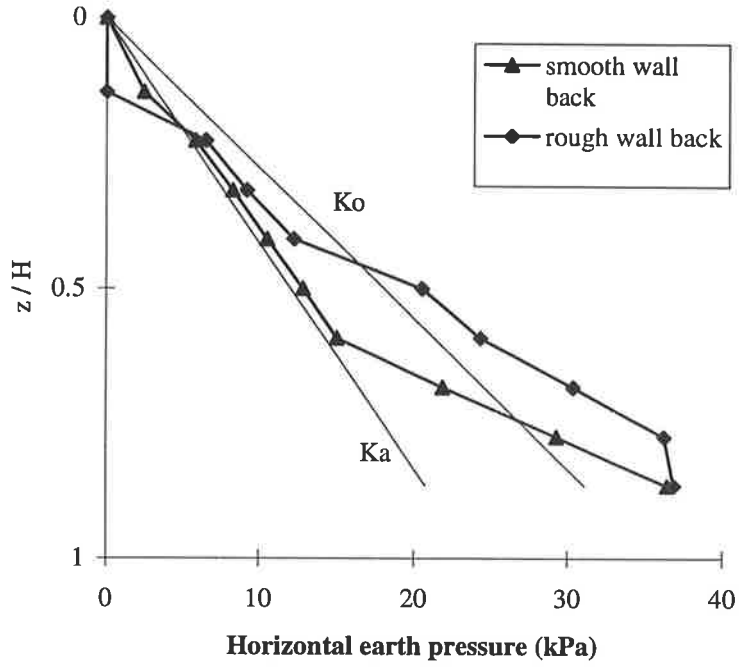

Figure 5.16 Effect of wall back roughness on the lateral earth pressure distribution behind cantilever L-walls.

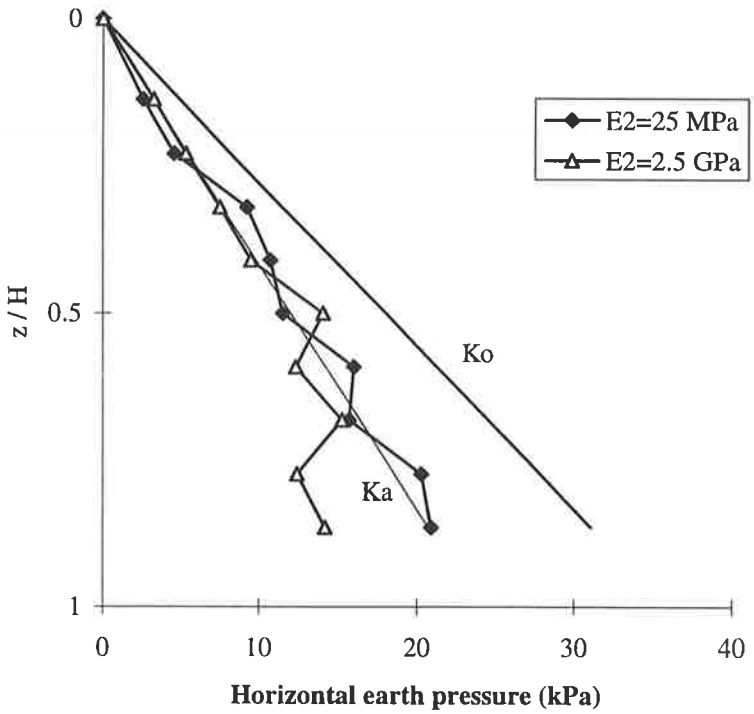

Figure 5.17 Effect of Young's modulus of the embankment, E_2, on the lateral earth pressure distribution behind cantilever L-walls.

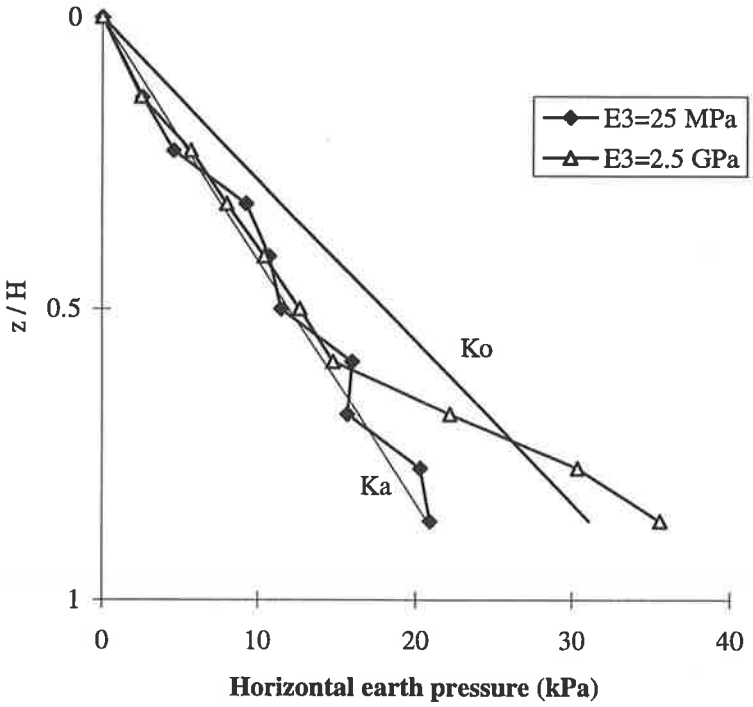

Figure 5.18 Effect of Young's modulus of the foundation subsoil, E_3, on the lateral earth pressure distribution behind cantilever L-walls.

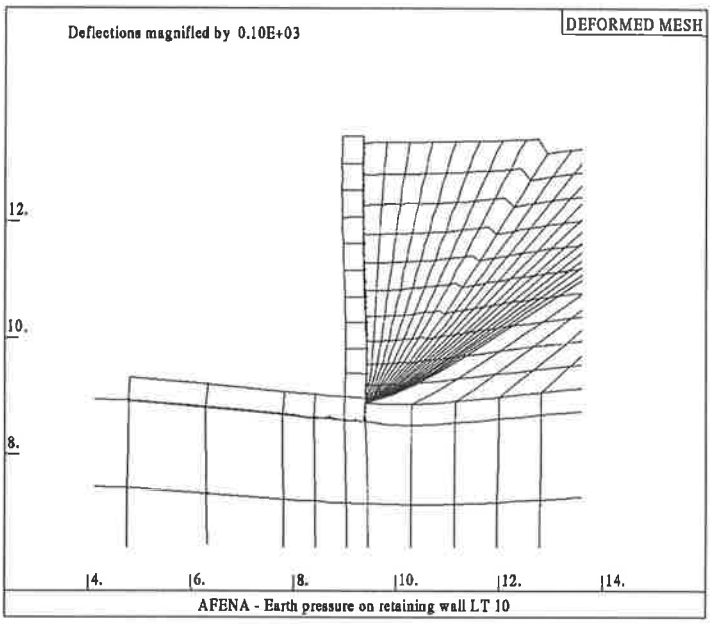

(a)

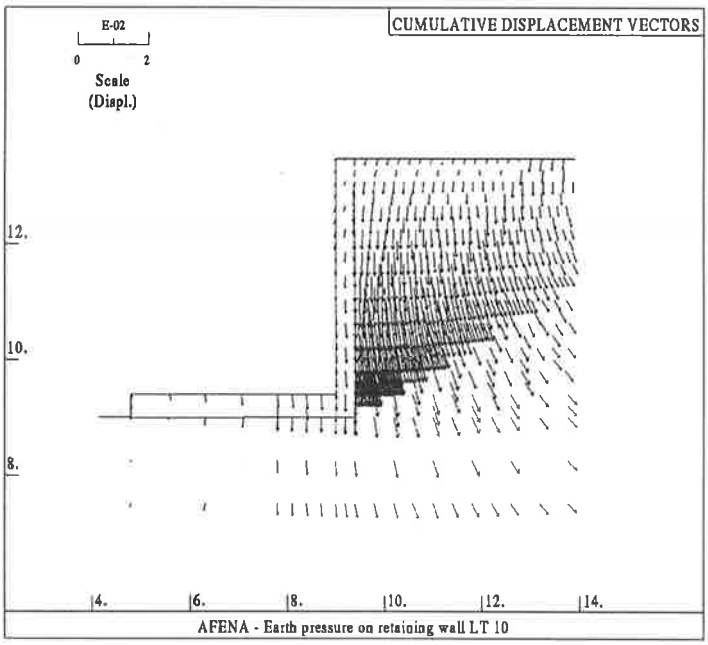

(b)

Figure 5.19 Cantilever L-wall with a triangular backfill with a/H=1.0: (a) wall and soil movements ; and (b) accumulative displacement vectors.

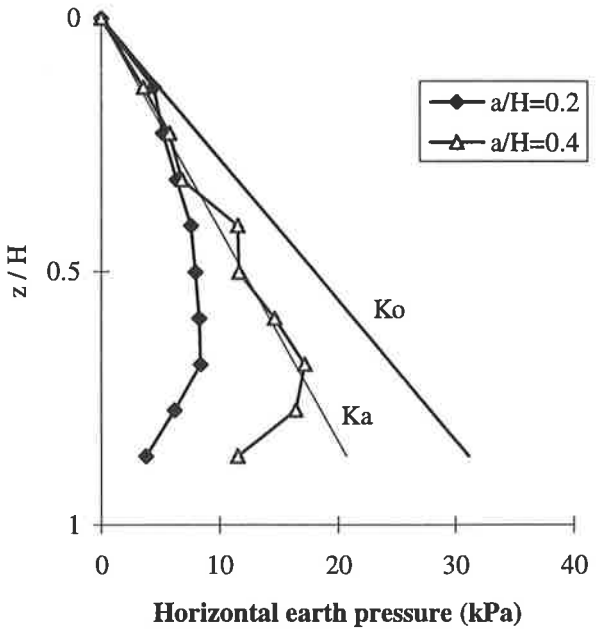

(a)

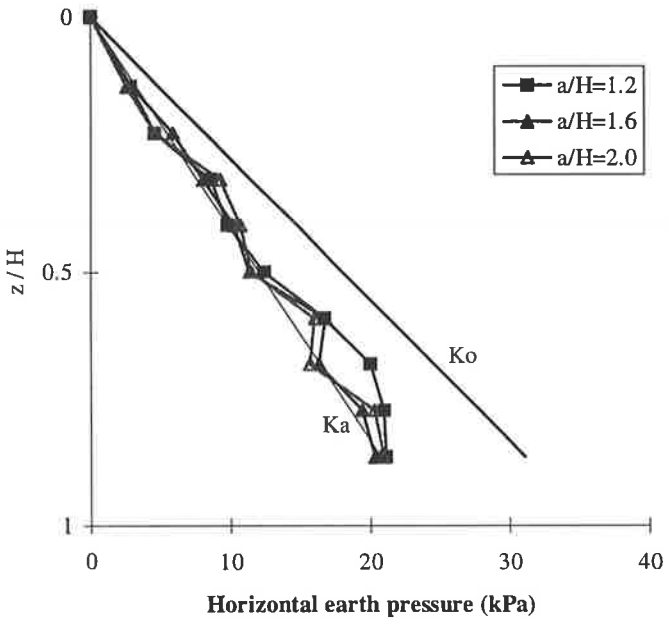

(b)

Figure 5.20 Typical lateral earth pressure distributions for L-walls with triangular backfills: (a) narrow backfills; and (b) wide backfills.

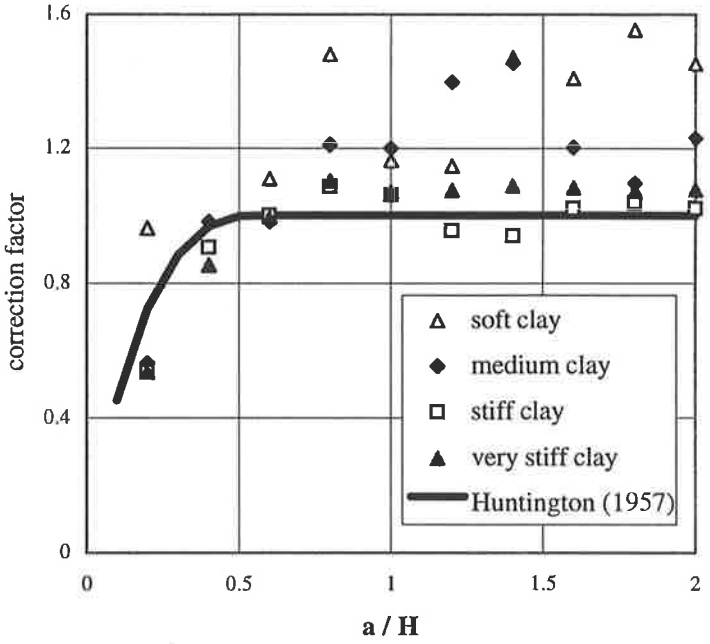

Figure 5.21 Variation of lateral thrust correction factor, β, with backfill size ratio, a/H, for L-walls having triangular backfills and founded in clays.

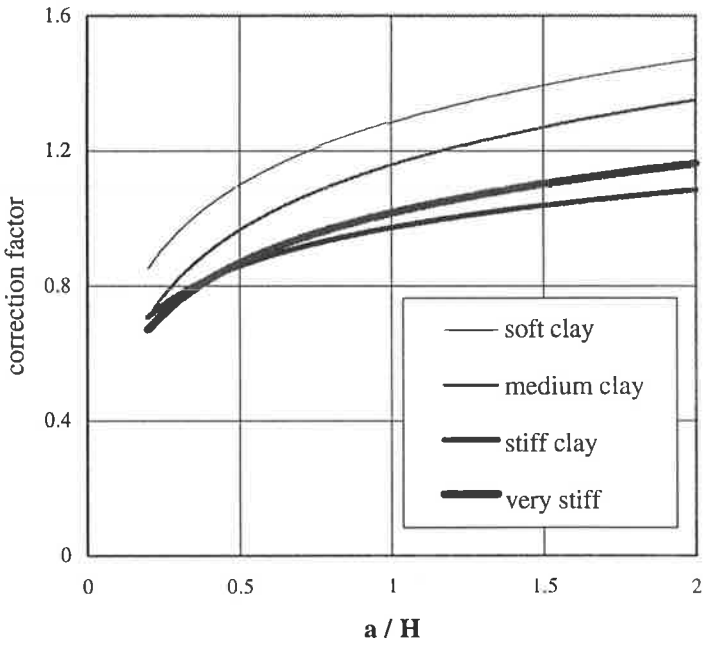

Figure 5.22 Design curves for lateral thrust correction factor, β, for L-walls having triangular backfills and founded in clays.

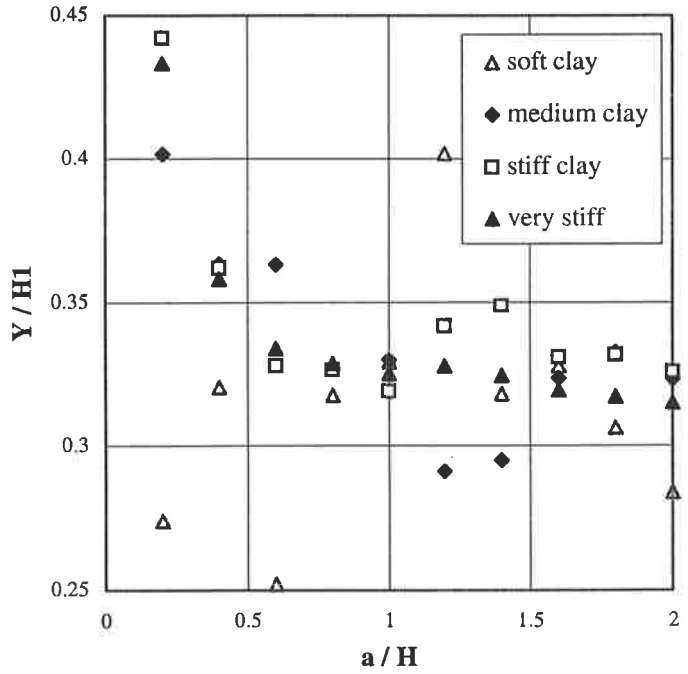

Figure 5.23 Variation of the normalised location of the lateral thrust, Y/H1, with a/H for L-walls having triangular backfills and founded in clays.

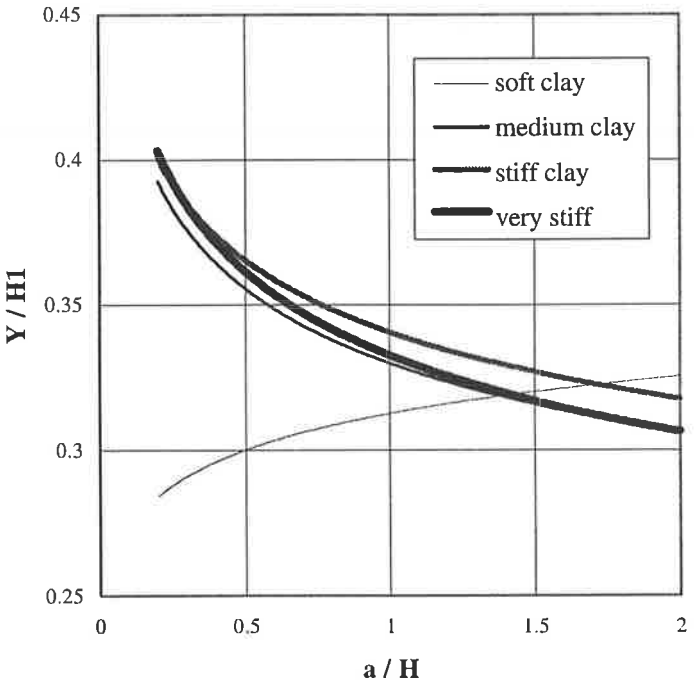

Figure 5.24 Design curves for the normalised location of the lateral thrust, Y/H1, for L-walls having triangular backfills and founded in clays.

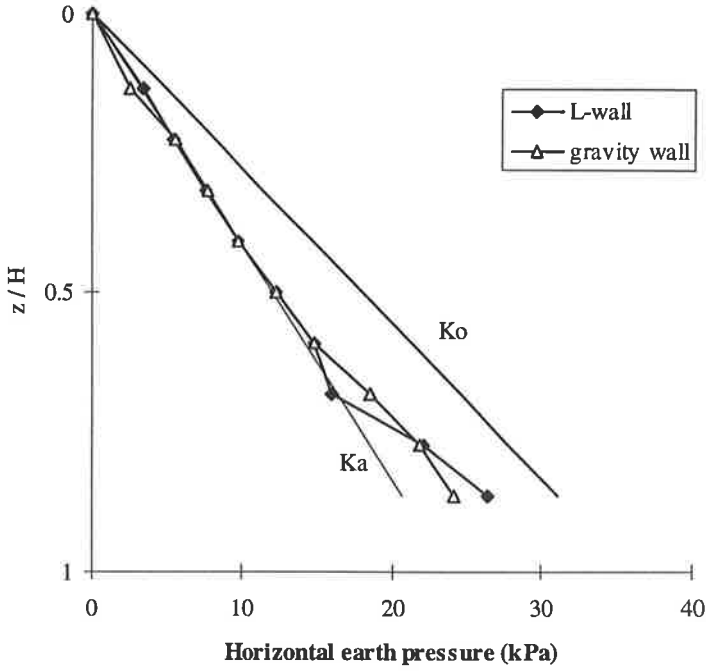

Figure 5.25 The lateral pressure distribution for gravity walls and L-walls with trapezoidal backfills, with c/H=2.0 and b/H=0.5, and founded on stiff clays.

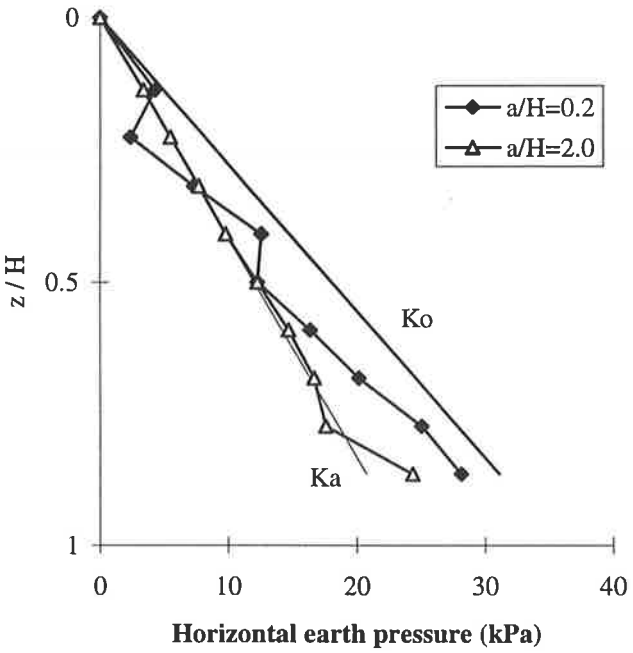

Figure 5.26 The lateral pressure distributions for L-walls with non-homogeneous backfills and founded on stiff clays.

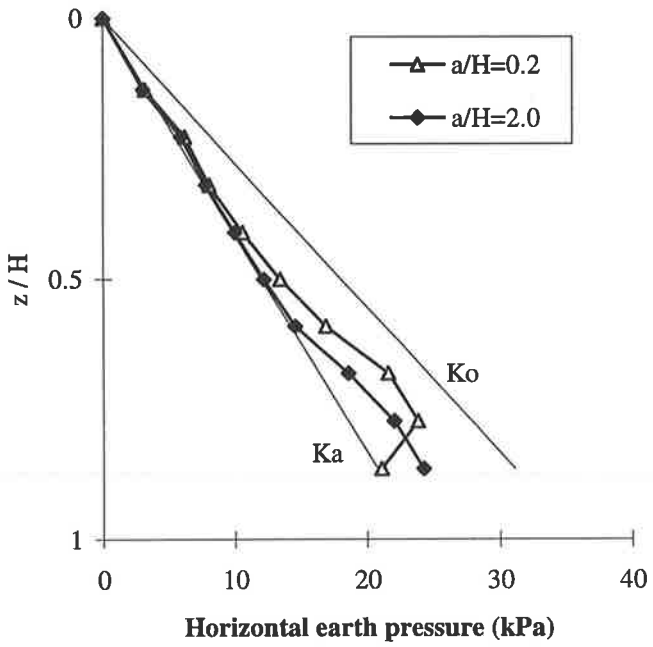

Figure 5.27 The lateral pressure distributions for gravity walls with non-homogeneous backfills and founded on stiff clays.

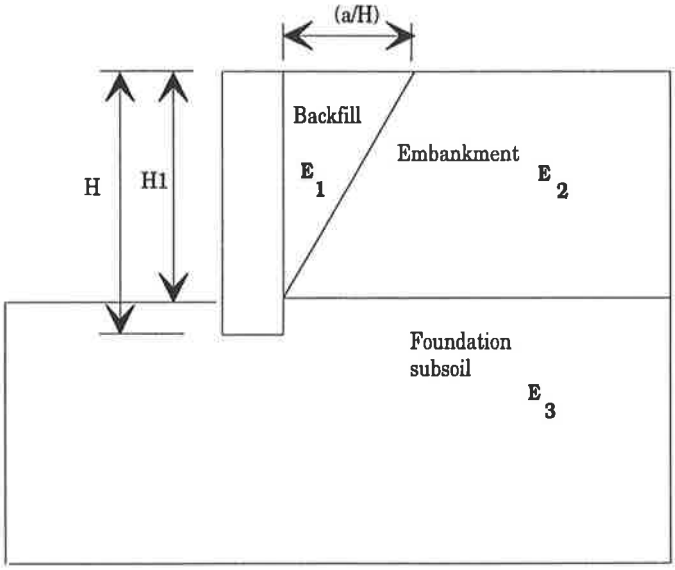

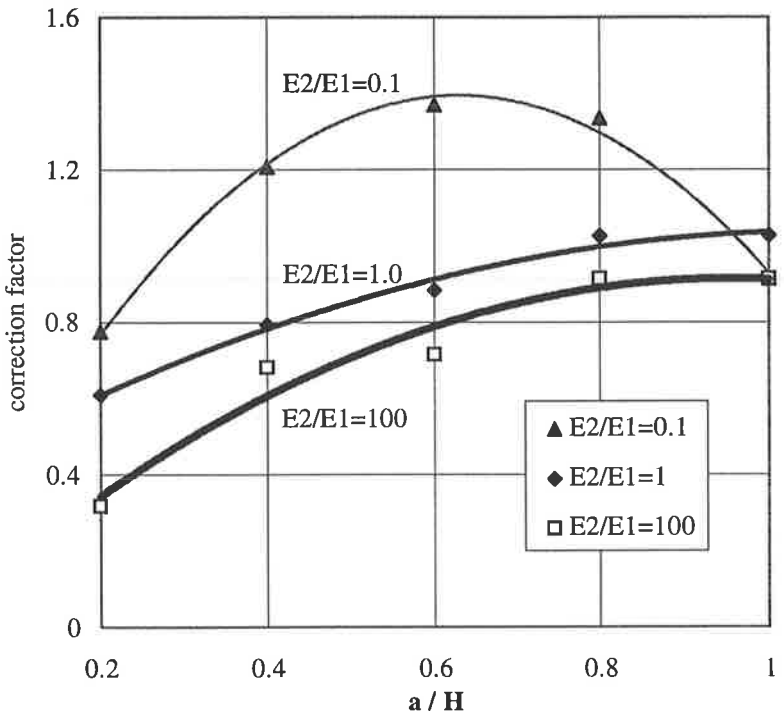

Figure 5.28 Variation of the lateral thrust correction factor, β, with a/H for gravity walls with triangular backfills and having different embankment stiffness.

Chapter 6

Application of Numerical Results to the Design of Retaining Walls

6.1 INTRODUCTION

The current practice of the design of retaining walls is reviewed, as well as the factors of the cost allocated for design, uncertainty of soil design parameters and insufficient information on different drainage systems. Simplified lateral earth pressure distributions are presented, based on the results of numerical studies of limited backfill conditions presented in Chapters 4 and 5. These design distributions are given for homogeneous and non-homogeneous backfills, in the form of upper and lower bounds. In order to present a rational method for design, a step-by-step design procedure for retaining walls with limited backfills is introduced. One case study of a retaining wall, built in the Adelaide metropolitan area, South Australia, is used to demonstrate the applicability of the proposed design method.

6.2 CURRENT DESIGN PRACTICE

The vast majority of design manuals, such as Code of Practice No. 2 for Earth Retaining Structures (1952), recommend that a drainage system be used behind retaining walls. However, no sufficient design data on drainage systems are provided that take into account different site conditions. This is to be expected because site specific factors and cost greatly vary from one site to another. A survey carried out by the author of the consulting engineers in Adelaide, South Australia, showed that the engineers have been left without guidance and there are many instances of poor practice. The reasons are many but include:

- minimal expenditure on design due to low overall construction costs of concrete retaining walls;
- insufficient data on drainage systems;
- uncertainties in the choice of soil design parameters, as a result of limited or no testing;
- use of classical earth pressure theories under inappropriate field conditions;
- Local Council requirements and regulations.

In routine design, the engineer is given the height of the retaining wall and incomplete data on in situ soil parameters. Accordingly, the engineer relies on experience in selecting appropriate soil design parameters. Using these parameters often overestimates the lateral pressures on the wall. It is common practice for the engineer to not clearly specify on the construction drawings the lateral extent of the drainage zone due to lack of data on drainage systems. Accordingly, the choice of the geometry and dimensions is left to the contractor who uses an in house drainage system (independent of the type of wall) without engineering support. As an example of this poor design, Figure 6.1 shows a construction drawing of a retaining wall that was designed and built in the metropolitan area of Adelaide. It can be seen that the dimensions of the drainage zone are not specified on the drawing provided by the consulting engineer.

6.3 SIMPLIFIED DESIGN DISTRIBUTIONS

The lateral earth pressure distributions presented in Chapters 4 and 5 showed only slight differences, from the design point of view, for the different types of walls considered. This is due to the fact that the three retaining walls moved slightly, with a maximum movement of $\Delta / H < 1.0\%$, and this movement was sufficient to reduce the lateral pressures, at least, at the upper half of the wall to their active values. However, the shear force along the base of the

wall increases the lateral pressures, particularly at the base of the wall. Therefore one distribution can be used, for the three walls, for design purposes.

In the following, the design distributions are developed for both homogeneous and non-homogeneous backfills. Note that these distributions are valid only for rigid retaining walls with smooth vertical backs and a horizontal ground surface. The distributions resulted in the case of the very stiff clay are not shown as they are very close to those of the stiff clay.

Although sufficient dimensions of the wall were selected, the prediction of the behaviour of retaining walls founded on soft clays and the associated lateral pressure distributions, involve a high level of uncertainty. This was partially due to incompatibility of strains close to the interface zone between the soft clay and the granular backfill. Therefore, the simplified lateral pressure distributions, presented in the current section, are not recommended for soft clays.

6.3.1 Homogeneous Backfills

It was discussed in Chapter 3 that trapezoidal and rectangular backfills are more likely to be found in the construction of cantilever T-walls. Therefore, the simplified lateral pressure distributions for these geometries are presented only for T-walls. On the other hand, the simplified distributions of triangular backfills are given for the three types of retaining wall.

Except for the soft clay, the results show that the limiting value of the backfill size ratio is close, from design point of view, to the classical value, $\lambda_c = \cot(45+\phi/2)$, which was recommended by Huntington (1957). Thus, the classical value of λ_c is recommended for design purposes to be used to define the boundary between narrow and wide backfills.

(a) Triangular Backfills

Figure 6.2 shows typical lateral earth pressure distributions for the three walls, having limited homogeneous triangular narrow backfills, with $a/H \leq \lambda_c$, and founded on medium and stiff clays. It can be seen that, there are slight differences in magnitudes of the LEPs for the corresponding a/H values, between the three types of retaining walls. Figure 6.3 shows typical lateral pressure distributions for the three walls having limited homogeneous triangular wide backfills, with $a/H > \lambda_c$, and founded on medium and stiff clays.

Figure 6.4 (a) shows the simplified lateral earth pressure distributions recommended for use in the design of rigid retaining walls with narrow triangular backfills, which are based on the data presented in Figure 6.2. As a lower bound of the LEPs, it is recommended to use a linear

$0.5\,K_a$ distribution in the upper half, and linearly decreasing the LEPs to zero in the lower half. For the upper bound, it is recommended to use a linear K_0 distribution in the upper half and a uniform $0.5\,K_0$ distribution in the lower half.

The simplified lateral earth pressure distributions recommended for wide triangular backfills are shown in Figure 6.4 (b), which are based on the data presented in Figure 6.3. It is recommended to use a linear K_a distribution over the full height of the wall, as a lower bound of the LEPs. For the upper bound, it is recommended to use a linear K_0 distribution in the upper half, and linearly increasing the LEPs in the lower half to reach a value of $2.5\,K_a$ at a depth, z=H.

(a) Rectangular Backfills

Figure 6.5 shows typical lateral earth pressure distributions for cantilever T-walls having narrow rectangular backfills, with $a/H \leq \lambda_c$, and founded on medium and stiff clays. Figure 6.6 shows typical lateral pressure distributions for cantilever T-walls having wide rectangular backfills, with $a/H > \lambda_c$, and founded on medium and stiff clays.

Figure 6.7 (a) shows the simplified lateral earth pressure distributions recommended for use in the design of cantilever T-walls with narrow rectangular backfills. As a lower bound of the LEPs, it is recommended to use: a linear $0.5\,K_a$ distribution in the upper half; and a uniform $0.25\,K_a$ distribution in the lower half. For the upper bound, it is recommended to use: a linear K_0 distribution in the upper half; and a uniform $0.5\,K_0$ distribution in the lower half.

The simplified lateral earth pressure distributions recommended for wide rectangular backfills are shown in Figure 6.7 (b). It is recommended to use a linear K_a distribution over the full height of the wall, as a lower bound of the LEPs. For the upper bound, it is recommended to use a linear K_0 distribution over the full height of the wall. Note that the LEPs are comparatively close to their lower bound (K_a), except for the upper third of the wall.

(a) Trapezoidal Backfills

It was concluded in Section 5.4 that the LEPs for L-walls and gravity walls with trapezoidal backfills, from design point of view, are close to wide triangular backfills. Accordingly, the simplified distributions developed for triangular backfills are recommended to be used for L-walls and gravity walls with trapezoidal backfills. Note that the LEPs for L-walls and gravity walls are comparatively close to the lower bound shown in Figure 6.4 (b).

Figure 6.8 shows typical lateral earth pressure distributions for cantilever T-walls having narrow trapezoidal backfills, with $a / H \leq \lambda_c$, and founded on medium and stiff clays. Figure 6.9 shows typical lateral pressure distributions for cantilever T-walls having wide trapezoidal backfills, with $a / H > \lambda_c$, and founded on medium and stiff clays.

Figure 6.10 (a) shows the simplified lateral earth pressure distributions, at the virtual back of the wall, recommended for use in the design of cantilever T-walls with narrow trapezoidal backfills. As a lower bound of the LEPs, it is recommended to use a linear 2/3 K_a distribution over the full height of the wall. For the upper bound, it is recommended to use a linear K_0 distribution in the upper half, but a uniform $0.5\,K_0$ distribution in the lower half. Note that this upper bound is the same one recommended for T-walls with narrow triangular backfills.

The simplified lateral earth pressure distributions, at the virtual back of the wall, recommended for wide trapezoidal backfills are shown in Figure 6.10 (b). It is recommended to use a linear K_a distribution in the upper two thirds of the wall, but a uniform $2/3\,K_a$ distribution in the lower third, as a lower bound of the LEPs. For the upper bound, it is recommended to use: a linear K_0 distribution in the upper two thirds of the wall; and a uniform $2/3\,K_0$ distribution in the lower third.

In Chapter 4, the results of T-walls with trapezoidal backfills showed some differences in magnitudes of the LEPs between lateral pressure distributions at the back of the wall and those developed at the virtual back. However, these differences are slight and can be neglected from design point of view. Also, the results showed that the lateral pressures exceeded the K_a values, and the term *narrow backfills* is not valid. Therefore, the simplified lateral pressure distributions presented in Figure 6.10 (b) are recommended to be used, at the back of the wall, for T-walls with trapezoidal backfills.

6.3.2 Non-Homogeneous Backfills

The results of analyses of retaining walls with non-homogeneous backfills demonstrated that the lateral thrust is often larger than the classical values. Figure 6.11 shows distributions of lateral earth pressures behind the three wall types founded on medium and stiff clays. Figure 6.12 shows the simplified lateral earth pressure distributions for the three retaining walls with non-homogeneous backfills and founded on medium, stiff and very stiff clays.

A linear K_a distribution is recommended to be used over the full height of the wall, as a lower bound of the LEPs. For the upper bound of the LEPs, it is suggested to use a linear K_0

distribution at the upper half, and linearly increasing the LEPs, in the lower half, to reach a value of $3\,K_a$ at a depth, z=H.

The simplified lateral pressure distributions, presented in the present section are valid only for:

- a rigid retaining wall having a vertical rear face and less than 4.5 m in height with a horizontal ground surface;
- a self supported cohesive embankment during construction, as there is no provision for temporary supports or allowance for large movements of the embankment, due to softening or wetting of the clay due to surface water or rainfall. The embankment is less than 4.1 m in height; and
- a loosely placed backfill, to provide the necessary drainage, as there was no compaction allowed in the granular backfill.

Based on the design distributions presented in the present section, it can be concluded that the linear K_0 distribution, which was recommended by Bowles (1988) for limited backfill conditions, represents an upper bound for the LEPs, at least in the upper half of the wall.

6.4 DESIGN PROCEDURE

Based on the analyses that have been carried out in the current numerical study and the results of the survey of the current design practice, a design procedure is recommended. This design process, for retaining walls, involves a number of steps that are summarised in a flow chart shown in Figure 6.13. The first step in this design process is the identification of design constraints such as site conditions, material availability and cost factors. After selecting a suitable type of the wall, which meets the design constraints, a preliminary design of the wall is required. Having the site conditions and the preliminary dimensions of the wall, a suitable drainage system can be chosen guided by those recommended by Huntington (1957). Obtaining a suitable size and geometry of the backfill, a favourable type of backfill material can be determined in step four, guided by the requirements of design codes, such as CP No. 2 (1951) for filter properties.

In step five, the engineer will be able to obtain the magnitude and location of the lateral thrust. If the properties of the natural deposit are known, it is recommended that the design curves presented in Chapters 4 and 5 be used according to the type of the wall. To use these design curves, an evaluation of properties of the clay deposit is required and the category of the clay should be determined, ie whether soft, medium, stiff or very stiff clay. Table 3.3 will help the engineer to fit each job to one of the four clay categories used in this research, by comparing the available parameters of the clay with those used in the analyses and using engineering judgement for intermediate values. From these design curves, the magnitude of the lateral thrust can be obtained as the product of β times the Rankine active lateral thrust. The location of the lateral thrust can be determined directly from the Y/H1 curves.

However, for a small design, if the soil parameters of the natural deposit are not known, which is often the case, the recommended distributions, presented in Section 6.3, can be used. These distributions are favourable for geotechnical engineers as they not only offer the magnitude and location of the lateral thrust, but also the location of the maximum bending moment can be determined by using the principles of linear-elastic-beam method. Thus, the magnitude and location of the lateral thrust can be readily obtained.

In step seven, sufficient information regarding the magnitude and location of the lateral thrust is obtained. In step eight, a number of classical steps are involved similar to any geotechnical design, that should be carried out to ensure the integrity of the retaining wall. These involve checking the overall stability, bearing capacity, and settlements. Attention should be paid to retaining walls founded on soft clays as they might experience shallow shear failure.

Structural design and dimensioning is carried out in step nine. Care should be given to the provision of haunches for T-walls, if required, at the critical section where the stem meets the base. This is because large lateral pressures were predicted by the FEM at this critical section for wide triangular backfills and non-homogenous backfills. If the wall, with its final dimensions, still satisfy the design constraints, a final step is carried out, including execution of construction drawings which should clearly specify the drainage system dimensions and material properties. However, if the wall does not satisfy the design constraints, a fine tuning step is required, in which it may be necessary to select another type of retaining wall.

6.5 CASE STUDY

A case study of an existing retaining wall is investigated to demonstrate the applicability of the design procedure discussed in the previous section and the simplified distributions presented in Section 6.3.

The wall was designed in 1990 by one of the consulting engineering firms in Adelaide, and was constructed in the metropolitan area of Adelaide, South Australia. The wall was built on a stiff clay with a limited granular backfill. Figure 6.14 shows the construction drawing of this wall, showing insufficient dimensions for the size and geometry of the backfill. It can be seen that the wall is a cantilever L-wall which forms a part of a basement. The wall is a 370 mm wide double leaf masonry wall. The total height of the wall, H=3.05 m and the embankment height, H1=2.6 m. Inspection of the calculation sheets demonstrated that the engineer over estimated the soil parameters in order to account for their uncertainty. The wall was assumed to have a smooth back, and the linear active Rankine distribution was used to determine the lateral pressures, without consideration of the geometry and size of the backfill.

As mentioned, the dimensions of the backfill were not provided, but the backfill size ratio can be roughly estimated as a/H=0.2 by scaling from Figure 6.14. Using the design procedure outlined in Section 6.4, a drainage system comprising: (i) an impervious surface layer to prevent infiltration of surface water, which is represented by the pavement around the building; (ii) a free draining granular soil; and (iii) weep holes, is used.

If the design curves given for L-walls are used, assuming: a triangular backfill; backfill size ratio, a/H=0.2; and a stiff clay deposit. Thus, the lateral thrust, $P = 0.7P_a$, from Figure 5.22 and the location of this thrust, Y=0.39H1, from Figure 5.24. Hence, the bending moment at the bottom of the stem is less than the design bending moment by 18%.

On the other hand, if the upper bound of the LEPs, given in Figure 6.4 (a), for a narrow triangular backfill is used, hence $P = 1.125P_a$ and Y=0.44H1. Thus, the estimated bending moment at the bottom of the stem is larger than the design value used by the engineer by 50%. On the other hand, if the lower bound of the LEPs is used, which is given in the same figure, hence $P = 0.5P_a$ and Y=0.5H1. Thus, the estimated bending moment at the bottom of the stem is lower than the design value used by the engineer by 25%.

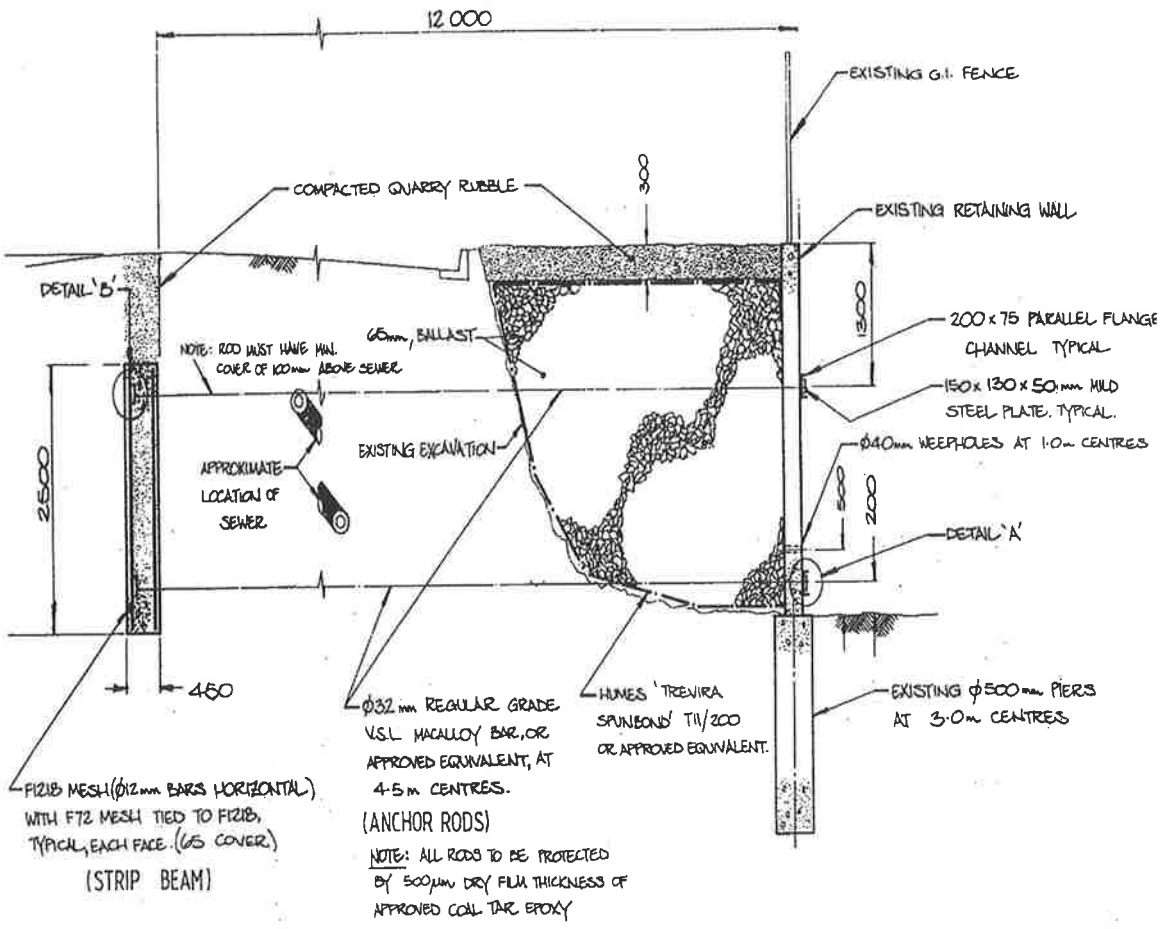

Figure 6.1 **A construction drawing of a retaining wall provided with a drainage system (*courtesy of M. B. Jaksa*).**

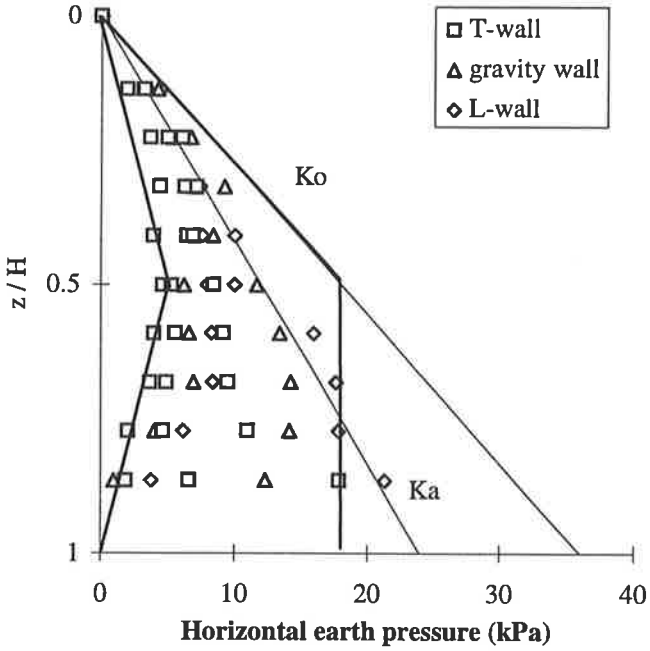

(a)

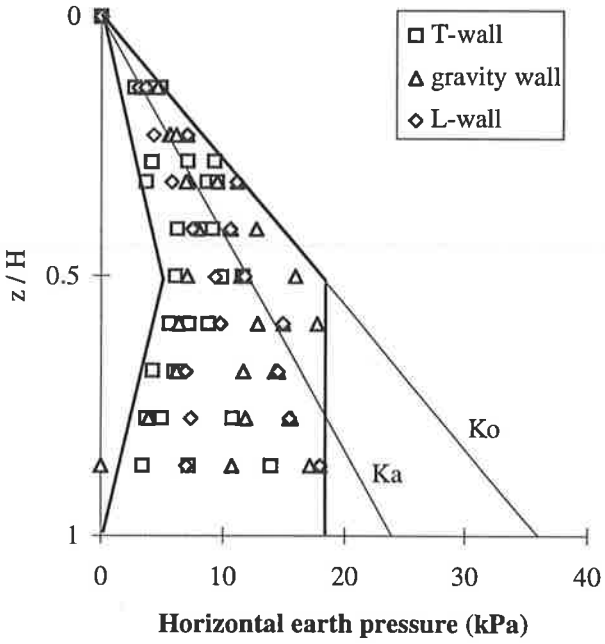

(b)

Figure 6.2 Typical lateral pressure distributions for rigid retaining walls having narrow triangular backfills and founded on: (a) medium clays; and (b) stiff clays.

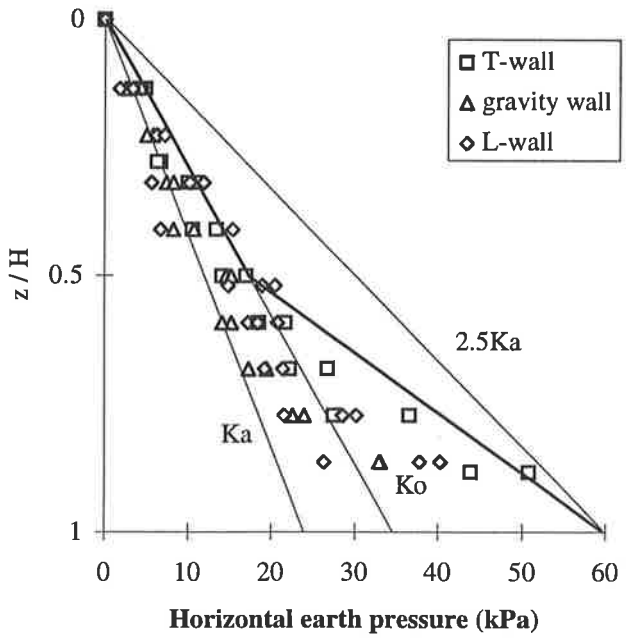

(a)

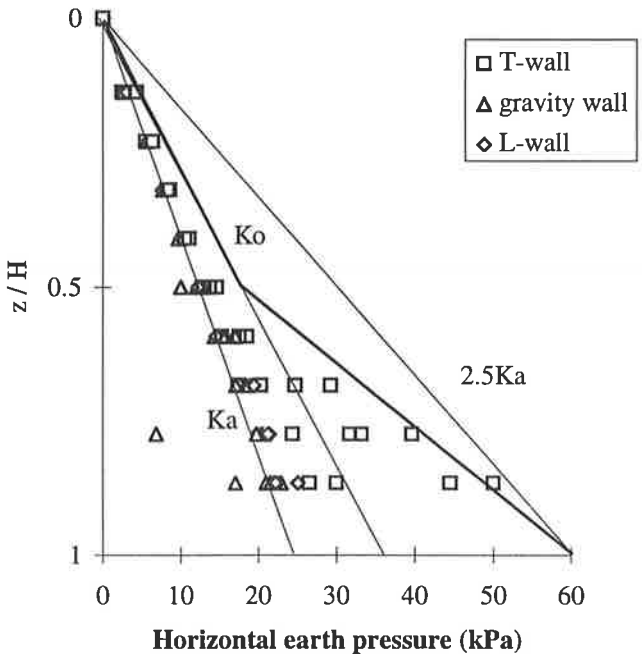

(b)

Figure 6.3 Typical lateral pressure distributions for rigid retaining walls having wide triangular backfills and founded on: (a) medium clays; and (b) stiff clays.

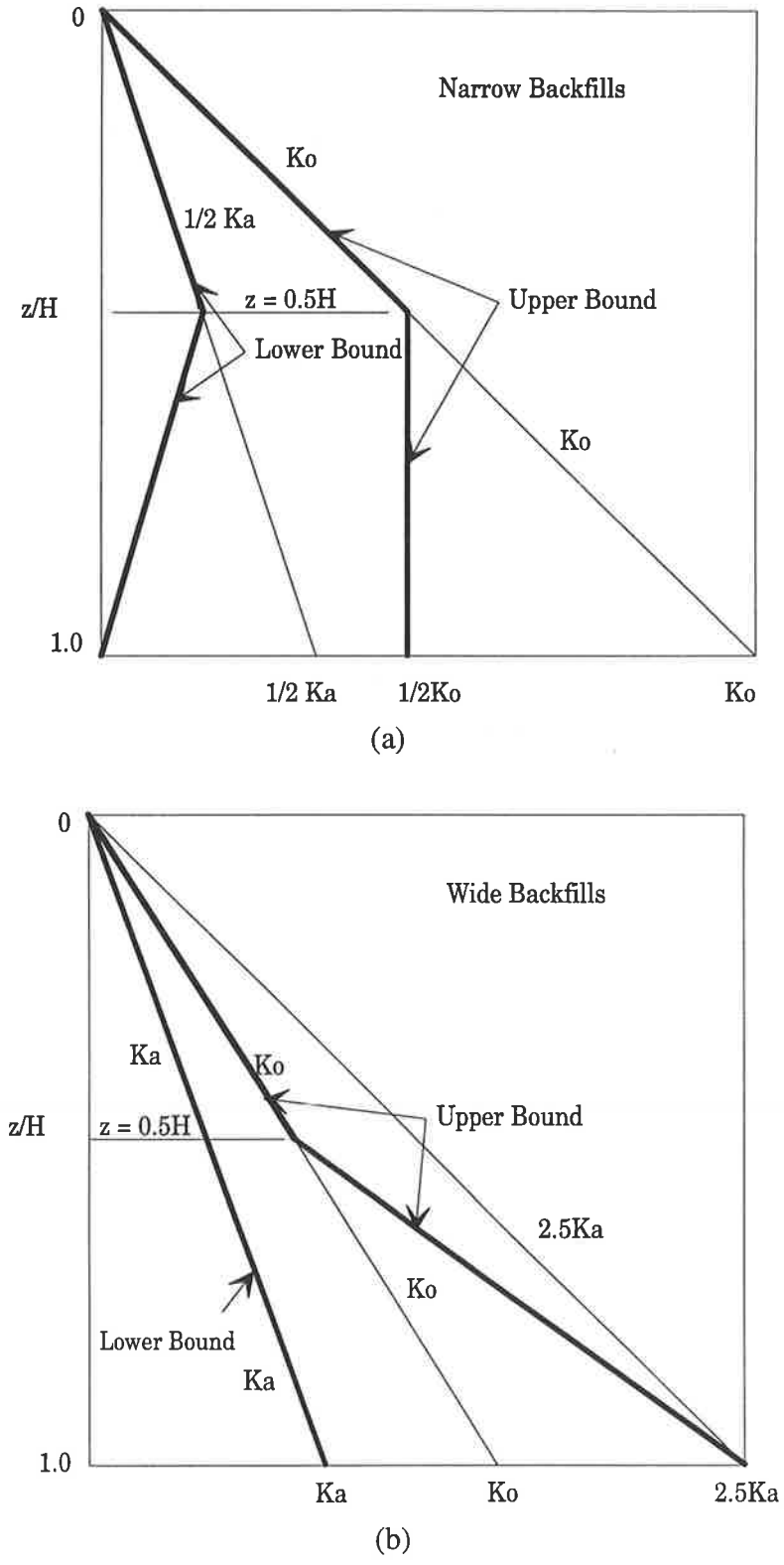

Figure 6.4 Simplified lateral earth pressure distributions for rigid retaining walls with triangular backfills, where the bold lines identify the upper and lower bounds: (a) narrow Backfills; and (b) wide Backfills.

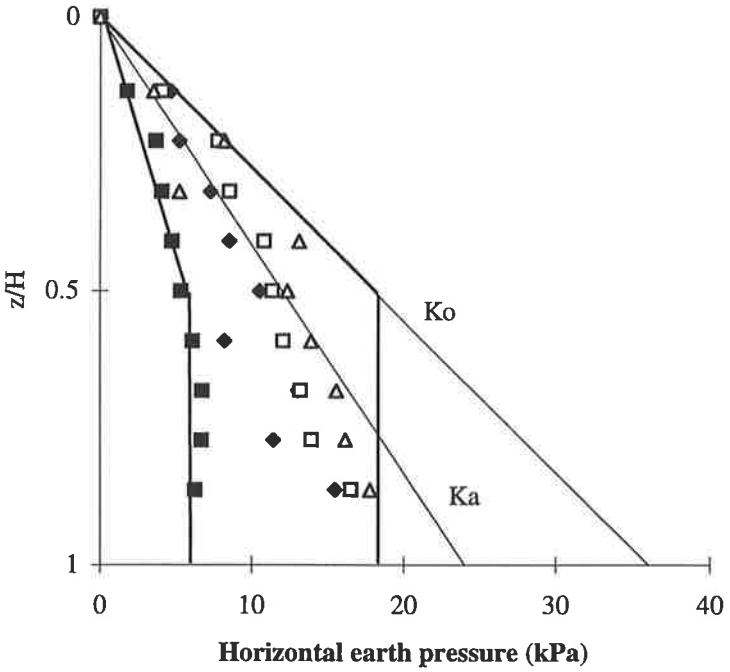

(a)

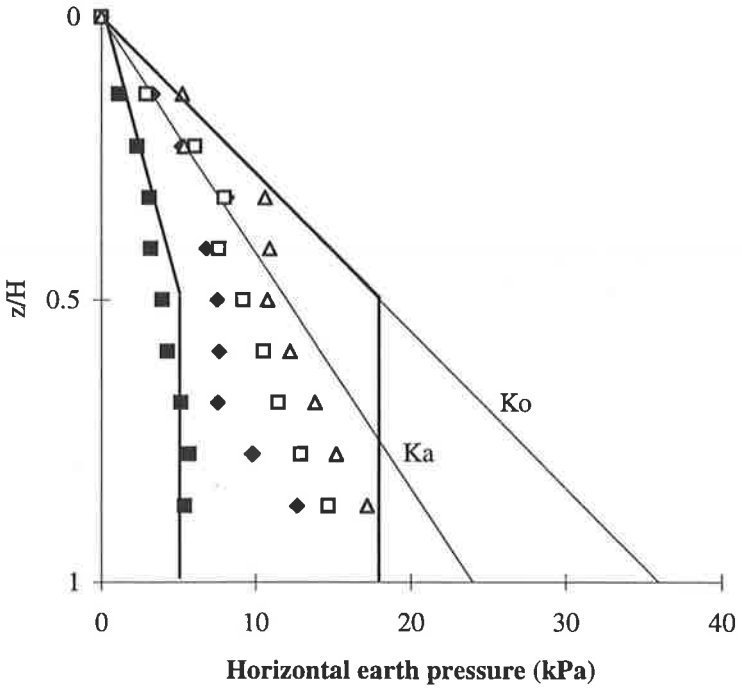

(b)

Figure 6.5 Typical lateral pressure distributions for cantilever T-walls having narrow rectangular backfills and founded on: (a) medium clays; and (b) stiff clays.

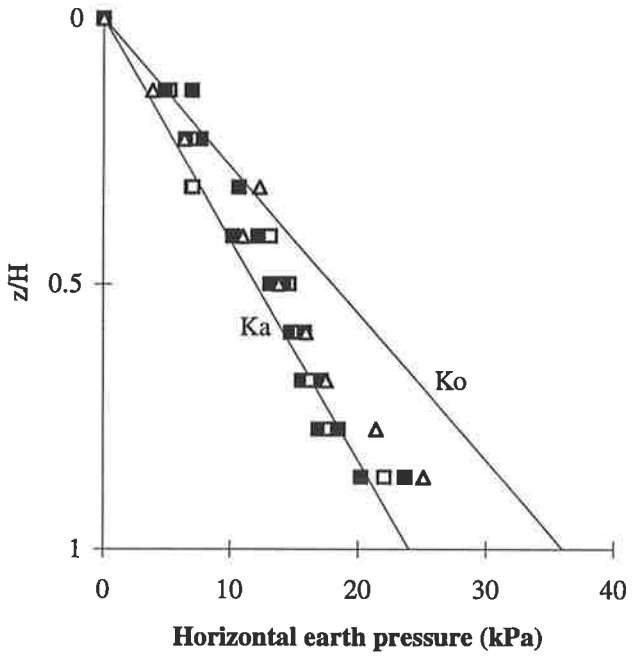

(a)

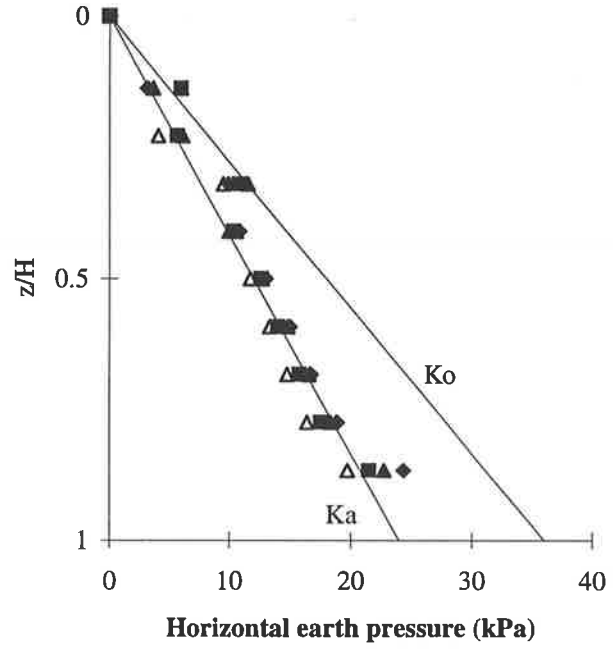

(b)

Figure 6.6 Typical lateral pressure distributions for cantilever T-walls having wide rectangular backfills and founded on: (a) medium clays; and (b) stiff clays.

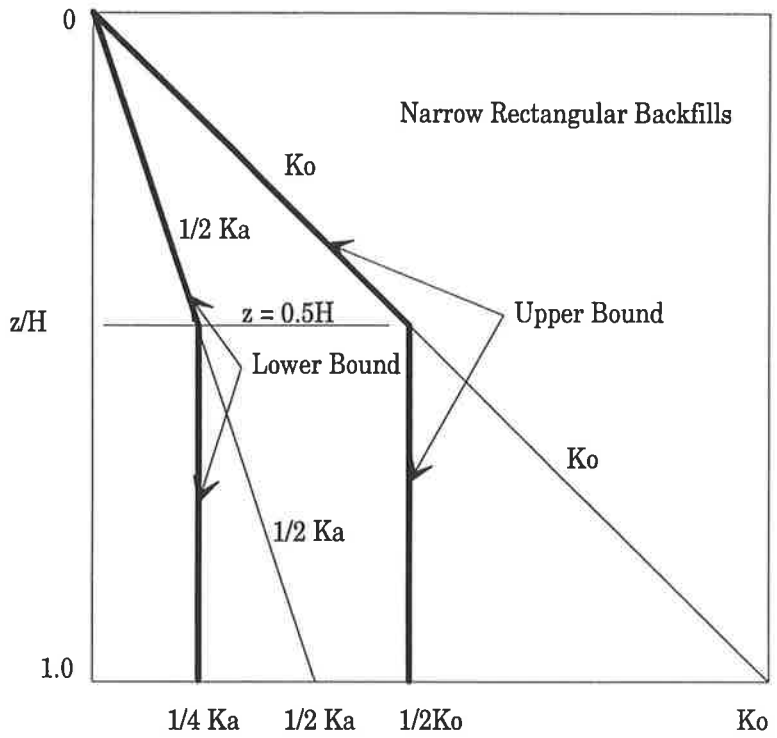

(a)

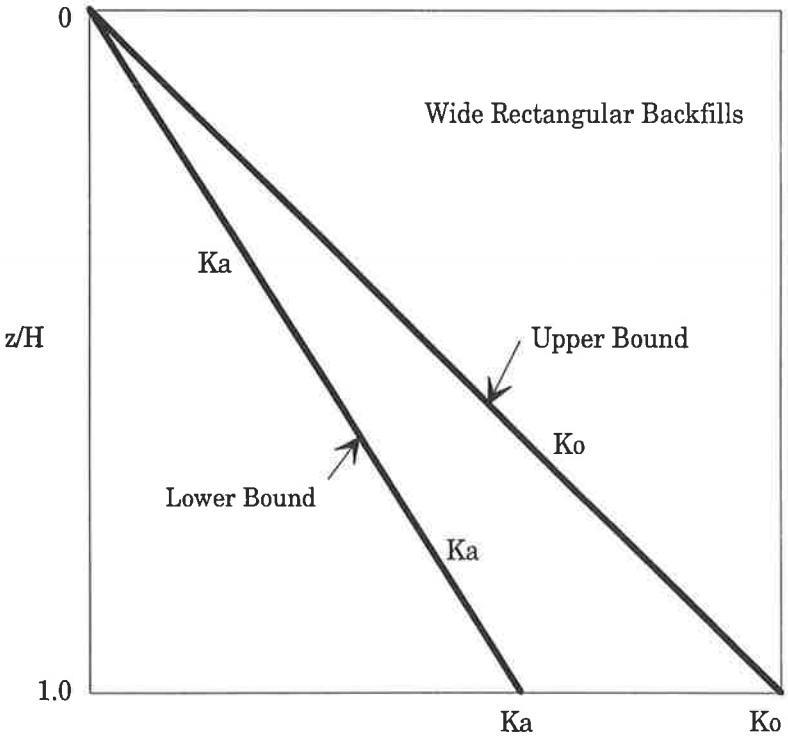

(b)

Figure 6.7 Simplified lateral earth pressure distributions for cantilever T-walls with rectangular backfills, where the bold lines identify the upper and lower bounds: (a) narrow Backfills; and (b) wide Backfills.

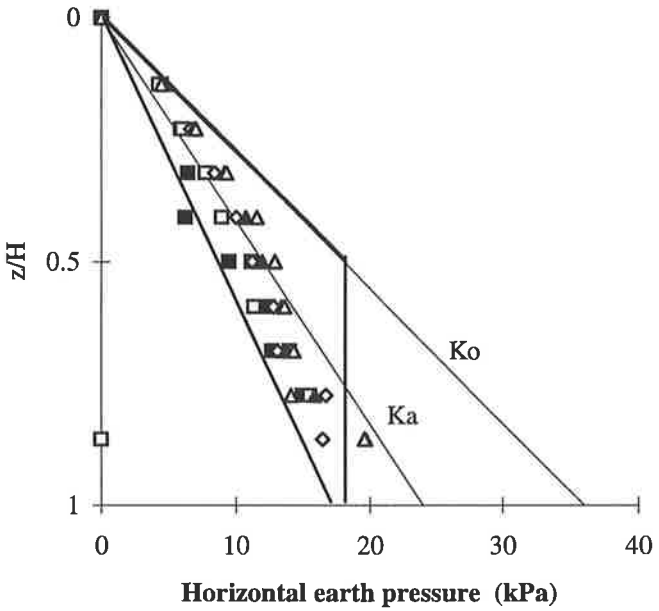

(a)

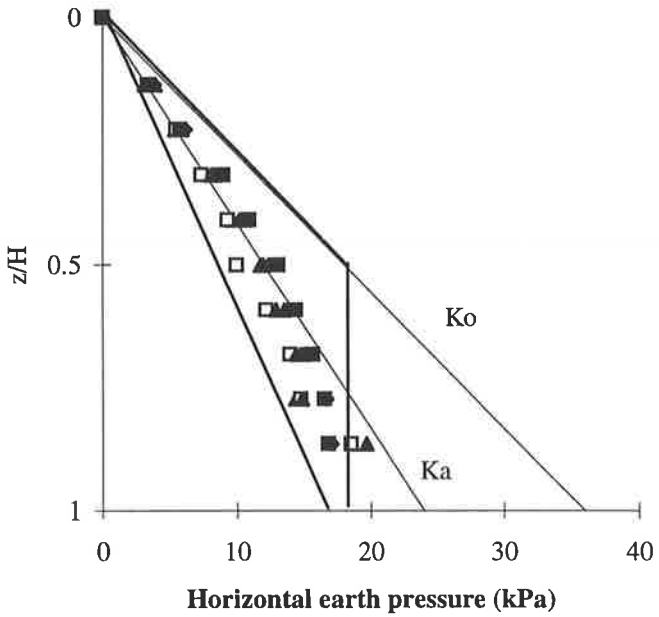

(b)

Figure 6.8 Typical lateral pressure distributions at the virtual back of cantilever T-walls having narrow trapezoidal backfills and founded on:
(a) medium clays; and (b) stiff clays.

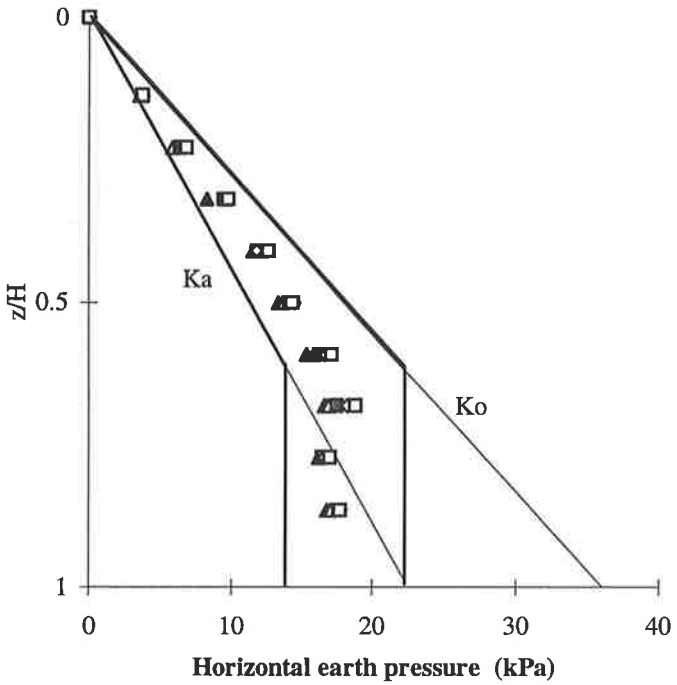

(a)

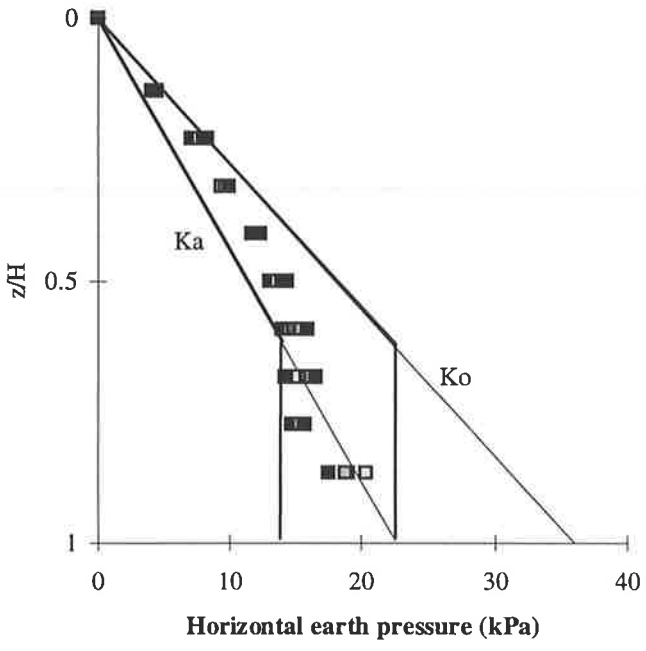

(b)

Figure 6.9 Typical lateral pressure distributions at the virtual back of cantilever T-walls having wide trapezoidal backfills and founded on: (a) medium clays; and (b) stiff clays.

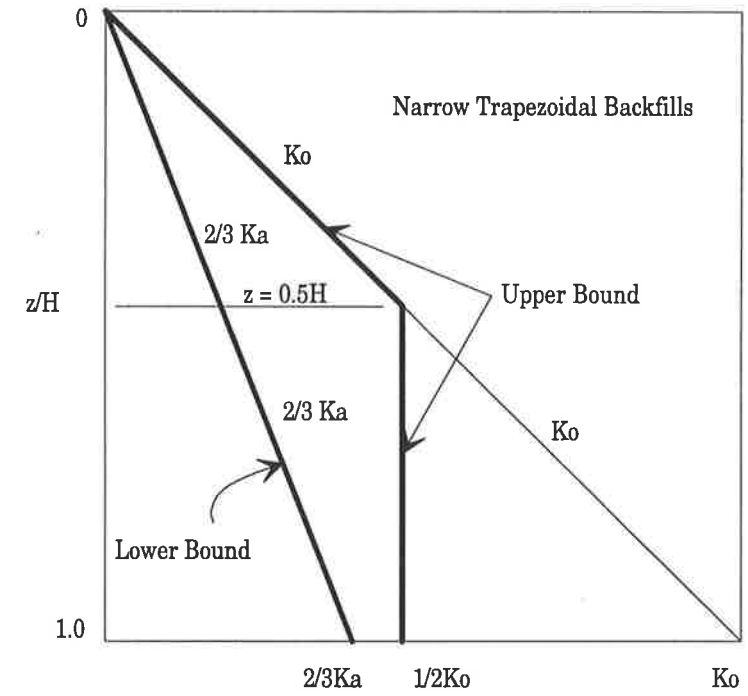

(a)

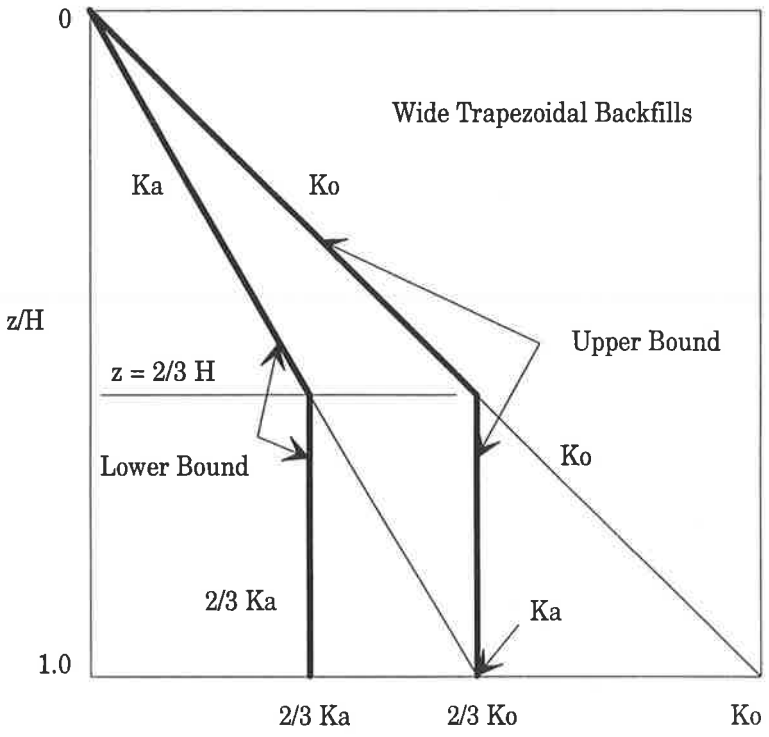

(b)

Figure 6.10 Simplified lateral earth pressure distributions for cantilever T-walls with trapezoidal backfills, where the bold lines identify the upper and lower bounds: (a) narrow Backfills; and (b) wide Backfills.

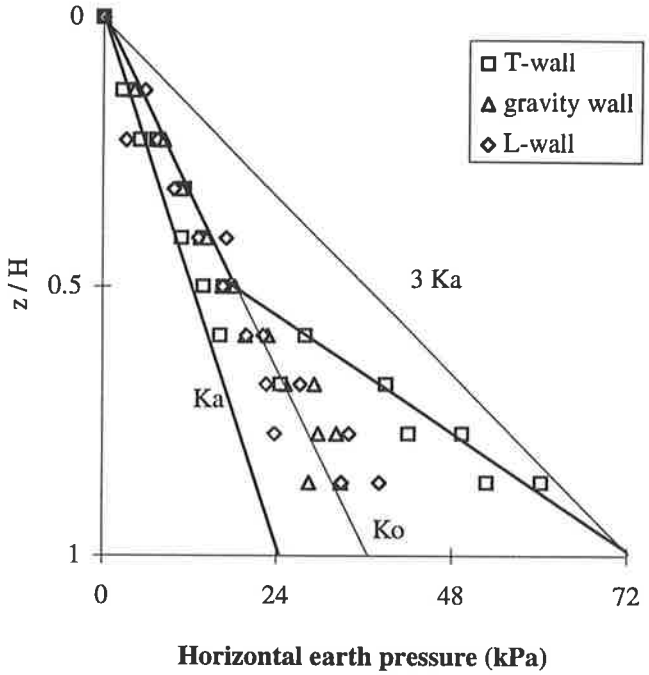

(a)

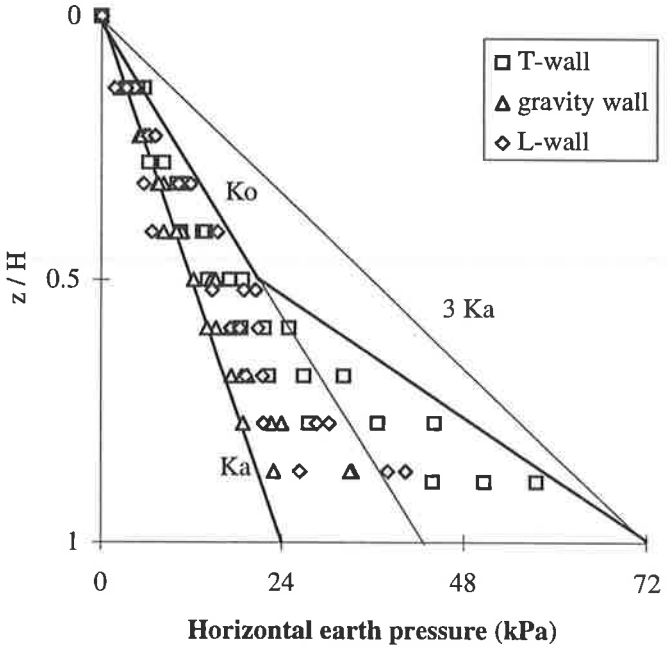

(b)

Figure 6.11 Typical lateral pressure distributions for rigid retaining walls having non-homogeneous backfills and founded on: (a) medium clays; (b) stiff clays.

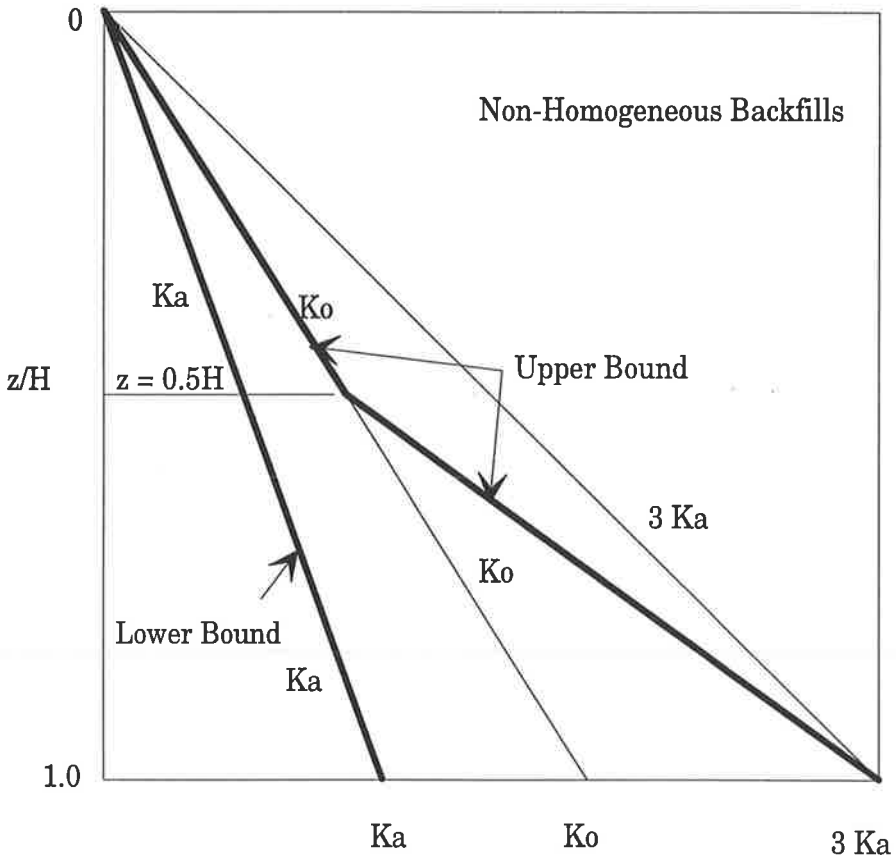

Figure 6.12 Simplified lateral earth pressure distributions for rigid retaining walls with limited non-homogeneous backfills, where the bold lines identify the upper and lower bounds.

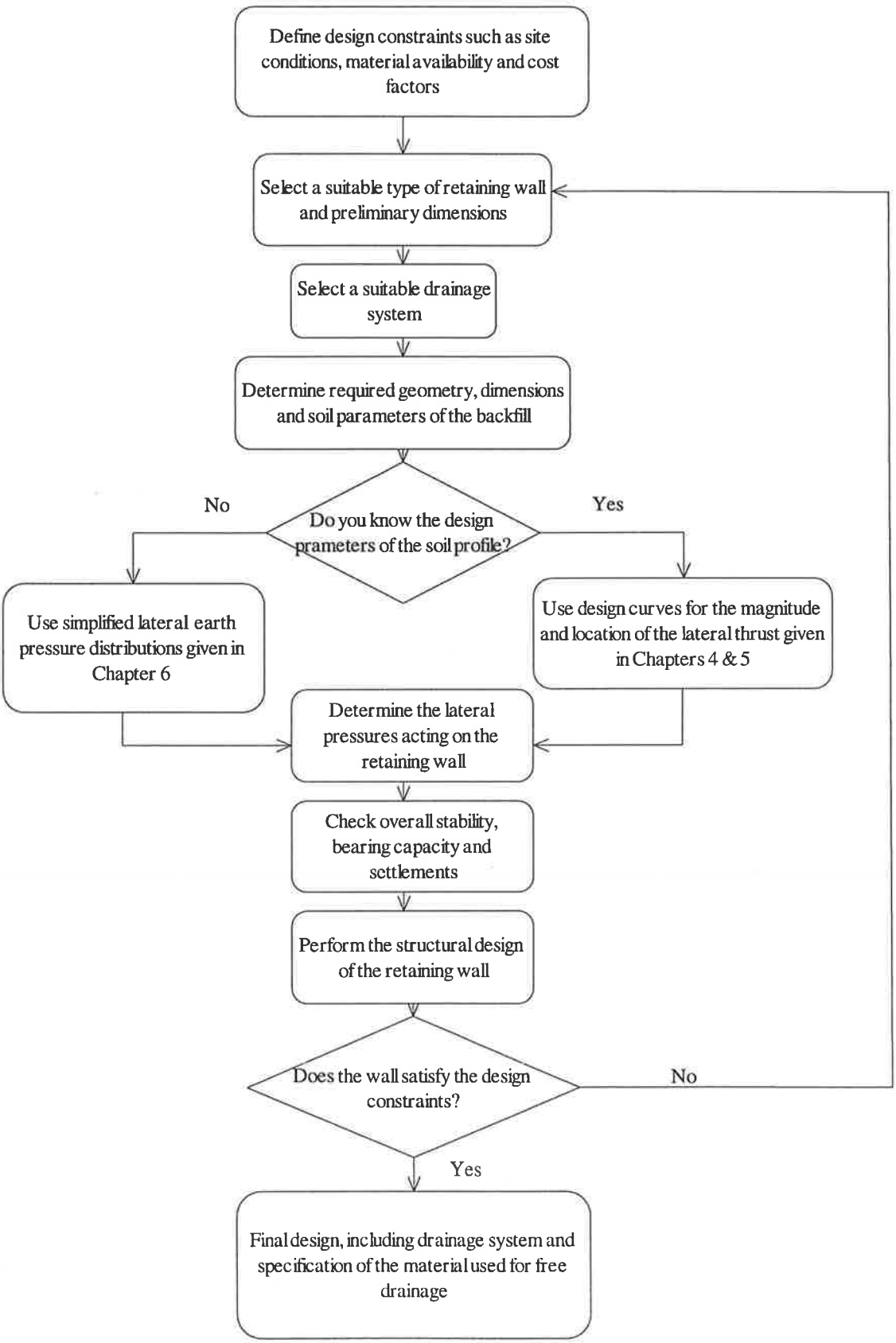

Figure 6.13 Recommended design procedure for retaining walls with limited backfills.

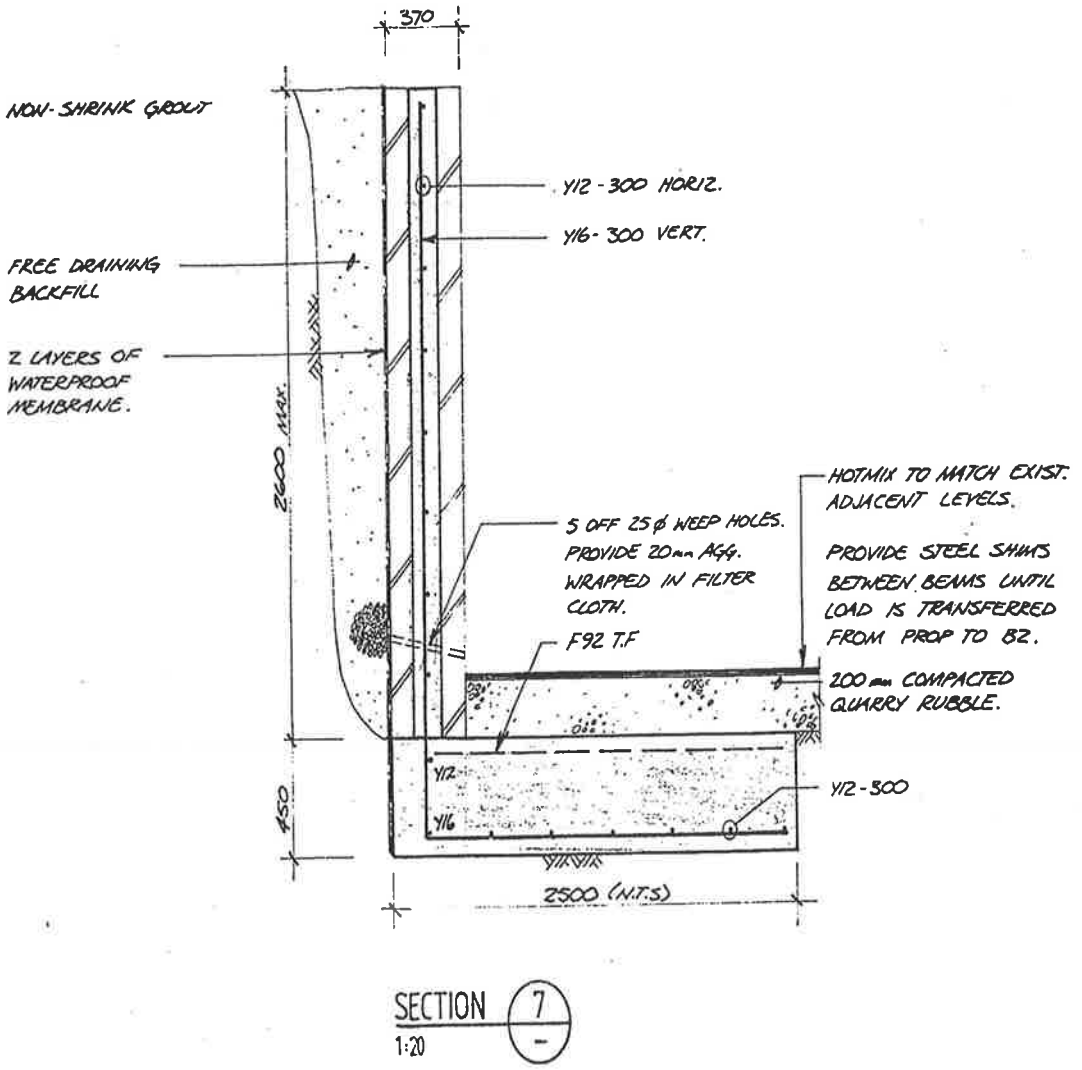

Figure 6.14 Part of the construction drawing of the cantilever L-wall used in the case study (*courtesy of J. Trezona*).

Chapter 7

Summary and Conclusions

7.1 SUMMARY

The principal objective of this research program was to develop design aids that reliably predict the behaviour of retaining walls having limited backfills and founded on cohesive deposits, thus enabling retaining walls to be designed safely and economically. In the following paragraphs the main aspects of the project are summarised.

Review of the literature showed that the determination of lateral earth pressures on retaining walls having limited backfills is poorly treated in major text books, design manuals and codes. The classical earth pressure theories assume that the backfill extends a sufficient distance behind the wall, whereas the trial wedge method is inappropriate for the analysis of limited backfill conditions. However, a number of analytical methods have been developed during the last 40 years or so for the analysis of retaining walls with limited backfills.

Some of the analytical methods are based on a rational theoretical basis, such as Huntington (1957), Bell (1987) and Bang and Tucker (1990). On the other hand, other methods are based on experience and engineering judgement, such as Teng (1962). The FEM was used to assess the suitability of the first group of these analytical methods for use in design.

The finite element program AFENA v4.6 (Carter and Balaam, 1994) was used to study the performance of three types of rigid retaining walls commonly used in residential and highway construction. These walls are: cantilever T-walls; gravity walls; and cantilever L-walls. These walls were modelled as having vertical smooth backs, at-rest initial stress conditions and a horizontal ground surface. Two types of backfill were examined: (i) homogeneous backfill with three different geometries, in which the backfill entirely consists of the granular soil used for drainage; and (ii) non-homogeneous backfill in which the backfill consists of two zones, the granular drainage zone directly behind the wall and a cohesive zone made up of the excavated material.

The cohesive deposit was categorised into four types: soft clay; medium clay; stiff clay; and very stiff clay. For convenience, unconsolidated undrained analyses were carried out and the ground water table was assumed below the foundation level. These conditions provide an adequate simulation of ground water conditions in Adelaide.

The FEM has been found successful in modelling cantilever and gravity retaining walls with different field conditions, particularly those having limited backfills. Two dimensional plane strain, 8-noded isoparametric elements with perfect elastic-plastic constitutive model and Mohr-Coulomb failure criterion were employed in AFENA. The 8-noded isoparametric elements were found appropriate for soil elements and suitable to account for bending rotations of cantilever walls. An incremental construction method was used to simulate a realistic construction sequence of placement of the backfill and simultaneous construction of the wall.

Some difficulties have been encountered with the use of zero-thickness interface elements: (i) insufficient literature on interface shear stiffness for cohesive soils; (ii) inefficient manual procedure when inserting these elements in AFENA.

Although, the numerical results are not supported by laboratory models or field testing, the results have been compared with a number of finite element studies and field measurements, and they were found in good agreement. The results have been

presented in the form of design curves and simplified lateral pressure distribution charts. The major results of the research can be summarised as follows:

- unlimited granular backfills showed reasonably accurate active pressure predictions for L-walls and gravity walls, whereas comparatively large lateral pressures resulted for T-walls particularly in the lower third of the wall.

- the limited homogeneous backfills can be divided into: narrow backfills where the critical backfill size $\lambda \leq \cot(45+\phi/2)$; and wide backfills where $\lambda > \cot(45+\phi/2)$. These values are conservative for the design of L-walls and gravity walls.

- for limited and unlimited backfills, wall movements were small and less than 1.0% but sufficient to mobilise the active conditions, at least in the upper half of the wall.

- Harr (1977) model, that accounts for rigid wall movements, was examined for the case of pure rotation about the base. It was found that this model significantly overestimated the lateral earth pressures, particularly in the lower half of the wall.

- for homogeneous narrow backfills, the distribution of lateral earth pressures are uniform and less than the Rankine active values. In wide homogenous backfills the lateral earth pressures are linear and exceed the Rankine active values within the lower third of the wall.

- the lateral thrust for homogeneous backfills increases as the backfill size increases and it is largest for soft cohesive deposits. In contrast, the lateral thrust decreases as the relative size of the granular zone to the cohesive zone increases, for non-homogenous backfills.

- Huntington's (1957) method for limited backfills can be used for narrow backfills but it considerably underestimates the magnitude of the lateral thrust for wide backfills.
- the results of Bang and Tucker (1990) are valid only for non-homogeneous backfills, where the lateral thrust decreases as the size of the granular backfill increases.

- the modified silo equation, developed by Bell (1987), is suitable for the determination of the lateral pressure distribution for retaining walls with narrow rectangular backfills where $b/H \leq \cot(45+\phi/2)$.

- in general, the lateral thrust increases as the embankment movements increase, and decreases as the settlements in the subsoil increase.

- the parametric study demonstrated that the lateral earth pressures are greatly affected by wall stiffness, stiffness of the embankment and stiffness of the subsoil, and interface parameters.

- although wall dimensions were chosen so as to ensure stability against sliding, overturning and shallow shear failure, erratic distributions were obtained for soft clays. This was found, during construction, due to large movements in the embankment and the subsoil. Therefore, the simplified lateral pressure distributions given in Chapter 6 are not valid for soft clays. However, for the design of retaining walls on soft clays the design curves developed in Chapters 4 and 5 may be used.

- in non-homogeneous backfills, the lateral earth pressures significantly exceed the Rankine active values in the lower half and reach three times the Rankine active values, in the case of T-walls founded on soft clays.

7.2 SUGGESTED FUTURE NUMERICAL STUDIES

The present study focused on the typical parameters of clays. A number of aspects have received limited attention. In future modelling of retaining walls it is favourable to use interface elements at the upper surface of the T-wall base. This may produce more accurate results as this may allow the wall to rotate away from the backfill soil.

It is worthwhile to study the influence of: sloping sites; shallow ground water table in the clay deposit; walls with sloping rear backs; a surface surcharge loading located at the surface of the backfill zone; and the effect of expansive clays.

It was pointed out in Chapter 3 that there is insufficient data on the interface parameters between concrete and cohesive soils. In future, it would be useful to carry

out some laboratory shear tests on a composite sample of soil and concrete to develop design values of interface shear stiffness for different types of concrete and clay.

The results presented in this thesis relate to loosely placed backfill. However, it is widely recognised that compacted backfills are common because they offer improvements in the shear strength of the soil. Excessive compaction is associated with larger at-rest lateral stresses which would be carried by a non-yielding retaining wall. It was previously discussed in Chapter 3, that compaction of the backfill will be an obstacle for drainage, but it may be used for the remaining region of the backfill to enhance the strength characteristics. It may be of interest to model non-homogeneous backfills, but introducing compaction in the region beyond the granular zone.

A limited parametric study was performed in Chapters 4 and 5 to identify the critical parameters affecting the lateral earth pressures. Only practical ranges of soil parameters were selected to aid the designer in the determination of lateral thrust on retaining walls. However, the results have shown complex effects of strength and stiffness parameters of embankment soil, foundation subsoil and wall-soil interface. It is therefore vital to carry out a detailed parametric study of these parameters so as to better quantify the relative effects of each factor.

A part of this detailed parametric study has already been carried out in order to quantify the effect of Young's modulus of the embankment, E_2, as shown in Figure 5.28. Similarly, these latter curves could be developed for Young's modulus of the foundation subsoil, E_3, by investigating a practical range of $E_3 / E_2 = 0.1$, 1.0, 10 and 100, while setting $E_3 / E_2 = E_3 / E_1$. These future unique combinations given in the form of β-a/H design curves would aid the designer in a wide range of field conditions.

The prediction of the behaviour of retaining walls founded on soft clays and associated lateral pressure distributions involves high uncertainty. In future, these walls should be modelled using the practical application of pile foundations underneath the base of the wall, instead of using a wide footing to provide the required stability, as used in the present research. This would provide a more realistic estimate of the lateral behaviour of the wall.

7.3 CONCLUSIONS

Based on the investigations presented in this thesis, the following can be concluded:

- the assumptions of the classical theories are most applicable to cantilever L-walls and gravity walls. For cantilever T-walls, the variation in the distribution of the LEPs is significantly different from the linear distribution.

- the use of the classical theories for the determination of the LEPs for retaining walls with wide rectangular backfills leads to minor errors;

- the classical theories overestimate the LEPs for retaining walls with narrow homogeneous backfills, while they underestimate the lateral earth pressure for retaining walls with wide backfills or non-homogeneous backfills;

- the parametric study demonstrated that the stiffness of the embankment, the stiffness of the natural deposit, and the interface parameters control the behaviour of retaining walls;

- the lateral earth pressure distribution is the product of the stress redistribution resulting from the complex interaction between the backfill, the embankment, the foundation subsoil and the retaining wall;

- the case of non-homogenous backfill was found to have significant effects, with the lateral pressures significantly exceeding the RAVs, particularly for the case of T-walls.

References

Acar, Y. B., Durgunoglu, H. T. and Tumay, M. T. (1982), Interface Properties of Sand, *Journal of Geotechnical Engineering, ASCE*, Vol. 108 (4), pp 648-654.

Bang, S. and Tucker, J. D. (1990), Active Lateral Earth Pressure Behind Retaining Structures with Interposed Backfill Soil Layer, *Proceedings 1990 Annual Symposium on Engineering Geology and Geotechnical Engineering*, Pocatello, ID, USA, pp 12.1-12.4.

Bell, A. L. (1915), The Lateral Pressure and Resistance of Clay and the Supporting Power of Clay Foundations, *A Century of Soil Mechanics*, Institution of Civil Engineers, London, pp 93-134.

Bell, F. G. (1987), *Ground Engineers Reference Book*, Butterworth, London, 1114 p.

Bishop, A. W. (1958), Test Requirements for Measuring the Coefficient of Earth Pressure at-rest, *Brussels Conference on Earth Pressures*, Brussels, Vol. 1, pp 2-14.

Booker, E. W. and Ireland, H. O. (1965), Earth Pressure at-rest Related to Stress History, *Canadian Geotechnical Journal*, Vol. 2, pp 1-12.

Boussinesq, J. (1885), *Application des Potentiels a l' Etude de l' Equilibre et du Mouvement des Solides Elastiques*, Gauthier-Villars, Paris.

Bowles, J. E. (1988), *Foundation Analysis and Design*, 4th Edn, McGraw-Hill Book Co., New York, 816 p.

Broms, B. B. and Ingelson, I. (1971), Earth Pressure Against the abutments of a Rigid Frame Bridge, *Geotechnique*, Vol. 21 (1), pp 15-28.

Broms, B. B. and Ingelson, I. (1972), Lateral Earth Pressure on a Bridge Abutment, *Proceedings 5th European Conference on Soil Mechanics and Foundation Engineering*, pp 117-123.

Bros, B. (1972), The Influence of Rigid Retaining Wall Displacements on Active and Passive Earth Pressures in Sand, *Proceedings 5th European Conference on Soil Mechanics and Foundation Engineering*, pp 241-249.

Caquot, A. (1934), *Equilibre des Massifs a Frottement Interne*, Gauthier-Villars, Paris.

Caquot, A. and Kerisel, J. (1948), Tables for the Calculation of Passive Pressure, *Active Pressure and Bearing Capacity of Foundations*, Gauthier-Villars, Paris.

Carder, D. R., Pocock, R. G. and Murray, R. T. (1977), Experimental Retaining Wall Facility, Lateral Stress Measurements with Sand Backfill, *Transport and Road Research Laboratory, Report No. LR. 766.*

Carter, J. P. and Balaam, J. B. (1994), *AFENA, v 4.6, Users Manual,* Centre for Geotechnical Research, University of Sydney, Australia.

Chang, C-Y. and Duncan, J. M. (1970), Analysis of Soil Movements Around a Deep Excavation, *JSMFE, ASCE*, Vol. 96, No. SM 5, pp 1655-1681.

Chen, W. F. and Liu, X. L. (1990), *Limit Analysis in Soil Mechanics*, Elsevier, Amsterdam, 447 p.

Chen, W. F. (1975), *Limit Analysis and Soil Plasticity*, Elsevier, Amsterdam, 638 p.

Christiano, P. and Chuntranuluck, S. (1974), Retaining Wall Under the Action of Backfill, *ASCE*, Vol. 100, No. GT4, pp 471-476.

CIRIA (1984), *Design of Retaining Walls Embedded in Stiff Clay*, Report 104, CIRIA Pub., London, pp 146.

Civil Engineering Code of Practice No. 2 (1951), *Earth Retaining Structures*, The Institute of structural Engineers, London, UK, pp 224.

Clough, G. W. (1969), *Finite Element Analyses of Soil-Structure Interaction in U-Frame Locks, PhD thesis*, University of California, Berkeley, California.

Clough. G. W. and Duncan, J. M. (1971), Finite Element Analysis of Retaining Wall Behaviour, *ASCE, Geotechnical Engineering Division*, Vol. 97, pp 1657-1673.

Clough, R. W. (1960), The Finite Element in Plane Stress Analysis, *Proceedings 2nd ASCE Conference on Electronic Computations*, Pittsburgh, Pa.

Clough, R. W. and Rashid, Y. (1965), Finite Element Analysis of Axi-symmetric Solids, *ASCE , EM Division*, Vol. 91, pp 71-85.

Clough. R. W. and Woodward, R. J. (1967), Analysis of Embankment Stresses and Deformations, *JSMFE, ASCE*, Vol. 93, No. SM 4, pp 529-539.

Coulomb, C. A. (1773), Essai sur une Application des Regles des Maximum et Minimumums a Quelques Problems de Statique Relatifs a L'architecture, *Memoris Academie Royal des Siences*, 3, 38.

Coyle, H. M., Bartoskewitz, R. E., Milberger, L. J. and Bulter, H. D. (1974), Field Measurement of Lateral Earth Pressures on a Cantilever Rctaining Wall, *Transportation Research Record 517*, pp 16-29.

Culmann, K. (1866), *Die Graphische Statik,* Zurich.

Davis, J. D., and Stephens, G. L. (1956), Pressure of Granular Materials Tests on Model Container, *Journal of Concrete and construction Engineering*, pp 32-43.

Desai, C. S. (1972), Theory and Application of the Finite Element Method in Geotechnical Engineering, *Proceedings Conference on Application of the Finite Element Method in Geotechnical Engineering*, Vicksburg, Mississippi, US Army Crops of Engineers, Vol. 1, pp 3-90.

Drucker, D. C. (1953), Limit Analysis of Two and Three Dimensional Soil Mechanics Problems, *Journal of Mechanics and Physics of Solids*, Vol. 1, pp 217-226.

Drucker, D. C., Prager, W. and Greenberg, H. J. (1952), Extended Limit Design Theorems for Continuous Media, *Quarterly of Applied Mathematics*, Vol. 9, No. 4, pp 381-389.

Duncan, J. M. and Dunlop, P. (1968), *Slopes in Stiff-Fissured Clays and Shales*, Contract Report No. TE 68-6, US Army Engineers Waterways Experiment Station, Vicksburg, Miss.

Duncan, J. M. and Seed, R. B. (1986), Finite Element Analysis, Compaction Induced Stresses and Deformations, *ASCE*, Vol. 112, GT1, pp 23-43.

Duncan, J. M. and Chang, C. Y. (1970), Non-Linear Analysis of Stress and Strain in Soils, *ASCE*, Vol. 56, SM5, pp 1625-1653.

Duncan, J. M., Clough, G. W. and Ebeling, R. (1990), Behaviour and Design of Gravity Earth Retaining Structures, *Proceedings Conference on Design and Performance of Earth Retaining Structures*, *ASCE*, No. 25, Cornell Uni, New York, USA, pp 20-44.

Fellenius, W. O. (1926), *Mechanics of Soils*, Statika Gruntov, Gosstrollzdat.

Girijavallabhan, C. V. and Reese, L. C. (1968), Finite Element Method for Problems in Soil Mechanics, *ASCE*, Vol. 94, No. SM2, pp 473-496.

Goh, A. T. C. (1984), *Finite Element Analysis of Retaining Walls*, *PhD thesis*, Monash University, Melbourne, Australia, 311 p.

Goh, A. T. C. (1994), Comparison of Methods of Determining Retaining Wall Earth Pressures from Surface Line Surcharge, *Australian Geomechanics Journal*, April, pp 87-91.

Goh, A. T. C. (1993), Behaviour of Cantilever Retaining Walls, *Journal of Geotechnical Engineering, ASCE*, Vol. 119 (10), pp 1751-1770.

Goodman, R. E., Taylor, R. L. and Brekke, T. L. (1968), A Model for the Mechanics of Jointed Rock, *ASCE*, Vol. 94, SM3, pp 637-659.

Hansen, J. B. (1953), *Earth Pressure Calculations*, 2nd Edn, Danish Technical Press, Institute of Danish Civil Engineering, Copenhagen, , 272 p.

Harr, M. H. (1977), *Mechanics of Particulate Media*, McGraw-Hill Book Co., New York, 542 p.

Hinton, E. and Owen, D. R. J. (1977), *Finite Element Programming*, Academic Press, London, 305 p.

Hong Kong Geotechnical Engineering Office (1993), *Guide to Retaining Wall Design, Geoguide 1*, Civil Engineering Department, Hong Kong Government, 267 p.

Huntington, W. C. (1957), *Earth Pressures and Retaining Walls*, John Wiley and Sons, New York, 534 p.

Islam, MD. Z., (1994), *Normalised Undrained Shear Strength and Deformation Properties of Remoulded Keswick Clay, M. Eng. Sc. thesis*, University of Adelaide, Australia, 172 p.

Jaky, J. (1948), Pressure in Silos, *Proceedings 2nd ICSMFE, Vol.* 1, pp 103-107.

James, R. G. and Bransby, P. L. (1970), Experimental and Theoretical Investigations of a Passive Earth Pressure Problem, *Geotechnique*, Vol. 20, No. 1, pp 17-37.

Jha, R. K. (1994), *Field and Laboratory Testing of Calcareous Sand, M. Eng. Sc. thesis*, University of Adelaide, Australia, 163 p.

Kaliakin, V. N. and Li, J. (1995), Insight into Difficulties Associated with Commonly Used Zero-Thickness Interface Elements, *Computers and Geotechniques*, Elsevier Applied Science, Vol. 17, No. 2, pp 225-252.

Kany, M. (1972), Measurements of Earth Pressures on a Cylinder 30 m in Diameter (Pump Storage Plant), *Proceedings 5th European Conference on Soil Mechanics and Foundations*, Madrid, pp 535-542.

Kotter, F. (1903), *Die Bestimmug des Druckes on Gekrummten Gleitflachen*, Sitzungsber. Kgl. Preuss. Akad. der Wiss., Berlin.

Kulhway, F. H. (1974), Analysis of a High Gravity Retaining Wall, *Proceedings ASCE Conference on Analysis and Design in Geotechnical Engineering*, University of Texas, Austin, Vol. 1, pp 159-172.

Lambe, T. W. and Whitman, R. V. (1969), *Soil Mechanics*, John Wiley and Sons, New York, 553 p.

Matsumoto, M., Kenmochi, S. and Yagi, H. (1978), Experimental Study on Earth Pressure of Retaining Wall by Field Tests, *Proceedings Japan Society of Soil Mechanics and foundation Engineering*, Vol. 18, No. 3, pp 27-41.

Mohr, O. (1871), Beitrage zur Theorie des Erddruckes, *Z. Arch. und Ing. Ver. Hannover*, Vol. 17, 1871, Vol. 18, 1872.

Morgenstern, N. R. and Eisenstein. Z. (1970), Method of Estimating Lateral Loads and Deformations, *Proceedings Conference on Lateral Stresses in Ground and Design Earth Retaining Structures*, pp 51-102.

New Zealand Ministry of Works and Development (1973), *Retaining Wall Design Notes*, Civil Engineering Division, Research and Development Section, 89 p.

Ozawa, Y. and Duncan, J. M. (1976), Elasto-Plastic Finite Element Analyses of Sand Deformations, *Proceedings 2nd International Conference on Numerical Methods in Geomechanics*, Vol I, pp 243-263.

Potts, D. M. and Burland, J. B. (1983), A Numerical Investigation of the Retaining Walls of the Bell Common Tunnel, *Transport Road Research Laboratory*, Report No. 783.

Rankine, W. J. M. (1857), On the Stability of Loose Earth, Philosophical, *The Royal Society*, 147(2), pp 9-27.

Reese, L. C. et al. (1970), Generalised Analysis of Pile Foundations, *JSMFD, ASCE*, Vol. 96, SM1, Jan., pp 235-250.

Rehnman, S. E. and Broms, B. B. (1972), Lateral Pressures on Basement Wall, Results From Full Scale Tests, *Proceedings 5th European Conference on Soil Mechanics and Foundations*, Madrid, pp 189-197.

Reimbert, M. and Reimbert, A. (1989), *Retaining Structures*, Lavoiser Pub. Inc., New York, 170 p.

Richards, B. G. (1980), Use of an Automatically Generated Joint Element for the Analysis of Collapse Load in Strain Softening Materials, *Proceedings 3rd Aust-NZ Geomechanics Conference*, Wellington, NZ., Vol. 2, pp 233-239.

Rockey, K. C., Evans, H. R., Griffiths, D. W., D. A. Nethercot (1983), 2nd Edn, *The Finite Element Method, A Basic Introduction for Engineers*, Blackwell Scientific Publications, Australia, Victoria, 239 p.

Rosenfarb, J. L. and Chen, W. F. (1972), Limit Analysis Solutions of Earth Pressure Problems, *Fritz Engineering Laboratory, Report No. 355.14*, Lehigh University, 53 p.

Schofield, A. N. and Wroth, C. P. (1968), *Critical State Soil Mechanics*, McGraw Hill, London, 310 p.

Seed, R. B. and Duncan, J. M. (1986), Compaction-Induced Earth Pressures Under K_0-Conditions, *ASCE*, Vol. 112, GT1, pp 1-22.

Sherif, M. A., Fang, Y. S. and Sherif, R. I. (1984), K_a and K_0 Behind Rotating and Non-yielding Walls, *ASCE*, Vol. 110, GT1, pp 44-56.

Simpson, B. and Wroth, C. P. (1972), Finite Element Computation for a Model Retaining Wall in Sand, *Proceedings 5th European Conference on Soil Mechanics and Foundation Engineering*, Madrid, pp 85-93.

Simpson, B., Calabresi, G., Sommer, H. and Wallays, M. (1979), Design Parameters for Stiff Clays, *Proceedings 7th European Conference on Soil Mechanics and Foundation Engineering*, Brighton, Vol. 5, pp 91-125.

Smith, I. M. (1982), *Programming the Finite Element Method with Applications to Geomechanics*, John Wiley and Sons, 313 p.

Sokoloviski, V. V. (1960), *Statics of Granular Media*, Translated from Russian by J. K. Luscher, Pergamon Press, London.

Stefanoff, G. and Venkov, V. (1972), Earth Pressure Exerted by a Stratified Backfill, *Proceedings 5th European Conference on Soil Mechanics and Foundation Engineering*, Madrid, pp 101-107.

Symons, I. F. and Clayton, C. R. I. (1992), Earth Pressures on Backfilled Retaining Walls, *Ground Engineering*, Vol. 25, April, pp 26-34.

Symons, I. F. and Wilson, D. S. (1972), Measurements of Earth Pressures in Pulverised Fuel Ash Behind a Rigid Retaining Wall, *Proceedings 5th European Conference on Soil Mechanics and Foundation Engineering*, Madrid, pp 569-575.

Teng, W. C. (1962), *Foundation Design*, Englewood Cliffs, N. J. Prentice-Hall, p 466.

Terzaghi, K. (1920), Old Earth Pressure Theories and New Test Results, *Engineering News Records*, Vol. 85, No. 14, pp 632-637.

Terzaghi, K. (1934), Large Retaining Wall Tests, *Engineering News Records*, Feb. 1, pp 136-140, Feb. 22, pp 259-262, Mar. 8, pp 316-318; Mar. 29, pp 403-406, April, Vol 19, pp 503-508.

Terzaghi, K. (1925-1940), A Fundamental Fallacy in Earth Pressure Computations, *Contributions to Soil Mechanics*, Boston Society of Civil engineers, Boston, pp 71-88.

Terzaghi, K. and Peck, R. B. (1967), *Soil Mechanics in Engineering Practice*, 2nd. Edn, John Wiley and Sons, New York, 729 p.

Tschebotarioff, G. P. (1951), *Soil Mechanics, Foundations and Earth Structures*, McGraw-Hill Book Co., New York, 655 p.

Valliappan, S (1978), *Short Course on Finite Element Analysis in Geomechanics*, University of NSW, Department of Civil and Environmental Engineering, Vol. 1, 2.

Wong, K. S. (1978), *Elasto-Plastic Analyses of Passive Pressure Tests, PhD Thesis*, University of California, Berkeley, USA.

Zienkiewicz, O. C. and Taylor, R. L. (1989), *The Finite Element Method*, Vol. 1, 4th Edn, McGraw-Hill Book Co., London, 648 p.